



Spatio-temporal patterns of throughfall
water and ion deposition under a
dominant beech tree (*Fagus sylvatica* L.)
in relationship to canopy structure

ir. Jeroen STAELENS



*The rain it rainth
on the good as on the bad fella
but more on the good
as the bad took his umbrella*

(Anonymous)

Promotors: Prof. dr. ir. K. Verheyen
Department of Forest and Water Management, Laboratory of
Forestry
Prof. dr. ir. N. Verhoest
Department of Forest and Water Management, Laboratory of
Hydrology and Water Management

Dean: Prof. dr. ir. H. Van Langenhove

Rector: Prof. dr. P. Van Cauwenberge

ir. Jeroen STAELENS

SPATIO-TEMPORAL PATTERNS OF THROUGHFALL WATER AND
ION DEPOSITION UNDER A DOMINANT BEECH TREE (*FAGUS*
SYLVATICA L.) IN RELATIONSHIP TO CANOPY STRUCTURE

Thesis submitted in fulfillment of the requirements
for the degree of Doctor (PhD) in Applied Biological Sciences

Ruimtelijke en temporele patronen van doorvalwater en ionendepositie onder een dominante beuk (*Fagus sylvatica* L.) in relatie tot de kroonstructuur

Staelens, J. 2006. Spatio-temporal patterns of throughfall water and ion deposition under a dominant beech tree (*Fagus sylvatica* L.) in relationship to canopy structure. Ph.D. thesis, Ghent University, Belgium.

ISBN-number: 90-5989-104-X

The author and the promotor give the authorisation to consult and to copy parts of this work for personal use only. Every other use is subject to the copyright laws. Permission to reproduce any material contained in this work should be obtained from the author

Woord vooraf

Allereerst wil ik mijn oorspronkelijke promotoren Prof. em. dr. ir. Noël Lust en Prof. em. dr. ir. Francois De Troch bedanken voor hun ondersteuning en vertrouwen tijdens de eerste jaren van dit onderzoek. Prof. dr. ir. Kris Verheyen en Prof. dr. ir. Niko Verhoest, die daarna het promotorschap overnamen, stonden altijd voor me klaar en motiveerden me onder meer door hun bemoedigende suggesties bij de teksten. Mijn dank gaat ook uit naar de andere co-auteurs en reviewers van publicaties die in dit proefschrift zijn opgenomen, evenals naar de leden van de examencommissie: Prof. dr. Niels De Pauw (voorzitter), Prof. dr. ir. Marc Van Meirvenne, Dr. ir. Roeland Samson, Dr. Klaus von Wilpert (Forstliche Versuchs- und Forschungsanstalt Baden-Württemberg, Freiburg, Duitsland) en Prof. em. dr. ir. Noël Lust. Hun constructieve opmerkingen waren van grote waarde en hebben in belangrijke mate bijgedragen tot de kwaliteit van dit werk.

Tijdens de voorbije jaren heb ik op het Laboratorium voor Bosbouw mogen ervaren hoe belangrijk samenwerking en collegialiteit zijn, en ik wil dan ook alle collega's bedanken voor de aangename sfeer. Ik ben An De Schrijver bijzonder erkentelijk voor haar expertise en enthousiasme en voor de talrijke stimulerende discussies. Met mijn vragen was ik ook altijd welkom bij onder meer Jan Mertens, Nancy Van Camp, Guy Geudens en Peter Van Gossum. Sebastiaan Luysaert lag mee aan de basis van het oorspronkelijke onderzoeksvorstel.

Mijn dank gaat verder uit naar Etienne De Bruycker voor de constructie van meettoestellen en naar Greet De Bruyn en Luc Willems voor de chemische analyses en de hulp bij het veldwerk. Philip Deman (Laboratorium voor Plantecologie, UGent) zorgde voor de goede werking van de meteorologische sensoren op de meettoeren in het Aelmoeseneiebos. Ik dank Philip Van Avermaet en de Vlaamse Milieumaatschappij (VMM) voor het gebruik van de wet-only toestellen, Truus Aelbers en Elke Adriaenssens voor de chemische analyses, en Leen Verlinden voor het bezorgen van luchtkwaliteitsgegevens van het telemetrisch meetnet van de VMM. Gerrit Genouw en Johan Neirynek van het Instituut voor Natuur- en Bosonderzoek (INBO) stelden gegevens ter beschikking van de Vlaamse Level II proefvlakken.

Mijn ouders wil ik bedanken voor hun onvoorwaardelijke vertrouwen en aanmoediging tijdens alle voorbije jaren. Mijn zus, vrienden en familie zorgden ook voor de nodige steun en gezelligheid. Tenslotte wil ik mijn allerliefste Tin in de bloemetjes zetten. Je warmte en geduld zijn onbeschrijfelijk.

Dit onderzoek was mogelijk dankzij een beurs als aspirant van het Fonds voor Wetenschappelijk Onderzoek - Vlaanderen (F.W.O.-Vlaanderen) en een werkingskrediet van het Bijzonder Onderzoeksfonds van Universiteit Gent.

Contents

WOORD VOORAF

LIST OF ABBREVIATIONS AND SYMBOLS

CHAPTER 1	INTRODUCTION.....	1
CHAPTER 2	BULK AND WET-ONLY PRECIPITATION AT TWO ADJACENT SITES.....	7
2.1	Abstract.....	7
2.2	Introduction.....	8
2.3	Materials and methods.....	10
2.3.1	Study site and meteorological conditions.....	10
2.3.2	Data collection.....	11
2.3.3	Chemical analysis and data quality.....	12
2.3.4	Data analysis.....	13
2.4	Results.....	14
2.4.1	Comparison of sites.....	14
2.4.2	Comparison of sampling devices.....	15
2.4.3	Atmospheric NH ₃ concentration.....	16
2.4.4	Wet and bulk precipitation deposition.....	16
2.5	Discussion.....	17
2.5.1	Rainfall amount.....	17
2.5.2	Deposition of Na ⁺ , K ⁺ , Ca ²⁺ , Mg ²⁺ , and Cl ⁻	17
2.5.3	Deposition of NH ₄ ⁺ , NO ₃ ⁻ , SO ₄ ²⁻ , F ⁻ , and H ⁺	18
2.5.4	Impact of temporal rainfall distribution on deposition.....	20
2.6	Conclusions.....	20
CHAPTER 3	RAINFALL PARTITIONING INTO THROUGHFALL, STEMFLOW, AND INTERCEPTION: INFLUENCE OF FOLIATION, RAIN EVENT CHARACTERISTICS, AND METEOROLOGY.....	21
3.1	Abstract.....	21
3.2	Introduction.....	22
3.3	Materials and methods.....	23
3.3.1	Study site.....	23
3.3.2	Data collection.....	24

3.3.2.1	Throughfall and stemflow	24
3.3.2.2	Precipitation	25
3.3.2.3	Meteorological data.....	26
3.3.3	Data analysis	26
3.3.3.1	Data handling and data exploration.....	26
3.3.3.2	Regression analysis	28
3.4	Results	28
3.4.1	Precipitation partitioning at the annual and semiannual level.....	28
3.4.2	Event rainfall partitioning as a function of rainfall amount and period of the year.	30
3.4.3	Rainfall characteristics and meteorological conditions.....	34
3.4.4	Event rainfall partitioning as a function of rainfall characteristics and meteorology ..	36
	36
3.5	Discussion	39
3.5.1	Precipitation partitioning at the annual and semiannual level.....	39
3.5.2	Interception loss in relationship to rainfall amount.....	40
3.5.3	Rainfall partitioning at the rain event level.....	41
3.5.4	Accuracy of interception measurements	43
3.6	Conclusions	44
CHAPTER 4	SPATIAL VARIABILITY AND TEMPORAL STABILITY OF THROUGHFALL WATER	
	AMOUNT IN RELATIONSHIP TO CANOPY STRUCTURE	45
4.1	Abstract	45
4.2	Introduction	46
4.3	Materials and methods.....	47
4.3.1	Data collection.....	48
4.3.1.1	Throughfall.....	48
4.3.1.2	Canopy structure	48
4.3.2	Data analysis	50
4.3.2.1	Spatial variability of throughfall	50
4.3.2.2	Temporal stability of spatial throughfall variability	51
4.3.2.3	Relationship between throughfall and canopy structure	52
4.4	Results	52
4.4.1	Spatial variability of throughfall	53
4.4.2	Temporal stability of spatial throughfall patterns	56
4.4.3	Relationship between throughfall and canopy structure	58
4.5	Discussion	62
4.5.1	Spatial variability of throughfall in the leafed and leafless season	62
4.5.2	Temporal stability of spatial throughfall patterns	63
4.5.3	Relationship between throughfall and canopy structure	64
4.6	Conclusions	66

CHAPTER 5 SEASONAL VARIATION IN THROUGHFALL AND STEMFLOW CHEMISTRY IN RELATION TO CANOPY PHENOLOGY	67
5.1 Abstract	67
5.2 Introduction	68
5.3 Materials and methods.....	70
5.3.1 Data collection.....	70
5.3.1.1 Water fluxes	70
5.3.1.2 Chemical analysis and data quality	71
5.3.2 Data analysis	72
5.3.2.1 Ion fluxes.....	72
5.3.2.2 Temporal variability of ion fluxes and correlation between ions.....	72
5.3.2.3 Canopy budget method.....	73
5.4 Results	74
5.4.1 Precipitation, throughfall, and stemflow deposition	74
5.4.2 Ion correlations in net throughfall deposition	78
5.4.3 Seasonal canopy budget method	82
5.5 Discussion.....	83
5.5.1 Throughfall enrichment in the leafed and leafless season.....	83
5.5.2 Sodium and chloride.....	84
5.5.3 Potassium, calcium, and magnesium.....	85
5.5.4 Nitrogen, hydrogen, and sulphur.....	86
5.5.5 Stemflow	89
5.6 Conclusions	90
 CHAPTER 6 SPATIAL VARIABILITY AND TEMPORAL STABILITY OF THROUGHFALL CHEMISTRY IN RELATIONSHIP TO CANOPY STRUCTURE	 91
6.1 Abstract	91
6.2 Introduction	92
6.3 Materials and methods.....	93
6.3.1 Data collection.....	93
6.3.2 Data analysis	94
6.3.2.1 Spatial variability of throughfall	94
6.3.2.2 Temporal stability of spatial throughfall variability	94
6.3.2.3 Relationship between throughfall and canopy structure	95
6.4 Results	95
6.4.1 Spatial variability of throughfall	95
6.4.2 Time stability of spatial throughfall patterns	97
6.4.3 Relationship between throughfall chemistry and throughfall water amount	98
6.4.4 Relationship between throughfall and canopy structure	100
6.5 Discussion.....	103

6.5.1	Spatial variability and temporal stability of throughfall	103
6.5.2	Spatial variability of throughfall in relationship to canopy structure.....	104
6.6	Conclusions	106
 CHAPTER 7 QUANTIFYING ATMOSPHERIC DEPOSITION ONTO A BEECH CANOPY USING VARYING FORMS OF THE CANOPY BUDGET METHOD AND AN INFERENTIAL TECHNIQUE		
7.1	Abstract.....	107
7.2	Introduction	108
7.3	Materials and methods.....	110
7.3.1	Study sites	110
7.3.2	Canopy budget method.....	111
7.3.2.1	‘Reference’ canopy budget method.....	111
7.3.2.2	Varying forms of the canopy budget method.....	113
7.3.3	Inferential method	115
7.4	Results	117
7.4.1	Net throughfall (+ stemflow) deposition.....	117
7.4.2	Canopy budget method.....	119
7.4.2.1	Beech plot.....	119
7.4.2.2	Mixed maple plot	122
7.4.3	Inferential method	124
7.5	Discussion.....	126
7.5.1	Time step, precipitation input, and tracer ion.....	126
7.5.2	Canopy uptake of nitrogen and protons	127
7.5.3	Comparison with inferential method.....	130
7.6	Conclusions	132
 CHAPTER 8 GENERAL DISCUSSION AND CONCLUSIONS.....		
133		
SUMMARY	143
SAMENVATTING	145
REFERENCES	149
CURRICULUM VITAE	165

List of abbreviations and symbols

Abbreviations

BD	Bulk precipitation deposition ($\text{mmol}_c \text{m}^{-2} \text{period}^{-1}$)
C	Ion concentration ($\mu\text{mol}_c \text{l}^{-1}$)
CE	Canopy exchange ($\text{mmol}_c \text{m}^{-2} \text{period}^{-1}$)
CL	Canopy leaching ($\text{CE} > 0$) ($\text{mmol}_c \text{m}^{-2} \text{period}^{-1}$)
CU	Canopy uptake ($\text{CE} < 0$) ($\text{mmol}_c \text{m}^{-2} \text{period}^{-1}$)
CV	Coefficient of variation (%)
DD	Dry deposition ($\text{mmol}_c \text{m}^{-2} \text{period}^{-1}$)
DL	Determination limit ($\mu\text{mol}_c \text{l}^{-1}$) of analytical method
I	Interception (mm period^{-1})
L	Leafed season
LAI	Leaf area index ($\text{m}^2 \text{m}^{-2}$)
NL	Leafless season
NSD	Net stand deposition ($= \text{TF} + \text{SF} - \text{WD}$) ($\text{mmol}_c \text{m}^{-2} \text{period}^{-1}$)
NTF	Net throughfall deposition ($= \text{TF} - \text{WD}$) ($\text{mmol}_c \text{m}^{-2} \text{period}^{-1}$)
P	Precipitation amount (mm period^{-1})
PAI	Plant area index ($\text{m}^2 \text{m}^{-2}$)
SD	Standard deviation
SF	Stemflow water (mm period^{-1}) or ion ($\text{mmol}_c \text{m}^{-2} \text{period}^{-1}$) flux
Site F	Field site (Melle, site of the Royal Meteorological Society of Belgium)
Site T	Tower site (Aelmoeseneie forest)
TF	Throughfall water (mm period^{-1}) or ion ($\text{mmol}_c \text{m}^{-2} \text{period}^{-1}$) flux
TF + SF	Stand deposition of water (mm period^{-1}) or ions ($\text{mmol}_c \text{m}^{-2} \text{period}^{-1}$)
TF/P	Relative throughfall fraction
vw	Volume-weighted (for ion concentrations)
WD	Wet-only precipitation deposition ($\text{mmol}_c \text{m}^{-2} \text{period}^{-1}$)
BC	So-called 'base cations' or neutral cations ($= \text{Na}^+ + \text{K}^+ + \text{Ca}^{2+} + \text{Mg}^{2+}$)
w.a.	Weak acids

Symbols

r	Pearson correlation coefficient
r_s	Spearman rank correlation coefficient
r^2	Coefficient of determination
r_a^2	Adjusted coefficient of determination
k	Canopy extinction coefficient
m	Number of sampling periods
n	Number of sampling collectors
p	Canopy gap fraction
$1 - p$	Canopy cover fraction

Chemical compounds

Ca^{2+}	Calcium
Cl^-	Chloride
H^+	Proton
HNO_3	Nitric acid
K^+	Potassium
Na^+	Sodium
N	Nitrogen
NH_3	Ammonia
NH_4^+	Ammonium
NH_x	Reduced nitrogen (NH_3 and NH_4^+)
NO	Nitric oxide
NO_2^-	Nitrite
NO_2	Nitrogen dioxide
NO_3^-	Nitrate
NO_x	NO and NO_2
NO_y	Oxidised nitrogen (NO_x , NO_3^- , HNO_3 , ...)
PO_4^{3-}	Phosphate
S	Sulphur
SO_2	Sulphur dioxide
SO_4^{2-}	Sulphate
SO_x	SO_2 and SO_4^{2-}

1 Introduction

Forest ecosystems represent a controlling factor of the global water cycle and interact with atmospheric gases and particles (Smith, 1981; Shuttleworth, 1989). The precipitation input passing through a forest canopy is affected in two ways. Quantitatively, precipitation water is reduced as it moves towards the forest floor due to interception and evaporation of water (Rutter *et al.*, 1971). Qualitatively, the chemical composition of the water flux to the forest floor is modified compared to the precipitation input due to wash-off of dry deposition as well as ion exchange processes within the canopy (Parker, 1983).

The water input by rain, hail, or snow passing through a forest canopy is partitioned into three fractions (Fig. 1.1): (i) throughfall, which reaches the ground directly through canopy gaps or indirectly after contact with the canopy, (ii) stemflow, which flows to the ground via branches and stems, and (iii) interception, which is the fraction of incident precipitation that remains on the vegetation and is evaporated during and after rain events (Shuttleworth, 1989).

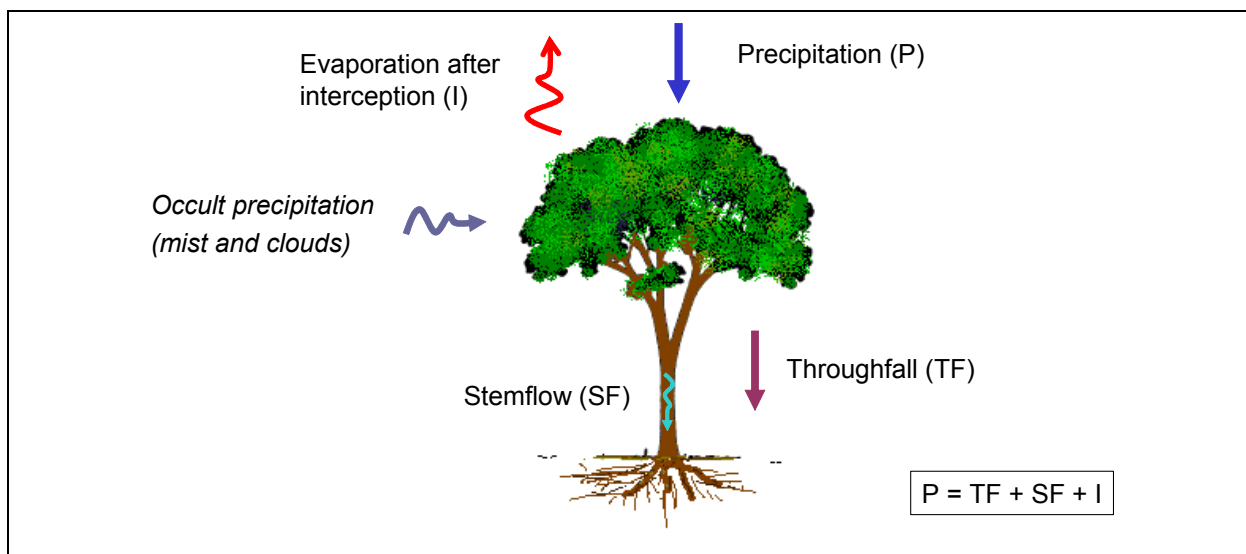


Fig. 1.1. Partitioning of precipitation water into throughfall, stemflow, and interception.

Consequently, the mass balance of partitioning of precipitation is expressed as (Crockford and Richardson, 2000):

$$P = TF + SF + I \tag{1.1}$$

where P is gross precipitation, TF is throughfall, SF is stemflow, and I is interception. The sum of throughfall and stemflow water is called net precipitation. In addition, so-called occult precipitation originating from fog, mist, and cloud moisture can contribute largely to the water budgets of high-elevation forest sites (Zimmermann and Zimmermann, 2002).

The evaporation of intercepted water from forest canopy surfaces is an important component of the hydrological budgets of forest ecosystems in temperate regions (Rutter *et al.*, 1971; Shuttleworth, 1989; Arora, 2002), and affects streamflow generation and groundwater recharge in watersheds (Armbruster *et al.*, 2004; Özyuvaci *et al.*, 2004). The intercepted fraction of precipitation is determined by forest type and climatic factors (Crockford and Richardson, 2000). In addition to a decreased net water input to the forest floor, forest canopies also reduce maximum intensities of precipitation, which leads to decreased soil erosion and overall greater stability of hill slopes under forest canopies (Keim and Skaugset, 2003).

In contrast to the water flux of throughfall and stemflow, ion fluxes to the forest floor by throughfall and stemflow may be higher or lower than the precipitation input. It is widely acknowledged that this transformation results from (i) wash-off of dry deposition as well as (ii) uptake and release of substances by plants and their associated microflora (Parker, 1983) (Fig. 1.2). Total atmospheric deposition onto lowland forest ecosystems consists of wet and dry deposition. Wet deposition is the above-canopy ion input by rain, hail, or snow (Krupa, 2002). Dry deposition is the direct deposition of particles and gases onto plant surfaces which is then washed off by precipitation (Lovett and Lindberg, 1984). At high-elevation sites, also occult ion deposition by fog, mist or cloud moisture can contribute significantly to forest ecosystem budgets (Lovett *et al.*, 1982; Zimmermann and Zimmermann, 2002).

The ion flux to the forest floor by throughfall and stemflow differs from the total atmospheric input due to ion exchange between canopy surfaces, including foliage, woody parts, epiphytes and micro-organisms, and the water passing through the canopy. This exchange includes both efflux from the canopy (leaching) and influx to the canopy (uptake). The mass balance for substances dissolved in canopy surface water can thus be written as (Lovett *et al.*, 1996):

$$TF + SF = WD + DD + CE \quad (1.2)$$

where TF is the throughfall ion flux, SF is the stemflow ion flux, WD is the wet deposition, DD is the dry deposition (including occult deposition), and CE is the ion source or sink within the canopy due to canopy exchange.

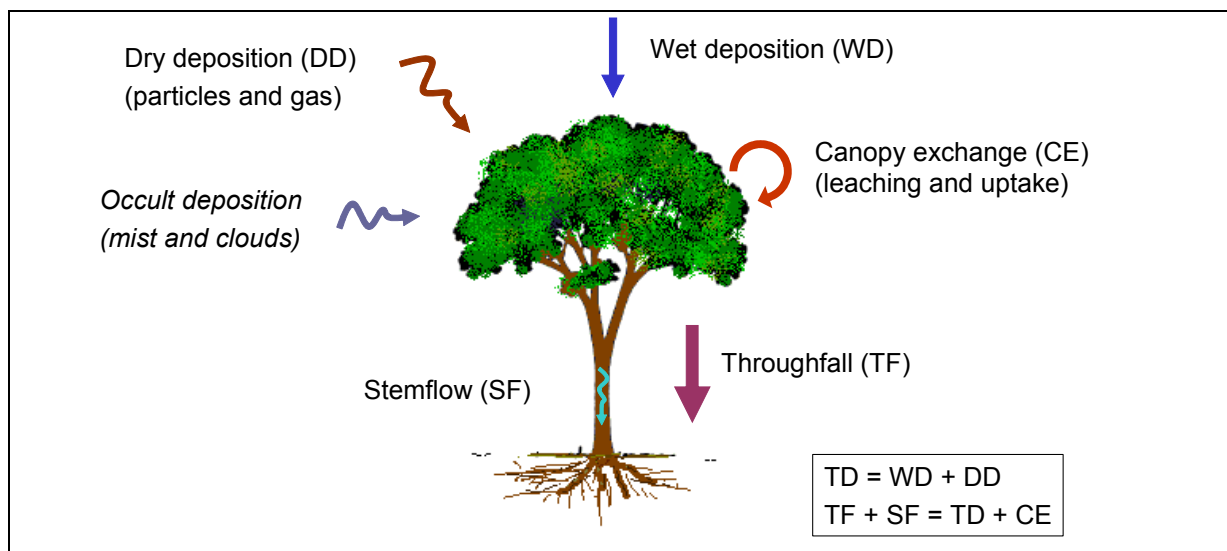


Fig. 1.2. Throughfall and stemflow ion deposition as a result of total atmospheric deposition (TD) and canopy exchange processes (CE).

It has long been recognized that the vegetative compartment of forest ecosystems functions as a sink for atmospheric components. On the one hand, the transfer of atmospheric gases and particles has been studied because the ability of woody plants to remove air pollutants and dust can improve air quality in urban and suburban areas (Chamberlain, 1967; Smith, 1981; Beckett *et al.*, 1998; Bolund and Hunhammar, 1999). The attenuation of atmospheric air pollution by vegetation has therefore been optimized using designed greenbelts around emission sources (Rao *et al.*, 2004; Yang *et al.*, 2005). On the other hand, there has been considerable interest in the filtering capacity of vegetation because of the acidifying and eutrophying impact of sulphur and nitrogen deposition on forest soils and waters (van Breemen *et al.*, 1982; Aber *et al.*, 1989, 1998; Bouwman *et al.*, 2002; de Vries *et al.*, 2003). The basis for this interest originates from reports of increased soil acidification as a causative factor of forest damage and decline in Europe and North America (Ulrich and Pankrath, 1983; Schulze, 1989; but see e.g., Binkley and Högberg, 1997).

In order to assess the impact of air pollution on forest ecosystems, an accurate quantification of total atmospheric deposition is needed. Dry deposition of chemical compounds is difficult to measure directly and thus inferential models have been developed (e.g., Hicks *et al.*, 1987, Wesely, 1989; Zhang *et al.*, 2002). Alternatively, dry atmospheric deposition is determined indirectly by measuring the ion enrichment of precipitation water passing through a forest canopy. To estimate dry (and occult) deposition of an element by its throughfall enrichment below the canopy, it is necessary to quantify canopy exchange processes (Draaijers *et al.*, 1996). Separating internal and external sources of ions in throughfall and stemflow has been

an ongoing concern for several decades (White and Turner, 1970; Mayer and Ulrich, 1978; Lovett and Lindberg, 1984; Draaijers and Erisman, 1995; Stachurski and Zimka, 2000). Foliar leaching is most pronounced for cations like potassium, calcium, and magnesium (Parker, 1983). Inorganic nitrogen, on the other hand, is retained and assimilated by above-ground vegetation (Harrison *et al.*, 2000; Gessler *et al.*, 2000; Horváth, 2004).

The impact of canopy cover on throughfall water and ion fluxes is generally studied at the stand level using annual average inputs. However, throughfall water and ion fluxes can vary largely within forest stands (e.g., Kimmins, 1973). Previous research in coniferous forests indicates that this spatial variability is not entirely random, but that the vegetation structure contributes to a systematic component of the spatial heterogeneity of throughfall (Beier *et al.*, 1993; Whelan and Anderson, 1996, 1998). Systematic spatio-temporal throughfall patterns may significantly affect spatially distributed processes in forests soils such as nitrification, root uptake, trace gas fluxes, and water and solute percolation (e.g., Manderscheid and Matzner, 1995; Raat *et al.*, 2002). Despite the general opinion that the structural elements of the canopy such as foliage, branches, and epiphytes, regulate inputs of matter and energy to the forest floor (Russel *et al.*, 1989; Frazer *et al.*, 2005), relatively few attempts have been made to relate fine-scale spatial throughfall patterns to canopy structure in a quantitative way (Nadkarni and Sumera, 2004). Particularly in broadleaved deciduous forest stands, little is known about the driving factors of the spatial distribution of the water and ion input to the forest floor. Furthermore, there is a seasonal variation in the canopy structure of deciduous trees, which likely affects the redistribution and chemical modification of rainfall passing through the canopy.

Therefore, the central hypothesis tested in this study is that the amount and ion enrichment of precipitation water passing through a forest canopy is significantly affected by the structure of the canopy that varies in space and time. The study aims at quantifying and explaining the fine-scale spatio-temporal variation of the water and ion fluxes to the forest floor beneath a broadleaved deciduous forest canopy, and the objectives were consequently:

- (i) to accurately quantify the water and ion input by precipitation above the canopy,
- (ii) to quantify the small-scale spatial heterogeneity of the water and ion fluxes under the deciduous canopy throughout the year and between years, and
- (iii) to relate the spatio-temporal variability of the water and ion fluxes to variations in the structure and phenology of the canopy.

To reach these aims, the study focused on the water and ion input to the forest floor under the canopy of one dominant tree. In this way, spatial variations in gross precipitation input, soil characteristics, and micrometeorological atmospheric conditions were minimized. The tree species studied is European beech (*Fagus sylvatica* L.), a shade-tolerant, late-successional species that occurs from south England, France and north Spain in its western limit to Poland and Romania in the east. Its latitudinal extension ranges from south Sweden to north Italy and Greece (Granier *et al.*, 2000). Beech forests have an important economic, ecological, and recreational value throughout Europe, and the percentage of beech or beech dominated forests in the total forest area varies from less than 10% in Belgium, France, and the Czech Republic over 30% in Slovakia and Romania, up to 70% in Slovenia (Anonymous, 2000; Hahn and Fanta, 2001; Vande Walle *et al.*, 2005).

The present research was conducted in the Aelmoeseneie forest (Melle-Gontrode, Belgium). In the stand where the studied beech tree is located, biogeochemical pools and fluxes are monitored in the framework of the International Co-operative Programme on the Assessment and Monitoring of Air Pollution Effects on Forests (ICP Forests) under the Convention of Long-Range Transboundary Air Pollution (UN/ECE, 2004). A measuring tower has been set up in the forest stand and there is a site of the Royal Meteorological Society of Belgium at 1 km distance.

The study consists of three parts (Fig. 1.3). First, the water amount and chemical composition of the precipitation input above the forest canopy is examined (Chapter 2). Second, the water amount beneath the canopy is studied at the plot level (Chapter 3) and the within-plot level (Chapter 4). Third, the chemical composition of the water fluxes under the canopy is analysed at the plot and the within-plot level (Chapters 5, 6, and 7). The influence of the canopy on throughfall and stemflow is investigated both in time and in space. Chapters 3 and 5 focus on the temporal variation of the water and ion fluxes at the plot level. Chapters 4 and 6 discuss the spatial variation of these fluxes throughout time at the within-plot level (Fig. 1.3).

(i) Above-canopy water amount and chemistry

An accurate quantification of the above-canopy precipitation input is required for determining the effect of a forest canopy on the water and ion fluxes to the forest floor. Therefore, the precipitation measured by commonly used bulk collectors was compared with the results of more advanced wet-only precipitation collectors at two adjacent sites (Chapter 2).

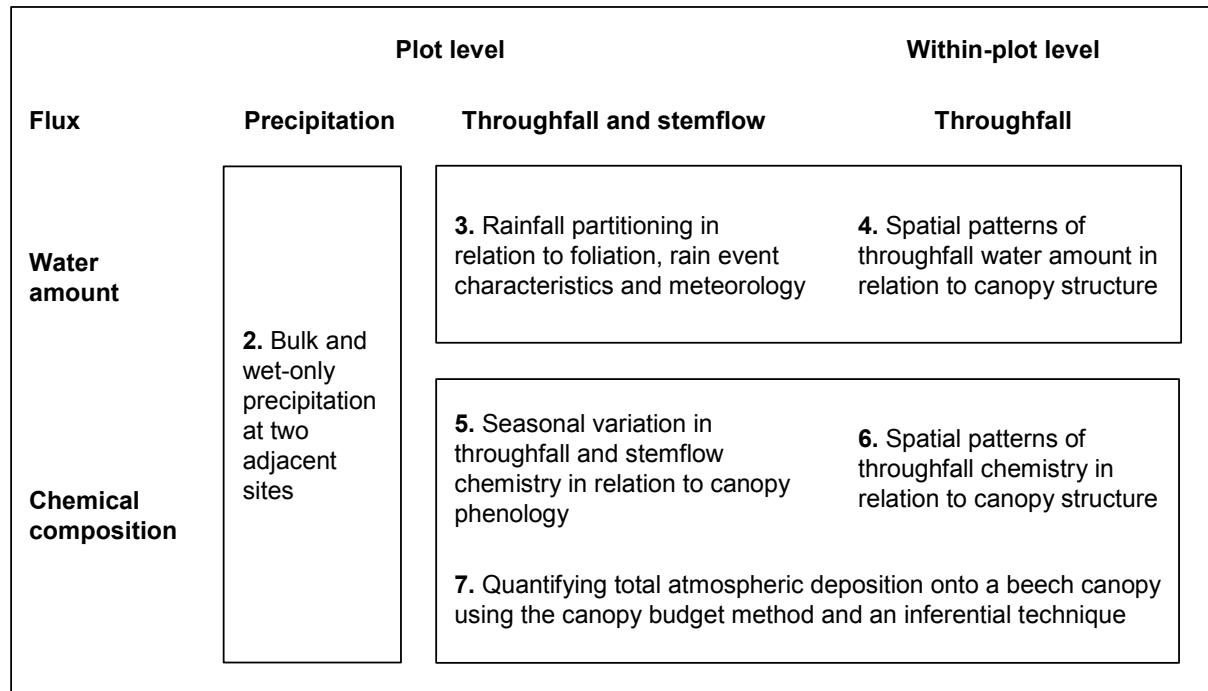


Fig. 1.3. Outline of the study

(ii) Below-canopy water amount

The partitioning of rainfall into throughfall, stemflow, and interception was studied at the plot level for individual rain events (Chapter 3). The temporal evolution of the water fluxes was examined in relation to foliation, rain event characteristics and meteorological conditions. Next, the spatial variability and temporal stability of the amount of throughfall water was quantified at the within-plot level and related to the local canopy structure (Chapter 4).

(iii) Below-canopy water chemistry

In a following step, the seasonal evolution of throughfall and stemflow chemistry was studied at the plot level to determine the impact of canopy phenology on the fluxes of major ions to the forest floor (Chapter 5). Then, similarly to Chapter 3 on the amount of throughfall water, the spatial variability and temporal stability of throughfall chemistry was studied in relation to the local canopy structure (Chapter 6). Finally, total atmospheric deposition onto the beech canopy was estimated by modelling ion exchange between precipitation water and the canopy and by an inferential method (Chapter 7).

The thesis is concluded by a general discussion (Chapter 8), relating the main findings of the study and indicating perspectives for further research.

2 Bulk and wet-only precipitation at two adjacent sites

After: Staelens J., De Schrijver A., Van Aevermaet P., Genouw G. and Verhoest N. 2005.
A comparison of bulk and wet-only deposition at two adjacent sites in Melle (Belgium).
Atmospheric Environment 39, 7-15.

2.1 Abstract

During nine months, the weekly bulk and wet-only precipitation depositions in an urbanized region of Flanders (Belgium) were compared at two sites with a different height and separated by 1 km. The amount of rainfall at the two sites was similar, and the difference in ion deposition between the two sites was generally less than 5%. While the amount of rainfall measured was almost the same for both collector types, bulk deposition was significantly ($p < 0.02$) higher than wet-only deposition for all ions other than H^+ and NH_4^+ . Averaged for both sites, the bulk deposition exceeded the wet-only deposition by 129% (K^+), 84% (Ca^{2+}), 51% (Cl^-), 50% (Mg^{2+}), 46% (Na^+), 32% (SO_4^{2-}), 27% (NO_3^-), 17% (F^-), and 11% (NH_4^+). The acidity of bulk samples was significantly ($p < 0.06$) lower than the acidity of wet-only samples. Bulk concentrations of NH_4^+ were only significantly ($p < 0.002$) higher than wet-only concentrations at one site because of the sensor-related, delayed closing of the wet-only lid at the second site. Although dry deposition significantly contributed to bulk precipitation measurements, bulk deposition exceeded the wet acidifying deposition of NO_3^- , NH_4^+ , and SO_4^{2-} by less than 25%.

2.2 Introduction

Atmospheric deposition contributes to the chemistry of plants, soils, and surface waters, and to the cycling of nutrients in ecosystems (Richter and Lindberg, 1988). Therefore, the accurate quantification of wet, dry, and occult deposition is important for a wide range of ecological disciplines. Wet deposition is defined as the process by which atmospheric compounds are attached to and dissolved in cloud and precipitation droplets and delivered to the earth's surface by rain, hail or snow (Krupa, 2002). In theory, wet deposition is best measured using wet-only samplers, which are covered by a lid during dry periods and open whenever precipitation is detected by a sensor. As wet-only collectors have the drawback of being expensive and requiring a power supply, continuously open funnels or bulk collectors are often used to collect precipitation in ecological studies.

Differences in the chemical composition of precipitation collected by wet-only and bulk collectors have been assessed in a number of comparative studies (Table 2.1), and average correction factors for the contribution of dry deposition onto the funnels have been derived from parallel measurements. However, the amount of dry deposition onto bulk precipitation collectors depends on local gas and aerosol concentrations, turbulence intensities and the collection efficiency of the samplers (Draaijers *et al.*, 1998). Calcium, magnesium and potassium concentrations are often higher in bulk samples than in wet-only samples because of the deposition of soil-derived particles on the walls of the collectors during dry periods (Thimonier, 1998). Differences for nitrate, ammonium, and sulphate are usually smaller, but local or regional sources of emissions can significantly influence the composition of bulk samplers (Stedman *et al.*, 1990).

If bulk samplers are used to quantify precipitation chemistry, short-term parallel wet-only and bulk measurements are recommended to estimate site-specific correction factors for the contribution of dry deposition onto funnels (Draaijers *et al.*, 1998). To our knowledge, no comparison between bulk and wet-only deposition has been made for Flanders. However, acidifying deposition in the north of Belgium is known to be among the highest in Europe (UN/ECE, 2003), and dry deposition is estimated to account for 40-55% of the atmospheric sulphur deposition and 50-80% of the nitrogen deposition onto forest and heather vegetation in Flanders (VMM, 2002).

Table 2.1. Ratio of volume-weighted mean bulk and wet-only concentrations in precipitation, as measured at several locations throughout the world: reference, sampling interval (SI), and bulk over wet-only ratio per ion. Values in *italic* indicate a non-significant ($p > 0.05$) difference between bulk and wet-only ion concentration.

Location	Reference	SI ^a	H ⁺	Na ⁺	K ⁺	Ca ²⁺	Mg ²⁺	NH ₄ ⁺	NO ₃ ⁻	SO ₄ ²⁻	Cl ⁻
Leadville, USA	Ranalli <i>et al.</i> (1997)	w	0.65	2.03	1.67	1.64	2.55	<i>1.26</i>	1.29	1.51	1.57
Oak Ridge, USA	Richter and Lindberg (1988)	5-w	<i>1.04</i>	-	4.41	2.44	-	-	0.68	1.15	-
Hong Kong, China	Tanner (1999)	d	0.86	1.03	1.09	1.57	1.06	-	<i>0.99</i>	<i>1.01</i>	<i>1.01</i>
Kobe, Japan	Aikawa <i>et al.</i> (2003)	w	0.29	-	-	3.96 ^b	-	1.56	1.84	1.48 ^b	-
Toyo-oka, Japan	Aikawa <i>et al.</i> (2003)	w	0.53	-	-	1.73 ^b	-	1.36	1.19	1.16 ^b	-
Kaibara, Japan	Aikawa <i>et al.</i> (2003)	w	0.79	-	-	1.87 ^b	-	1.24	1.20	1.19 ^b	-
Delhi, India	Kulshrestha <i>et al.</i> (1995)	d	0.63 ^c	1.01 ^c	1.30 ^c	2.03 ^c	2.06 ^c	0.93 ^c	1.08 ^c	1.02 ^c	1.16 ^c
Istanbul, Turkey	Akkoyunlu and Tayanç (2003)	w	0.52 ^d	1.63 ^d	2.82 ^d	2.60 ^d	2.15 ^d	1.36 ^d	1.26 ^d	4.39 ^d	1.64 ^d
Pallanza, Italy	Mosello <i>et al.</i> (1988)	w	0.98	1.10	1.50	1.32	1.29	1.06	1.12	1.08	1.08
Manchester, UK	Lee and Longhurst (1992)	w	0.50	-	-	1.87	-	1.21	1.17	1.18	-
Esksdalemuir, UK	Stedman <i>et al.</i> (1990)	w	1.00	0.97	0.89	1.14	0.90	0.87	1.00	0.98	0.93
Stoke Ferry, UK	Stedman <i>et al.</i> (1990)	w	1.28	1.41	1.00	1.45	1.42	0.84	1.10	1.05	1.39
Ludlow, UK	Stedman <i>et al.</i> (1990)	w	1.09	1.93	1.33	1.86	1.88	1.12	1.36	1.23	1.88
Lough Navar, UK	Stedman <i>et al.</i> (1990)	w	0.83	0.99	0.94	1.18	0.99	0.60	0.85	0.94	1.01
Barcombe Mills, UK	Stedman <i>et al.</i> (1990)	w	1.22	1.35	1.53	1.76	1.29	1.00	1.30	1.36	1.33
Yarner Wood, UK	Stedman <i>et al.</i> (1990)	w	1.07	0.85	0.85	1.05	0.83	0.72	1.00	0.95	0.84
High Muffles, UK	Stedman <i>et al.</i> (1990)	w	0.97	1.14	1.22	1.37	1.13	0.92	1.04	0.99	1.10
Strathvaich Dam, UK	Stedman <i>et al.</i> (1990)	w	1.23	1.29	1.00	0.73	1.17	0.55	0.92	1.03	1.29
Glen Dye, UK	Stedman <i>et al.</i> (1990)	w	1.02	1.38	1.22	1.16	1.29	0.88	0.98	1.01	1.29
Ghent, Belgium	Present study	w	0.37	1.46	2.28	1.84	1.50	1.11	1.27	1.32	1.51

^a Sampling interval of bulk precipitation measurements: d: daily, w: weekly.

^b Non-marine fraction.

^c Significance of the difference between bulk and wet-only concentrations was not tested.

^d Ratio of arithmetic mean concentration of bulk and wet-only precipitation.

Bulk precipitation is sampled in the framework of the Pan-European network programme for intensive and continuous monitoring of forest ecosystems (ICP Forests; UN/ECE, 2004) and the data are, for example, used to quantify acidifying and eutrophying deposition onto forest vegetation. Precipitation is normally measured at a site in the open field located in the vicinity of the studied forest stand, instead of the rainfall being measured above the forest canopy. The aims of this chapter were therefore: (i) to assess the systematic bias on precipitation chemistry measured by using continuously open funnel collectors, and (ii) to compare the precipitation amount and chemistry measured at different heights at two sites separated by 1 km.

2.3 Materials and methods

2.3.1 Study site and meteorological conditions

Both bulk and wet-only precipitation were measured at two neighbouring sites (Fig. 2.1) in Melle (50°58' N, 3°49' E, 16 m a.s.l.) in the north of Belgium, ca. 60 km from the North Sea. Average precipitation between 1980 and 2002 was 755 mm yr⁻¹ and mean annual temperature was 10.2 °C (data of the Royal Meteorological Society of Belgium). Regional land use is a mixture of arable land and urban zones. At one site (site T), precipitation was collected on top of a 35-meter-high tower located in a mixed deciduous forest of 28 ha with a mean tree height of 27 m. The shortest distance from the tower to the forest edge is 60 m (Fig. 2.1). A cattle farm is located next to the forest.

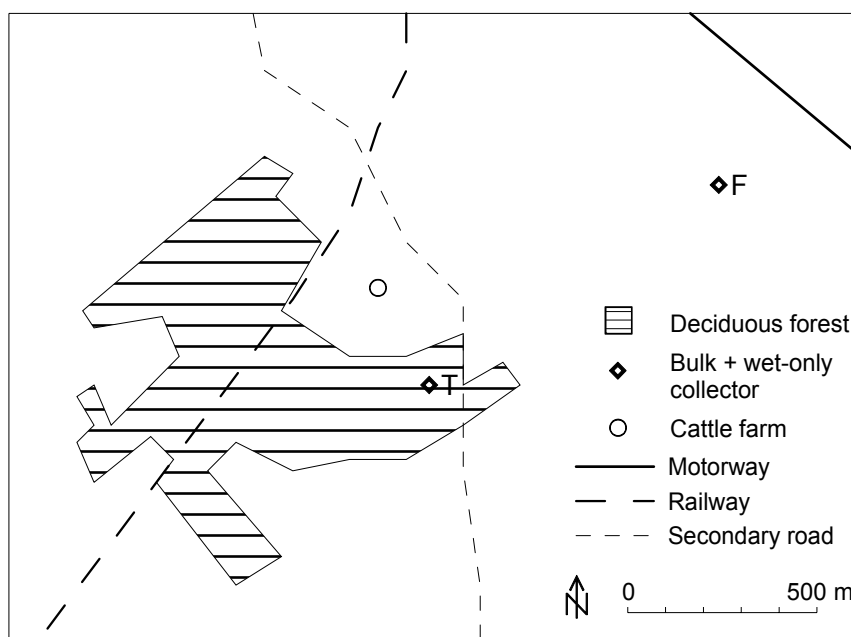


Fig. 2.1. Location of the tower (T) and field (F) site in Melle, Belgium.

The second site (site F) was located in the open field, on grass vegetation surrounded by meadows and arable land. One of the main motorways in Belgium is situated at a distance of about 250 m from the site (Fig. 2.1). Site F is a meteorological station of the Royal Meteorological Society of Belgium, and the amount of precipitation is measured at 10-minute intervals by a tipping bucket gauge. The chemical composition of bulk precipitation at site F has been measured since 1994 within the framework of ICP Forests (UN/ECE, 2004).

During 11 of the 40 measured weeks (4 March to 9 December 2003), the amount of weekly precipitation measured was less than 1 mm (Fig. 2.2). No snowfall occurred during the study period. Weekly average wind speeds at site F ranged from 1.7 to 4.6 m s⁻¹, with a nine-month average of 2.8 m s⁻¹. The main wind direction was southwest.

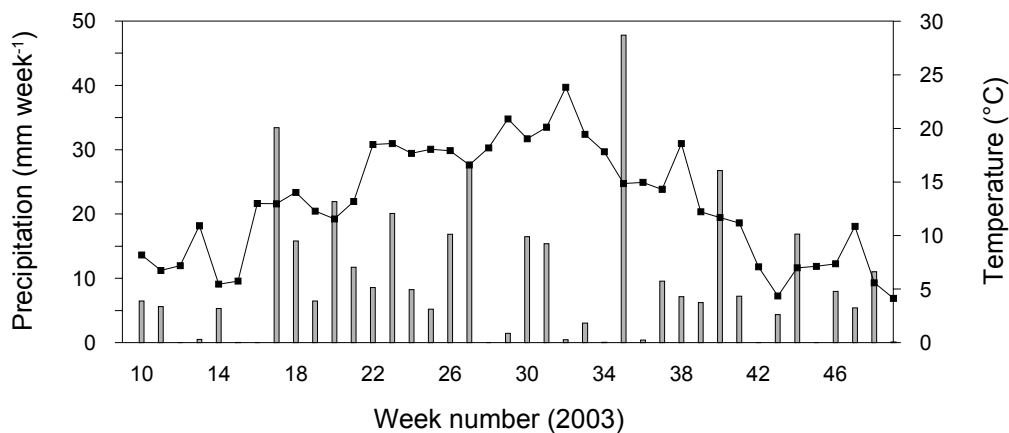


Fig. 2.2. Weekly precipitation (mm) and mean temperature (°C) at the field site.

2.3.2 Data collection

The quantity and chemistry of wet-only and bulk precipitation were measured weekly from 4 March to 9 December 2003. Wet-only precipitation was collected by automatic wet-only samplers (Eigenbrodt) with an orifice diameter of 25.4 cm, set at a height of 1.9 m. For site T, the actual height of the collecting surface was 36.9 m above ground level or 9.9 m above the mean stand height. Rainfall sensors with a delay time of 1 s activated the opening of the lid. An electrical, resistance-driven rain sensor (RS 85, Eigenbrodt) was used at site T and an optical sensor (IRSS 88, Eigenbrodt) at site F. Rainwater was stored in five-litre glass bottles that were refrigerated at a temperature of 4 °C. All parts of the collector that came into contact with rainwater were made of teflon, and were cleaned once every two weeks using demineralised water. The reproducibility of the wet-only sampling system has been tested thoroughly by means of paired measurements (VMM, 2002).

Bulk precipitation was collected using polyethylene funnels with a diameter of 24.2 cm, a sharp-edged vertical rim and a slope of 45°, set at a height of 1.5 m above ground level (36.5 m above ground level for site T). Two bulk precipitation collectors were used at site T and four bulk precipitation collectors at site F. A nylon wire mesh placed in the funnels prevented contamination by large particles. Funnels were supported by and drained into two-litre polyethylene bottles. At site F, collecting bottles were placed below ground level to avoid the growth of algae and to keep the samples cool. As placing below ground level was not possible at site T, bottles were wrapped in aluminium foil. Funnels, wire meshes, and bottles were replaced weekly with equipment that had been cleaned using demineralised water.

At both sites two passive samplers (Palmes tubes, Gradko, UK) were exposed in an open box to adsorb atmospheric ammonia (NH_3) during 4-week sampling periods. The passive samplers were installed at a height of 36.5 m above ground level (9.5 m above the mean stand height) at site T and at a height of 2 m above ground level at site F. The passive samplers adsorb NH_3 as NH_4^+ by phosphoric acid. Atmospheric NH_4^+ salts are not adsorbed since they cannot penetrate the sampler wall (Swaans and Aerts, 2004).

2.3.3 Chemical analysis and data quality

Rain samples were kept cool during transport, and stored in darkness at 4 °C in the laboratory. Water pH (pH meter CG841, Schott) and conductivity (Konduktometer CG855, Schott) were measured within one week after sampling. Anions (F^- , Cl^- , PO_4^{3-} , SO_4^{2-} , NO_3^- , NO_2^-) and cations (NH_4^+ , Na^+ , K^+ , Mg^{2+} , and Ca^{2+}) were determined using ion chromatography (Dionex DX300 and DX120) according to the ISO-10304 standard within one month after sampling. Ion chromatograph samples passed 20 μm and 5 μm in-line filters (Dionex) before analysis. H^+ concentrations were derived from pH measurements. Determination limits (DL, $\mu\text{mol}_c \text{ l}^{-1}$) of the chemical analyses were 5.7 (Na^+), 1.8 (K^+), 11 (Ca^{2+}), 1.7 (Mg^{2+}), 1.7 (NH_4^+), 1.0 (NO_3^-), 2.9 (SO_4^{2-}), 1.0 (Cl^-), 9.1 (PO_4^{3-}), 1.6 (F^-), and 1.1 (NO_2^-). The analytical accuracy was evaluated by checking the ion balance ($< 0.2 \text{ mmol}_c \text{ l}^{-1}$) and by comparing the measured and calculated conductivity of water samples. Phosphate concentration was below the DL in all measured rain samples, indicating that samples were not contaminated by bird droppings (Erisman *et al.*, 2003). Nitrite was below the DL in about 50% of the samples, and therefore the NO_2^- results have not been used. On the few occasions that K^+ and F^- concentrations were below the DL, the concentrations were assumed to be equal to half of the DL.

Within one week after exposure, the passive NH₃ samplers were desorbed with 10 ml ultrapure water, which was then analysed using spectrophotometry. For each sampling period two blank samplers were analysed. The average NH₃ concentration ($\mu\text{g m}^{-3}$) in each sampling period was calculated using an experimentally-determined sampling rate of $3.9 \text{ cm}^3 \text{ s}^{-1}$ (Swaans and Aerts, 2004). The relative standard deviation between the two samplers for each site and sampling period was generally below 5%. No correction was made for temperature or relative humidity.

2.3.4 Data analysis

Three methods were used to compare the weekly rainfall amounts and ion concentrations between collector types and sites. First, scatter plots of wet-only against bulk concentration measurements of each ion were visually inspected for both sites. Second, Wilcoxon signed rank tests were performed to test whether weekly rainfall amounts and ion concentrations were significantly different between collector types. This non-parametric test was used because according to the Shapiro-Wilk test the differences between the wet-only and bulk precipitation variables did not approximate a normal distribution ($p < 0.05$). Third, mean ion concentrations in bulk and wet-only samples were calculated as precipitation volume-weighted (vw) means, so as to account for the effect of precipitation amount on ion concentrations.

Pearson correlation coefficients were calculated between the variables in the wet-only data and the bulk data of both study sites together. The role of NH₄⁺, Ca²⁺, and Mg²⁺ in neutralizing rainwater acidity was validated by calculating neutralization factors as the ratio of the concentration ($\mu\text{mol}_e \text{ l}^{-1}$) of each ion to the sum of NO₃⁻ and SO₄²⁻ concentration ($\mu\text{mol}_e \text{ l}^{-1}$) (Kulshrestha *et al.*, 1995). The deposition of non-marine SO₄²⁻ was calculated using an equivalent SO₄²⁻:Na⁺ seawater ratio of 0.12 (Stedman *et al.*, 1990, VMM, 2002) and assuming that all deposited Na⁺ originated from seawater. A paired samples t-test was used to compare the atmospheric NH₃ concentrations between the two sites because according to the Shapiro-Wilk test the difference in concentration between the sites approximated a normal distribution ($p = 0.92$). All statistical analyses were performed using SPSS for Windows (SPSS Inc., 2003).

2.4 Results

2.4.1 Comparison of sites

Almost the same rainfall amounts were measured at both study sites (Table 2.2), and the Wilcoxon signed rank tests revealed no statistically significant differences. Over the study period, the total rainfall at site F was 0.7% higher for the wet-only samplers ($p = 0.76$) and 1.7% higher for the bulk samplers ($p = 0.21$) compared to site T. At site F, the wet-only rainfall was 2.1% lower and the bulk rainfall 1.4% lower than the rainfall amount measured by the Royal Meteorological Society of Belgium.

Table 2.2. Bulk and wet-only precipitation at two adjacent sampling sites: amount (mm) and volume-weighted (vw) mean pH (-) and ion concentrations ($\mu\text{mol}_e \text{ l}^{-1}$), ratio of the vw mean bulk and wet-only concentrations, and significance of the difference between bulk and wet-only concentrations (Wilcoxon signed rank test).

	Site T (tower)				Site F (field)			
	Wet	Bulk	Ratio	Sign.	Wet	Bulk	Ratio	Sign.
Water	382.1	381.2	1.00	0.310	384.8	387.7	1.01	0.765
pH ^a	5.19	5.45	-	0.082	5.00	5.58	-	0.002
H ⁺	6.51	3.55	0.54	0.061	10.08	2.61	0.26	0.001
Na ⁺	36.98	56.04	1.52	< 0.001	37.49	52.83	1.41	0.016
K ⁺	1.96	4.27	2.18	< 0.001	1.93	4.61	2.39	< 0.001
Ca ²⁺	26.87	48.90	1.82	< 0.001	25.06	46.59	1.86	< 0.001
Mg ²⁺	9.25	14.32	1.55	< 0.001	9.43	13.65	1.45	< 0.001
NH ₄ ⁺	65.65	68.98	1.05	0.370	62.16	72.93	1.17	0.002
NO ₃ ⁻	31.26	39.77	1.27	< 0.001	30.62	38.81	1.27	< 0.001
Cl ⁻	33.37	51.99	1.56	< 0.001	33.70	49.06	1.46	< 0.001
SO ₄ ²⁻	47.32	61.47	1.30	< 0.001	44.79	59.68	1.33	< 0.001
F ⁻	1.59	2.15	1.35	< 0.001	1.48	1.97	1.32	< 0.001

^a pH-values were calculated as the negative logarithm of the corresponding mean vw H⁺ concentrations.

The composition of rainfall was similar at both sites (Table 2.2). Volume-weighted (vw) mean ion concentration generally differed by less than 5% between the two sites and always by less than 10%, except for H⁺. For the wet-only samples, vw mean H⁺ concentration was 35% lower at site T than at site F, whereas the bulk H⁺ concentration was on average 35% higher at site T. According to the Wilcoxon tests, weekly wet-only concentrations of NH₄⁺ and NO₃⁻ were significantly ($p < 0.05$) higher at site T than at site F. Bulk NH₄⁺ concentration was lower at site T, but not significantly ($p = 0.44$). Finally, bulk rainfall concentrations differed significantly ($p < 0.05$) between sites for H⁺, NO₃⁻, Cl⁻, and F⁻.

2.4.2 Comparison of sampling devices

Almost the same rainfall amounts were measured for both collector types (Table 2.2). Over the study period, the wet-only sampler collected 0.2% more rainfall than the bulk sampler at site T ($p = 0.31$) and 0.7% less than the bulk sampler at site F ($p = 0.72$).

According to the Wilcoxon signed rank tests, weekly bulk rainfall concentrations were significantly ($p < 0.02$) higher than wet-only concentrations for all ions, except for NH_4^+ and H^+ (Table 2.2). Although the NH_4^+ concentrations were higher in bulk rainfall than in wet-only rainfall at both sites, the difference between the two collector types was only significant ($p = 0.002$) at site F (Fig. 2.3). In contrast to all other ions, H^+ concentrations were significantly ($p < 0.06$) lower in bulk rainfall than in wet-only rainfall.

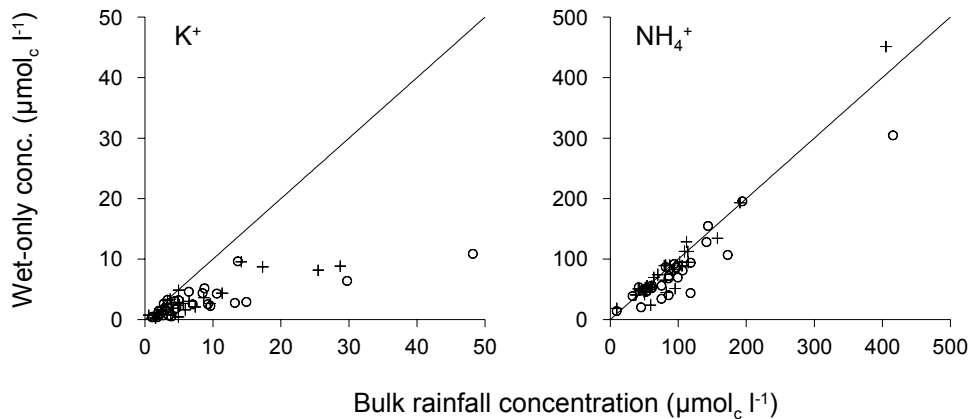


Fig. 2.3. Weekly ($n = 29$) bulk and wet-only rainfall concentration ($\mu\text{mol}_c \text{l}^{-1}$) of K^+ and NH_4^+ at the tower site (+) and the field site (o). The diagonal line indicates the 1:1 ratio.

The calculated vw mean ion concentrations were higher in bulk rainfall than in wet-only rainfall for all ions except H^+ , in agreement with the Wilcoxon tests. The greatest difference was found for K^+ , for which the vw mean bulk concentration was 2.2 times higher than the wet-only concentration at site T, and 2.4 times higher at site F (Table 2.2). Arranged according to decreasing concentration ratios of bulk over wet-only rainfall, the ion order was K^+ , Ca^{2+} , Cl^- , Mg^{2+} , Na^+ , SO_4^{2-} , NO_3^- , NH_4^+ , and H^+ .

High and significant ($p < 0.001$, $n = 58$) Pearson correlation coefficients were found in wet-only and bulk precipitation of both sites between the concentration of Na^+ and Cl^- ($r > 0.97$), and between NH_4^+ , NO_3^- , and SO_4^{2-} ($r > 0.92$). Calcium was more strongly correlated with K^+ ($r = 0.92$) and SO_4^{2-} ($r = 0.95$) in the bulk precipitation than in the wet-only precipitation ($r = 0.65$ and 0.85 , respectively). Magnesium, on the other hand, was more strongly correlated

with Na^+ ($r = 0.97$) and Cl^- ($r = 0.97$) in the wet-only precipitation than in the bulk precipitation ($r = 0.82$ and 0.82 , respectively). All concentrations were significantly ($p < 0.05$) negatively correlated with the precipitation amount, except for pH and H^+ , and Cl^- in the wet-only data, for which no significant correlations were found. The values of the neutralization factor (Kulshrestha *et al.*, 1995) for NH_4^+ , Ca^{2+} , and Mg^{2+} were 0.83, 0.34, and 0.12 in the wet-only samples and 0.71, 0.48, and 0.14 in the bulk samples, respectively.

2.4.3 Atmospheric NH_3 concentration

The average NH_3 concentration measured by the passive samplers over the study period was $5.6 \mu\text{g NH}_3 \text{ m}^{-3}$ at site T, which was significantly lower ($p = 0.031$) than the concentration of $6.2 \mu\text{g NH}_3 \text{ m}^{-3}$ at site F. There was a seasonal variation in atmospheric NH_3 concentration, with peaks in March and August (Fig. 2.4).

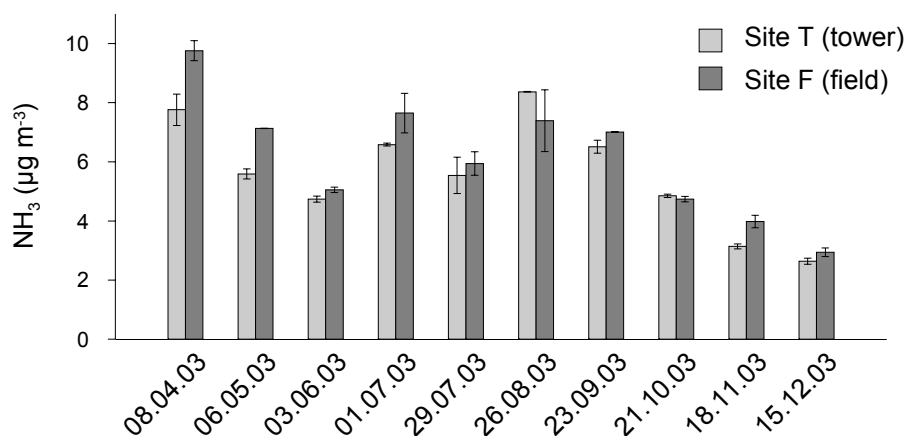


Fig. 2.4. Atmospheric NH_3 concentration measured by passive samplers during 4-weekly periods at two adjacent sites. The error bars indicate standard deviations ($n = 2$).

2.4.4 Wet and bulk precipitation deposition

As the measured precipitation amount was almost equal for both collector types, the bulk:wet-only deposition ratios equal the bulk:wet-only vw mean concentration ratios (Table 2.2). Averaged for both sites, bulk deposition was 129% (K^+), 84% (Ca^{2+}), 51% (Cl^-), 50% (Mg^{2+}), 46% (Na^+), 32% (SO_4^{2-}), 27% (NO_3^-), 17% (F^-), and 11% (NH_4^+) higher than wet-only deposition, while the bulk deposition of H^+ was 60% lower. Over the 9-month study period, the wet acidifying deposition of SO_4^{2-} , NO_3^- , and NH_4^+ was $55.1 \text{ mmol}_c \text{ m}^{-2}$ at site T and $52.9 \text{ mmol}_c \text{ m}^{-2}$ at site F. The bulk acidifying deposition was $64.9 \text{ mmol}_c \text{ m}^{-2}$ at site T and $66.5 \text{ mmol}_c \text{ m}^{-2}$ at site F. This calculation of potentially acidifying deposition takes into account

the microbial transformation of reduced nitrogen (NH_x) to nitrate with the resultant release of a hydrogen ion.

2.5 Discussion

2.5.1 Rainfall amount

The collection efficiency of a precipitation sampler is determined by the disturbance of the airflow over and around the collector, height above the ground, evaporation of collected rainwater, and, in the case of a wet-only collector, the efficiency of the rain sensor (Stedman *et al.*, 1990). In general, wet-only devices are reported to collect less precipitation than other samplers, which is commonly attributed to their higher aerodynamic blockage. In the United Kingdom, for example, the collection efficiency of nine wet-only collectors relative to bulk collectors ranged from 71 to 92% and generally decreased with increasing wind speed at the site (Stedman *et al.*, 1990). Yet, in the present study, the total amount of rainfall collected by bulk and wet-only devices differed by less than 1%. This might be due to the relatively low wind speeds at the sites. With respect to sensor sensitivity, no delayed opening of the wet-only lid was observed in the field, even at low rainfall intensities.

Elevated gauges may underestimate precipitation amounts due to the modification of airflow around the gauge, particularly when wind speeds are high and raindrop size is small (Allerup *et al.*, 1997; Crockford and Richardson, 2000). Nevertheless, no significant differences were found between the total amount of rainfall measured above the canopy and at the adjacent field site, in agreement with other studies (e.g., Lloyd *et al.*, 1988; Loustau *et al.*, 1992; Aboal *et al.*, 1999).

2.5.2 Deposition of Na^+ , K^+ , Ca^{2+} , Mg^{2+} , and Cl^-

The greatest difference between bulk and wet-only precipitation collectors was found for the neutral or so-called ‘base’ cations and for Cl^- , with mean concentration ratios of bulk:wet-only rainfall of 2.3 for K^+ , 1.8 for Ca^{2+} , and 1.5 for Mg^{2+} , Na^+ , and Cl^- . Therefore during the study period, dry deposition of sedimenting particles onto the bulk samplers contributed between 50 and 130% of the bulk deposition of base cations and Cl^- , depending on the ion. These findings correspond well to previously reported research (Table 2.1). However, it should be noted that a considerable variation in bulk:wet-only ratios has been observed, depending on sampler type, location, meteorological circumstances, and sampling interval. The variability in bulk:wet-only ratios is usually smaller between ions than between locations,

which suggests that the dry deposition rate of cations is influenced more by local circumstances than by the ion concerned. Similarly, in a Canadian study (Houle *et al.*, 1999b), regression analysis suggested that the wet:dry ratio of Na^+ was the same for the other base cations.

The high correlation between Cl^- and Na^+ or Mg^{2+} in the precipitation indicates a common source, i.e. marine. Ca^{2+} and K^+ had a stronger correlation in bulk than in wet-only samples, which confirms that both cations readily undergo dry deposition and mainly originate from the same source, i.e. soil particles (Akkoyunlu and Tayanç, 2003). No difference in base cation deposition by rainfall was found between sites at a different height. This is in contrast to Kulshrestha *et al.* (1995), who found that the mean Ca^{2+} and Mg^{2+} concentrations in India were 122% and 68% higher for bulk collectors at a height of 13 m than at a height of 30 m.

2.5.3 Deposition of NH_4^+ , NO_3^- , SO_4^{2-} , F^- , and H^+

Bulk deposition of NO_3^- , SO_4^{2-} , and F^- was 30% higher ($p < 0.001$) than wet-only deposition, while the bulk H^+ deposition was significantly ($p < 0.06$) lower than the wet-only deposition. Although the measured atmospheric NH_3 concentrations were relatively high (Walker *et al.*, 2004), almost all NH_4^+ collected by bulk samplers was the result of wet deposition.

The most pronounced differences between sites were found for NH_4^+ and H^+ . Scatter plots showed that the weekly bulk concentration of NH_4^+ generally was higher than the wet-only concentration at both sites (Fig. 2.3). However, the difference between bulk and wet-only NH_4^+ concentration was only significant ($p = 0.002$) at the field site (Table 2.2) due to the significantly ($p < 0.05$) lower wet-only deposition and the higher bulk deposition at the field site compared to the tower site. The higher bulk deposition of NH_4^+ at the field site suggests a higher dry deposition of NH_4^+ onto bulk funnels. This is in line with the significantly ($p < 0.05$) higher atmospheric NH_3 concentrations at the field site (Fig. 2.4), which is surrounded by manured fields. The significantly higher wet-only NH_4^+ deposition at the tower site than at the field site was most probably due to different rainfall sensors being used at the two sites. While the optically-driven wet-only lid at the field site was closed immediately after rain events, the electrical, resistance-driven lid at the tower site remained opened for a longer time (until 15 minutes) after rain events. As the highest dry deposition rates of NH_3 (Cape and Leith, 2002) and particles (Ruijgrok *et al.*, 1997) are obtained for wet surfaces, this longer opening time probably resulted in a higher dry deposition of NH_3 and NH_4^+ particles onto the wet-only collector after rain events. Mean wet-only concentrations of SO_4^{2-} and NO_3^- were

also higher at the tower site than at the field site.

Cape and Leith (2002) experimentally found that the amount of SO_2 deposited on wet funnel surfaces was closely related to the amount of NH_3 deposited. This was mainly attributed to the oxidation of dissolved SO_2 , which retains dissolved NH_3 as involatile $(\text{NH}_4)_2\text{SO}_4$ salts as the water evaporates. Co-deposition of NH_4^+ and SO_4^{2-} is also suggested in the present study by the high correlation between the concentration of these ions in bulk deposition. However, other SO_4^{2-} containing salts than $(\text{NH}_4)_2\text{SO}_4$ may be deposited onto funnel surfaces (Cape and Leith, 2002), which explains why the measured bulk:wet-only ratios were higher for SO_4^{2-} than for NH_4^+ . Ammonium, SO_4^{2-} , and NO_3^- mainly originate from anthropogenic sources (Tanner, 1999). Assuming that all deposited Na^+ originates from seawater, non-marine SO_4^{2-} contributed 90% of the wet SO_4^{2-} deposition.

The acidity of a rainwater sample is determined by the balance of the anions and other cations present. This is demonstrated by plotting pH as a function of the equivalent concentration ratio of $(\text{NH}_4^+ + \text{Ca}^{2+} + \text{Mg}^{2+})$ to $(\text{SO}_4^{2-} + \text{NO}_3^-)$ (Fig. 2.5). The calculated neutralization factors indicate that NH_4^+ was the main acid-neutralizing ion. Therefore, the difference in NH_4^+ concentration between sites for similar collecting devices explains most of the difference in H^+ concentration between sites (Table 2.2). The hydrogen concentrations in bulk rainfall were significantly ($p < 0.06$) lower than in wet-only rainfall. The neutralization factors show that the lower H^+ concentration in the bulk rainfall compared to the wet-only rainfall was mainly due to the extra reduction of acidity by dry deposited Ca^{2+} compounds (Lee and Longhurst, 1992).

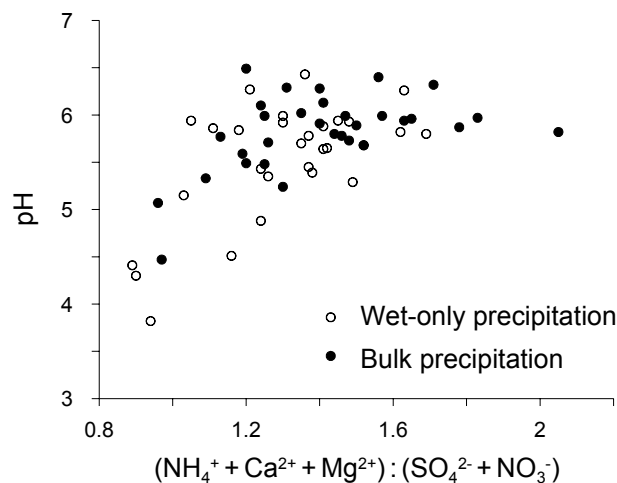


Fig. 2.5. Wet-only and bulk precipitation pH at the field site in relation to the ratio of equivalent $(\text{NH}_4^+ + \text{Ca}^{2+} + \text{Mg}^{2+}) : (\text{SO}_4^{2-} + \text{NO}_3^-)$ precipitation concentrations.

2.5.4 Impact of temporal rainfall distribution on deposition

The summer of 2003 was exceptionally dry (cf. Ciais *et al.*, 2005; Leuzinger *et al.*, 2005). During the 9-month period 382 mm precipitation was collected, which is only 63% of the average 1980-2002 amount of 606 mm for this period and location (data of the Royal Meteorological Society of Belgium). The low precipitation amount explains why wet deposition of ions was relatively low compared to other years. Dry deposition fluxes can vary considerably, depending on the nature and position of the receptor surfaces and on the meteorological conditions. Dry deposition onto bulk funnels depends on how long and how often funnel surfaces are wetted (Cape and Leith, 2002). Therefore, the occurrence of 25% of dry weeks combined with the weekly replacement of bulk samplers by clean equipment has probably resulted in an underestimation of the dry deposition onto bulk precipitation funnels. In other words, the bulk:wet-only ratios presented are conservative estimates, and in years with higher precipitation amounts, the systematic bias on precipitation composition measured by bulk funnels might be higher.

2.6 Conclusions

Bulk deposition was 30 to 130% higher ($p < 0.02$) than the wet deposition of all major ions, with the exception of NH_4^+ . The acidity of bulk precipitation was significantly ($p < 0.06$) lower than the acidity of wet-only precipitation. Therefore, wet-only samplers are preferred for accurately determining wet deposition fluxes. Alternatively, bulk measurements should be corrected for dry deposition onto the funnels by site-specific bulk over wet-only factors. The chemistry of wet-only precipitation was almost identical at the two study sites with different heights that were located about 1 km from each other. A small but significant difference in wet-only deposition between the sites was only found for NH_4^+ and NO_3^- , which could be attributed to the delayed closing of the wet-only lid by the electrical, resistance-driven rain sensor at one site. The measured bulk:wet-only ratios show that the major fraction of the ions measured in bulk rainwater samples was removed from the atmosphere by wet deposition rather than by dry deposition, except for K^+ . Bulk deposition exceeded the wet acidifying deposition of SO_4^{2-} , NO_3^- , and NH_4^+ by less than 25%. Yet, bulk collectors do not provide reliable estimates of the total wet and dry deposition, as the collection efficiency of bulk samplers for gases and particles is substantially different from that of a natural landscape.

3 Rainfall partitioning into throughfall, stemflow, and interception: influence of foliation, rain event characteristics, and meteorology

After: Staelens, J., De Schrijver, A., Verheyen, K. and Verhoest, N.E.C. Rainfall partitioning into throughfall, stemflow, and interception within a single beech (*Fagus sylvatica* L.) canopy: influence of foliation, rain event characteristics, and meteorology. Hydrological Processes, accepted with minor revisions.

3.1 Abstract

While the hydrological balance of forest ecosystems has often been studied at the annual level, quantitative studies on the factors determining rainfall partitioning of individual rain events are less frequently reported. Therefore, the effect of the seasonal variation in canopy cover on rainfall partitioning was studied for a mature deciduous beech (*Fagus sylvatica* L.) tree over a 2-year period. At the annual level, throughfall was 71% of precipitation, stemflow 8%, and interception 21%. Rainfall partitioning at the event level depended strongly on the amount of rainfall and differed significantly ($p < 0.001$) between the leafed and the leafless period of the year. Therefore, water fluxes of individual rain events ($n = 205$) were described using a multiple regression analysis with foliation, rain event characteristics and meteorological variables as predictor variables. For a given amount of rainfall, foliation significantly increased interception and decreased throughfall and stemflow amounts. In addition, rainfall duration, maximum rainfall rate, vapour pressure deficit, and wind speed significantly affected rainfall partitioning at the event level. Increasing maximum hourly rainfall rate increased throughfall and decreased stemflow generation, while higher hourly vapour pressure deficit decreased event throughfall and stemflow amounts. Wind speed decreased throughfall in the growing season only. Since foliation and the event rainfall amount largely determined interception loss, the observed net water input under the deciduous canopy was sensitive to the temporal distribution of rainfall.

3.2 Introduction

The interception of precipitation by vegetation and subsequent evaporation during and after rain events is an important component of the hydrological budget of terrestrial ecosystems, and is, particularly in forest ecosystems, a significant component of evapotranspiration (Crockford and Richardson, 2000). Net precipitation, which is the amount of water that reaches the forest floor, consists of throughfall and stemflow. Throughfall reaches the ground directly through gaps in the canopy cover or as canopy drip, while stemflow flows down tree boles. As direct measurement of the intercepted precipitation fraction is complicated (Teklehaimanot and Jarvis, 1991; Bouten *et al.*, 1996), interception is commonly calculated as the difference between gross precipitation measured above the canopy or in an adjacent open area and net precipitation sampled on the forest floor.

Rainfall partitioning in forest stands is a function of rainfall characteristics, meteorological conditions, vegetation structure, and the interaction between these factors (Rutter and Morton, 1977; Gash, 1979; Crockford and Richardson, 2000; Xiao *et al.*, 2000b). Firstly, rainfall partitioning is affected by the amount, intensity, and duration of rainfall and the temporal distribution of rain events. Throughfall and stemflow are often strongly correlated with the amount of rainfall (Bellot and Escarre, 1998; Marin *et al.*, 2000; Xiao *et al.*, 2000b; Huber and Iroumé, 2001; Iroumé and Huber, 2002). Rainfall of high intensity and short duration may yield higher net precipitation input than events of low intensity and long duration (Bellot and Escarre, 1998). The temporal distribution of precipitation affects the number of canopy wetting and drying cycles (Link *et al.*, 2004), and thus, for a given number of rain hours, interception is greater if rainfall is not continuous (Rutter and Morton, 1977; Zeng *et al.*, 2000). Secondly, meteorological conditions control the evaporation rate of the intercepted water that is temporarily stored on the leaves, branches, and trunks. Consequently, the amount of net precipitation is affected by wind speed, air humidity deficit (Rutter and Morton, 1977; Teklehaimanot and Jarvis, 1991) and net radiation (Klaassen, 2001). Thirdly, interception depends on forest structure characteristics such as species composition (Aussenac and Boulangeat, 1980), stand age, basal area (Forgeard *et al.*, 1980), stand density (Peck and Mayer, 1996), spatial distribution of trees (Teklehaimanot and Jarvis, 1991), leaf area index (Marin *et al.*, 2000), branch angle (Huber and Iroumé, 2001), and leaf shape (Crockford and Richardson, 2000). Tree species also differ in hydrophobicity or water repellency of leaf and wood (Herwitz, 1985). The review of Crockford and Richardson (2000) illustrates that it is difficult to draw general conclusions about interception by a particular forest type because of

the combined effect of several tree and stand characteristics and the dependency on climatic conditions. For modelling rainfall interception, forest structure is generally described by canopy cover and storage capacity (Rutter and Morton, 1977; Gash, 1979; Davie and Durocher, 1997; Liu, 1997).

In deciduous forests, rainfall partitioning is more affected by the period of the year than in coniferous forests (Augusto *et al.*, 2002). During the leafed growing season, net precipitation is generally smaller and stemflow constitutes a smaller part of the net precipitation than during the leafless dormant season (Levia and Frost, 2003). However, to assess the effect of a forest canopy on rainfall partitioning, it is important to separate the effect of seasonal changes in rainfall characteristics and meteorological conditions from the effect of the variation in canopy structure throughout the year.

The relationship between precipitation and interception depends on the temporal scale considered (Llorens *et al.*, 1997), and data obtained over a longer period cannot be extrapolated to a shorter scale. Consequently, measurements at the scale of individual rain events are recommended for examining rainfall redistribution (Whelan and Anderson, 1996). Although many studies have quantified annual hydrological balances in forest ecosystems, event-based studies are less frequently reported, particularly for broadleaved deciduous forests (Hörmann *et al.*, 1996). Therefore, the aims of this chapter were (i) to quantify the partitioning of rainfall into throughfall, stemflow, and interception under a deciduous beech tree at the individual rain event scale, and (ii) to determine the influence of foliation, rainfall characteristics, and meteorological variables on rainfall partitioning.

3.3 Materials and methods

3.3.1 Study site

The Aelmoeseneie forest (50°58' N, 3°49' E, 16 m a.s.l.) is a mixed deciduous forest near Ghent in the north of Belgium, ca. 60 km from the North Sea. The forest has a total area of 28 ha and the dominant trees are about 85 years old. Mean annual precipitation (1980-2002) is 755 mm, and mean annual temperature is 10.2 °C. The study plot is located in a forest stand dominated by pedunculate oak (*Quercus robur* L.) and European beech (*Fagus sylvatica* L.). Stand density was 345 trees ha⁻¹ in 1997, and mean canopy height was 27 m (Vande Walle *et al.*, 1998). Pedunculate oak and beech represent 49% and 27% of the total basal area of 26.6 m² ha⁻¹, respectively. The understory consists of rowan (*Sorbus aucuparia* L.), hazel (*Corylus avellana* L.), and maple (*Acer pseudoplatanus* L.). Maximum leaf area index during the 1996

growing season was 5.5 (Mussche *et al.*, 2001). The forest soil has developed from a quaternary layer of sand loam (0.5 -1 m) on a shallow impermeable clay and sand complex of tertiary origin. According to the Belgian soil legend, the soil is classified as is a strongly gleyic sandy loam soil with a structural B-horizon and a clay substratum starting at 60 cm depth. In the World Reference Base (ISSS-ISRIC-FAO, 1998) the soil is classified as a Gleyic Cambisol. The forest stand contains a Level II observation plot of the Pan-European network programme for intensive monitoring of forest ecosystems (UN/ECE, 2004), and throughfall and stemflow water have been measured at the plot level since 1994.

In the oak-beech stand one dominant beech tree¹ was chosen with a diameter at breast height (1.3 m) of 0.68 m and a height of 30 m. The studied tree was surrounded by several pedunculate oaks, an American red oak (*Quercus rubra* L.), and a beech tree (Fig. 3.1). The understory layer was removed in the research plot of 15 x 12 m² to determine solely the effect of the tree crown on rainfall redistribution. The beech trees at the study site were leafless from 8 November 2002 to 25 April 2003 and from 18 November 2003 to 22 April 2004.

3.3.2 Data collection

3.3.2.1 Throughfall and stemflow

From 17 May 2002 to 16 May 2004, the amount of throughfall water (TF) was sampled using 20 tipping bucket rain gauges with a funnel diameter of 24.2 cm (460 cm²) placed in a 3 x 3 m grid (Fig. 3.1). The output of the tipping buckets was recorded by a data logger system (Campbell Scientific Inc.) with a temporal resolution of 5 minutes. The funnels were set at a height of 1.5 m and had a sharp-edged vertical rim and a slope of 45°. The resolution of the self-constructed tipping buckets, determined by repeated dynamic calibration, was approximately 0.2 mm per tip. Stemflow from the beech tree was collected by a spiral type gauge and measured by means of a self-constructed tipping bucket with bucket content of 0.2 l. As a check, the outflow was collected in a 200 l container, which was read and emptied at least weekly. Stemflow volume was transformed to depth (mm) using the surface area of the horizontal canopy projection, which was approximately 180 m².

¹ According to the inventory and mapping of the scientific area of the Aelmoeseneie forest (Vande Walle *et al.*, 1998), the studied beech tree was tree number 472 with coordinates $x = 101.9$ m , $y = 66.9$ m.

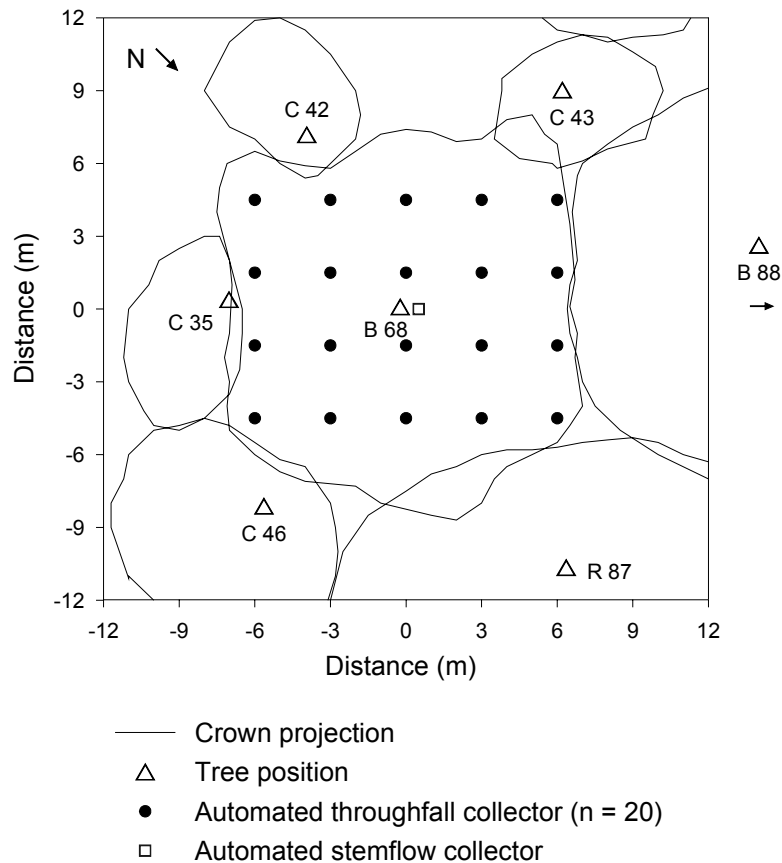


Fig. 3.1. Experimental setup in the Aelmoeseneie forest, Gontrode (Belgium) to measure the partitioning of rainfall. Tree labels indicate tree species (C: common oak, B: European beech, R: American red oak) and diameter (cm) at 1.3 m height.

3.3.2.2 Precipitation

In the forest stand a 36 m high meteorological tower was installed at a distance of 50 m from the study plot (Samson and Lemeur, 2001). Precipitation was measured on top of the tower using two tipping bucket rain gauges with a resolution of about 0.2 mm. In addition, from 11 November 2002 onwards, two manual rain gauges on top of the tower were read and emptied weekly. One self-registering rain gauge (Delta-T-Devices) had a funnel diameter of 25.0 cm (491 cm²). The other tipping bucket was self-constructed and identical to the TF collectors, with a funnel diameter of 24.2 cm (460 cm²). The two manual collectors consisted of identical funnels as the self-constructed collectors (24.2 cm diameter) that drained into 2-l bottles. The output of the self-constructed tipping bucket was recorded by the TF data logger system (Campbell Scientific Inc.), whilst the output of the Delta-T-Devices tipping bucket was recorded by a second data logger system (HP 75000 and HP 34970). The accuracy of the tipping buckets was confirmed by the linear regression between event rainfall amounts (≥ 1 mm) measured by the self-constructed device and the Delta-T device, as the coefficients did

not differ significantly from zero intercept (0.004 ± 0.033 , mean \pm standard error) and unit slope (1.002 ± 0.004) ($r^2 = 0.997$; paired t-test $p = 0.430$; $n = 188$).

3.3.2.3 Meteorological data

Net radiation (REBS) was measured at 36 m height, as well as incoming and reflected short-wave solar radiation (Delta-T-Devices). At 1, 8, 15, 22, 29 and 36 m above soil level, air temperature was measured with shielded (aluminium housing) Pt100 sensors. Relative air humidity was measured at 22 and 29 m using ventilated, shielded psychrometers (Vector Instruments). Wind speed was measured using a 4-cup anemometer (Delta-T-Devices) at 29 m and wind-direction was measured at 36 m (Delta-T-Devices). Leaf wetness sensors (ELE International) were installed at two heights in the canopy (15 and 22 m) to monitor the surface wetness status of the leaves. All above-canopy meteorological readings were measured every 10 s, and stored at 10 min steps by a data logger (HP 75000 and HP 34970).

3.3.3 Data analysis

3.3.3.1 Data handling and data exploration

Interception loss (I) was calculated by subtracting plot-average throughfall (TF) and stemflow (SF) from the above-canopy precipitation (P). This chapter focuses on the plot-average ($n = 20$) TF water amount whereas the spatial variability of TF will be discussed in Chapter 4. Rainfall partitioning was studied at the event level using the tipping bucket data. A rainfall event was defined as a period with more than 1 mm of total rainfall. Two subsequent events were separated in the data analysis when both leaf wetness sensors were dry for at least one hour, indicating complete drying of the canopy foliage. This separation of events generally corresponded to differentiating between individual events based on a lack of precipitation for at least 4 h (e.g., Xiao *et al.*, 2000b). Rainfall event duration was calculated as the time between the first and last recorded tipping bucket measurement of a rainfall event. Six snow events occurred during the study period, which were excluded from the analyses at the event level. To calculate the total water input, snowfall amounts were estimated as the maximum TF amount measured during the events because of the undercatch of above-canopy snowfall measurements (Allerup *et al.*, 1997). Potential evaporation from wet surfaces was calculated by the Penman-Monteith equation (Monteith, 1965) with canopy resistance set to zero using the 10-min meteorological measurements above the canopy. The aerodynamic resistance was calculated from the measured wind speed (Dolman, 1986) with zero plane displacement and

surface roughness length set to 80% and 10% of the stand height, respectively (Herbst *et al.*, 1999; Samson and Lemeur, 2001).

Rainfall events were initially divided into four canopy development phases, i.e. leaf emergence, fully leafed period, leaf senescence, and leafless period. After inspection of the I-P relationship, as discussed in section 3.4.2, two canopy development stages were retained: the leafed and the leafless season. Rain events during leaf emergence and leaf senescence were included into the leafed season, except for the last week of leaf senescence, which was included into the leafless season because only few leaves were present at that time.

Rainfall characteristics and meteorological conditions during rain events (Table 3.1) were compared between the leafed and leafless seasons with the Wilcoxon rank sum test, and Spearman correlations coefficients (r_s) were calculated between the event variables. Non-parametric tests were used because according to the Shapiro-Wilk test the distribution of all rainfall and meteorological variables at the event level, except temperature, deviated significantly ($p < 0.01$) from normality.

Table 3.1. Event rainfall characteristics and meteorological conditions measured at the study site, and their median values during individual rain events in the leafed ($n = 115/103$) and leafless ($n = 95/85$) seasons. Bold values within rows are significantly ($p < 0.05$) higher according to a Wilcoxon rank sum test.

Variable	Symbol	Unit	Median value		Sign.
			Leafed ($n = 115$)	Leafless ($n = 95$)	
Rainfall characteristic of events			($n = 115$)	($n = 95$)	
Amount of rainfall	P	mm event ⁻¹	3.60	3.67	0.804
Duration of rainfall	D	h	5.50	8.50	0.011
Average rainfall intensity	R	mm h ⁻¹	0.80	0.58	0.010
Maximum 10-min rainfall intensity	R ₁₀	mm h ⁻¹	4.16	3.12	0.002
Maximum 60-min event intensity	R ₆₀	mm h ⁻¹	1.56	1.39	0.075
Meteorological conditions during events			($n = 103$)	($n = 85$)	
Average wind direction	WD	° from north	224	187	0.026
Average wind speed	V	m s ⁻¹	1.36	2.36	0.000
Maximum 10-min wind speed	V ₁₀	m s ⁻¹	2.49	4.04	0.000
Net radiation	NR	W m ⁻²	19.08	-1.04	0.000
Air temperature (29 m)	T	°C	13.24	6.84	0.000
Vapour pressure deficit (29 m)	VPD	kPa h ⁻¹	0.44	0.31	0.010
Potential evaporation rate	E _{pot}	mm h ⁻¹	0.31	0.40	0.051
Duration of antecedent dry period	DDP	d	0.92	0.64	0.134

3.3.3.2 Regression analysis

First, for all events during the study period in which $P \geq 1$ mm, linear regressions (SPSS Inc., 2003) were calculated between the amount of P and the amount of TF, SF, and I (mm event^{-1}):

$$Y = a_0 + a_1 \cdot P \quad (3.1)$$

where $Y = \text{TF, SF, or I}$. Only regression coefficients significant at $p < 0.01$ were retained. It should be noted that these regressions are only meaningful, i.e. lead to positive values for Y, when P is larger than $-a_0/a_1$. Next, the relationships between Y and P were quantified for events in the leafed and leafless seasons separately. To test directly whether regression coefficients a_0 and a_1 differed significantly between the two seasons of the year, a so-called dummy variable ‘foliation’ (F) (Neter *et al.*, 1996) was added to Eq. 3.1, and the following multiple linear regressions were computed by adding and removing the independent variables stepwise forward (SPSS Inc., 2003):

$$Y = (a_0 + a_1 \cdot F) + (a_2 + a_3 \cdot F) \cdot P \quad (3.2)$$

where $F = 0$ in the leafless season and $F = 1$ in the leafed period. Then, for determining the actual effect of foliation on rainfall partitioning, each rainfall or meteorological variable X (Table 3.1) was added individually to Eq. 3.2:

$$Y = (a_0 + a_1 \cdot F) + (a_2 + a_3 \cdot F) \cdot P + (a_4 + a_5 \cdot F) \cdot X + (a_6 + a_7 \cdot F) \cdot X \cdot P \quad (3.3)$$

allowing interaction between rainfall amount P, rainfall characteristic X, and period of the year F. By allowing a three-way interaction term, the possible interaction between P and X could differ between the leafed and the leafless season. Finally, all variables X and their two-way and three-way interactions with P and F were used as independent variables in the TF, SF, and I regressions. The goodness-of-fit of all multiple linear regressions was expressed by the adjusted r^2 (r_a^2) to account for the number of variables used (Neter *et al.*, 1996).

3.4 Results

3.4.1 Precipitation partitioning at the annual and semiannual level

Between 17 May 2002 and 16 May 2004 a total precipitation amount (P) of 1448 mm was collected (Fig. 3.2, Table 3.2), of which an estimated 4% was snowfall. On the average, this amount was partitioned into 71% throughfall (TF), 8% stemflow (SF), and 21% interception loss (I) (Table 3.2).

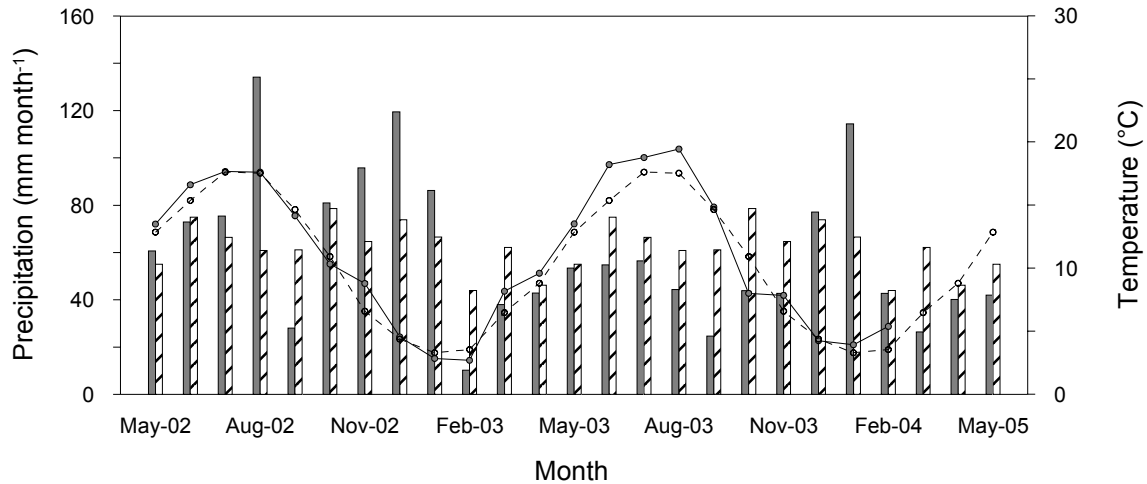


Fig. 3.2. Monthly precipitation (full bars) and average temperature (solid line) during the study period. The hashed bars and dashed line indicate the long-term (1980-2002) monthly averages.

The intercepted fraction was three times higher during the leafed season (31% of P) than in the leafless season (10%), which was mainly due the lower TF fraction in the leafed season (Table 3.2). Interception loss during the leafed season was higher in 2003 (34%) than in 2002 (28%). While the SF fraction of gross precipitation was considerably higher in defoliated conditions, SF contributed similarly to net precipitation (TF+SF) to the forest floor during the leafed (9.2%) and leafless season (10.6%). Rainfall events ≥ 1 mm ($n = 210$) accounted for 96% of P and more than 99% of TF and SF, while events ≥ 5 mm ($n = 78$) contributed 72% of P, 79% of TF, and 87% of SF (Table 3.3).

Table 3.2. Partitioning of precipitation (rainfall and snowfall) into throughfall, stemflow, and evaporation of intercepted water during the leafed season (foliation $F = 1$) and the leafless season ($F = 0$) from 17 May 2002 to 16 May 2004.

Measurement period	F	Precipitation		Throughfall		Stemflow		Interception	
		(mm)	(%)	(mm)	(%)	(mm)	(%)	(mm)	(%)
17 May 02 - 31 Oct 02	1	411.5	100	271.8	66	26.1	6.3	113.6	28
1 Nov 02 - 24 Apr 03	0	357.5	100	292.8	82	33.6	9.4	31.1	9
25 Apr 03 - 11 Nov 03	1	328.4	100	195.7	60	21.6	6.6	111.1	34
12 Nov 03 - 21 Apr 04	0	320.4	100	253.2	79	31.1	9.7	36.1	11
22 Apr 04 - 16 May 04	1	30.0	100	15.7	52	1.5	4.9	12.8	43
Leafed season	1	769.9	100	483.3	63	49.2	6.4	237.5	31
Leafless season	0	677.9	100	546.0	80	64.6	9.5	67.2	10
Total study period		1447.8	100	1029.3	71	113.8	7.9	304.7	21

Table 3.3. Cumulative rainfall (P, mm), average throughfall (TF, $n = 20$), stemflow (SF), and interception loss (I) (% of P) per rainfall class (mm) for 344 events during the leafed (L) and the leafless season (NL).

Rainfall (mm)	No. of events		Rainfall (mm)		TF (% of P)		SF (% of P)		I (% of P)	
	L	NL	L	NL	L	NL	L	NL	L	NL
0 - < 1	72	62	26	24	3.2	44	0.0	1.5	97	54
1 - < 2	32	24	43	37	16	68	0.1	2.2	84	29
2 - < 5	37	39	118	135	50	75	3.3	7.3	47	17
5 - < 10	22	13	142	89	65	79	5.9	11	30	10
10 - < 15	11	6	131	84	74	85	7.1	11	18	4.0
15 - 35	13	13	310	246	73	83	8.9	13	18	4.1
Total	187	157	769	614	63	79	6.4	10	31	11

3.4.2 Event rainfall partitioning as a function of rainfall amount and period of the year

For all rainfall events of at least 1 mm during the entire study period ($n = 210$), TF ($r_a^2 = 0.98$, $p < 0.001$; Fig. 3.3a-b) and SF ($r_a^2 = 0.85$; Fig. 3.3c-d) were strongly correlated with P. Interception of all rainfall events was significantly but weakly ($r_a^2 = 0.29$, $p < 0.001$) correlated with P (Fig. 3.3e-f). Although I was always positive at the weekly time interval, negative I values (-0.05 to -0.67 mm event⁻¹, Fig. 3.3e) were observed for six events during the leafless season, five of which exceeded 1 mm rainfall. The exclusion of these five events did not have a meaningful impact on the TF-P and SF-P regressions, but did increase the fit of the I-P regression ($r_a^2 = 0.40$, $n = 205$).

When multiple linear regressions that took the period of the year into consideration were derived, the adjusted regression coefficients increased for all water fluxes ($r_a^2 = 0.99$ for TF and 0.89 for SF, $n = 210$) but particularly for I ($r_a^2 = 0.73$). In the TF-P relationship for events with $P \geq 1$ mm, both the slope and the intercept were statistically different ($p < 0.001$) between the leafed (L) and the leafless season (NL) (Fig. 3.3a):

$$TF_L = -0.835 + 0.777 \cdot P \quad (r^2 = 0.99, p < 0.001, n = 115) \quad (3.4)$$

$$TF_{NL} = -0.302 + 0.850 \cdot P \quad (r^2 = 0.99, p < 0.001, n = 95) \quad (3.5)$$

Consequently, a given amount of P generated significantly more TF in the leafless season than in the leafed season. The regression coefficients indicate that TF occurred when P exceeded 1.1 mm during the growing season and 0.4 mm during the dormant season, in accordance with the observations (Fig. 3.3b). For P values lower than 1.1 mm (leafed season) or 0.4 mm (leafless season), the regressions were not meaningful.

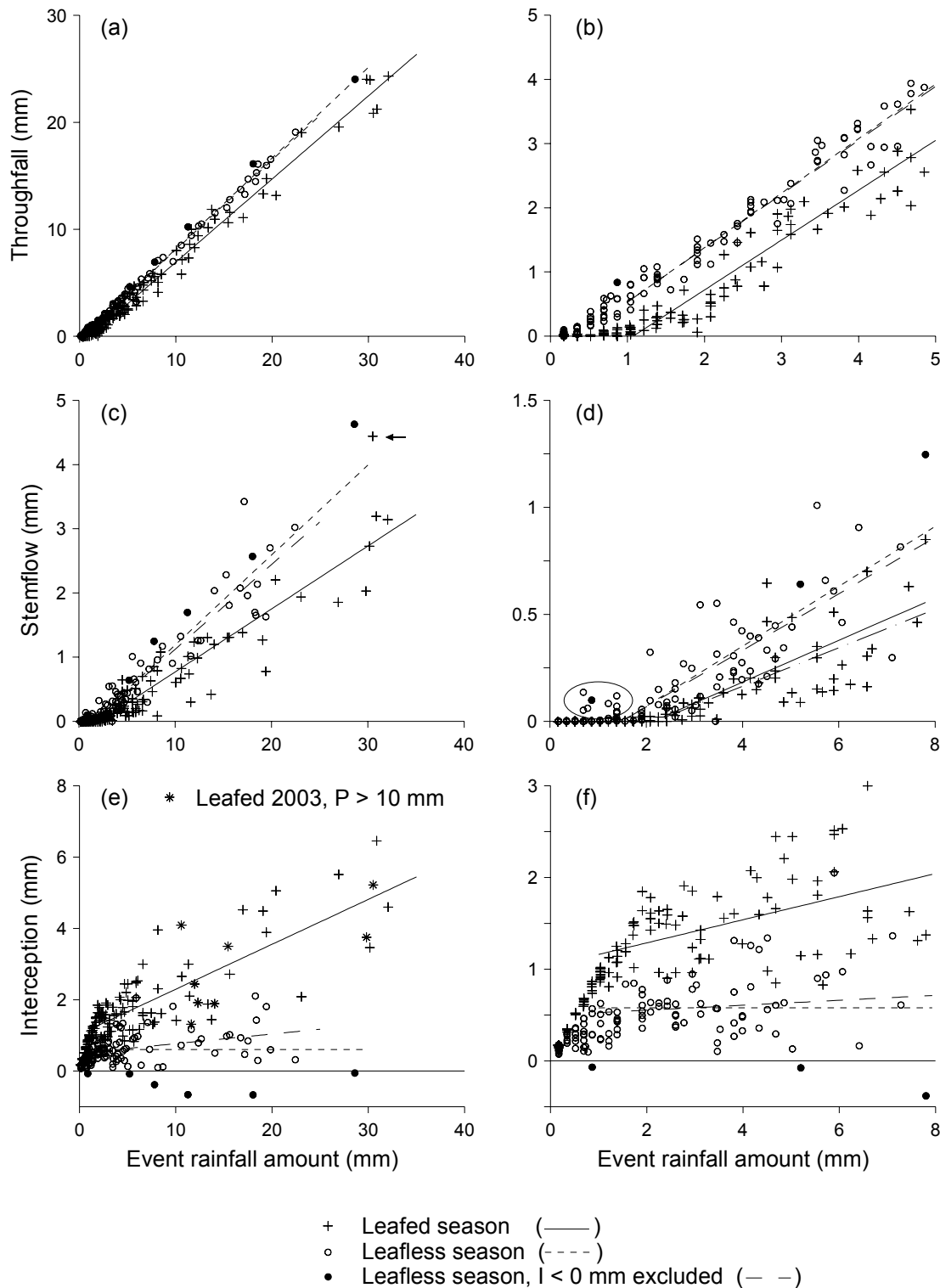


Fig. 3.3. (a-b) Throughfall, (c-d), stemflow, and (e-f) interception (mm event⁻¹) from 17 May 2002 to 16 May 2004 as a function of rainfall (mm event⁻¹). Plot (b), (d), and (f) are magnifications of (a), (c), and (e), respectively. The linear regressions were calculated per period of the year for events in which rainfall ≥ 1 mm.

The difference between the two periods of the year is clearly illustrated when TF is expressed as a percentage of P (Fig. 3.4a). During the leafed season, the TF fraction increased from an

average of 16% of P for 1 to 2 mm rain events, over 50% for 2 to 5 mm events, to 74% for events ≥ 10 mm (Table 3.3). The TF fraction in the leafless season was greater than in the leafed season for all rainfall classes, and stabilized at an average of 83% of P for events ≥ 5 mm. The events in which a negative interception was calculated all had high TF fractions (Fig. 3.4a, $I < 0$ mm), but the linear TF-P regression for the leafless season (Fig. 3.3a-b) was hardly affected by excluding these events and could not be distinguished from the relationship determined for all rainfall events, including those with $I < 0$ mm.

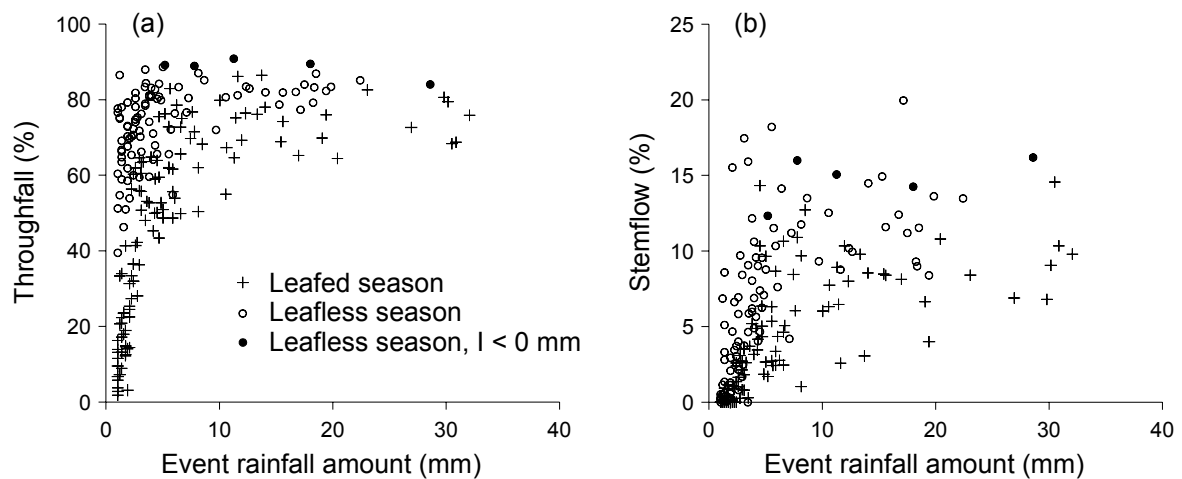


Fig. 3.4. (a) Throughfall and (b) stemflow as a percentage of rainfall (mm event^{-1}) for events during the leafed and leafless season.

In the SF-P relation, only the slope was significantly influenced by the period of the year, and consequently a multiple regression was fitted with equal intercepts in both seasons. A given amount of P yielded more SF water when the tree was defoliated (Fig. 3.3c-d):

$$SF_L = -0.209 + 0.098 \cdot P \quad (r^2 = 0.88, p < 0.001, n = 115) \quad (3.6)$$

$$SF_{NL} = -0.209 + 0.140 \cdot P \quad (r^2 = 0.90, p < 0.001, n = 95) \quad (3.7)$$

The regression coefficients indicate that SF occurred for rainfall events of more than 2.1 mm and 1.5 mm for the leafed and leafless season, respectively. These are lower SF generating P values than observed (Fig. 3.3d). Therefore, the SF-P regressions were recalculated using only events that were certainly large enough to generate SF (e.g., $P \geq 3$ mm, Fig. 3.3d), resulting in calculated minimum rainfall amounts of 2.5 mm and 1.9 mm in the growing and dormant season, respectively. Neither slope nor intercept of the SF-P regression was significantly different when calculated for events ≥ 1 mm or ≥ 3 mm rainfall. In the leafless season, unexpected SF amounts were observed for eight small events ($P < 1.9$ mm), as indicated by an

ellipse in Fig. 3.3d. A common characteristic of six of those events was that the temperature was between 0 and 3°C. The rain events with negative I generally had high SF amounts, and their exclusion decreased the slope of the SF-P regression in the leafless season (Fig. 3.3c), but not significantly ($p > 0.05$). For one of the larger rainfall events ($P = 30$ mm) during summer, indicated by an arrow in Fig. 3.3c, a SF amount was measured that was more in the order of a winter SF yield. Excluding this outlier did not significantly ($p > 0.05$) decrease the slope of the SF-P regression in the leafed season. While relative SF in the leafless season stabilized at an average of 12% of P for events ≥ 5 mm (Table 3.3, Fig. 3.4b), no stabilization of SF as a fraction of P was observed for events in the leafed season.

The slope and the intercept of the I-P regression differed significantly between the growing and dormant season. Interception depth (mm) increased with event rainfall during the leafed season, but not during the leafless season (Fig. 3.3e). Consequently, P was only retained in the relationship for leafed season events ($P \geq 1$ mm), while a constant interception depth of 0.6 mm was predicted for events in the leafless season:

$$I_L = 1.035 + 0.126 \cdot P \quad (r^2 = 0.70, p < 0.001, n = 115) \quad (3.8)$$

$$I_{NL} = 0.603 \quad (\text{n.s.}, n = 95) \quad (3.9)$$

After excluding the five events ($P \geq 1$ mm) with $I < 0$ mm, a weak but significant relationship was also found between I and P for the rainfall events in the leafless season (Fig. 3.3e):

$$I_{NL} = 0.499 + 0.027 \cdot P \quad (r^2 = 0.14, p = 0.001, n = 90) \quad (3.10)$$

As indicated by the low r^2 of Eq. 3.10, the deviation between predicted and observed I amounts was considerable in the defoliated season (Fig. 3.3e-f). When the amount of P increased, the fraction of I decreased (Fig. 3.5, Table 3.3), in the leafed season from 84% for 1 to 2 mm events to an average of 18% for ≥ 10 mm events, and in the leafless season from 29% for 1 to 2 mm events to 4% for ≥ 10 mm events. The best fit between P (≥ 1 mm) and relative I was obtained by the following power equations (Fig. 3.5):

$$I_L (\% \text{ of } P) = 0.941 \cdot P^{-0.604} \quad (r^2 = 0.84, p < 0.001, n = 115) \quad (3.11)$$

$$I_{NL} (\% \text{ of } P) = 0.404 \cdot P^{-0.792} \quad (r^2 = 0.50, p < 0.001, n = 90) \quad (3.12)$$

in which both coefficients differed significantly ($p < 0.001$) between the leafed and the leafless season. Eq. 3.12 was calculated with the exclusion of events where I was negative, since a power model cannot be fitted to negative values. Fig. 3.5 shows that it was justified to

use only two canopy development stages, because the relative I of events during the period of leaf emergence was similar to the relative I for events during the fully leafed period, while events during the last week of leaf senescence could not be distinguished from the events during the leafless season.

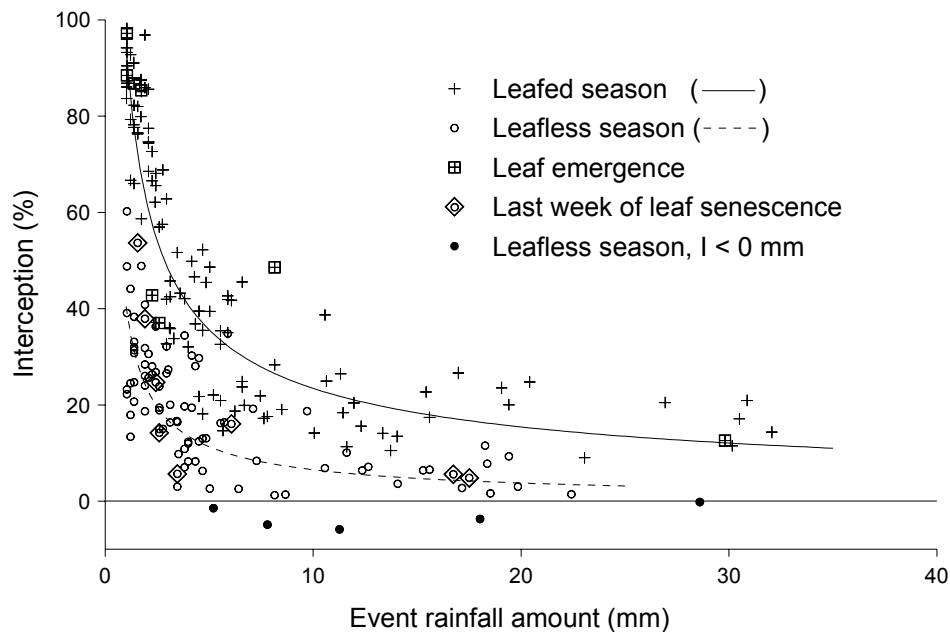


Fig. 3.5. Interception loss as a percentage of rainfall (mm event^{-1}) for events during different canopy development phases. The lines indicate power functions calculated per period of the year for events ≥ 1 mm rainfall, excluding events where $I < 0$ mm (see Eq. 3.11 - 3.12).

Finally, the I-P relationship was examined for events in the leafed season of 2002 and 2003 separately, but neither the slope nor the intercept differed significantly ($p > 0.80$) between the regressions of the two measuring years. However, the regression plots showed a different distribution of event rainfall amount between 2002 and 2003. As illustrated by asterisks in Fig. 3.3e, large rain events (≥ 10 mm) were scarce in the growing season of 2003, and events ≥ 15 mm accounted for only 23% of rainfall compared to 52% in the growing season of 2002. Hence, small rain events (< 10 mm) contributed 60% and 30% of the leafed season rainfall in 2003 and 2002, respectively.

3.4.3 Rainfall characteristics and meteorological conditions

Complete meteorological measurements were available for 188 of the 210 events ≥ 1 mm rainfall. Rainfall events lasted significantly ($p < 0.01$) longer in the leafless season than in the leafed season, and consequently had lower event-average rainfall intensities (Table 3.1). The

statistical difference in rainfall intensity between the two seasons was most pronounced for the maximum 10-min rates of rain events (Table 3.1, Fig. 3.6a). Rainfall was accompanied by significantly ($p < 0.001$) higher wind speeds in the leafless season than in the leafed season (Fig. 3.6b), with median values of 2.4 and 1.4 m s⁻¹, respectively (Table 3.1). Wind direction during rain also differed statistically ($p = 0.03$). Net radiation (NR), temperature, and hourly vapour pressure deficit (VPD) during rain were significantly ($p < 0.01$) higher for events in the leafed season. The median value of the NR of leafless season events was negative due to negative values at night time. The calculated potential evaporation rate was higher ($p = 0.05$) in the leafless season due to the higher wind speeds in that period. Rain events in the leafed season were preceded by longer dry periods than in the leafless season, but the difference was not significant (Table 3.1).

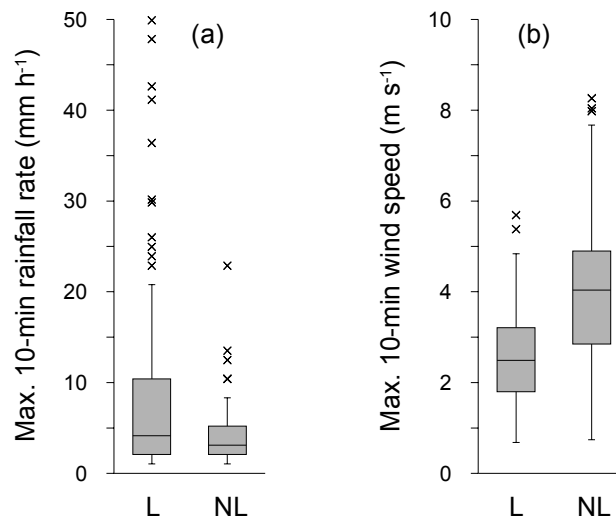


Fig. 3.6. Maximum 10-minute (a) rainfall intensity (mm h⁻¹) and (b) wind speed (m s⁻¹) for rain events ≥ 1 mm rainfall during the leafed (L, $n = 115/103$) and the leafless season (NL, $n = 95/85$). The boxplots indicate the minimum, lower quartile, median, upper quartile, and maximum values of the variables. Values outside the 1.5 interquartile ranges are indicated by x.

Spearman correlations between water fluxes and climatic factors were generally similar in the leafed and in the leafless season, except for I. The event amounts of P, TF, and SF were positively correlated with rainfall duration D ($r_s > 0.56$, $p < 0.001$, $n = 210$) and rainfall rate, while this held true for I in the leafed season only. P, TF, and SF correlated more closely with the maximum hourly rainfall rate R_{60} ($r_s > 0.71$) and 10-minute rate R_{10} ($r_s > 0.48$) than with the average rate R ($r_s < 0.40$, $p < 0.001$) of rain events. Rainfall duration D was negatively related to R ($r_s = -0.44$), weakly positively to R_{60} ($r_s = 0.24$, $p = 0.01$) and not significantly to

R_{10} ($p = 0.09$). Wind direction was not significantly ($p > 0.10$) correlated with any other event variable measured. A strong correlation ($r_s > 0.86$) was observed between the average and maximum 10-min wind speeds. For rain events in the leafed season, net radiation, temperature and hourly vapour pressure deficit were weakly correlated ($r_s = 0.20$ to 0.40 , $p < 0.04$).

3.4.4 Event rainfall partitioning as a function of rainfall characteristics and meteorology

The influence of rainfall and meteorological variables was first tested individually in Eq. 3.3 (Table 3.4), excluding the five events with $I < 0$ mm. Variables that were not significant ($p < 0.01$) were excluded from the stepwise multiple regressions. In general, when an event variable was added to the regressions, the intercept and slope still differed significantly between the two periods of the year, as indicated by the non-zero values of the coefficients a_1 and a_3 (Table 3.4). The tested variables rarely affected TF and SF in the leafless season (coefficient a_4 and a_6 not significant), but often significantly influenced the intercept or slope of the regressions for events in the leafed season (a_5 and a_7) (Table 3.4). For example, when rainfall duration (D) of events was used in addition to P and F for describing the event TF amount, a multiple regression was obtained ($r_a^2 = 0.991$, $n = 205$) in which the significantly lower slope of the TF-P relationship in the growing season was expressed as a function of D:

$$TF_L = -0.819 + (0.844 - 0.002 \cdot D) \cdot P \quad (r^2 = 0.99, p < 0.001, n = 115) \quad (3.13)$$

In contrast to TF, the generation of SF for a given amount of P was not affected by event duration (Table 3.4). With respect to rainfall interception, the intercept in the I-P regression during the growing season was significantly higher for events of longer duration (Table 3.4):

$$I_L = (0.719 + 0.063 \cdot D) + 0.096 \cdot P \quad (r^2 = 0.74, p < 0.001, n = 115) \quad (3.14)$$

The second event characteristic tested was rainfall rate. For TF and SF, higher fits of the multiple regressions (Eq. 3.3) were obtained using maximal rainfall intensity R_{10} and R_{60} than using the average event intensity R. Controlling for P, higher maximum rainfall rates significantly ($p < 0.01$) increased the TF amount and decreased the SF amount of rain events (Table 3.4). This is illustrated by plotting the residual errors of the single linear regressions between event P and TF (Eq. 3.4 - 3.5) and P and SF (Eq. 3.6 - 3.7) as a function of maximum hourly rainfall rate (Fig. 3.7).

Table 3.4. Coefficients (a_i) and adjusted fit (r_a^2) of multiple linear regressions ($n = 205/184$, $P \geq 1$ mm, $I \geq 0$ mm) with throughfall, stemflow, and interception amount (mm event⁻¹) as dependent variables, and rainfall amount (P, mm event⁻¹), foliation ($F = 1$ in the leafed season, $F = 0$ in the leafless season), a variable X (see Table 3.1), and their 2-way and 3-way interactions as independent variables (Eq. 3.3).

X	Leafed season				Leafless season				r_a^2
	(cst)	P	X	P·X	(cst)	P	X	P·X	
	$a_0 + a_1$	$a_2 + a_3$	$a_4 + a_5$	$a_6 + a_7$	a_0	a_2	a_4	a_6	
Throughfall									
-	-0.835	0.777	-	-	-0.309	0.840	-	-	0.989
D	-0.819	0.844	n.s.	-0.002	-0.313	0.844	n.s.	n.s.	0.991
R ₁₀	-0.778	0.706	0.023	0.002	-0.309	0.840	n.s.	n.s.	0.992
R ₆₀	-0.857	0.680	0.190	0.005	-0.463	0.813	0.190	n.s.	0.992
V	-0.801	0.838	n.s.	-0.049	-0.290	0.838	n.s.	n.s.	0.990
T	-0.788	0.630	n.s.	0.010	-0.302	0.840	n.s.	n.s.	0.990
VPD	-0.843	0.777	n.s.	n.s.	-0.302	0.840	n.s.	n.s.	0.989
E _{pot}	-0.789	0.801	n.s.	-0.093	-0.302	0.840	n.s.	n.s.	0.990
Stemflow									
-	-0.196	0.097	-	-	-0.196	0.132	-	-	0.890
D	-0.196	0.097	n.s.	n.s.	-0.196	0.132	n.s.	n.s.	0.890
R ₁₀	-0.122	0.115	-0.022	n.s.	-0.122	0.146	-0.041	n.s.	0.925
R ₆₀	-0.127	0.125	-0.095	n.s.	-0.127	0.146	-0.095	n.s.	0.912
V	-0.196	0.097	n.s.	n.s.	-0.196	0.132	n.s.	n.s.	0.890
T	-0.208	0.133	n.s.	-0.002	-0.208	0.133	n.s.	n.s.	0.891
VPD	-0.221	0.129	0.179	-0.082	-0.221	0.129	n.s.	n.s.	0.902
E _{pot}	-0.188	0.108	n.s.	-0.036	-0.188	0.131	n.s.	n.s.	0.896
Interception									
-	1.035	0.126	-	-	0.499	0.027	-	-	0.749
D	0.719	0.096	0.063	n.s.	0.719	n.s.	n.s.	n.s.	0.765
R ₁₀	0.907	0.179	n.s.	-0.002	0.560	n.s.	n.s.	0.003	0.789
R ₆₀	0.994	0.200	-0.105	-0.005	0.666	n.s.	-0.105	0.012	0.787
V	1.000	0.066	n.s.	0.048	0.500	n.s.	n.s.	0.010	0.784
T	1.004	0.238	n.s.	-0.008	0.520	n.s.	n.s.	0.003	0.758
VPD	1.086	0.079	-0.226	0.122	0.540	n.s.	-0.226	0.122	0.783
E _{pot}	1.049	0.085	-0.172	0.148	0.510	n.s.	-0.172	0.090	0.810

Note: All coefficients are significant at $p < 0.01$, except otherwise stated. Non-significant (n.s.) variables were excluded from the stepwise multiple regressions. The symbol “-” indicates that only P was used as dependent variable, corresponding to the single linear regressions given in Eq. 3.4 - 3.10 for $n = 210$ (i.e. including events with negative I).

According to the multiple regressions, higher wind speeds (V) significantly decreased the TF_L amount and increased I (Table 3.4, $n = 184$). Net radiation (NR) was not retained as a significant variable. When only event temperature (T) was used in Eq. 3.3, the different slope of the TF-P, SF-P, and I-P relationships between the two periods of the year was statistically expressed as a function of T. A higher hourly vapour pressure deficit (VPD) and calculated hourly potential evaporation rate (E_{pot}) significantly increased interception for rainfall events

throughout the year. Of all variables tested individually, the highest fit for I was obtained using E_{pot} ($r_a^2 = 0.81$) (Table 3.4).

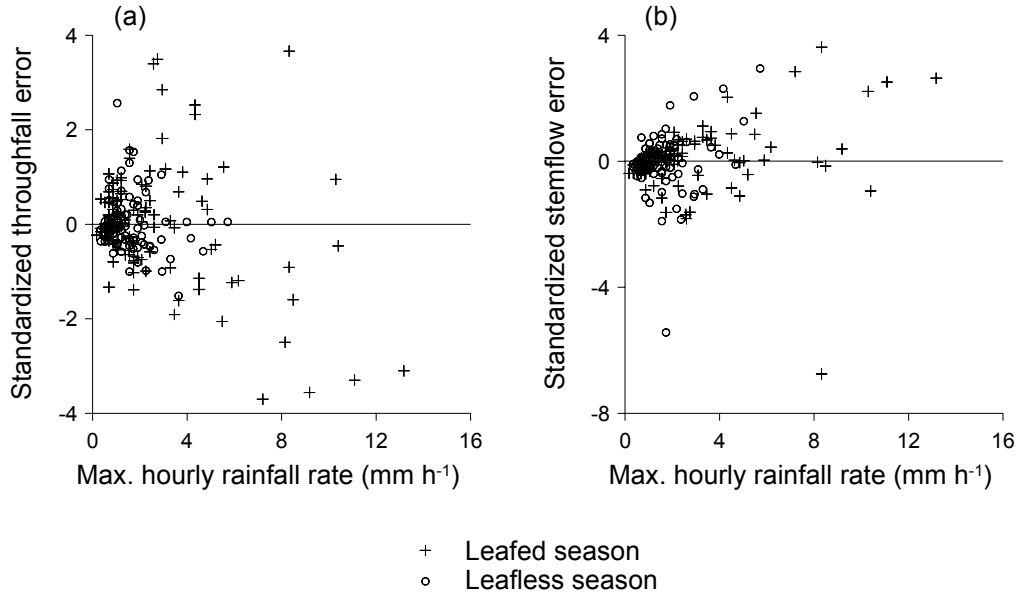


Fig. 3.7. Standardized residual errors of event amount of (a) throughfall and (b) stemflow predicted by Eq. 3.4 - 3.5 and Eq. 3.6 - 3.7, respectively, as a function of the maximum hourly rainfall rate (mm h^{-1}) ($n = 205$). Standardized errors are positive when the regression overestimates the observed value.

When Eq. 3.3 was computed testing all variables X_i (D , R_{60} , V , T , NR , VPD , E_{pot}) as predictors, the following multiple regression ($r_a^2 = 0.993$, $n = 184$, $p < 0.001$) was obtained for TF:

$$TF = -0.367 - 0.046 \cdot F \cdot D + 0.183 \cdot R_{60} - 0.031 \cdot T + (0.812 - 0.035 \cdot F \cdot V - 0.039 \cdot VPD) \cdot P \quad (3.15)$$

indicating that the TF amount of rain events ($P \geq 1 \text{ mm}$) increased with increasing maximum hourly rainfall rate and decreasing vapour pressure deficit and temperature throughout the year, while in the growing season the duration and wind speed of rain events negatively affected the TF amount. The final multiple regression ($r_a^2 = 0.930$) for SF at the event level ($P \geq 1 \text{ mm}$) was:

$$SF = -0.259 - 0.039 \cdot F \cdot R_{60} + (0.154 - 0.071 \cdot P) \cdot VPD + (0.158 - 0.003 \cdot R_{60}) \cdot P \quad (3.16)$$

showing a negative effect of maximum rainfall rate and vapour pressure deficit (when $P \geq 2.2$ mm) on stemflow generation; the lower slope of the SF-P relationship in the growing season was expressed as a function of the maximum hourly rainfall rate. For the event amount of I, the following multiple regression was obtained ($r_a^2 = 0.853$):

$$I = 0.466 + (0.586 + 0.032 \cdot D - 0.169 \cdot R_{60}) \cdot F + (0.069 \cdot P - 0.173) \cdot E_{pot} \quad (3.17) \\ + (0.115 \cdot F + 0.061 \cdot VPD) \cdot P$$

indicating a higher interception loss for events ($P \geq 1$ mm) with higher vapour pressure deficit and potential evaporation rate. Eq. 3.17 shows that, controlling for other variables, both the intercept and the slope (dI/dP) of the I-P regression differed significantly between the two periods of the year. For rainfall events during the leafed season, interception increased with longer duration and lower maximal intensity of rainfall.

3.5 Discussion

3.5.1 Precipitation partitioning at the annual and semiannual level

The partitioning of precipitation measured during two years under a dominant beech tree (Table 3.2) corresponds well with previous research. In the ICP Forests Level II plot located in the same oak-beech stand, mean annual throughfall in the period 1994-2003 was 74% of the precipitation input (67 to 76%) and mean annual interception loss was 23% (19 to 27%) (Genouw, unpublished data). According to the review of Augusto *et al.* (2002), precipitation interception by *Fagus sylvatica* averages 22% in Europe with a standard deviation of 5% ($n = 30$), while Peck and Mayer (1996) reported interception values of 5 to 48% of precipitation for beech stands, with an average value of 20% ($n = 19$).

In the present study, relative interception loss was significantly higher in the leafed season than in the leafless season, which is in agreement with findings for other beech stands and deciduous forests (Augusto *et al.*, 2002; Levia and Frost, 2003; Armbruster *et al.*, 2004). In a 80-yr old beech stand in France, for example, interception loss was 21% in the growing season and 6% in the dormant season (Ausenac and Boulangeat, 1980). Nevertheless, Forgeard *et al.* (1980) did not find evidence for a relationship between interception loss and beech phenology, and suggested that the high intensity of rain events in summer may have compensated the possible increase in interception due to the presence of leaves. In a lowland beech plantation in southern England, lowest interception losses occurred during winter, but

because of occult precipitation during winter months, it was not clear to which degree interception changed as a function of foliation (Neal *et al.*, 1993).

It is widely acknowledged that stemflow from beech represents a significant input of water (and elements) to the forest soil, mainly due to its branching architecture and smooth bark (Levia and Frost, 2003). Stemflow contributed about 10% of the annual soil water input under the studied tree crown, which falls well within the reported range of 7 to 20% for beech stands (Chang and Matzner, 2000b), although it is higher than in the adjacent ICP Forests plot (on average 6% in 1994-2003; Genouw, unpublished data) because of the presence of both oak and beech trees in that plot. The stemflow fraction of net precipitation (TF+SF) was almost unaffected by the period of the year, in contrast to Neal *et al.* (1993), but the stemflow fraction of gross precipitation (P) was significantly lower in the growing season than in the dormant season. Likewise, stemflow amounted to 3% of gross precipitation in summer and 9% in winter according to Aussenac and Boulangeat (1980), and for events exceeding 5 mm, stemflow in a beech coppice was always lower in the leafed season (Giacomin and Trucchi, 1992).

3.5.2 Interception loss in relationship to rainfall amount

The present study confirms that the largest percentage of rainfall interception occurs during small rain events (Llorens *et al.*, 1997, Price and Carlyle-Moses, 2003), but the inverse relationship between relative interception and rainfall amount was much clearer in the growing season than in the dormant season (Fig. 3.5). During the growing season, throughfall as a percentage of gross rainfall remained quasi-constant for events exceeding 10 mm, similar to the results of a mature mixed-deciduous forest in Canada (Price and Carlyle-Moses, 2003). The interception loss for events in the leafless season was only weakly related to the amount of rainfall. For a dense oak forest in the Netherlands, the slope of the regression between daily interception and precipitation was also significantly lower in winter ($n = 14$ days) than in summer ($n = 44$) (Dolman, 1987).

Although the average annual rainfall during the 2-year study period was close (96%) to the long-term average, the growing season of 2003 was relatively dry and warm (Fig. 3.2). The higher intercepted rainfall fraction in the growing season of 2003 than in 2002 (Table 3.2) was not caused by a modified relationship between event interception loss and rainfall amount, but by a different rainfall distribution (Fig. 3.3e). While the majority of rainfall in the growing season of 2002 was delivered by large events (≥ 15 mm), the lower total rainfall

amount in the growing season of 2003 was mainly comprised of smaller events (< 10 mm), which have a higher relative interception loss. This indicates that the water balance of forest ecosystems is sensitive to the temporal rainfall distribution, which is important for evaluating the effects of changing climatic conditions (Herbst and Hörmann, 1998; Bellot and Escarre, 1998).

3.5.3 Rainfall partitioning at the rain event level

Although many variables may affect the amount of throughfall and stemflow at the individual rain event level, the observed water fluxes were principally explained by the gross rainfall input and foliation. Similar relationships between precipitation and throughfall or stemflow amounts have been reported for different forest types (Neal *et al.*, 1993; Bellot and Escarre, 1998; Marin *et al.*, 2000; Xiao *et al.*, 2000b; Huber and Iroumé, 2001). The regression analysis shows that, controlling for variations in rainfall characteristics and meteorological factors, foliation significantly increased the interception loss for a given amount of rainfall and significantly decreased the amount of throughfall and stemflow.

Free throughfall and canopy drip were lower in the leafed season than in the leafless season because the gap fraction is lower in foliated conditions and the surface area from which intercepted rainfall water can evaporate is larger (Rutter *et al.*, 1975; Link *et al.*, 2004; Pypker *et al.*, 2005). Furthermore, the evaporation rate for wetted woody surfaces is lower than for wetted foliage, mainly because of the differences in boundary layer thickness (Rutter *et al.*, 1975) and the development of detained water films in porous bark tissue (Herwitz and Levia, 1997). In addition to foliation, the different throughfall generation in the two periods of the year for a given rainfall amount was partly explained by other event characteristics. Because of possible correlations between the studied variables, the influence of rainfall and climatic variables is better interpreted based on the results of the multiple regressions than of the single regressions. For example, examining the relationship between canopy interception and rainfall intensity is only meaningful when the analysis controls for duration (Keim, 2004), which is complicated by the fact that large events tend to last longer than small events and thus tend to have lower average intensities ($r_{s,D-R} = -0.44$). However, the maximum 10-min and hourly rainfall intensities were not or very weakly correlated with rainfall duration, and still significantly increased the throughfall amount of rain events (Eq. 3.15, Table 3.4, Fig. 3.6a). Throughfall was also correlated ($r = 0.57$) with maximum rainfall intensity in a holm-oak forest (Bellot and Escarre, 1998), but no correction was made for the likely relationship

between rainfall amount, intensity and duration. For two broadleaved trees in California, higher average rainfall rates increased winter throughfall, but the effect was not significant at the 95% level (Xiao *et al.*, 2000b).

After controlling for other event characteristics, the constant in the regression between event interception loss and rainfall amount was significantly higher in the growing season than in the dormant season (Table 3.4, Eq. 3.17). In other words, a higher amount of rainfall was necessary to induce throughfall in the growing season, indicating a higher water storage capacity of the leafed canopy. The significantly lower slope of the throughfall-rainfall regression in the growing season (Fig. 3.3a) was partly explained by the higher vapour pressure deficit in summer (Table 3.1), but still differed between the two periods of the year, expressed as a function of wind speed (Eq. 3.15). According to the Penman-Monteith equation, higher wind speeds increase the evaporation rate and hence decrease throughfall, but wind may also increase throughfall by decreasing canopy storage capacity (Hutchings *et al.*, 1988; Hörmann *et al.*, 1996; Klaassen *et al.*, 1996). As wind speed significantly decreased throughfall both in the single (Table 3.4) and multiple regressions (Eq. 3.15), its influence on the evaporation rate appeared to dominate at our study site. In contrast to wind speed and air humidity deficit, net radiation did not significantly affect interception. This confirms that wet forests are well coupled to the lower atmosphere (Klaassen, 2001), so that evaporation from a wet canopy is driven by advected energy rather than by net radiation (Teklehaimanot and Jarvis, 1991).

With respect to stemflow, leaves on the one hand favour water collection, but on the other hand prevent branches from becoming wet and conducting water down the trunk (Giacomin and Trucchi, 1992; Herwitz and Levia, 1997; Crockford and Richardson, 2000). Stemflow occurred for events of more than 2.1 and 1.5 mm rainfall in the growing and dormant season, respectively (Eq. 3.6 - 3.7, Fig. 3.3d), which is lower than the reported rainfall amounts of 5 mm (Chang and Matzner, 2000b) and 8 mm (Neal *et al.*, 1993) derived from biweekly sampling intervals. In a laurel forest, the antecedent rainfall amount for the initiation of stemflow was 1.5 to 4.9 mm for different species (Aboal *et al.*, 1999). Stemflow yield of plants has been observed to decrease with the intensity of incident gross precipitation (Levia and Frost, 2003), though quantitative reports are scarce. In the present study, a significant decrease of stemflow amount was found for events with higher maximal rainfall rates, particularly during the leafed season (Eq. 3.16, Fig. 3.7). A probable explanation is that intense rain events increase the probability of branch drip by overloading preferential flow

paths on tree trunks and forcing stemflow to become throughfall (Crockford and Richardson, 2000). No significant effect of wind speed on stemflow yield was found for the studied forest tree, in contrast to the increased stemflow generation with increasing wind speed that has been observed for two open-grown trees (Xiao *et al.*, 2000b).

3.5.4 Accuracy of interception measurements

In the present study, negative interception loss was observed for six rain events during leafless conditions, even though the weekly water balance was always positive. When interception is calculated as the difference between above and below-canopy water fluxes, measurement accuracy of both the gross and net precipitation is critical.

Elevated gauges may underestimate gross precipitation due to the modification of airflow around the gauge, particularly when wind speeds are high and raindrop size is small (Allerup *et al.*, 1997; Crockford and Richardson, 2000). However, at the study site no significant differences were found between the 9-monthly amount of rainfall measured above the canopy and in an adjacent grassland (see section 2.4.1), in agreement with other studies (Lloyd *et al.*, 1988; Loustau *et al.*, 1992; Aboal *et al.*, 1999). A possible explanation for negative interception values is that gross precipitation was underestimated due to fog interception, although fog drip, i.e. throughfall without rainfall, was not registered at this lowland forest site. Throughfall water is known to have a considerable spatial variability in most forest stands, even at the plot level (see Chapter 4), but throughfall errors are expected to be minor in the present study because of the relatively large sampling density. The plot-average throughfall water amount was lower than the rainfall input for all events. A major problem associated with stemflow is scaling up measurements from tree level to stand level, for which various methods can be used (Aboal *et al.*, 1999). The areal stemflow flux for the studied beech tree was calculated using the crown projected area, and errors in stemflow are likely mainly associated with the determination of this area.

We remarked that four of the six events with negative interception loss occurred at near zero-temperatures (0 to 3°C), two of which were preceded by snowfall, which may have contributed additional stemflow when melting (Levia and Underwood, 2004). The other two events occurred shortly after each other and were preceded by 10 mm of rainfall the day before. So, possibly the tree bole was not completely dry at the beginning of all rainfall events with negative interception loss. Unexpected stemflow amounts were observed for several small winter events (Fig. 3.3d), most of which also occurred at low temperatures but only

once after snowfall. While the accuracy of the stemflow tipping bucket may have been lower at temperatures just above freezing point, the anomalous stemflow findings could also be caused by a higher stemflow generation due to increased kinematic viscosity and surface tension of water at low temperatures (Levia and Herwitz, 2000).

3.6 Conclusions

The partitioning of rainfall into throughfall, stemflow, and interception loss is affected by rainfall characteristics, meteorological factors and vegetation structure. In deciduous forests, tree phenology alters the surface area of the forest canopy, thereby influencing canopy water storage and interception loss. In addition to a different canopy cover, rain events lasted longer, had lower maximal intensity and were accompanied by higher wind speed and lower temperature, net radiation and vapour pressure deficit in the dormant season. The present study demonstrates the significant influence of foliation on rainfall partitioning by controlling for variations in rainfall characteristics and meteorological conditions during individual rain events. Key variables such as rainfall rate, wind speed, and vapour pressure deficit also significantly affected the observed water fluxes but were less important than foliation. As the relative interception loss of events decreased with increasing rainfall amount, the intercepted rainfall fraction during the growing season was affected by a different distribution of rainfall in the two measuring years. Since foliation and rainfall amount of individual events were the major factors determining rainfall partitioning, the net precipitation input beneath the studied beech canopy depends on the temporal distribution of gross precipitation.

4 Spatial variability and temporal stability of throughfall water amount in relationship to canopy structure

After: Staelens, J., De Schrijver, A., Verheyen, K. and Verhoest, N.E.C. Spatial variability and temporal stability of throughfall water under a dominant beech (*Fagus sylvatica* L.) tree in relationship to canopy structure. Journal of Hydrology, moderate revisions.

4.1 Abstract

Although the spatial heterogeneity of throughfall water (TF) under forest canopies has been related to vegetation structure in several forest types, few reports have been made of the driving factors of small-scale TF variability in deciduous stands. Therefore, the spatial variability of the amount of TF water under one dominant beech tree (*Fagus sylvatica* L.) was quantified in high temporal and spatial resolution over a 2-year period to examine the temporal stability of spatial TF variability and to relate spatial TF patterns to canopy structure. Plant area index (PAI) was derived from canopy cover determined in three zenith angles above each throughfall collector ($n = 48$). The spatial variability of TF was significantly higher during the leafed season (coefficient of variation (CV) = 18%) than during the leafless season (CV = 8%), and a strong negative relationship was observed between the CV of event TF and the TF fraction of rainfall in the open field. Geostatistical analysis showed that the cumulative TF water during the leafed season was spatially correlated up to a distance of 3-4 m. There was a significant temporal stability of spatial TF patterns in the growing season and in the dormant season, but not between the two periods of the year. The TF water amount during the growing season significantly decreased with increasing canopy cover and PAI above the sampling locations ($r = -0.66$, $p < 0.01$, $n = 20$), but was more closely correlated with branch cover ($r = -0.82$, $p < 0.001$). However, the spatial pattern of TF during defoliated conditions was not related to the measured variation in branch cover.

4.2 Introduction

Precipitation falling on a forest canopy is reduced and redistributed as it moves towards the forest floor. Throughfall water (TF) and interception loss are known to be very variable in space, even at the plot scale (e.g., Kimmins, 1973). Previous research suggests that the canopy architecture of vegetation may contribute to a systematic component of spatial TF variability (Lloyd and Marques, 1988; Beier *et al.*, 1993; Whelan and Anderson, 1996), and in several forest types a negative relationship between canopy density and the amount of TF water at individual soil points has been observed (Burghouts *et al.*, 1998; Llorens and Gallart, 2000; Loescher *et al.*, 2002; Nadkarni and Sumera, 2004).

Spatial patterns in TF input can affect the heterogeneity of hydrological, biogeochemical, and ecological processes on the forest floor and in the mineral soil. In a 30-year old Douglas fir stand, spatial distributions of yearly water uptake and percolation fluxes were strongly affected by TF patterns (Bouten *et al.*, 1992). The rewetting pattern of the upper 30 cm of soil in a mixed spruce-beech stand reflected the different interception efficiency of both species (Schume *et al.*, 2003). Durocher (1990) found that the spatial variability of stemflow and rainfall interception in a beech plantation might play an important role in small-scale soil moisture heterogeneity. As preferential root growth into moister soil regions is observed (Joslin *et al.*, 2000), TF 'hot spots' and stemflow can be expected to influence horizontal root distribution in forest stands. In a mature Norway spruce stand, the spatial variation of annual seepage water fluxes at 0.9 m depth was highly correlated with the spatial pattern of TF ($r^2 = 0.98$, $n = 20$) (Manderscheid and Matzner, 1995). However, spatial patterns in forest floor water contents are a result of patterns in forest floor thickness, evaporation, root uptake, drainage to the mineral soil, and TF. As such, it is not possible to relate spatial patterns in TF directly to patterns in forest floor water content (Raaijmakers *et al.*, 2002).

In contrast to coniferous forests, to our knowledge no significant relationships between the small-scale variability of TF and canopy structure have been reported for deciduous forests. Lower TF corresponded to higher leaf area index (LAI) values in a resprouted holm-oak forest, but the difference between four LAI classes was not significant (Bellot and Escarre, 1998). Throughfall was not related to PAI in two red oak forests in Mexico (Carlyle-Moses *et al.*, 2004). Robson *et al.* (1994) concluded that canopy structure caused systematic effects on TF in a beech stand, but without quantifying canopy characteristics and based on only three rain events. In deciduous forest stands, the spatial distribution of TF water amount has mainly been quantified to derive sample size requirements from it (see references in Table 4.1), and

generally little attention is paid to the spatio-temporal patterns of TF water fluxes and its driving factors. Furthermore, most studies use sampling intervals of one week or longer, while hydrological measurements at the rain event level (Llorens *et al.*, 1997) or intra-event level (Xiao *et al.*, 2000b) yield the best results for predicting interception, and hence for studying TF variability.

Table 4.1. Sampling strategy and spatial coefficient of variation (CV) of throughfall water (TF) in temperate hardwood forests: reference, forest type and age, number (n) and collecting area (A) of TF collectors, number (m) and sampling interval (SI) of TF collections, median and range of the CV (%) of TF.

Reference	Forest		TF collector		Sampling		CV (%)	
	Type	Age (yr)	n	A (cm ²)	m	SI ^a	Median	Range
Bellot and Escarre (1998)	Holm oak	-	50	-	60	e	-	-
Duijsings <i>et al.</i> (1986)	Oak-beech	45-105	11	350	26	2-w	15 ^b	7-30
Durocher (1990)	Red oak plantation	40	15	108	1	w	21	-
Houle <i>et al.</i> (1999a)	Mixed hardwood	80-120	36/72	577	163	w	22	7-44
Kostelnik <i>et al.</i> (1989)	Mixed hardwood	90	40	1134	6	e	18	13-22
Peterson and Rolfe (1979)	Oak-hickory	-	96	189	12	e	14	9-23
Puckett (1991)	Mixed hardwood	80	50	182	5	e	16	12-18
Robson <i>et al.</i> (1994)	Beech	20-40	48	-	3	2-w	-	-
Rodrigo and Avila (2001)	Holm oak	30-50	32	79	64	w	-	-
Present study	Beech	85	20	460	236	e	20	8-144
Present study	Beech	85	48	460	83	w	17	8-50

^a Sampling interval: e = rainfall event, w = weekly

^b Mean spatial coefficient of variation of throughfall water

Therefore, in the present study, the spatial variability of TF water was measured in high temporal and spatial resolution over a 2-year period. The aims of this chapter were (i) to quantify the spatial heterogeneity of the water flux to the forest soil under a beech (*Fagus sylvatica* L.) canopy, (ii) to examine the temporal stability of spatial TF patterns, and (iii) to relate spatial TF patterns to easily measurable canopy characteristics.

4.3 Materials and methods

The study area is described in section 3.3.1. To analyse the spatial variability of throughfall water, the experimental setup described in section 3.3.2 has been used. The collected data were identical with respect to precipitation water (3.3.2.2) and leaf wetness status (3.3.2.3),

but the sampling of throughfall water with tipping buckets was extended with two types of manual collectors.

4.3.1 Data collection

4.3.1.1 Throughfall

Throughfall water (TF) was measured using three types of collectors. To determine the spatial variability of TF amount at high temporal resolution, 20 automated tipping bucket collectors with a funnel diameter of 24.2 cm (460 cm²) were used. To enhance sampling density at reasonable costs, these automated collectors were combined with a set of 28 manual TF collectors with a funnel diameter of 24.2 cm. The spatial variability below the 0.75 m scale was examined using 50 TF collectors with a funnel diameter of 14.2 cm (158 cm²). This chapter is mainly based on data of the collectors with a 24.2 cm funnel diameter ($n = 20 + 28 = 48$). Data of the 14.2 cm funnel collectors were only used for the geostatistical analysis.

From 17 May 2002 to 16 May 2004, TF was sampled with 20 tipping bucket rain gauges (automated collectors), placed in a 3 x 3 m grid (Fig. 4.1). The output of the tipping buckets was recorded by a data logger system (Campbell Scientific Inc.) with a temporal resolution of 5 minutes. Additionally, TF was sampled weekly from 27 June 2002 to 16 May 2004 by 28 manual TF collectors, which consisted of a funnel above a receiving 2-l polyethylene bottle. The resulting sampling design was a combination of a 2.1 x 2.1 m grid and two orthogonal transects with an intermediate funnel distance of 0.75 m (Fig. 4.1). All 48 funnels of the manual and automated collectors were identical, with a diameter of 24.2 cm, a sharp-edged vertical rim and a slope of 45°, and were set at a height of approximately 1.5 m. The resolution of the self-constructed tipping buckets, determined by repeated dynamic calibration, was 0.2 mm per tip. Finally, TF was sampled monthly from June 2002 to May 2004 along a transect with 50 collectors consisting of a 14.2 cm diameter funnel placed in a 2-l polyethylene bottle. At two sides of the beech stem, 25 funnels were set with an intermediate distance between funnel centres of 0.25 m.

4.3.1.2 Canopy structure

To determine the canopy gap fraction (p), digital non-hemispherical colour photographs (Canon Powershot S30) were taken vertically above each TF collector location (Whelan and Anderson, 1996; Llorens and Galart, 2000). Photographs were taken during overcast sky conditions in August 2002 (foliated conditions) and March 2003 (non-foliated conditions).

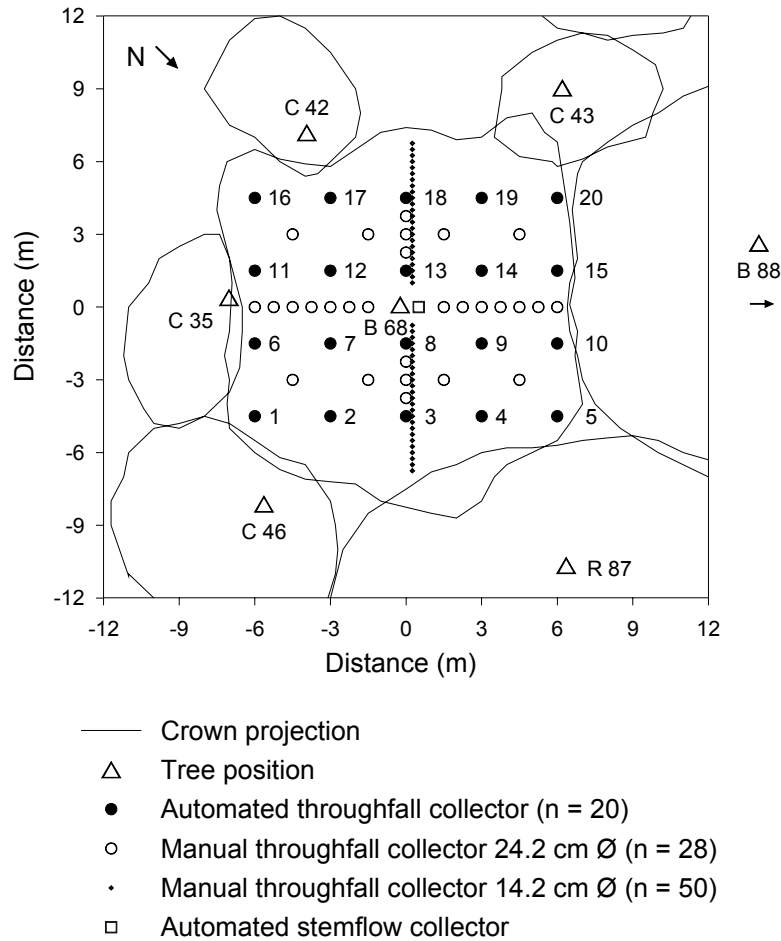


Fig. 4.1. Experimental setup in the Aelmoeseneie forest, Gontrode (Belgium) to measure the spatial variability of the amount of throughfall water. Tree labels indicate tree species (C: common oak, B: European beech, R: American red oak) and diameter (cm) at 1.3 m height.

The camera was mounted on a 1.5 m high tripod and levelled with a spirit level. The canopy cover ($1 - p$) for both seasons was determined for circles with a radius of 0.5, 1.0, and 1.5 m at a height of 15 m above the TF collectors, equivalent to zenith angles of 1.9, 3.8, and 5.7° respectively, using Gap Light Analyzer software. Plant area index (PAI) above each collector, i.e. the one-sided area of leaves, twigs, and stems per unit ground surface area, was calculated by inverting the Beer-Lambert extinction law (Holst *et al.*, 2004):

$$PAI = -(1/k) \cdot \ln(I/I_0) \quad (4.1)$$

where k is the canopy extinction coefficient and I/I_0 is the ratio between the radiation below and above the canopy, which is equivalent to p for small zenith angles. The value of k was calculated for the leafed and leafless season separately by rearranging Eq. 4.1 (Bréda, 2003), based on the average p measured by canopy photographs (zenith angle = 3.8°, $n = 20$) and

independent measurements of PAI. For the leafed period, the mean PAI in the k -value calculation was assumed to equal the maximum stand LAI (Bréda, 2003), as determined directly by litterfall collection (Mussche *et al.*, 2001). Independent PAI estimates for the leafless period were derived from LAI-2000 Plant Canopy Analyzer measurements (Mussche *et al.*, 2001).

4.3.2 Data analysis

The experimental design allows analysis of the spatial variability of TF at several temporal scales. In the first place, TF was studied at the rain event level using the 2-year tipping bucket collector ($n = 20$) data. A rain event was defined as a period with more than 1 mm of total rainfall. Two subsequent events were separated in the data analysis when both leaf wetness sensors were dry for at least one hour, indicating complete drying of the canopy foliage. The rare snowfall events ($n = 6$) were excluded from the analysis. To calculate the total water input, snowfall amount was estimated as the maximum amount of TF measured during the event because of the undercatch of above-canopy snowfall measurements (Allerup *et al.*, 1997). Second, individual rain events were grouped within five rainfall classes (1 to <2, 2 to <5, 5 to <10, 10 to <15, and ≥ 15 mm rainfall), since the spatial variability of TF has been reported to depend on event rainfall amount (Llorens *et al.*, 1997; Gómez *et al.*, 2002). These rainfall classes will further be indicated as 1-2, 2-5, 5-10, 10-15, and ≥ 15 mm. Third, data of all TF collectors with a funnel diameter of 24.2 cm ($n = 48$) were used to study TF at weekly and longer time intervals. The studied period then was from 27 June 2002 to 16 May 2004, since no manual TF collectors were in use between 17 May and 27 June 2002.

Throughout this chapter, a distinction is made between the leafed and leafless season (see 3.3.1 for the exact dates). Like in Chapter 3, the last week of leaf senescence was included into the leafless season because only very few leaves were present at that time and their influence on interception loss appeared to be negligible (see section 3.4.2, Fig. 3.5).

4.3.2.1 Spatial variability of throughfall

The spatial TF variability was expressed by means of the coefficient of variation (CV), i.e. the standard deviation as proportion of the mean. The CV of TF was calculated for temporal scales ranging from the rain event to the six-month interval, and for the cumulative TF of the rain events divided into the five above defined rainfall classes. The Mann-Whitney test was used to compare the CV of TF between the leafed and the leafless season. A non-parametric

test was used since the Shapiro-Wilk test showed that the CV distribution significantly ($p < 0.001$) deviated from normality.

The spatial patterns of the six-monthly cumulative TF in the leafed and the leafless season were also examined by geostatistical analysis, in which two steps can be distinguished (Deutsch and Journel, 1998): (i) defining the semivariogram, which indicates the degree of spatial autocorrelation among the data, and (ii) interpolating values between measured points based on the degree of autocorrelation encountered. Experimental semivariograms of TF water were computed with Surfer 7.0 software (Golden Software, 1999) for the small (14.2 cm diameter, $n = 50$) and large (24.2 cm, $n = 48$) TF collectors, using the smallest lag distance for which stable variograms were obtained. No anisotropy could be detected in the data. Spherical or Gaussian models with a nugget effect were fitted interactively by checking the statistical strength of the visually fitted model to allow a better focussing on the first lags (Schume *et al.*, 2003). A contour map of the TF water amount was obtained by global ordinary kriging (Golden Software, 1999).

4.3.2.2 Temporal stability of spatial throughfall variability

Two techniques were applied to investigate the temporal stability of the observed spatial patterns. The first technique was a correlation analysis. Pearson (r) and Spearman rank (r_s) correlation coefficients were calculated between the the annual TF amounts of both measuring years and among the six-month periods using all 24.2 cm diameter collectors ($n = 48$). Pearson r and Spearman r_s coefficients measure the extent of linearity and monotonicity of a relationship between two variables, respectively. Using the automated collectors ($n = 20$), correlation coefficients were calculated between the cumulative TF amounts per rainfall class as well as between the TF of individual events within the same rainfall class.

The second technique was the ‘time stability’ method (Vachaud *et al.*, 1985; Raat *et al.* 2002). For m periods and n locations, the method calculates the mean relative difference over time of the TF collected at location j ($\bar{\delta}_j$):

$$\bar{\delta}_j = \frac{1}{m} \sum_{t=1}^m \delta_{t,j} \quad (4.2)$$

where $\delta_{t,j}$ is the relative deviation from the mean at time t :

$$\delta_{t,j} = \frac{TF_{t,j} - \overline{TF}_t}{\overline{TF}_t} \quad (4.3)$$

and \overline{TF}_t is the mean TF over all locations j at time t :

$$\overline{TF}_t = \frac{1}{n} \sum_{j=1}^n TF_{t,j} \quad (4.4)$$

By plotting $\overline{\delta}_j$ ranked from smallest to largest, this parametric method of relative differencing graphically presents the constancy of temporal stability among locations. The time stability method was used for event TF after classifying events in five rainfall classes.

4.3.2.3 Relationship between throughfall and canopy structure

The relationship between canopy structure and TF amount was examined by calculating Pearson correlation coefficients between the TF amount at each sampling location and the canopy cover or plant area index above a location determined in the leafed and leafless season for three zenith angles. This correlation analysis was done for the six-month TF, the cumulative TF of events divided in rainfall classes, and TF at the rain event level.

At the level of individual rainfall events, the correlation between TF and canopy cover was related to rain event characteristics such as event rainfall amount, duration, and intensity (average, maximum 10-min and 60-min intensity), and average event wind speed. The determination of these rain event variables has been given in sections 3.3.2.3 and 3.3.3.1. The correlation between different rain event characteristics is discussed in section 3.4.3.

4.4 Results

Between 17 May 2002 and 16 May 2004 a total rainfall amount of 1384 mm was collected and an estimated snowfall amount of 63 mm (4% of gross precipitation), as reported in Chapter 3 (see section 3.4.1). The average annual precipitation of 724 mm was partitioned into 71% throughfall, 8% stemflow, and 21% interception. The throughfall fraction of rainfall was much lower in the leafed season (63%) than in the leafless season (81%), and was lower in the leafed season of the second measuring year (60%) than in the first year (66%). Stemflow amounted to 6% and 10% of rainfall in the growing and dormant season, respectively.

4.4.1 Spatial variability of throughfall

The spatial variability of TF water amount, as expressed by the median coefficient of variation (CV), decreased with increasing length of the sampling interval and was significantly ($p < 0.001$) higher during the leafed season than during the leafless season for each interval considered (Table 4.2).

Table 4.2. Minimum, median, mean \pm standard deviation (SD), and maximum coefficients of variation (%) of throughfall water calculated for different sampling intervals during the leafed season (L) and the leafless season (NL) using 20 (event sampling) or 48 collectors (weekly sampling interval and longer).

Sampling interval	No. of periods		Coefficient of variation (%)							
			Minimum		Median		Mean \pm SD		Maximum	
			L	NL	L	NL	L	NL	L	NL
Rain event	115	95	11	8	30	16	45 \pm 34	17 \pm 6	144	37
Week	43	40	10	8	24	12	24 \pm 7	13 \pm 4	50	25
Month	14	13	11	8	20	12	21 \pm 5	12 \pm 3	28	19
Six months	2	2	16	8	18	8	18 \pm 3	8 \pm 1	20	9

At the six-month sampling interval, the median CV of TF amount was 18% for the leafed season and 8% for the leafless season (Table 4.2). The range of relative TF as a fraction of the precipitation input was much higher in the leafed than in the leafless season (Fig. 4.2).

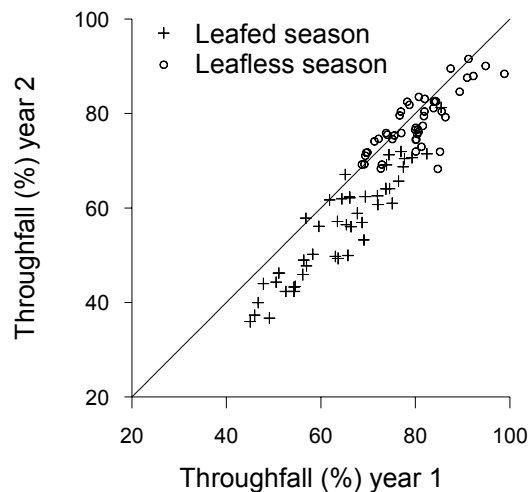


Fig. 4.2. Semi-annual throughfall (% of rainfall) during the leafed and leafless season for the two measuring years (2002-2003 and 2003-2004). The diagonal line indicates the 1:1 ratio.

Geostatistical analysis of the TF measured by the small collectors (14.2 cm diameter) showed that the semi-annual TF amount at two sampling locations with intermediate distance of 0.25

m was almost equal, and that the spatial correlation of TF in the growing as well as in the dormant season declined with increasing lag distance (Fig. 4.3a). According to the large TF collectors (24.2 cm diameter), the TF in the leafed season was spatially correlated up to a range of about 3-4 m, while the TF in the leafless season showed no spatial dependence (Fig. 4.3b). A contour plot of the TF amount during the leafed season of 2003 (Fig. 4.4) was obtained by ordinary kriging between the 48 sampling locations of the large TF collectors. A plot with a similar pattern was yielded for the leafed season TF of 2002.

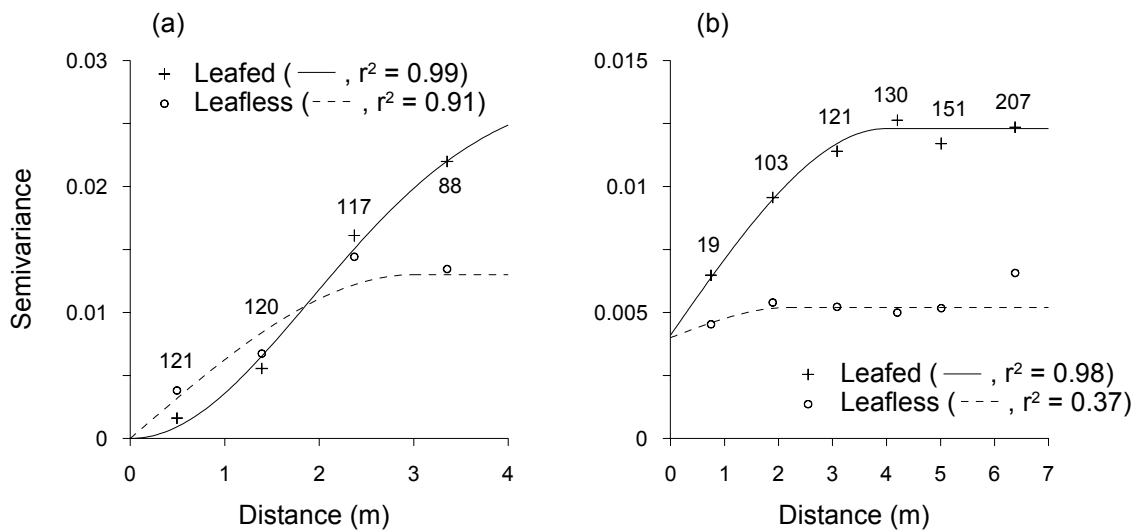


Fig. 4.3. Experimental semivariograms and fitted models of cumulative throughfall during the leafed and the leafless season of 2003-2004 based on measurements performed with (a) 50 collectors with a funnel diameter of 14.2 cm and (b) 48 collectors with a funnel diameter of 24.2 cm. The strength of the model fit and the number of pairs per lag distance are indicated.

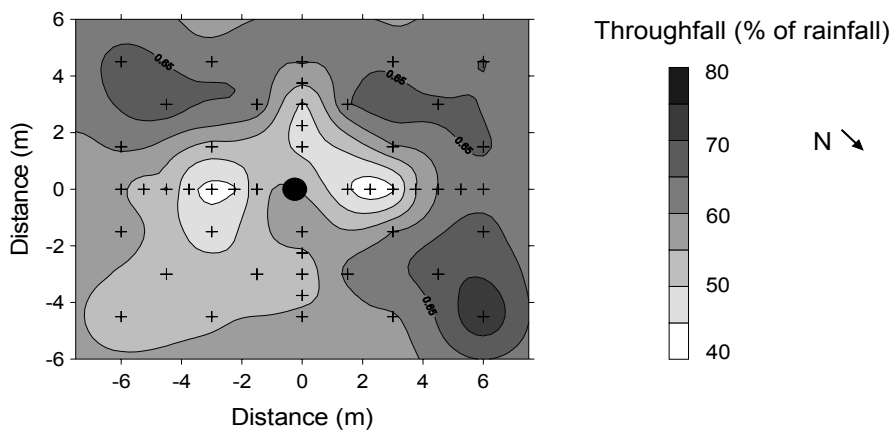


Fig. 4.4. Contour map of cumulative throughfall in the leafed season of 2003 obtained by ordinary kriging using the semivariogram of Fig. 4.3b. The positions of the 48 throughfall collectors and of the beech tree are indicated by crosses and a black dot, respectively.

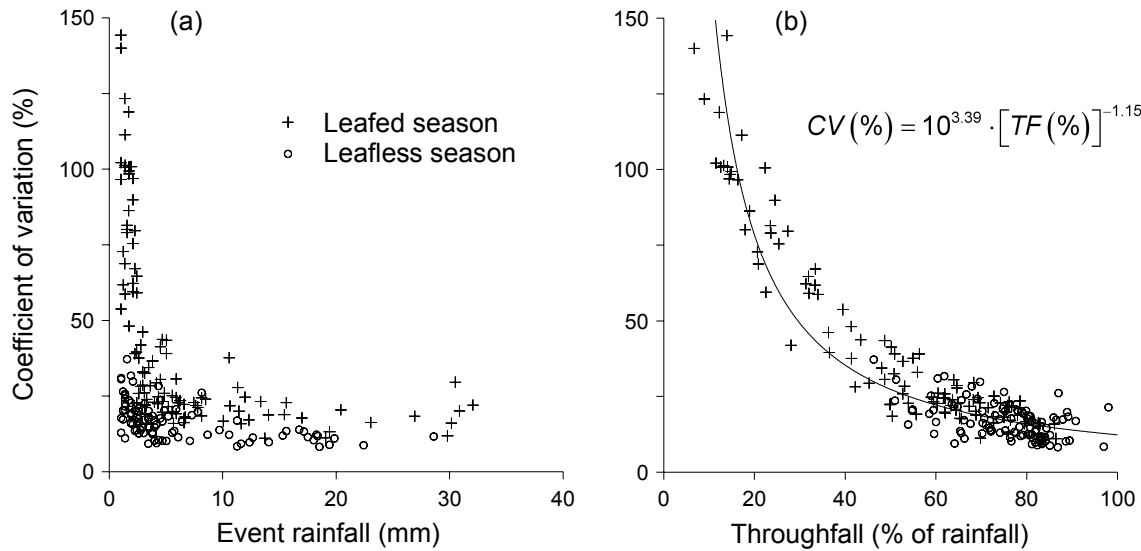


Fig. 4.5. Decline of the spatial coefficient of variation (%) of throughfall with (a) increasing rainfall amount (mm) and (b) increasing plot-average relative throughfall (% of rainfall) for rain events during the leafed season ($n = 115$) and the leafless season ($n = 95$).

At the rain event level, the spatial CV of TF decreased asymptotically with increasing rainfall amount (Fig. 4.5a). During the leafed season, the CV of TF decreased from a median value of 101% for events of 1-2 mm rainfall to stabilize at a median value of 19% for events ≥ 10 mm rainfall (Table 4.3). During the leafless season, the CV of TF decreased from 21% for 1-2 mm events to 11% for ≥ 10 mm events.

Table 4.3. Cumulative rainfall (mm), throughfall and stemflow (% of rainfall), as well as median spatial variation coefficient of throughfall (CV (%), $n = 20$) per rainfall class (mm) for 344 events during the leafed (L) and the leafless season (NL) of both measuring years.

Rainfall (mm)	No. of events		Rainfall (mm)		Throughfall (%)		Stemflow (%)		Median CV (%)	
	L	NL	L	NL	L	NL	L	NL	L	NL
0 - < 1	72	62	26	24	0.2	2.2	0.0	0.6	-	-
1 - < 2	32	24	43	37	1.5	5.3	0.1	1.3	101	21
2 - < 5	37	39	118	135	12	21	8	16	33	16
5 - < 10	22	13	142	89	19	14	17	16	22	14
10 - < 15	11	6	131	84	20	15	19	15	20	10
15 - 32	13	13	310	246	47	42	56	51	18	12
Total	187	157	769	614	100	100	100	100	29	16

Thus, similarly to the semi-annual TF, event TF was spatially significantly ($p < 0.001$) more variable during the leafed season than during the leafless season. Nevertheless, a strong negative relationship was observed between the CV of event TF and the proportion of rainfall

reaching the forest floor as TF throughout the whole year (Fig. 4.5b). The best fit was obtained with the following power function:

$$CV_{TF}(\%) = 10^{3.39} \cdot [TF(\%)]^{-1.15} \quad (r^2 = 0.82, p < 0.001, n = 210) \quad (4.5)$$

4.4.2 Temporal stability of spatial throughfall patterns

At the annual level, a strong correlation was observed between the TF amounts in the first and the second measuring year (Pearson $r = 0.88$, Spearman $r_s = 0.86$, $p < 0.001$, $n = 48$). The semi-annual TF amounts were more closely correlated among the leafed periods ($r = 0.92$, $r_s = 0.91$) than among the leafless periods ($r = 0.78$, $r_s = 0.74$) (Fig. 4.2), and were not correlated between the two periods ($r = 0.01$, $r_s = -0.05$, $p > 0.50$). Since the r and r_s values were very similar also for the correlation analyses discussed in the next paragraph, only r_s values are reported below.

At the scale of the cumulative TF of events divided into five rainfall classes (Table 4.4), correlation coefficients were highest between the summed TF of events with similar rainfall amounts. For example, the cumulative TF amount of 1-2 mm rain events during the leafed season was more closely correlated with the TF amount of 2-5 mm events ($r_s = 0.88$) than with the TF amount of 5-10 mm events ($r_s = 0.68$) (Table 4.4). The cumulative TF amounts of the rainfall classes were not significantly correlated between the leafed and leafless season, similarly to the result of the six-month TF.

Table 4.4. Spearman rank correlation coefficients ($n = 20$) between the cumulative throughfall (TF) of rain events within rainfall classes in the leafed season (values upper right) and the leafless season (values lower left), and between the leafed and the leafless season (italic values on the diagonal). The time stability at the rain event level is given by the percentage of pairs of events within a rainfall class that was significantly ($p < 0.05$) positively correlated.

TF (mm)	TF of events within rainfall class (mm)					Time-stable* pairs of events (%)	
	1 - < 2	2 - < 5	5 - < 10	10 - < 15	15 - 32	Leafed	Leafless
1 - < 2	<i>0.36</i>	0.88***	0.68**	0.69**	0.57**	42	14
2 - < 5	0.87***	<i>0.10</i>	0.86***	0.83**	0.74***	74	30
5 - < 10	0.65**	0.84***	<i>-0.29</i>	0.85***	0.71***	41	45
10 - < 15	0.73***	0.86***	0.66**	<i>-0.11</i>	0.83***	45	33
15 - 32	0.51*	0.71***	0.47*	0.81***	<i>0.19</i>	50	37

Significance levels: * $p < 0.05$; ** $p < 0.01$; *** $p < 0.001$. Non-significant ($p > 0.05$) values are indicated in italic.

At the level of individual rainfall events, TF amounts of events within the same rainfall class were generally positively correlated with each other. A significant ($p < 0.05$, $n = 20$) positive Spearman correlation coefficient between event TF was found for 56% of the pairs of events ($n = 1526$) within the same rainfall class during the leafed season and for only 28% of the pairs of events ($n = 1188$) during the leafless season (Table 4.4).

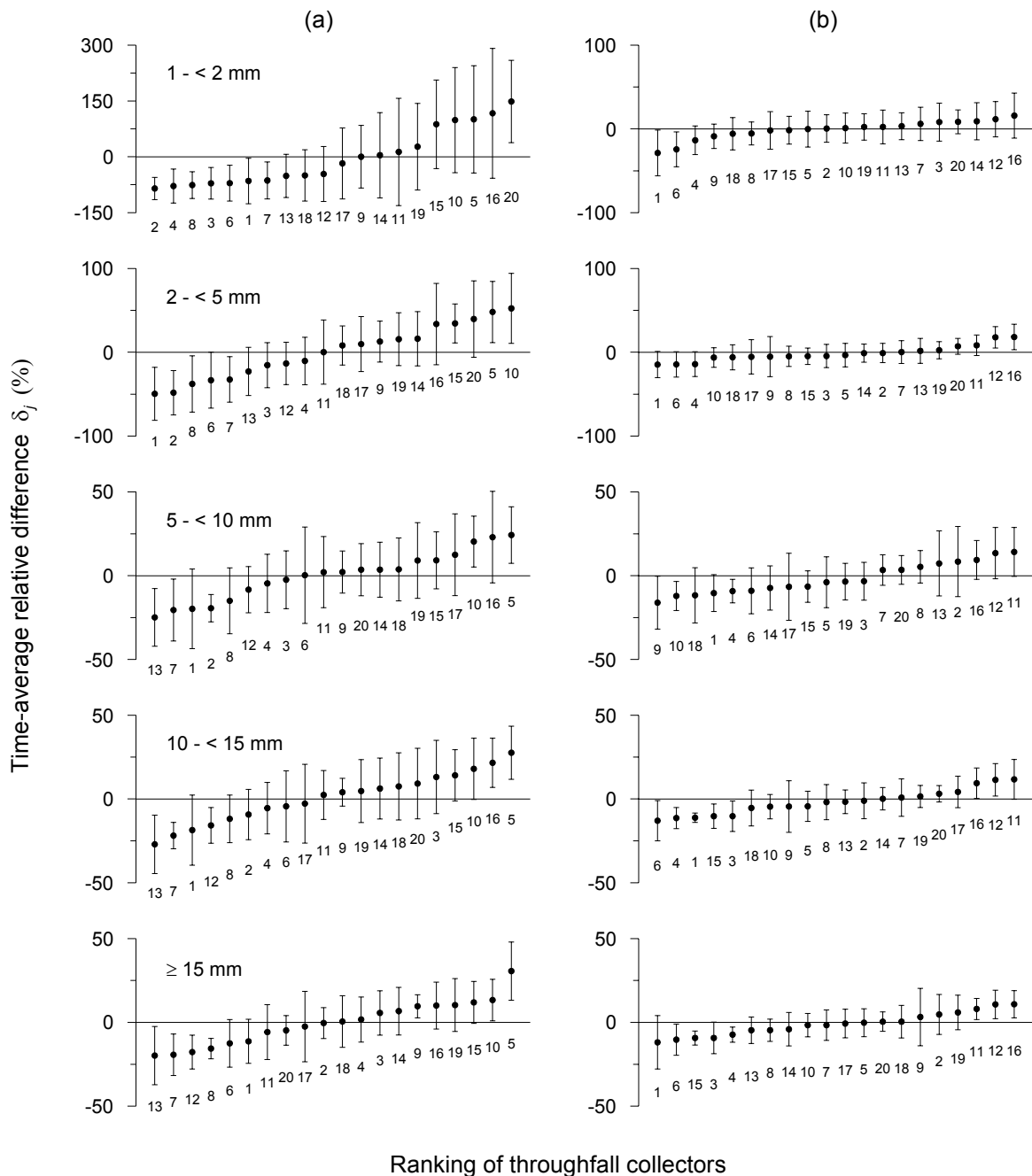


Fig. 4.6. Time stability plots for throughfall water (TF). Time-average relative deviation of TF amount (Eq. 4.2) by collectors for events grouped within five rainfall classes during (a) the leafed season and (b) the leafless season. Error bars are plus and minus one standard deviation; numbers refer to collector number ($n = 20$) (cf. Fig. 4.1). The number of events in each rainfall class is given in Table 4.3.

The degree of time stability of TF water at the event scale is visualized in Fig. 4.6. For example, the collector that received on average the lowest TF amount for 1-2 mm rainfall events in the leafed season (collector 2, Fig. 4.6a), received on average also low TF amounts for 2-5 mm and 5-10 mm events. Nevertheless, for the leafed season events ≥ 15 mm rainfall, this collector (2) received on average the mean plot TF amount (Fig. 4.6a). The error bars indicate the considerable temporal deviation around the mean relative difference for each sampling point. The collector numbers (cf. Fig. 4.1) in Fig. 4.6 confirm the lack of relationship between TF amounts in the two periods of the year that was already expressed by the correlation analyses (cf. Table 4.4). The time stability plots also illustrate that the spatial variability of TF was greater in the leafed than in the leafless season (cf. Table 4.2).

4.4.3 Relationship between throughfall and canopy structure

The plot-average canopy cover was 94% (PAI = 4.8) during the leafed season and 55% (PAI = 0.9) during the leafless season. Canopy cover above the TF collectors determined with a zenith angle of 3.8° ranged from 81 to 99.7% in the leafed season and from 35 to 72% in the leafless season. The measured canopy structure above the sample locations was significantly positively correlated between the leafed and the leafless season ($r = 0.79$ for cover, $r = 0.71$ for PAI, $p < 0.001$, $n = 20$). The computed values for the canopy extinction coefficients (Eq. 4.1) used to derive PAI from canopy cover were 0.7 in summer and 0.9 in winter.

The total TF water amount in the leafed season (TF_L) was significantly negatively correlated with canopy cover above the 20 automated collectors measured for zenith angles of 3.8° ($r = -0.54$, $p = 0.014$) (Fig. 4.7a, Table 4.5) and 5.7° ($r = -0.66$, $p = 0.001$) (Table 4.5). According to the correlation coefficients, TF_L was only slightly better correlated with leafed PAI (PAI_L) than with leafed canopy cover (Table 4.5). However, the relationship between TF_L and canopy cover for zenith angles of 1.9° and 3.8° was not confirmed for some sampling points near the canopy edge that had a canopy cover of less than 90% (Fig. 4.7a). Excluding these points led to a better correlation between TF_L and canopy cover determined for the 3.8° zenith angle ($r = -0.63$, $p = 0.005$, $n = 18$), and resulted in a significant correlation coefficient for the smallest zenith angle (1.9°) ($r = -0.62$, $p = 0.004$, $n = 17$).

When canopy cover was converted to plant area index (PAI_L), the sample points with canopy cover $< 90\%$ hardly affected the relationship between TF_L and PAI_L (e.g., for the 3.8° zenith angle, $r = -0.56$ for $n = 20$, $r = -0.53$ for $n = 18$) (Fig. 4.7b). Note that the calculated correlation coefficients were not influenced by the value of the canopy extinction coefficient

(Eq. 4.1). Correlations coefficients for all 48 TF collectors were approximately equal to those for the 20 TF collectors on the 3 x 3 m grid, but are not reported because of the spatial autocorrelation between sampling locations closer than 3 m (Fig. 4.3b).

Table 4.5. Pearson correlation coefficients ($n = 20$) between throughfall water amount (TF) in the leafed season (semi-annual TF and summed TF of events within rainfall classes) and canopy cover or plant area index (PAI) determined in the leafed and leafless season for three zenith angles above the automated TF collectors.

Season	Parameter	Angle (°)	TF in the leafed season					
			Semi-annual TF	Summed TF of events within rainfall class (mm)				
				1 - < 2	2 - < 5	5 - < 10	10 - < 15	15 - 32
Leafed	Canopy cover	1.9	-0.35	-0.64**	-0.45*	-0.30	-0.38	-0.19
		3.8	-0.54*	-0.73***	-0.59**	-0.53*	-0.52*	-0.37
		5.7	-0.66**	-0.75***	-0.69***	-0.62**	-0.56**	-0.55*
	PAI	1.9	-0.43	-0.63**	-0.51*	-0.38	-0.41	-0.29
		3.8	-0.56**	-0.73***	-0.67**	-0.59**	-0.46*	-0.38
		5.7	-0.60**	-0.72***	-0.68***	-0.61**	-0.47*	-0.47*
Leafless	Branch cover	1.9	-0.71***	-0.72***	-0.70***	-0.68***	-0.73***	-0.57**
		3.8	-0.77***	-0.74***	-0.75***	-0.78***	-0.75***	-0.63**
		5.7	-0.82***	-0.68***	-0.74***	-0.82***	-0.77***	-0.75***

Significance levels: * $p < 0.05$; ** $p < 0.01$; *** $p < 0.001$. Non-significant ($p > 0.05$) values are indicated in italic.

TF_L was more closely correlated with the branch architecture determined in winter than with the foliated canopy structure determined in summer (Fig. 4.7, Table 4.5). The relationship of TF_L to branch and twig cover was equal as to the derived woody PAI (Fig. 4.7d), because, according to Eq. 4.1, PAI is almost linearly related to canopy cover if cover is less than 90%. The correlation coefficients between TF_L and branch cover increased for greater zenith angles, but the difference in correlation was less pronounced than between TF_L and the leafed canopy cover (Table 4.5). In contrast to the significant negative correlation between TF_L and branch cover, the total TF amount in the leafless season (TF_{NL}) was not significantly correlated with the branch cover for any of the zenith angles used ($r > -0.22$, $p > 0.20$, $n = 20$). At the level of the TF amount of rainfall events divided into classes, the negative correlation between TF_L and PAI_L was stronger for the two largest zenith angles (Table 4.5), in consistence with the results for the semi-annual TF_L, and was stronger for the cumulative TF_L of small rain events (1-2 mm) than for larger events (≥ 15 mm). In contrast, the relationship

between TF_L and branch cover was significant ($p < 0.01$) for all rainfall classes, without declining trend in terms of the correlation coefficients (Table 4.5). The amount of TF_{NL} within rainfall classes was not significantly negatively correlated with branch cover ($r = -0.33$ to -0.05 , $p > 0.15$), except for the summed TF_{NL} of 5-10 mm events, which was positively but not-significantly correlated with branch cover ($r = 0.07$ to 0.22 , $p > 0.35$).

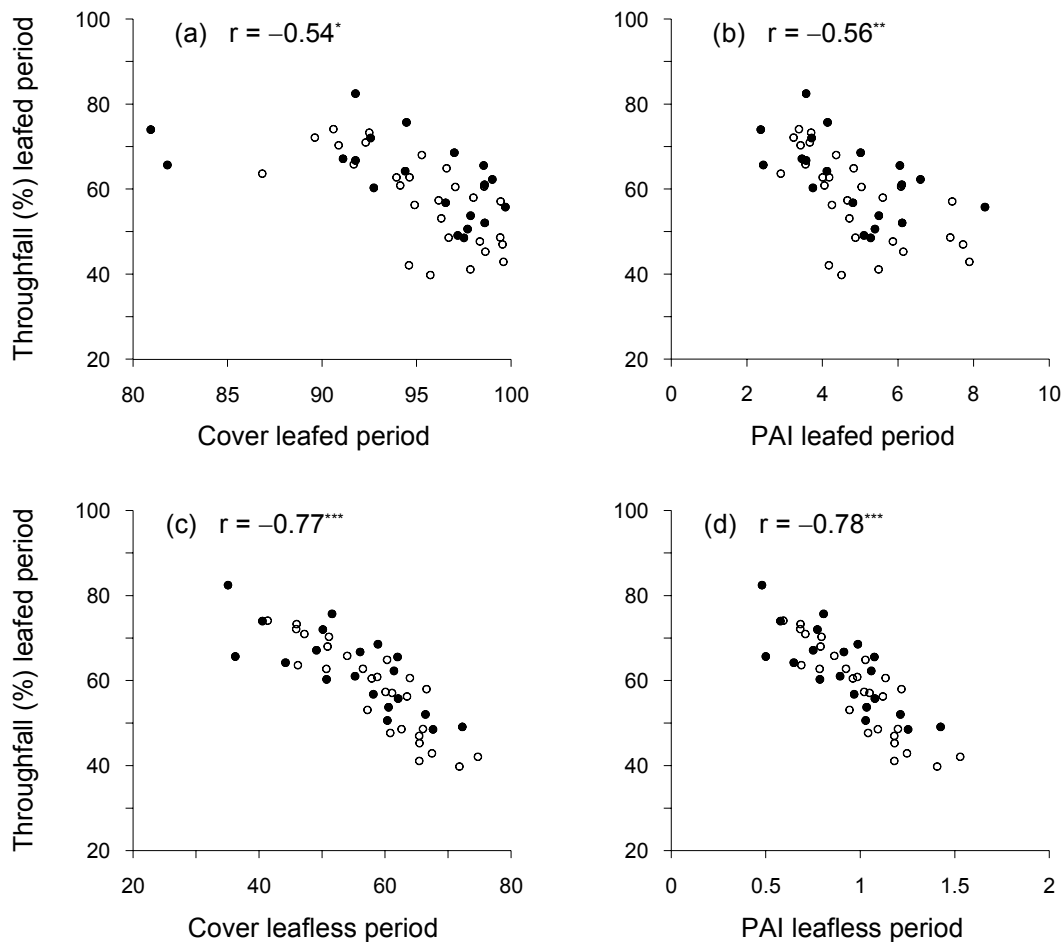


Fig. 4.7. Cumulative throughfall (% of rainfall) of the leafed season of both measuring years in relation to the canopy cover and derived plant area index (PAI) determined in the leafed and leafless season using a zenith angle of 3.8° above the sampling locations. The 20 automated and 28 manual collectors (cf. Fig. 4.1) are indicated by full and open circles, respectively. Pearson correlation coefficients are calculated for the 20 automated collectors only; significance levels cf. Table 4.5.

Finally, at the level of individual rain events, significant ($p < 0.05$) negative Pearson correlation coefficients between TF_L and branch cover were found for 57, 68, and 70% of the 115 events in the growing season using a 1.9 , 3.8 , and 5.7° zenith angle, respectively (Fig. 4.8). In contrast, TF_{NL} was only significantly negatively related to branch cover for 4% of the

90 rain events in the dormant season, and sometimes non-significant positive correlations were found (Fig. 4.8).

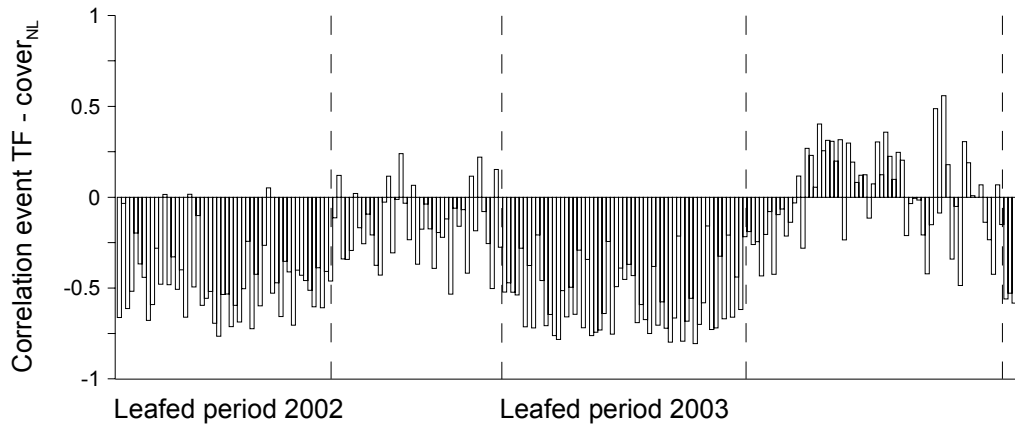


Fig. 4.8. Temporal development of the Pearson correlation coefficient between event throughfall and branch cover (determined using a zenith angle of 3.8° above the 20 automated collectors). Each bar represents one rain event (≥ 1 mm rainfall, $n = 210$); the x-axis is not linearly related to time. The dashed lines separate the leafed and leafless seasons. Correlation coefficients > 0.5 or < -0.5 are significant at $p < 0.02$.

To explain the variation within rain events in the relationship between event TF and woody cover above sampling points (cf. Fig. 4.8), the correlation between TF and woody cover was examined as a function of rain event characteristics. A significant relationship was only found in the leafed season for event wind speed. For rain events in the leafed season, the correlation between TF_L and woody canopy cover was weakly related ($r = 0.38$, $p < 0.001$, $n = 103$) to the average wind speed during rainfall (Fig. 4.9).

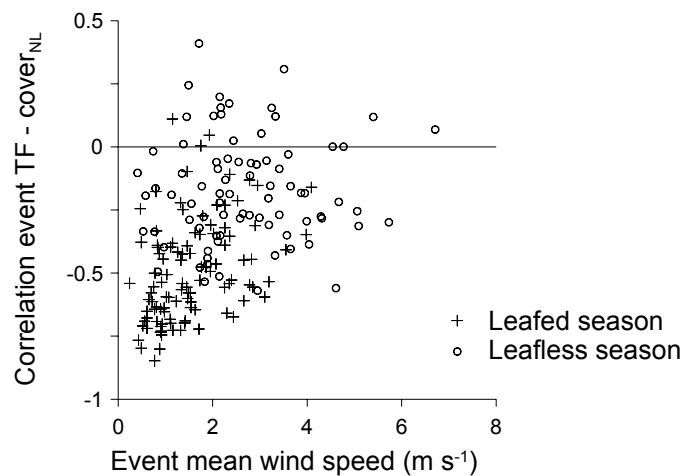


Fig. 4.9. Pearson correlation coefficient between event throughfall and branch cover (determined using a zenith angle of 1.9° above the 20 automated collectors) as a function of mean wind speed ($m s^{-1}$) during rain events.

4.5 Discussion

4.5.1 Spatial variability of throughfall in the leafed and leafless season

The present study confirms that forest canopies modify the spatial distribution of net precipitation reaching the forest floor. Under the canopy of one dominant beech tree, the weekly amount of TF water had a median spatial variation coefficient (CV) of 17%, which falls well within the range of 14% to 21% that has been observed at the stand scale in other temperate hardwood forests (Table 4.1). The results clearly demonstrate that the spatial variability of TF water is significantly ($p < 0.001$) higher during the leafed season than during the leafless season for each investigated time scale. Similarly, in an oak-hickory stand, Peterson and Rolfe (1979) found that there was considerably more variability in TF data in the summer than in other seasons, and attributed this primarily to the presence of a leafed canopy, which provides more sheltered areas and drip points than due to branch arrangement alone. Furthermore, we found that the median CV of TF decreased with increasing sampling interval (Table 4.2). Analogously, spatial variability of TF water in a mixed hardwood forest decreased exponentially according to the length of the study period from a median CV of 22% for weekly TF, 18% for monthly TF, to 14% for three-monthly and semi-annual TF (Houle *et al.*, 1999a).

It is well known that the variability of TF declines with increasing rainfall amount (Loustau *et al.*, 1992; Bellot and Escarre, 1998; Whelan and Anderson, 1996). For small rainfall amounts, differences in canopy interactions are relatively large resulting in a higher degree of spatial TF variability (Lin *et al.*, 1997) than for larger rain events, in which the water storage capacity of the canopy is satisfied (Carlyle-Moses *et al.*, 2004). The present study confirms the inverse relationship between TF variability and event rainfall amount, but shows that this relationship differs significantly between the growing and dormant season. Nevertheless, irrespective of foliage, the decline of TF variability could accurately be described as a function of the relative TF fraction of rainfall ($r^2 = 0.82$, Fig. 4.5b). Since relative TF was significantly lower in the growing season than in the dormant season, this suggests that both the lower TF fraction and the higher TF variability in the growing season are caused by a higher evaporated interception loss from the foliated canopy. A power function very similar to Eq. 4.5 was reported for events during the growing season in a mixed deciduous forest in Canada (Price and Carlyle-Moses, 2003; coefficients $10^{3.27}$ and -1.11 , $r^2 = 0.85$, $n = 28$).

The six-monthly amount of TF under the beech tree studied was spatially autocorrelated up to a range of about 3-4 m in the growing season. TF during the dormant season showed spatial dependence for the small TF collectors but not for the large ones, and a nugget effect was only observed in the semivariograms of the large collectors (Fig. 4.3). These two differences between collector types are likely due to the higher minimum intermediate distance of the large TF collectors, resulting in a lack of information on the spatial autocorrelation at the scale below 0.75 m. The negligible nugget effect of TF measured by the small collectors is important, as it implies that TF was almost equal at two locations with an intermediate distance of 0.25 m. Similar geostatistical studies of small-scale spatial TF patterns are scarce. According to Bouten *et al.* (1992), semivariograms showed that spatial patterns of TF around Douglas fir trees can be determined very effectively, but no further details were mentioned. No spatial autocorrelation between individual TF collectors was observed in a maritime pine stand (Loustau *et al.*, 1992) and a resprouting holm-oak forest (Bellot and Escarre, 1998). The small spatial range of TF in the present study suggests that perhaps no spatial dependence was found in these studies because the minimum sampling distance exceeded the possibly present spatial range of TF variability. TF water in an old-growth tropical wet forest in Costa Rica exhibited an autocorrelation range of 43 m, which appeared to be due to the high structural variability of the forest, characterized by large areas dominated by either individual tree canopies or by treefall gaps (Loescher *et al.*, 2002).

4.5.2 Temporal stability of spatial throughfall patterns

Previous studies have found both a systematic temporal trend in the spatial distribution of TF (Whelan and Anderson, 1996; Robson *et al.*, 1994) as well as a random TF distribution over time (Loustau *et al.*, 1992; Lin *et al.*, 1997), although the temporal stability has mostly been assessed for few events and in a non-quantitative way. In the present study, a significant time stability of TF patterns was found, which was higher in the leafed than in the leafless season and increased as the length of the sampling interval increased. At the six-monthly level, similar spatial TF patterns occurred in the two measuring years (Fig. 4.2). This was particularly true during the growing season, even though the TF fraction in the second growing season was lower than in the first one (Fig. 4.2) because of a different rainfall distribution (see section 3.5.2). Time-stability of the six-monthly TF is the result of many separate rain events with a correlated spatial TF variability. Although the degree of spatial variability differed between rain events of different rainfall classes (Table 4.3), the summed

TF amounts per rainfall class within the leafed and leafless seasons were significantly correlated with each other (Table 4.4). However, spatial TF patterns were not significantly correlated between the two considered periods of the year (Table 4.4). Although some rainfall characteristics and meteorological parameters during rain events differed significantly between the growing and dormant season (see section 3.4.3), this obviously indicates that foliage affected the spatial distribution of canopy drip to the forest floor. The time stability of spatial TF was lowest at the level of individual rain events, particularly for small events in non-foliated conditions (Table 4.4).

4.5.3 Relationship between throughfall and canopy structure

The observed negative relationship between beech canopy cover and the amount of TF during the leafed season confirms the results obtained in other forest types. In a lowland dipterocarp rain forest, annual TF decreased significantly with increasing litterfall ($r_s = -0.70$, $p < 0.001$, $n = 30$), which was assumed to be indicative of canopy biomass (Burghouts *et al.*, 1998). Mean normalized TF of seven collection periods of intermediate rainfall intensity (10-40 mm day⁻¹) was closely related ($r = -0.89$, $p < 0.001$, $n = 32$) to the amount of foliage in an old-growth coniferous forest (Nadkarni and Sumera, 2004). Whelan and Anderson (1996) quantified canopy cover to model the observed spatial variability of event TF water in a spruce forest. Significant negative relationships between TF and canopy cover were also found in a Mediterranean pine stand ($r_s = -0.54$, $p < 0.001$, $n = 40$) (Llorens and Gallart, 2000), and, more weakly, in a tropical wet forest in Costa Rica ($r = -0.33$, $p < 0.02$, $n = 36$) (Loescher *et al.*, 2002).

Research in spruce forests (Beier *et al.*, 1993; Hansen, 1996; Whelan and Anderson, 1996) shows that a systematic heterogeneous water distribution under forest canopies can be due to (i) non-homogeneous distribution of rain drops as a consequence of turbulent air flow just above and within the canopy, (ii) translocation of water within the canopy, and/or (iii) differences in interception loss related to canopy density. In the present study, the effect of a non-homogeneous rainfall distribution on TF variability was assumed to be negligible because of the small plot size, and also the possible effect of non-vertical rainfall on interception patterns (Herwitz and Slye, 1995) was assumed to be small because of the low wind speeds at the site. We found that the TF amount during the leafed season (TF_L) was significantly negatively correlated with the canopy cover or PAI above sampling locations (Table 4.5, Fig. 4.7), indicating that the canopy structure contributes to the spatial distribution

of TF_L by a heterogeneous interception and subsequent evaporation of rainfall. PAI better described the decline in TF_L over the total cover range than canopy cover (Fig. 4.7). The finding that the amount of TF_L was more closely related to the canopy structure determined using the larger zenith angles (3.8 and 5.7°) suggests that the water input at a point of the forest floor is affected by a relatively large canopy volume. Similarly, Llorens and Gallart (2000) found a better relationship between TF and the canopy cover for a zenith angle of 7.8° than for smaller ones, while Nadkarni and Sumera (2004) related TF to the amount of foliage measured within a cylinder of 1 m radius above the sampling locations. Whelan and Anderson (1996) quantified canopy cover for an area of approximately 1.6 x 2.3 m² at 15 m height. Besides a systematic component in the variability of throughfall, non-systematic throughfall variability occurs which may be due to turbulence above the canopy, wind direction (Weihe, 1984), and wind speed (Hörmann *et al.*, 1996). We found little evidence for the influence of event characteristics other than rainfall amount on the relationship between canopy structure and the throughfall pattern beneath the canopy. During the leafed season, the correlation between TF_L and branch cover tended to decline with increasing event wind speed (Fig. 4.9), which may be due to water drops falling more inclined to the forest floor by the wind.

The spatial variability of TF_L was better explained by the degree of branch cover than by the combined cover of leaves and branches together (Fig. 4.7, Table 4.5), but TF_{NL} was not related to branch cover. Because the local canopy structure was significantly positively correlated between the growing and the dormant season, a straightforward explanation for the higher correlation between TF_L and branch cover could be that photographs in non-foliated conditions more reliably estimate potential local foliage density than summer photographs. However, the strength and the significance of the relationship between TF_L and foliated canopy cover declined with increasing rainfall amount class, while the relationship between TF_L and branch and twig cover was significant for all five classes (Table 4.5). Therefore, the results suggest that branches and twigs additionally affect the spatial distribution of TF_L , which may be due to enhanced water interception and stemflow generation. First, branches have a larger water storage capacity than leaves (Herwitz, 1985; Llorens and Gallart, 2000), and hence may contribute to the spatial variability of TF water for large rain events, in contrast to leaves, whose influence on TF patterns declines after complete wetting (Carlyle-Moses *et al.*, 2004). Second, the funnel-like branching architecture and smooth bark of beech trees lead to an efficient gathering of water from the branches to the stem (Herwitz, 1987; Levia and Frost, 2003), which may reduce TF under canopy parts with high branch cover.

In contrast to the growing season, the spatial variability of TF water in the dormant season (TF_{NL}) could not be explained by the simple measure of branch structure used. This may be related to the low interception loss in the dormant season, decreasing the decline of TF water with increasing branch cover. More importantly, there was no clear relationship between the spatial variability of TF_L and TF_{NL} (Table 4.4), which indicates that other factors drive the variability of TF in the dormant season than in the growing season. As illustrated in Fig. 4.9, the generally higher wind speed during rain events in the dormant season (see section 3.4.3) could not explain the lacking correlation between TF_{NL} and woody canopy cover. Stemflow water amounted to a larger fraction of rainfall in the dormant season, but the local stemflow generation apparently was too small to contribute significantly to the spatial TF variability and/or was only weakly correlated with the amount of twigs and branches. Using the data of the automated collectors, we noticed that TF_{NL} at some sampling points exceeded the rainfall input for some individual rain events, although this seldom occurred for weekly sampling intervals. The occurrence of such temporary ‘dripping points’ may explain why TF_{NL} at the rain event level had a low temporal stability (Table 4.4) and was sometimes positively though not significantly correlated with branch cover (Fig. 4.8).

4.6 Conclusions

The spatial variability of the amount of throughfall water (TF) under one dominant beech tree was similar to the previously reported stand-scale variability of TF. As the length of the sampling period increased, the spatial variability of TF decreased and the temporal stability of the TF pattern increased. The spatial TF pattern in the growing season was better explained by branch cover than by the foliated canopy structure, showing that branching architecture is an important parameter for rainfall redistribution when the canopy is fully leafed. The spatial TF pattern in the dormant season was less pronounced than in the growing season due to the lower interception loss. Although time stability of TF was also observed during the dormant season, the spatial TF pattern under the defoliated tree was not related to the growing season pattern and could not be explained by the measured branch cover above sampling locations. We conclude that during the growing season both canopy leaves and tree branches affect the spatial variability of TF water amount by the process of interception loss. Most studies on throughfall and stemflow generation in deciduous forests are conducted in the leafed season, and further research is necessary to improve our understanding of the spatial redistribution of precipitation during the leafless season.

5 Seasonal variation in throughfall and stemflow chemistry in relation to canopy phenology

After: Staelens, J., De Schrijver, A. and Verheyen, K. Seasonal variation in throughfall and stemflow chemistry beneath a beech (*Fagus sylvatica* L.) tree in relation to canopy phenology. Submitted to an international journal with peer review.

5.1 Abstract

Precipitation, throughfall and stemflow were measured biweekly over a 1-year period to examine the effect of canopy phenology on major ion fluxes beneath a mature beech (*Fagus sylvatica* L.) tree. Annual and semiannual ion fluxes to the forest floor were significantly ($p < 0.001$) higher than the incoming wet-only deposition for all measured ions other than H^+ , which was significantly reduced after canopy passage. Stemflow contributed 9 to 19% of the annual ion input to the forest floor except for H^+ (40%). The ratio of annual throughfall to wet deposition ranged from 2.1 to 4.8, except for K^+ (43) and H^+ (0.16). Throughfall enrichment ratios of K^+ , Ca^{2+} , Mg^{2+} , and NO_3^- were significantly higher in the leafed than in the leafless season, while Na^+ , NH_4^+ , and H^+ were more enriched in the leafless season. The analysis of throughfall and stemflow enrichment for four phenological canopy phases indicated leaching of Na^+ , Cl^- , and NH_4^+ from emerging leaves and of Cl^- and SO_4^{2-} from senescing leaves, in addition to leaching of K^+ , Ca^{2+} , and Mg^{2+} throughout the leafed season. Using a modified seasonal canopy budget method, the contribution of canopy leaching to annual net throughfall and stemflow was estimated at 96% (K^+), 54% (Ca^{2+}), 40% (Mg^{2+}), 12% (Cl^-), and 7% (Na^+ , SO_4^{2-}). Dry deposition estimates accounted for 58-75% of the total atmospheric deposition onto the beech canopy. The relatively high throughfall enrichment during the leafless season indicated a much higher particulate and gaseous dry deposition onto the woody canopy than expected in the absence of foliage as well as K^+ release from beech branches.

5.2 Introduction

Throughfall water can contribute large amounts of nutrients to forest floors (Parker, 1983), and may have some control on the acid-base status of the soil by altering incoming precipitation (Bélanger *et al.*, 2004). Furthermore, throughfall ion deposition is often used for estimating total atmospheric input to forests to assess potential effects of air pollution on the diversity, and functioning of forest ecosystems (de Vries *et al.*, 2003). Interpreting throughfall measurements in nutrient cycling and atmospheric deposition studies requires a distinction between in-canopy sources and atmospheric input of chemical compounds, since both wash-off of dry deposition and ion exchange processes contribute to the modified ion composition of water flowing through a forest canopy (Lovett and Lindberg, 1984). Dry deposition is the direct deposition of particles and gases from the atmosphere to the vegetation without involvement of precipitation or fog droplets (Andersen and Hovmand, 1999). Canopy exchange comprises passive ion diffusion and/or exchange between the water layer covering canopy tissues and the underlying apoplast, as well as uptake of gases through stomata (Draaijers *et al.*, 1997).

The contribution of dry deposition and canopy exchange to throughfall enrichment is ion-specific. Canopy exchange of sodium and chloride is generally considered to be negligible (Draaijers *et al.*, 1997), and Na^+ and Cl^- enrichment in throughfall compared to precipitation is attributed to washing off of dry deposition only. Likewise, sulphur is usually assumed to be conservative with respect to the canopy, as stomatal uptake of SO_2 is thought to be balanced by canopy leaching of SO_4^{2-} in throughfall (Butler and Likens, 1995; Kovács and Horváth, 2004). For nitrogen, in contrast, significant canopy uptake and assimilation of gaseous compounds and dissolved ammonium and nitrate ions have been reported (Boyce *et al.*, 1996; Harrison *et al.*, 2000; Gessler *et al.*, 2000). Calcium, magnesium, and potassium are known to be leached from vegetative surfaces, and this leaching has partly been attributed to canopy retention of H^+ (Cronan and Reiners, 1983) and NH_4^+ (Roelofs *et al.*, 1985) by ion exchange reactions (Stachurski and Zimka, 2002).

Both dry deposition and canopy exchange processes are influenced by a large number of variables and can vary significantly in space and time (Lovett *et al.*, 1996; Morris *et al.*, 2003). The dry deposition of gases and particles from the atmosphere to a receptor surface is governed by air concentration and by turbulent transport processes in the aerodynamic boundary layer, as well as by the chemical and physical nature of the depositing compound and the capability of the surface to capture gases and particles (Erisman and Draaijers, 2003).

Consequently, the amount of dry deposition at a given time and place depends on meteorological factors such as wind speed and air humidity, the strength and proximity of emission sources, and on vegetation characteristics such as tree species, tree height, and leaf area index (Lovett *et al.*, 1996; Andersen and Hovmand, 1999) that affect surface roughness. Precipitation characteristics influencing canopy exchange include the composition and acidity of precipitation (Schaefer *et al.*, 1988, Hansen, 1996, Lovett *et al.*, 1996), and precipitation amount (Potter *et al.*, 1991; Lovett *et al.*, 1996), duration (Reiners and Olson, 1984), and intensity (Hansen *et al.*, 1994). Furthermore, canopy exchange is affected by ion contents in the canopy, which depends on tree species, age, and nutrient status of the forest (Parker, 1983; Houle *et al.*, 1999b), canopy leaf area (Lovett *et al.*, 1989), and physiological state of the vegetation (Morris *et al.*, 2003).

Because several of these factors act at relatively large scales, the spatio-temporal variability of throughfall deposition at the plot scale can be expected to depend mostly on atmospheric conditions, precipitation characteristics and the local canopy structure. With respect to the spatial heterogeneity of throughfall within forest stands, previous research indicates that the input of water and nutrients to the forest floor may be related to the local canopy and branch structure (Beier *et al.*, 1993; Whelan and Anderson, 1996; see Chapter 6). With respect to the temporal variability of throughfall, most attention has been paid to the relationship between throughfall chemistry and the temporal distribution and composition of precipitation events (Potter *et al.*, 1991; Lovett *et al.*, 1996).

In broadleaved deciduous forest stands, a considerable temporal variation in canopy cover and physiological activity occurs throughout the year, which likely affects both dry deposition and canopy exchange. Nevertheless, throughfall and stemflow fluxes in deciduous forest types have mostly been measured during the leafed growing season. Even when ion fluxes are quantified during the leafless season, research often focuses on annual means, so that there is relatively little information on the interaction of incident precipitation with the woody canopy of trees during the dormant season (Houle *et al.*, 1999b; Levia and Frost, 2003; Pryor and Barthelmie, 2005). Therefore, the aims of this chapter were (i) to quantify throughfall and stemflow ion deposition throughout the year beneath a deciduous beech (*Fagus sylvatica* L.) canopy, (ii) to examine the effect of seasonal changes in canopy cover and phenology on throughfall and stemflow chemistry, and (iii) to estimate ion exchange within the deciduous canopy per phenological canopy phase.

5.3 Materials and methods

The study site is described in section 3.3.1. The chemical composition of throughfall water was measured during one year using a subset of the experimental setup described in section 3.3.2. The beech trees at the study site were in leaf from 25 April until 18 November 2003. These 30 weeks subsequently will be called the leafed season. Within the leafed season a distinction was made between three periods: leaf emergence, the fully leafed period, and leaf senescence, as described below (section 5.3.2.2).

5.3.1 Data collection

5.3.1.1 Water fluxes

Bulk precipitation and throughfall (TF) were sampled weekly from 4 March 2003 to 4 March 2004. Wet-only precipitation was sampled weekly from 4 March 2003 to 9 December 2003. In the forest stand a 35 m high meteorological tower is located 50 m from the study plot. Wet-only precipitation was measured on top of the tower by an automatic wet-only sampler (Eigenbrodt). An electrical, resistance-driven rain sensor (RS 85, Eigenbrodt) with a delay of 1 s activated the opening of the lid. Additional information on the sampling of wet-only precipitation is given in section 2.3.2. Bulk precipitation was measured on top of the tower using two collectors with a funnel diameter of 24.2 cm (460 cm²). The funnels had a sharp-edged vertical rim, a slope of 45°, and were set at a height of 36.5 m above ground level. Precipitation drained into 2-l polyethylene bottles at 35 m height that were wrapped in aluminium foil to keep the samples cool. A nylon 1-mm wire mesh placed in the funnels prevented contamination by large particles.

TF water was measured using 12 collectors that were set in a 3 x 3 m grid under the beech canopy (Fig. 5.1). TF collectors were of the same type as the bulk precipitation samplers, and were set at a height of 1.5 m above ground level. The collecting bottles were placed below ground level to avoid the growth of algae and to keep the samples cool. Funnels, wire meshes, and bottles were replaced weekly by equipment rinsed by demineralised water. Precipitation and TF water amounts were determined by weight in the laboratory. Stemflow water of the beech tree was collected by a spiral type gauge, and measured by means of a self-constructed tipping bucket with bucket content of 0.2 l. The outflow was collected in a 200 l container and sampled at least weekly from 4 March 2003 to 4 March 2004.

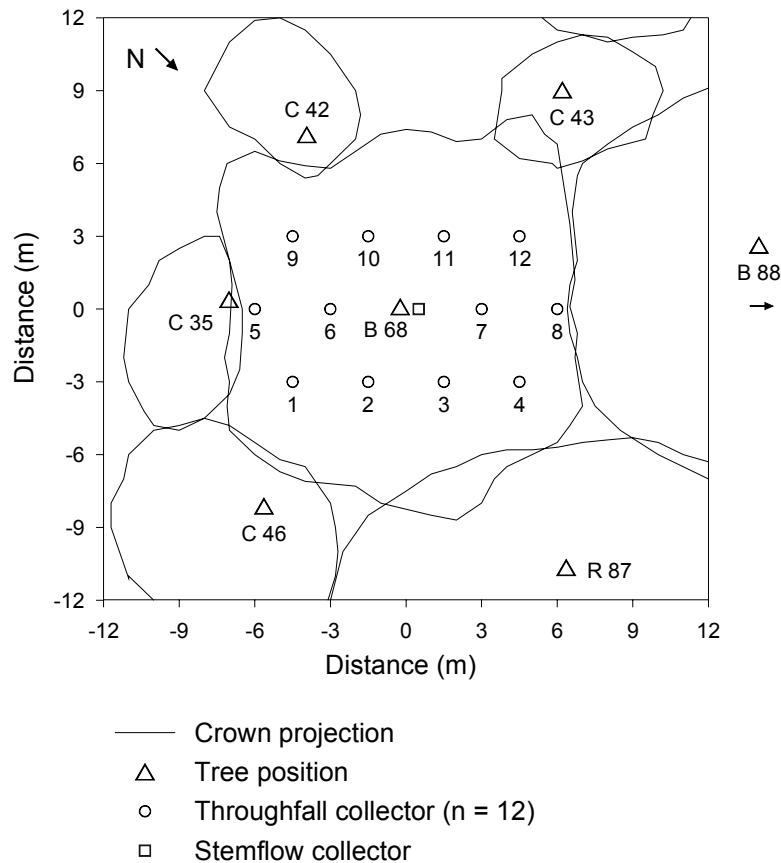


Fig. 5.1. Experimental set up in the Aelmoeseneie forest, Gontrode (Belgium) to measure ion fluxes to the forest floor. Tree labels indicate tree species (C: common oak, B: European beech, R: American red oak) and diameter (cm) at 1.3 m height.

5.3.1.2 Chemical analysis and data quality

Precipitation and stemflow water were analysed weekly until December 2003 and biweekly afterwards. Weekly samples of TF were pooled biweekly for chemical analysis. Water samples were transported and stored in darkness at 5 °C, and pH (ion-specific electrode) and conductivity were measured within 24 h after sampling. After filtering through a 0.45- μm nylon membrane filter, NO_3^- , SO_4^{2-} , PO_4^{3-} , and Cl^- were determined with ion chromatography (Dionex) within one week after sampling. Ammonium was analysed by the photometric determination of a reaction product of NH_4^+ at 660 nm (Dutch standard method NEN 6567), and K^+ , Ca^{2+} , Mg^{2+} , and Na^+ were determined by flame atomic absorption spectrophotometry. H^+ concentrations were derived from the pH measurements.

The chemical analyses were validated by including method blanks and repeated measurements of internal and certified standard reference samples (CRM 409, Quevauviller *et al.*, 1993). Determination limits (DL, $\mu\text{mol}_\text{c} \text{ l}^{-1}$) of the chemical analyses were 1.8 (Na^+), 1.0 (K^+), 4.4 (Ca^{2+}), 1.6 (Mg^{2+}), 4.2 (NH_4^+), 4.0 (NO_3^-), 5.2 (SO_4^{2-}), 5.6 (Cl^-), and 6.3 (PO_4^{3-}). The

coefficient of variation of five repeated measurements of CRM 409 samples throughout the year was smaller than 5% and the recovery was higher than 95% for all ions. Furthermore, the quality of the chemical analyses was evaluated by comparing measured (x) and calculated (y) conductivity of water samples (mean \pm standard error of regression slope = 0.926 ± 0.020 and $r^2 = 0.982$ for precipitation; slope = 0.992 ± 0.014 and $r^2 = 0.996$ for TF; slope = 0.996 ± 0.005 and $r^2 = 0.996$ for SF) and by checking the ion balance. When all major ions are analysed, the charge difference between cations and anions is ascribed to the presence of organic anions, or to bicarbonate for samples with sufficiently high pH (Driscoll *et al.*, 1989; Chiwa *et al.*, 2004). The bicarbonate concentration of water samples was estimated from the pH, using a dissociation constant pK_{CO_2} of 7.8 and a partial CO₂ pressure of 0.3 mbar (de Vries *et al.*, 2001). Phosphate concentration was below or around DL, indicating that samples were not contaminated by bird droppings (Erisman *et al.*, 2003).

5.3.2 Data analysis

5.3.2.1 Ion fluxes

Ion deposition ($\text{mmol}_e \text{ m}^{-2}$) was calculated by multiplying the amount of water collected by ionic concentration divided by the area of the collector openings. Stemflow volume was transformed to depth using the surface area of the horizontal canopy projection, which was approximately 180 m^2 . Snowfall occurred during one week of the study period. Because of the undercatch of above-canopy snowfall measurements (Allerup *et al.*, 1997), the precipitation amount for this sampling week was assumed to be equal to the maximum TF amount measured in this week. The bulk precipitation measurements from 9 December 2003 to 4 March 2004 were corrected for dry deposition of particles and gases onto the funnels by site-specific bulk:wet-only concentration factors, derived at the study site from 4 March 2003 to 9 December 2003 (see Chapter 2). Wet deposition was calculated by multiplying wet-only rainfall concentrations with the rainfall amounts collected by the bulk collectors, because the latter were identical to the throughfall collectors. Wet-only and bulk rainfall amounts were not significantly different (see section 2.4.2).

5.3.2.2 Temporal variability of ion fluxes and correlation between ions

The temporal evolution of the biweekly wet deposition (WD), throughfall (TF), and stemflow (SF) fluxes was first examined visually. To account for seasonal variations in WD, the biweekly net throughfall (NTF) flux was calculated as TF-WD, and the net stand deposition

(NSD) at the plot level as $TF+SF-WD$. In addition, the biweekly ratio of TF to WD (TF:WD) was determined (Neary and Gizyn, 1994; Michopoulos *et al.*, 2001). One-sample t-tests ($n = 12$) were used to examine whether the annual and semiannual NTF and NSD deposition differed significantly from zero. Positive net ion fluxes indicate ion enrichment by the canopy due to dry deposition and/or internal canopy leaching, negative values indicate uptake of ions from throughfall by the canopy.

Then, the significance of the differences between the leafed (25 April until 18 November 2003) and the leafless season was determined. For each ion, WD, plot-average TF, and SF were compared between the leafed ($m = 13$ sampling intervals) and the leafless ($m = 9$) season with a Wilcoxon rank sum test for independent samples. Since the TF ion deposition was determined for individual collectors ($n = 12$), TF, NTF, and TF:WD could also be compared statistically between the leafed and leafless season with a Wilcoxon signed rank test for two related samples. As the growing season was longer than the dormant season, this analysis was performed on the average biweekly ion deposition per collector in the two periods of the year, calculated by dividing the deposition in the leafed (30 weeks) and leafless (22 weeks) season by 15 and 11, respectively. There were two biweekly sampling intervals without precipitation in both the leafed and leafless season.

Finally, relations between ions in NTF deposition were examined by visual inspection of plots of ion pairs and by correlation and regression analysis. Spearman rank correlation coefficients (r_s) were calculated between the NTF deposition of 12 individual collectors for 22 sampling intervals ($n_{tot} = 264$), and by distinguishing four phenological phases: the leafed season was divided into (i) period of budbreak and leaf unfolding (25 April to 6 May), subsequently indicated as leaf emergence, (ii) fully leafed period (6 May to 30 September), and (iii) leaf senescence (1 October to 18 November), in addition to (iv) the leafless season. All statistical analyses were performed with SPSS for Windows (SPSS Inc., 2003).

5.3.2.3 Canopy budget method

To estimate the contribution of dry deposition (DD) and canopy exchange (CE) to the net stand deposition, a modified version of the canopy budget method reported by Draaijers and Erisman (1995) was used. The canopy budget method is presented and discussed in detail in Chapter 7. In this method, the NSD ($TF+SF-WD$) of Na^+ , Cl^- , NO_3^- , and SO_4^{2-} is assumed to be due to DD only, and CE is assumed to be zero. Furthermore, the ratio of DD to WD of Na^+ is assumed to be valid for particles containing K^+ , Ca^{2+} , and Mg^{2+} . The annual DD of the

latter cations X is calculated by multiplying WD_X by $(DD:WD)_{Na}$, and canopy leaching is estimated as $(NSD-DD)_X$. Canopy uptake of NH_4^+ and H^+ is assumed to be equal to the canopy leaching of K^+ , Ca^{2+} , and Mg^{2+} that is not associated with weak acid release; with NH_4^+ and H^+ taken up in a proportion equal to their average ratio in WD and TF+SF but accounting for a more efficient uptake of H^+ by a factor of 6 (see Eq. 7.8). The canopy release of weak acid anions is calculated by assuming that the DD of weak acids equals the WD.

Based on the results of the present research, the canopy budget method was slightly modified and applied for each of the four phenological canopy phases separately instead of annually. The method was modified to include canopy leaching of Na^+ , Cl^- , and SO_4^{2-} during leaf emergence and/or senescence, and to account for the leaching of weak acids as well as Na^+ , Cl^- , and SO_4^{2-} to estimate canopy uptake of H^+ and NH_4^+ .

5.4 Results

5.4.1 Precipitation, throughfall, and stemflow deposition

The annual precipitation amount of 613 mm (4 March 2003 to 2004) was partitioned into 67% throughfall (TF), 8% stemflow (SF), and 25% interception (Table 5.1). Annual as well as semiannual ion deposition to the forest floor (TF+SF) was significantly ($p < 0.001$) higher than the incoming wet deposition (WD) for all measured ions, except for H^+ , which was significantly reduced after canopy passage (Table 5.1).

Table 5.1. Annual wet-only deposition (WD), bulk deposition (BD), throughfall (TF, mean \pm standard deviation, $n = 12$), stemflow (SF), and net stand deposition (NSD = TF+SF-WD) of water (mm) and major ions ($mmol_c m^{-2}$), and ratio of throughfall to wet-only deposition (TF:WD) and stemflow to stand deposition (SF:(TF+SF)).

	Annual water (mm) and ion ($mmol_c m^{-2}$) deposition					Ratio (-)	
	WD	BD	TF	SF	NSD	TF:WD	SF:(TF+SF)
Water	612.6 ^a	612.6	410.4 \pm 31.9	51.6	-150.5	0.67	0.11
H^+	4.0	1.9	0.6 \pm 0.1	0.4	-3.0	0.16	0.38
Na^+	30.0	44.3	77.3 \pm 7.3	18.1	65.5	2.6	0.19
K^+	1.2	2.5	49.6 \pm 6.9	5.1	53.4	42.8	0.09
Ca^{2+}	10.9	19.2	47.4 \pm 6.6	5.3	41.8	4.3	0.10
Mg^{2+}	6.8	10.2	25.7 \pm 3.7	3.3	22.2	3.8	0.11
NH_4^+	33.5	36.9	89.5 \pm 16.7	15.2	71.2	2.7	0.15
NO_3^-	18.2	22.7	38.8 \pm 4.5	4.1	24.7	2.1	0.10
SO_4^{2-}	27.7	35.8	105.0 \pm 16.5	14.8	92.1	3.8	0.12
Cl^-	33.0	50.2	100.4 \pm 10.6	23.6	91.1	3.0	0.19
w.a. ^b	7.5	6.4	46.0 \pm 10.3	4.7	43.2	4.8	0.09

^a Wet deposition calculated by wet-only rainfall concentrations and bulk rainfall amounts.

^b Weak acids (w.a.) calculated as the difference between measured cations and anions.

Consequently, the ratio of annual TF to wet deposition (WD) exceeded one for all ions other than H^+ , and generally ranged from 2.1 to 4.8 (Table 5.1). The annual TF:WD ratio of K^+ (43) was much higher than for the other ions. The most important ions in net stand deposition (NSD) were NH_4^+ , Na^+ , SO_4^{2-} , and Cl^- . The HCO_3^- fluxes calculated from the pH hardly contributed to the annual fluxes of the sum of measured anions in WD (3%), TF (1%), and SF (0.4%). The contribution of SF to the annual TF + SF ion deposition was 38% for H^+ , 15-19% for NH_4^+ , Na^+ , and Cl^- , and about 10% for the other measured ions (Table 5.1).

According to the unrelated samples rank test, WD of Na^+ , Cl^- , and Mg^{2+} was significantly ($p < 0.05$) higher in the leafless season than in the leafed season (Fig. 5.2, Table 5.2), while in TF, fluxes of Na^+ , Cl^- , and SO_4^{2-} were higher ($p < 0.05$) in the leafless than in the leafed season.

Table 5.2. Average biweekly wet deposition (WD), throughfall (TF), stemflow (SF), and ratio of throughfall to wet-only deposition (TF:WD) in the leafed (L) and the leafless (NL) season. Bold values indicate whether a deposition flux or ratio was significantly ($p < 0.05$) higher in the leafed or leafless season of the year.

	Biweekly water (mm) and ion ($mmol_c m^{-2}$) deposition						Ratio (-)	
	WD ^a		TF ^b		SF ^a		TF:WD ^b	
	L	NL	L	NL	L	NL	L	NL
Water	22.40	25.14	12.88	19.75	1.53	2.61	0.57	0.79
H^+	0.15	0.16	0.01	0.05	0.00	0.03	0.04	0.31
Na^+	0.64	1.85	1.51	4.97	0.16	1.44	2.35	2.69
K^+	0.04	0.05	2.49	1.11	0.14	0.26	58.77	23.39
Ca^{2+}	0.42	0.42	2.09	1.46	0.07	0.38	4.95	3.52
Mg^{2+}	0.17	0.39	0.87	1.15	0.03	0.26	5.25	2.93
NH_4^+	1.30	1.27	3.26	3.69	0.50	0.70	2.51	2.90
NO_3^-	0.78	0.59	1.83	1.03	0.14	0.18	2.35	1.76
SO_4^{2-}	1.00	1.16	3.71	4.49	0.31	0.92	3.71	3.88
Cl^-	0.72	2.01	2.19	6.15	0.22	1.85	3.03	3.05
w.a. ^c	0.23	0.37	2.51	0.75	0.23	0.11	11.14	2.01

Note: The leafed season includes leaf emergence, fully leafed period, and leaf senescence.

^a Wilcoxon rank sum test between plot-average deposition per sampling interval in the leafed season ($m = 15$) and leafless season ($m = 11$).

^b Wilcoxon signed rank test between time-average biweekly deposition of individual TF collectors ($n = 12$) in the leafed and leafless season.

^c Weak acids (w.a.) calculated as the difference between measured cations and anions.

However, for TF and its derived variables TF-WD and TF:WD, a more powerful related samples rank test was possible, which demonstrated that the TF deposition of all ions differed significantly ($p < 0.01$, $p = 0.023$ for NH_4^+) between the leafed and leafless season (Table 5.2, Fig. 5.2). The TF deposition of K^+ , Ca^{2+} , NO_3^- , and calculated weak acids was higher in the leafed season, while TF of all other measured ions was higher in the leafless season.

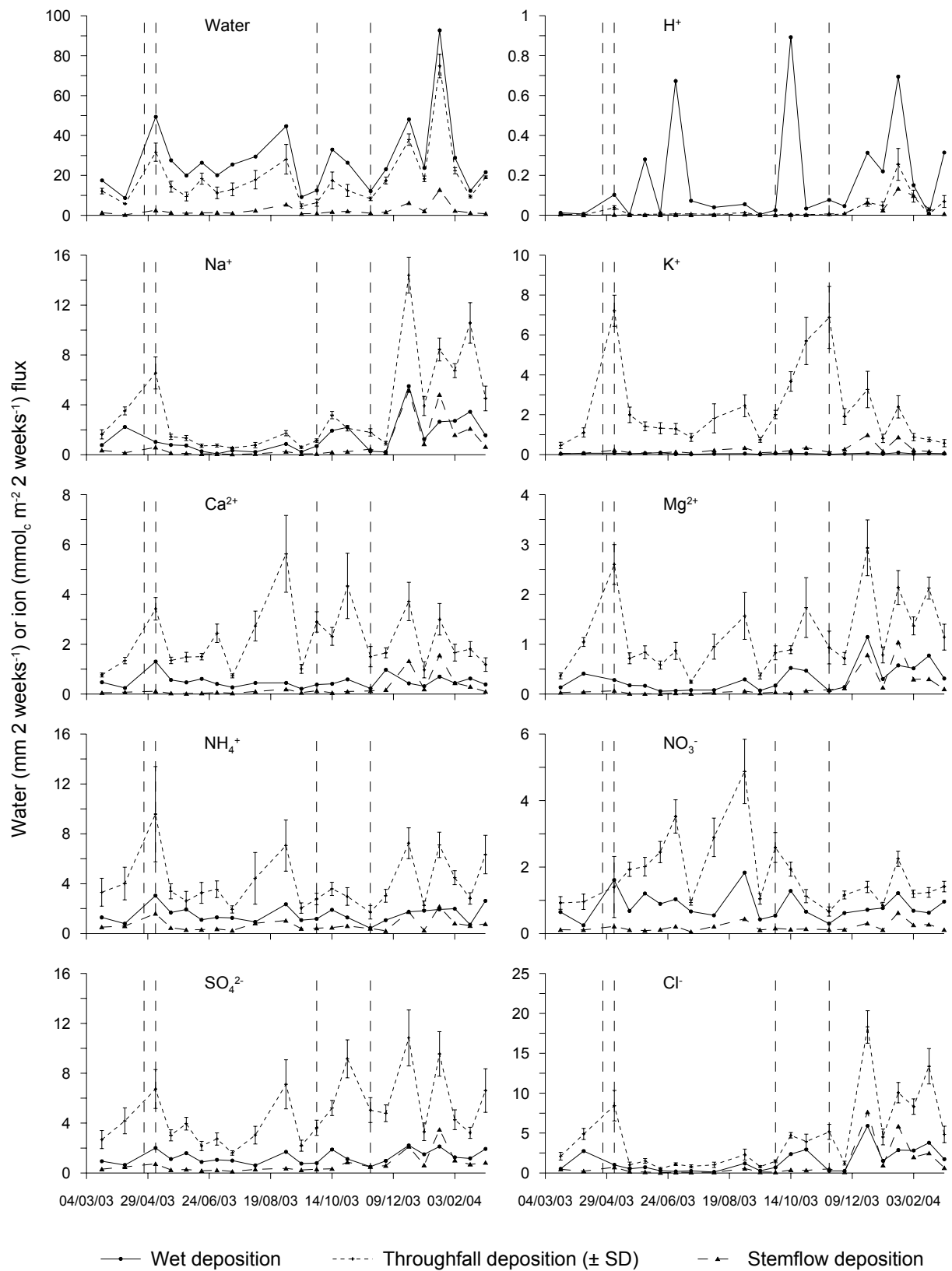


Fig. 5.2. Wet-only precipitation, throughfall (\pm standard deviation, $n = 12$), and stemflow water ($\text{mm } 2 \text{ weeks}^{-1}$) and ion flux ($\text{mmol}_c \text{ m}^{-2} 2 \text{ weeks}^{-1}$) from 4 March 2003 to 4 March 2004. The dashed vertical lines separate the phenological canopy phases.

In general, similar statistical results as for TF were obtained for TF-WD and TF:WD. For Mg^{2+} , TF-WD differed not significantly between the leafed and leafless season. The TF:WD ratio of Mg^{2+} was significantly higher in the leafed than in the leafless season (Table 5.2) because the strong Mg^{2+} increase in WD during the leafless season (+130% compared to the leafed season) was accompanied by only a moderate Mg^{2+} increase in TF (+30%). For Cl^- and SO_4^{2-} , TF:WD differed not significantly between the leafed and leafless season. The most pronounced temporal pattern was observed for K^+ , with strongly increasing TF:WD during leaf emergence and leaf senescence (Fig. 5.2, Fig. 5.3). Almost half (48%) of the annual NTF of K^+ occurred during leaf emergence and senescence, although these periods accounted for only 15% of the study time. The TF to WD ratio also increased for Na^+ , Mg^{2+} , and Cl^- during the short period of leaf emergence, and for Ca^{2+} and SO_4^{2-} during leaf senescence (Fig. 5.3).

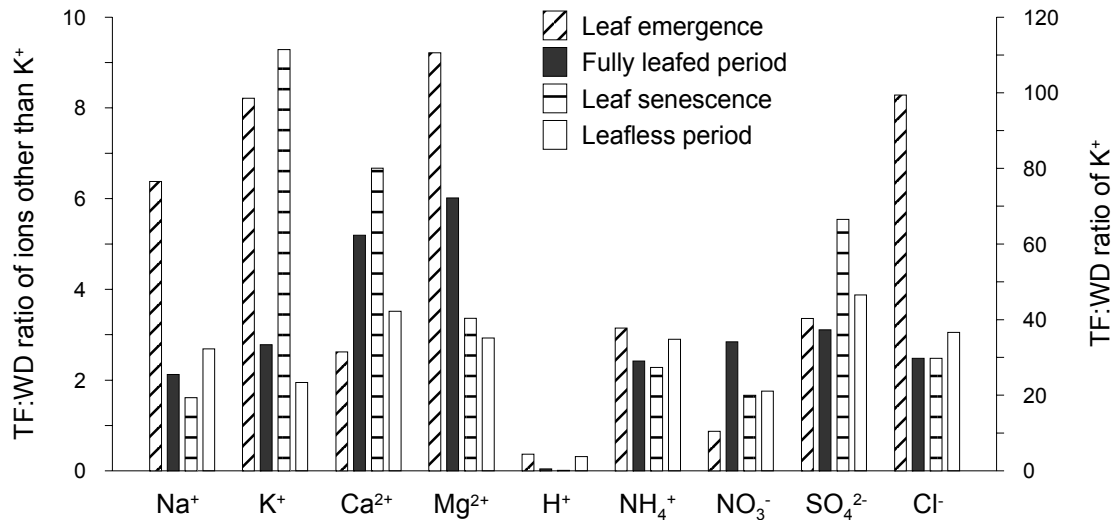


Fig. 5.3. Ratios of throughfall to wet ion deposition (TF:WD) during four phenological canopy phases.

Ion deposition by SF was significantly ($p < 0.02$) higher in the dormant season than in the growing season for all ions other than NO_3^- and NH_4^+ (Table 5.2). The higher SF deposition in the dormant season was due to significantly ($p < 0.07$) higher ion concentrations as well as higher (n.s.) water fluxes in SF. The average volume-weighted (vw) ion concentrations of SF were similar in the leafed and leafless season for NO_3^- , NH_4^+ , and K^+ , but increased in the leafless season for the other ions by 1.7 (SO_4^{2-}), 3.2 (Ca^{2+}) to more than 5 times (Na^+ , Cl^- , and Mg^{2+}). This increase in SF concentration during the leafless season was not due to seasonal differences in rainfall concentration for Ca^{2+} and SO_4^{2-} , as the mean vw ion concentration of WD was similar in the two periods of the year. For Na^+ , Cl^- , and Mg^{2+} , the vw concentration

of WD was 2 to 2.6 higher during the leafless than the leafed season, which is less than the fivefold increase in SF. For H^+ , the vw concentration of SF was an order of magnitude higher (13 times) in the leafless season than in the leafed season. In contrast to the negligible H^+ input by TF ($0.10 \text{ mmol}_c \text{ m}^{-2}$) and SF ($0.02 \text{ mmol}_c \text{ m}^{-2}$) during the leafed season, higher H^+ depositions occurred during the leafless season (0.65 and $0.39 \text{ mmol}_c \text{ m}^{-2}$ by TF and SF, respectively). During the leafed season, the average vw pH increased from 5.2 in WD to 6.3 in TF (Fig. 5.4) and to 6.0 in SF. During the leafless season, the pH of WD (5.2) increased to only 5.6 in TF and decreased to 4.9 in SF.

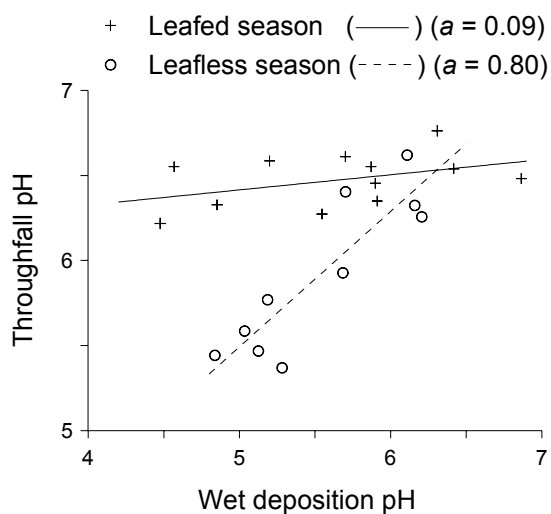


Fig. 5.4. Relation between pH of biweekly wet deposition and throughfall (plot-average, $n = 12$) in the leafed season (including leaf emergence and senescence) and the leafless season. The lines indicate single linear regressions ($y = a \cdot x + b$) fitted to the seasonally divided data, for which the slope (a) is given. Leafed season: $y = 0.09 \cdot x + 6.0$ ($r^2 = 0.17$, $p = 0.18$, $m = 12$); leafless season: $y = 0.80 \cdot x + 1.5$ ($r^2 = 0.87$, $p = 0.001$, $m = 10$).

5.4.2 Ion correlations in net throughfall deposition

The relation between the biweekly NTF deposition (TF-WD, $\text{mmol}_c \text{ m}^{-2} \text{ 2 weeks}^{-1}$) of the sum of measured cations (H^+ , NH_4^+ , Na^+ , K^+ , Ca^{2+} , and Mg^{2+}) and the sum of anions (measured Cl^- , NO_3^- , SO_4^{2-} and calculated HCO_3^-) clearly differed between the four distinguished canopy phases. The anion deficit in NTF, which represents the flux of unmeasured anions of weak organic acids, was negligible during the leafless season, pronounced during leaf emergence, and moderate during the fully leafed period and during leaf senescence (Fig. 5.5). During leaf emergence, the calculated weak acid flux in NTF was significantly positively correlated with the NTF flux of Mg^{2+} ($r_s = 0.57$, $p = 0.05$, $n = 12$) and NH_4^+ ($r_s = 0.89$, $p < 0.001$) (Fig. 5.6a). During the fully leafed period, weak acid deposition in NTF was significantly ($p < 0.001$, $n =$

108) correlated with all cations other than H^+ ($r_s = 0.81$ for NH_4^+ (Fig. 5.6a), $r_s = 0.71$ for K^+ (Fig. 5.6b), $r_s \sim 0.50$ for Ca^{2+} and Mg^{2+}). The smaller NTF flux of weak acids during leaf senescence (Fig. 5.5) was significantly ($p < 0.001$, $n = 36$) correlated with Mg^{2+} ($r_s = 0.74$), K^+ ($r_s = 0.66$), and Ca^{2+} ($r_s = 0.52$).

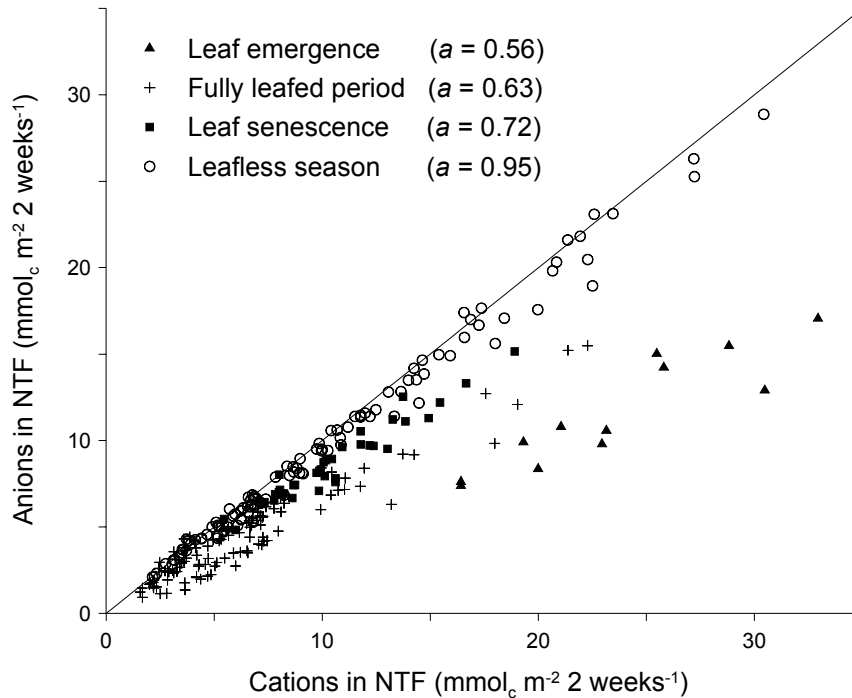


Fig. 5.5. Relationship between net throughfall (NTF) deposition ($mmol_c m^{-2} 2 weeks^{-1}$) of anions and cations for 12 individual throughfall collectors during four phenological canopy phases ($n_{tot} = 264$). For each period the slope (a) of the linear regression ($y = a \cdot x + b$) is given. The diagonal line indicates the 1:1 ratio. Leaf emergence: $y = 0.56 \cdot x - 1.6$ ($r^2 = 0.81$); fully leafed period: $y = 0.63 \cdot x + 0.6$ ($r^2 = 0.92$); leaf senescence: $y = 0.72 \cdot x + 0.8$ ($r^2 = 0.92$); leafless season: $y = 0.95 \cdot x - 0.1$ ($r^2 = 0.99$). All regressions significant at $p < 0.001$.

The relationship between cations and anions was examined per anion, beginning with Cl^- . During the short period of leaf emergence, the NTF deposition of both Na^+ and Cl^- increased strongly compared to the fully leafed and leaf senescence periods (Fig. 5.2, Fig. 5.7). During the last two weeks of leaf senescence, in contrast, NTF deposition of Cl^- increased while NTF of Na^+ remained relatively low (Fig. 5.7). Hence, the Cl^- to Na^+ ratio in NTF during this November sampling was significantly higher ($2.7 mol_c mol_c^{-1}$) than during the rest of the year ($1.3 mol_c mol_c^{-1}$). The biplots (not shown) suggested that the additional Cl^- flux in NTF during the last two weeks of senescence, calculated from the Cl^- to Na^+ ratio of the rest of the year, was most closely correlated with K^+ ($r_s = 0.76$, $p = 0.004$, $n = 12$).

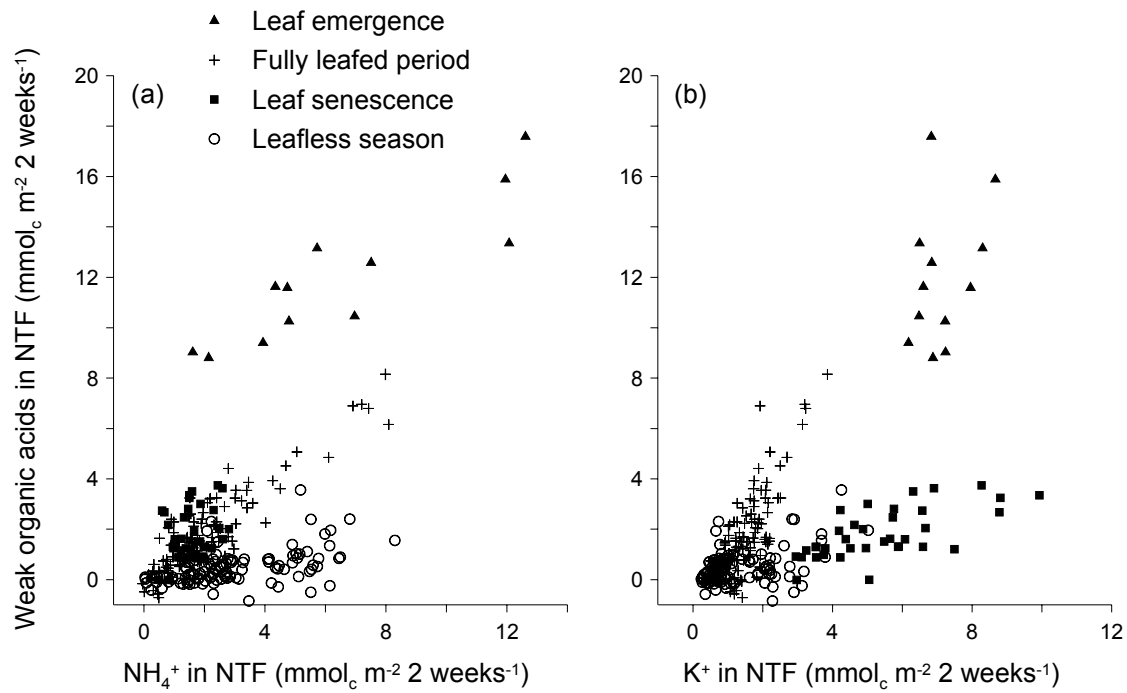


Fig. 5.6. Relationship between net throughfall (NTF) deposition ($\text{mmol}_c \text{m}^{-2} 2 \text{ weeks}^{-1}$) of weak organic acids (calculated as the anion deficit) and (a) NH_4^+ , and (b) K^+ for 12 individual throughfall collectors during four phenological canopy phases ($n_{tot} = 264$).

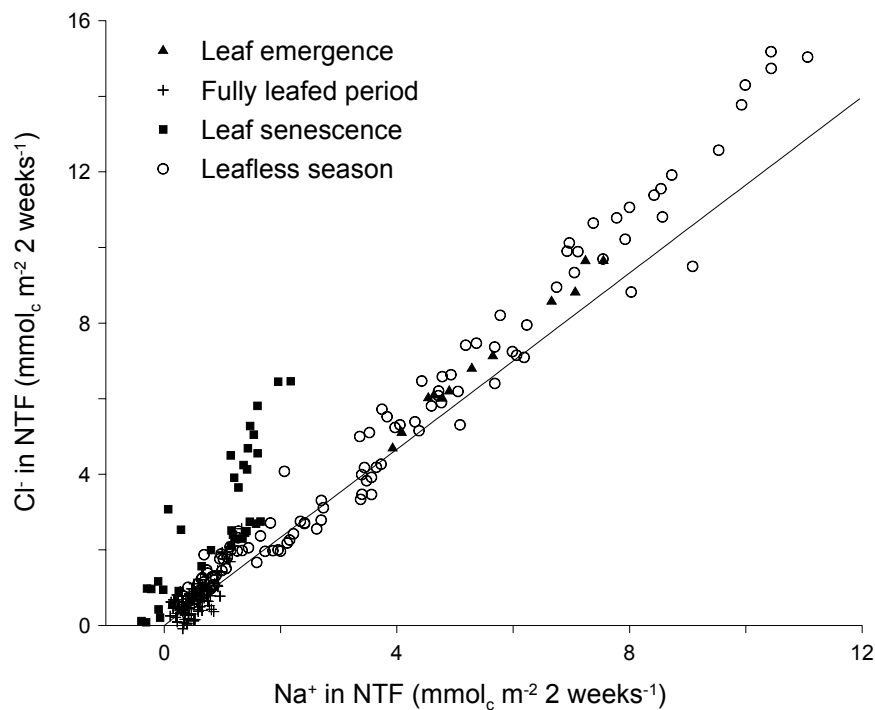


Fig. 5.7. Relationship between net throughfall (NTF) deposition ($\text{mmol}_c \text{m}^{-2} 2 \text{ weeks}^{-1}$) of Cl^- and Na^+ for 12 individual throughfall collectors during four phenological canopy phases ($n_{tot} = 264$). The diagonal line indicates the $\text{Cl}^-:\text{Na}^+$ ratio of seawater ($1.166 \text{ mol}_c \text{mol}_c^{-1}$; de Vries *et al.*, 2003).

With respect to SO_4^{2-} , a distinct seasonal difference was observed in the relationship between the NTF deposition of Ca^{2+} and SO_4^{2-} (Fig. 5.8a). During the fully leafed period, similar NTF amounts of SO_4^{2-} ($22 \text{ mmol}_c \text{ m}^{-2}$) and Ca^{2+} ($17 \text{ mmol}_c \text{ m}^{-2}$) were measured ($r_s = 0.83$, $p < 0.001$, $n = 108$), while the slope of the SO_4^{2-} to Ca^{2+} regression was 2.2 to 2.9 during the other three canopy phases. This confirms that the throughfall enrichment of Ca^{2+} was highest during the fully leafed period, in contrast to the enrichment of SO_4^{2-} (Fig. 5.3). Regarding to Mg^{2+} , an increased Mg^{2+} to SO_4^{2-} ratio was observed in NTF during leaf emergence (Fig. 5.8b; $r_s = 0.78$, $p = 0.003$, $n = 12$), in agreement with the increased NSD:WD ratio of Mg^{2+} at that time (Fig. 5.3). During leaf senescence, the NTF of SO_4^{2-} was correlated with Mg^{2+} ($r_s = 0.84$), Ca^{2+} ($r_s = 0.70$), and K^+ ($r_s = 0.59$). During the leafless season, in contrast, the NTF of SO_4^{2-} was closely correlated with NH_4^+ ($r_s = 0.88$, $p < 0.001$). The NTF fluxes of SO_4^{2-} and NH_4^+ were also closely correlated during the fully leafed period ($r_s = 0.78$; $p < 0.001$).

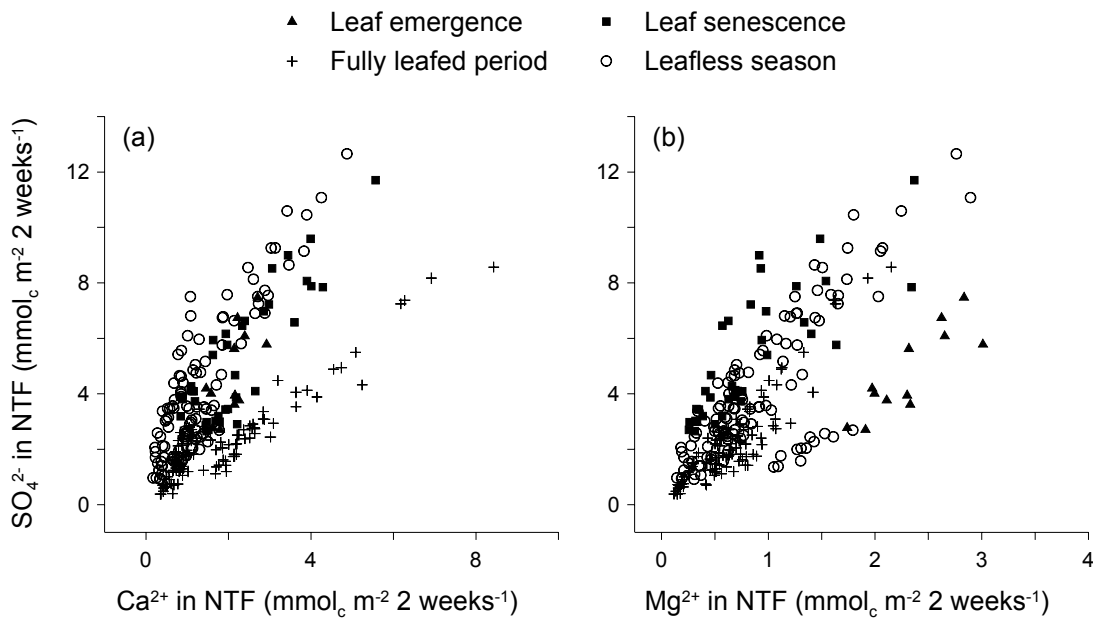


Fig. 5.8. Relationship between net throughfall (NTF) deposition ($\text{mmol}_c \text{ m}^{-2} \text{ 2 weeks}^{-1}$) of SO_4^{2-} and (a) Ca^{2+} , and (b) Mg^{2+} for 12 individual throughfall collectors during four phenological canopy phases ($n_{tot} = 264$).

The biweekly NTF deposition of NO_3^- was higher during the fully leafed period than in the other phenological canopy phases (Fig. 5.2), and was then correlated with Ca^{2+} ($r_s = 0.89$), Mg^{2+} and NH_4^+ ($r_s = 0.86$) (not shown). During leaf senescence, Ca^{2+} was the only cation that was weakly correlated ($r_s = 0.38$, $p = 0.02$) with NO_3^- in NTF.

5.4.3 Seasonal canopy budget method

Using the version of the canopy budget method originally reported by Draaijers and Erisman (1995), cation leaching was estimated to contribute 95% (K^+), 43% (Ca^{2+}), and 33% (Mg^{2+}) of the annual net stand deposition (NSD). Canopy exchange of Na^+ , Cl^- , SO_4^{2-} , and NO_3^- was set to zero. The computed canopy uptake of NH_4^+ was $29 \text{ mmol}_c \text{ m}^{-2} \text{ yr}^{-1}$, which resulted in an estimated dry deposition of $100 \text{ mmol}_c \text{ m}^{-2} \text{ yr}^{-1}$. Neglecting weak acid leaching resulted in a calculated uptake of $54 \text{ mmol}_c \text{ NH}_4^+ \text{ m}^{-2} \text{ yr}^{-1}$. The uptake of H^+ was estimated at $11 \text{ mmol}_c \text{ m}^{-2} \text{ yr}^{-1}$, yielding a dry deposition of $8.4 \text{ mmol}_c \text{ m}^{-2} \text{ yr}^{-1}$.

The canopy budget method was applied separately for each phenological canopy phase, and slightly adapted based on the previous results (5.4.1 and 5.4.2). Because of the indication of Na^+ and Cl^- leaching during leaf burst (Fig. 5.2), the dry deposition factor (DDF = NSD:WD) of Na^+ during leaf emergence was set equal to its DDF of the fully leafed period. In this way, DD and leaching of Na^+ from sprouting buds and unfolding leaves could be estimated. Then, DD of Cl^- during leaf emergence and senescence was determined as the product of DD_{Na} and the average ratio of Cl^- to Na^+ in NSD during the rest of the year. This allowed estimating Cl^- leaching from the emerging and senescent leaves. Next, DD and leaching of SO_4^{2-} during leaf senescence was estimated by multiplying the WD of SO_4^{2-} during senescence with the NSD:WD ratio of SO_4^{2-} during the rest of the year. Lastly, canopy uptake of H^+ and NH_4^+ was estimated from the leaching of base cations corrected for the estimated canopy leaching of weak acids, Cl^- and SO_4^{2-} .

Using this modified seasonal canopy budget method, the estimated contribution of canopy leaching to the annual NSD was 96% (K^+), 54% (Ca^{2+}), 40% (Mg^{2+}), 12% (Cl^-), and 7% (Na^+ , SO_4^{2-}) (Table 5.3). During leaf burst, the estimated Na^+ leaching was 78% of its NSD. Canopy leaching of K^+ contributed more than 90% of the NSD, irrespective of the canopy phase considered. For Ca^{2+} and Mg^{2+} , about 70% of the NSD was attributed to canopy leaching during the fully leafed period. During the leafless season, 28% of the NSD was attributed to branch leaching for Ca^{2+} and 5% for Mg^{2+} . During leaf burst, estimated canopy leaching was low for Ca^{2+} (22% of NSD) but pronounced for Mg^{2+} (84%), while during leaf senescence, leaching was important for both Ca^{2+} (86%) and Mg^{2+} (67%). Similarly to Mg^{2+} , the relative fraction of Cl^- leaching in NSD was highest during leaf burst (78% of NSD) and meaningful during leaf senescence (50%). The calculated leaching of SO_4^{2-} contributed 39% of the NSD during leaf senescence. Net canopy uptake of NH_4^+ was estimated at $32 \text{ mmol}_c \text{ m}^{-2} \text{ yr}^{-1}$, with a small amount of NH_4^+ leaching from the canopy calculated during leaf burst.

Table 5.3. Wet deposition (WD), estimated dry deposition (DD), and estimated canopy exchange (CE > 0 indicates ion leaching from the canopy, CE < 0 indicates uptake) (mmol_c m⁻² period⁻¹) of ions during four phenological canopy phases and the total studied year. The number of weeks in each period is given in brackets.

Canopy phase	Flux	Ion flux (mmol _c m ⁻² period ⁻¹)									
		H ⁺	Na ⁺	K ⁺	Ca ²⁺	Mg ²⁺	NH ₄ ⁺	NO ₃ ⁻	SO ₄ ²⁻	Cl ⁻	w.a. ^a
Leaf emergence (<i>m</i> = 2)	WD	0.1	1.0	0.1	1.3	0.3	3.0	1.6	2.0	1.0	1.2
	DD	-0.4	1.4	0.1	1.7	0.4	5.3	0.0	5.5	1.8	1.2
	CE	0.3	4.7	7.3	0.5	2.0	2.9	0.0	0.0	6.3	11.4
Fully leafed (<i>m</i> = 21)	WD	1.0	4.2	0.4	3.8	1.2	12.8	7.8	9.5	4.3	2.0
	DD	1.8	5.6	0.6	5.1	1.5	33.2	15.9	22.2	7.7	2.0
	CE	-2.9	0.0	14.2	11.5	4.4	-10.6	0.0	0.0	0.0	16.7
Senescence (<i>m</i> = 7)	WD	1.0	4.4	0.1	1.2	1.1	3.6	2.2	3.5	5.6	0.2
	DD	2.1	3.6	0.1	1.0	0.9	9.8	1.9	10.8	4.8	0.2
	CE	-3.1	0.0	16.7	6.2	1.8	-3.7	0.0	6.9	4.7	6.3
Leafless (<i>m</i> = 22)	WD	1.8	20.3	0.5	4.6	4.3	14.0	6.5	12.7	22.1	4.1
	DD	4.3	50.1	1.3	11.3	10.6	46.1	6.9	46.8	65.8	4.1
	CE	-5.1	0.0	13.3	4.4	0.5	-11.8	0.0	0.0	0.0	1.3
Year (<i>m</i> = 52)	WD	4.0	30.0	1.2	10.9	6.8	33.5	18.2	27.7	33.0	7.5
	DD	7.8	60.7	2.1	19.1	13.4	94.4	24.7	85.2	80.1	7.5
	CE	-10.8	4.7	51.4	22.7	8.8	-23.2	0.0	6.9	11.0	35.7

^a Weak acids (w.a.) calculated as the difference between measured cations and anions.

5.5 Discussion

5.5.1 Throughfall enrichment in the leafed and leafless season

The throughfall deposition under the deciduous beech tree studied was significantly higher than the wet deposition input during both the growing and dormant season for all ions except H⁺ (Table 5.2). The finding that leafed as well as leafless forest canopies interact with incident precipitation is in line with other studies in temperate deciduous forest stands. In two Canadian hardwood forests, throughfall deposition of all ions other than H⁺, NO₃⁻, and NH₄⁺ exceeded wet deposition during the leafless season, with enrichment ratios varying from 1.04 to 4.7 (Neary and Gizyn, 1994) and from 1.3 to 7.5 (Houle *et al.*, 1999b). In an oak-hickory stand in Georgia - where only 24% of precipitation was sampled in the 2-year study period - throughfall enrichment ratios of ions other than H⁺ and NH₄⁺ ranged from 1.4 to 44 during the leafless season (Cappellato *et al.*, 1993). In an oak-hickory stand in Kansas, throughfall deposition exceeded wet deposition for five of eight elements during the dormant season, but the difference was only significant for phosphate (Hamburg and Lin, 1998).

While foliation in the present study decreased the net water flux to the forest floor (see also Chapter 3), varying seasonal patterns were observed for the major ions. The throughfall to wet deposition ratios were significantly higher during the growing season for K^+ , Ca^{2+} , Mg^{2+} , and NO_3^- , but significantly higher during the dormant season for Na^+ , NH_4^+ , and H^+ (Table 5.2).

5.5.2 Sodium and chloride

Sodium and chloride are generally considered as conservative elements showing only minor canopy exchange (Parker, 1983; Johnson and Lindberg, 1992, Draaijers *et al.*, 1996). Our results indicate canopy leaching of Na^+ but particularly of Cl^- . The net throughfall deposition of both Na^+ and Cl^- strongly increased during the short leaf emergence period compared to the rest of the fully leafed period (Fig. 5.3, Fig. 5.7). Assuming that dry deposition of these ions did not increase in these two weeks, both Na^+ and Cl^- must have leached from the breaking buds and/or emerging leaves. During the last biweekly sampling period of leaf senescence, the high Cl^- enrichment was not accompanied by a similar Na^+ enrichment (Fig. 5.7), indicating Cl^- leaching from the senescent leaves. This may be due to the fact that Cl^- is a highly mobile anion that is readily taken up by plants (Marschner, 1995) but not retranslocated during senescence. According to the correlation analysis, Cl^- leaching mainly occurred as KCl salt. A similar increase in plant-derived chloride in throughfall during autumn has previously been reported for other hardwood species (Cronan and Reiners, 1983; Neary and Gizyn, 1994; Houle *et al.*, 1999b). After experimental $CaCl_2$ addition to the soil, canopy leaching of Cl^- increased with elevated Cl^- content of sugar maple foliage (Berger *et al.*, 2001). Therefore, it appeared reasonable to modify the canopy budget method to include Cl^- leaching during leaf senescence. The Cl^- to Na^+ ratio of 1.32 in the net throughfall flux during the fully leafed period and the leafless season was slightly higher than in seawater (1.17, de Vries *et al.*, 2003; Fig. 5.7). This may be due to dry deposition of $MgCl_2$, HCl and/or NH_4Cl besides the dominant fraction of Na^+ and Cl^- aerosol. Throughfall deposition of Na^+ was significantly higher than wet deposition throughout the year, even though meaningful Na^+ leaching most likely only occurred during leaf emergence. Furthermore, the throughfall enrichment ratio of Na^+ was higher during the dormant than the growing season, in line with previous results (Neary and Gizyn, 1994; Houle *et al.*, 1999b; Devlaeminck *et al.*, 2005). This demonstrates considerable dry deposition of Na^+ and Cl^- to twigs and branches of the leafless tree despite the lower collecting canopy surface than in the leafed season, and may be attributed to the combined effect of (i) higher atmospheric turbulence within the canopy during the dormant

season due to the absence of leaves and the generally higher wind speeds in that period (see 3.4.3), increasing the dry deposition velocity (Beckett *et al.*, 2000; Freer-Smith *et al.*, 2004), and (ii) enhanced atmospheric sea spray concentrations during winter time, as indicated by the temporal pattern in wet deposition of Na^+ , Cl^- , and Mg^{2+} (Fig. 5.2; Table 5.2).

5.5.3 Potassium, calcium, and magnesium

In contrast to Na^+ , the throughfall to wet deposition ratios of K^+ , Ca^{2+} , and Mg^{2+} were significantly higher during the leafed than the leafless season (Table 5.2), indicating canopy leaching of these cations from physiologically active leaves. Similarly, enrichment ratios of K^+ and Mg^{2+} beneath a deciduous *Fagus moesiaca* Cz. canopy were significantly higher in the growing periods of the year (Michopoulos *et al.*, 2001). Canopy leaching was the main mechanism of K^+ enrichment in throughfall, in agreement with previous research (Parker, 1983; Houle *et al.*, 1999b; Balestrini and Tagliaferri, 2001). Potassium is more susceptible to canopy leaching than Ca^{2+} and Mg^{2+} because its principal function in plants is that of stomatal regulation, so that it is not bound in structural tissues or enzyme complexes (Marschner, 1995). The estimated amount of canopy leaching was higher for Ca^{2+} than for Mg^{2+} , but the contribution of Ca^{2+} leaching to net stand deposition was smaller during leaf emergence than during senescence (Table 5.3). This is in line with the fact that calcium occurs in considerable quantities in cell walls as relatively insoluble pectates and is hardly retranslocated from leaves into woody components in autumn (Marschner, 1995). While increased cation leaching during leaf senescence is commonly reported (Cronan and Reiners, 1983; Neary and Gizyn, 1993; Houle *et al.*, 1999b), the effect of budbreak and leaf unfolding on throughfall chemistry has rarely been discussed. Our results suggest that Mg^{2+} , NH_4^+ , and K^+ were leached during leaf burst, accompanied by significant leaching of organic acids. Leaching of Mg^{2+} and K^+ has also been found for young oak leaves (Draaijers *et al.*, 1992). The estimated leaching of weak organic acids during leaf senescence was smaller than during leaf emergence. This suggests that base cation leaching from senescent leaves was not only associated with release of organic anions (Cronan and Reiners, 1983; Balestrini and Tagliaferri, 2001), but also with uptake of NH_4^+ or H^+ (Draaijers and Erisman, 1995; Chiwa *et al.*, 2004), and/or the release of one or more of the measured anions, like Cl^- and SO_4^{2-} . The leaching of base cations as well as organic acids may be underestimated when insoluble salts are formed in the throughfall solution that cannot be measured in filtered samples (Chiwa *et al.*, 2004).

Significant throughfall enrichment of base cations was observed also during the dormant season (Table 5.2), and most likely resulted from both dry deposition and canopy exchange. Controlled experiments demonstrate strongly increasing dry deposition velocities of particles with increasing wind speed (Beckett *et al.*, 2000; Freer-Smith *et al.*, 2004). Furthermore, different aerodynamic properties of leaves and branches may lead to relatively high dry deposition onto leafless deciduous trees with a complex branching structure (Freer-Smith *et al.*, 2004), like the beech tree studied. Little is known about canopy leaching from deciduous tree species during the leafless season. Branchflow fluxes of K^+ and Mg^{2+} differed significantly between tree species and the enrichment was higher for precipitation events of longer duration (Levia and Herwitz, 2002), indicating ion release from tree branches. Tukey (1970) also reported that stems and branches of woody plants lose nutrients by leaching during both the growing and dormant season. In the present study, throughfall enrichment of K^+ and Ca^{2+} during the leafless season was attributed partly to ion leaching from twigs and branches according, while estimated leaching of Mg^{2+} was negligible (Table 5.3) according to the modified seasonal canopy budget method. There is evidence of cation leaching from forest canopies due to snowfall (Cappellato *et al.*, 1993; Neary and Gizyn, 1994), particularly for snow-to-rain events at temperatures around the freezing point (Levia, 2003). In the present study, snowfall occurred only once, so that base cation leaching in defoliated conditions was almost completely due to rainfall water interacting with the leafless canopy.

5.5.4 Nitrogen, hydrogen, and sulphur

Throughfall enrichment ratios of NH_4^+ and H^+ were significantly lower during the growing season than during the dormant season (Table 5.2), in contrast to the NO_3^- enrichment ratio. A decrease in throughfall enrichment of inorganic N during the growing season is commonly attributed to the retention of N by canopy leaves and/or their microbial communities (Neary and Gizyn, 1994; Hamburg and Lin, 1998). For deciduous canopies, ion exchange of both NH_4^+ (Roelofs *et al.*, 1985; Stachurski and Zimka, 2002) and H^+ (Puckett, 1990; Cappellato *et al.*, 1993; Lovett *et al.*, 1996) with K^+ , Ca^{2+} , and Mg^{2+} has been reported. During autumn, increased canopy retention of NH_4^+ (Cronan and Reiners, 1983; Neary and Gizyn, 1994; Houle *et al.*, 1999b), NO_3^- , and H^+ (Cronan and Reiners, 1983; Houle *et al.*, 1999b) has been observed in hardwood stands. Since this uptake occurs at the moment of leaf senescence, it is probably linked to nitrogen retranslocation by trees (Houle *et al.*, 1999b). Increased ion exchange between $NH_4^+ + H^+$ and base cations by senescent beech leaves, as estimated by the

modified seasonal canopy budget method, can explain why the observed leaching of K^+ , Ca^{2+} , and Mg^{2+} in autumn did not lead to an equivalent anion deficit in net throughfall (Fig. 5.5, Table 5.3). A relatively large amount of canopy uptake was also calculated during the leafless season. Although the main route for N uptake is considered to be via the foliage, increasing evidence suggests that uptake via twig, branch, and stem surfaces may be at least as important (Bowden *et al.*, 1989; Boyce *et al.*, 1996; Macklon *et al.*, 1996; Wilson and Tiley, 1998). The estimated canopy leaching of NH_4^+ during leaf emergence (Table 5.3) is supported by the correlation analysis of net throughfall, which suggested simultaneous release of NH_4^+ and weak acids at that time (Fig. 5.6a). By including the estimated leaching of weak acids as well as Cl^- and SO_4^{2-} to determine NH_4^+ uptake, the calculated canopy absorption was $0.33 \text{ g N m}^{-2} \text{ yr}^{-1}$ ($3.3 \text{ kg N ha}^{-1} \text{ yr}^{-1}$). This is in the lower range of other studies, in which N uptake was 0.1 to $1.2 \text{ g N m}^{-2} \text{ yr}^{-1}$ (Brumme *et al.*, 1992; Lovett and Lindberg, 1993). When leaching of K^+ , Ca^{2+} , and Mg^{2+} was only attributed to canopy uptake of NH_4^+ and H^+ (de Vries *et al.*, 2003), the calculated retention of reduced N (NH_x) was more than twice as high ($0.77 \text{ g N m}^{-2} \text{ yr}^{-1}$).

Nitrate enrichment in net stand deposition was significantly higher during the leafed than the leafless season, although there was significant enrichment compared to wet deposition in both seasons (Fig. 5.2, Table 5.2). Nitrate leaching from the canopy was assumed to be negligibly small, since we have no knowledge of a generally accepted method to estimate NO_3^- exchange within the canopy directly from throughfall and precipitation measurements. Nitrate can be taken up by tree canopies, although NH_4^+ is retained and assimilated more preferentially than NO_3^- (Bowden *et al.*, 1989; Brumme *et al.*, 1992; Boyce *et al.*, 1996; Stachurski and Zimka, 2002). The higher throughfall enrichment of NO_3^- in the growing season may be attributed to the presence of a leafed canopy, by which dry deposition of oxidised N was enhanced through stomatal uptake but apparently without being assimilated in the canopy. Dry deposition of oxidised N (NO_y) is mainly due to nitrogen dioxide (NO_2), nitric acid vapor (HNO_3), and particulate NO_3^- (Hanson and Lindberg, 1991). Dry deposition of NO_2 to vegetation shows a marked diurnal and annual cycle because its canopy uptake is largely controlled by stomatal opening (Duyzer and Fowler, 1994; Gessler *et al.*, 2000). Our results suggest that NO_2 that is taken up through leaf stomata is largely released as NO_3^- in throughfall afterwards. The lower throughfall enrichment in the leafless season for NO_3^- was not found for NH_4^+ (and SO_4^{2-}), likely because NH_3 is not only taken up through stomata but also by moist surfaces (Wesely and Hicks, 2000). In addition, higher assimilation of NH_x in the growing season probably masked the potentially higher dry deposition of NH_x onto the leafed canopy.

Our results confirm that deciduous forest canopies exhibit substantial buffering of pH during the growing season and less buffering during the leafless season (Bredemeier, 1988; Houle *et al.*, 1999b; Michopoulos *et al.*, 2001; Pryor and Barthelmie, 2005). Based on throughfall only, the canopy neutralized 96% of the free rainfall acidity in the growing season and 69% in the dormant season. Including the stemflow flux of H^+ , however, only 48% of the wet H^+ input was neutralized in the dormant season. The actual fraction of neutralized H^+ is higher because of dry deposition of H^+ originating from H_2SO_4 , $(NH_4)HSO_4$, HNO_3 , and HCl (Draaijers and Erisman, 1995). The estimated dry deposition and uptake of H^+ (and of NH_4^+) (Table 5.3) depends on the assumed canopy uptake equation and exchange efficiency (see also Chapter 7). The reduction of acidity after canopy passage is generally attributed to ion exchange removal of free H^+ by the canopy or to organic anion leaching from the foliage (Cronan and Reiners, 1983), but can also be due to proton consumption by dry deposited NH_3 gas (De Schrijver *et al.*, 2004) and Ca^{2+} compounds (Lee and Longhurst, 1992) (see section 2.5.3), or to canopy uptake of HNO_3 (Cappellato *et al.*, 1993; Stachurski and Zimka, 2002).

The throughfall to wet deposition enrichment ratio of SO_4^{2-} differed not significantly between the leafed and leafless season (Table 5.2). When canopy processes of sulphur (S) are assumed negligible compared to wet and dry deposition (Lindberg and Lovett, 1992), considerable amounts of S were dry deposited onto both the leafed (0.75 g S m^{-2}) and leafless (0.72 g S m^{-2}) beech canopy ($1.47 \text{ g S m}^{-2} \text{ yr}^{-1}$). Dry deposition of S mainly originates from SO_2 (besides particulate SO_4^{2-} , see also section 7.4.3), for which the deposition rate is strongly affected by stomatal resistance (Wesely and Hicks, 2000). Therefore, lower S enrichment was expected in leafless conditions. However, deposition of SO_2 onto leafless forests may be considerable underestimated based on stomatal uptake when ambient NH_3 concentrations are sufficiently large because of the enhanced co-deposition of SO_2 and NH_3 on canopy surfaces under humid conditions (Erisman and Wyers, 1993; Wesely and Hicks, 2000; Cape and Leith, 2002). For example, Cape *et al.* (1998) found that fumigation of a Scots pine canopy with NH_3 notably increased S deposition. The dissolution of NH_3 in a water film increases the pH, which promotes the dry deposition of SO_2 and results in the formation of $(NH_4)_2SO_4$ (Derome *et al.*, 2004). The high throughfall enrichment of both NH_4^+ and SO_4^{2-} (Table 5.2) and the close correlation between the net throughfall fluxes of NH_4^+ and SO_4^{2-} suggests enhanced dry deposition of NH_3 and SO_2 due to co-deposition of both gases. The molar ratio of N over S in the estimated dry deposition, accounting for canopy uptake of N and leaching of S (Table 5.3), was 2.71 in the leafed season and 1.97 in the leafless season.

Although throughfall enrichment of SO_4^{2-} beneath various canopy types is generally attributed to dry S deposition rather than canopy leaching (Lindberg and Garten, 1988; Butler and Likens, 1995; Kovács and Horváth, 2004), both canopy absorption (Cappellato *et al.*, 1993; Quilchano *et al.*, 2002) and leaching of S (Lovett and Lindberg, 1984; Neary and Gizyn, 1994; Cappellato *et al.*, 1998) have been reported for leafed deciduous canopies. Sulphate enrichment in the present study increased during leaf senescence (Fig. 5.3). Assuming no enhanced dry deposition of SO_x during this period, $0.11 \text{ g S m}^{-2} \text{ yr}^{-1}$ was leached from the senescing leaves, which slightly decreased the estimated dry deposition in the leafed season to 0.61 g S m^{-2} (Table 5.3). Canopy leaching of S during senescence has also been reported for a beech forest in southern Sweden (Staaf, 1982). Observations by Meiwes and Khanna (1981) suggest that $0.22 \text{ g S m}^{-2} \text{ yr}^{-1}$ could be leached from senescent beech leaves.

5.5.5 Stemflow

Stemflow contributed significantly to the annual below-canopy fluxes of water (11%) and ions (9-19%) in the studied beech plot, and particularly for H^+ (38%). In German beech forests, stemflow accounted for 15% (Chang and Matzner, 2000b) and 37-66% (Sah, 1990) of the annual stand deposition of H^+ . The high contribution of H^+ by stemflow in the present study was entirely due its low pH values during the dormant season. As stemflow infiltrates on a small area around the trunk, the substantial stemflow fluxes of smooth-barked tree species such as European beech can contribute to spatial patterns of water percolation under the rooting zone (Chang and Matzner, 2000b) and lead to enhanced soil acidification (Matschonat and Falkengren-Grerup, 2000; Chang and Matzner, 2000b), nitrification (Chang and Matzner, 2000a) and mineral weathering (Rampazo and Blum, 1992) close to beech trees.

Stemflow concentrations of most ions were higher in the dormant season than in the growing season, and could not be explained by enhanced rainfall concentrations. According to Levia and Frost (2003), increased chemical enrichment of stemflow in winter may be due to the larger portion of the woody tree crown that is exposed to incident gross precipitation, which enhances bark leaching, and to increased residence times of stemflow water on the bark surface by lower air temperatures and lower rainfall intensities. However, the increased Na^+ , Cl^- , and Mg^{2+} concentration in the dormant season stemflow was not observed for the readily leached K^+ , which suggests an efficient dry deposition of seasalt aerosols onto fine beech twigs (Freer-Smith *et al.*, 2004) and/or the tree bole (Becker *et al.*, 2000) rather than increased ion leaching in leafless conditions.

5.6 Conclusions

The chemical enrichment of throughfall and stemflow deposition beneath a deciduous beech tree compared to wet deposition was clearly influenced by foliation and physiological canopy activity, and differed between the major ions studied. The seasonal pattern of throughfall and stemflow enrichment indicated that elements that are often thought to behave conservatively with respect to forest canopies were released from the beech canopy during leaf emergence and/or senescence, although the estimated contribution of canopy leaching was low compared to the annual dry deposition. Weak acid excretion by leaves, as derived from the anion deficit in net throughfall, was highest during leaf emergence and the fully leafed period and should be taken into account when studying ion exchange within forest canopies. The applied canopy budget model allows more insight in processes affecting throughfall chemistry than observed net throughfall fluxes, but additional research is needed to verify underlying assumptions. The high dry deposition of reduced nitrogen due to NH_3 emissions in the study region masked the likely canopy retention of nitrogen. Although throughfall enrichment was higher during the leafed season, significant enrichment of all ions other than H^+ was also observed during the leafless season. The high throughfall to wet deposition ratios in the leafless season indicated that K^+ and Ca^{2+} were leached from beech branches and twigs by rainfall. Furthermore, the estimated contribution of dry deposition of seasalt derived aerosols, sulphur and reduced N onto the leafless canopy was as least as high as onto the foliated canopy, despite the lower collecting canopy surface in the absence of leaves.

6 Spatial variability and temporal stability of throughfall chemistry in relationship to canopy structure

After: Staelens, J., De Schrijver, A., Verheyen, K. and Verhoest, N.E.C. Spatial variability and temporal stability of throughfall deposition under beech (*Fagus sylvatica* L.) in relationship to canopy structure. Environmental Pollution, in press.

6.1 Abstract

Although the spatial variability of throughfall (TF) in forests can have important ecological implications, little is known about the driving factors of within-stand TF variability, in particular for deciduous forests. The spatial variability of annual TF deposition beneath a dominant beech (*Fagus sylvatica* L.) tree was highest for H^+ and NH_4^+ (coefficient of variation $\sim 20\%$), intermediate for SO_4^{2-} , Mg^{2+} , K^+ , and Ca^{2+} ($\sim 15\%$), and lowest for NO_3^- , Na^+ , Cl^- , and water (12-8%). The spatial variation of TF water amount and H^+ deposition was significantly ($p < 0.01$) higher in the leafed season than in the leafless season and was not related between the two periods of the year. For the major ions studied, in contrast, the spatial variability was not significantly different between the leafed and leafless season, and similar spatial TF deposition patterns were found in both periods of the year. The semiannual TF depositions of all ions other than H^+ were significantly positively correlated ($r = 0.68$ to 0.90 , $p < 0.05$, $n = 12$) with the canopy structure above sample locations during the leafed and the leafless season. The throughfall water and H^+ fluxes during the leafed season were negatively correlated with branch cover. We conclude that the spatial heterogeneity in TF ion deposition beneath a beech canopy was strongly affected by the canopy structure throughout the entire year. Both leaves and branches significantly influence spatial patterns of TF deposition under deciduous forest canopies.

6.2 Introduction

Throughfall (TF) is an important pathway of nutrients to the forest floor (Parker, 1983), and is often used to estimate atmospheric deposition to forests (de Vries *et al.*, 2003). TF water passing through a forest canopy is generally enriched compared to the incoming precipitation because of two primary processes: (i) wash-off of dry deposited particles and gases and (ii) ion exchange between the canopy surfaces and their associated microflora and the water passing over them (Schaefer *et al.*, 1988; Lovett *et al.*, 1996). TF dynamics of nitrogen can also be influenced by phytophagous insects (Stadler *et al.*, 2001, 2005) and epiphytic lichens (Oyarzún *et al.*, 2004) in forest canopies.

The water flow and matter transport in forest ecosystems can show considerable spatial heterogeneity within a forest stand (Zirlewagen and von Wilpert, 2001), and previous research indicates that the forest canopy architecture may contribute to a systematic component of spatial variability of TF (Beier *et al.*, 1993; Robson *et al.* 1994; Whelan and Anderson, 1996). The spatial variability of TF water and ion input within stands has been related to (i) distance to the forest edge, (ii) distance to the nearest tree stem, and (iii) local canopy structure. First, numerous reports indicate that upwind edges of forest plots receive considerably more dry deposition than do other areas of the same plot (e.g., Draaijers *et al.*, 1988; De Schrijver *et al.*, 1998; Devlaeminck *et al.*, 2005). Second, within coniferous forest stands, TF ion depositions are generally higher closer to the stem while water fluxes are lower, which has mostly been explained by higher foliar densities close to the stem (Beier *et al.*, 1993; Seiler and Matzner, 1995; Whelan *et al.*, 1998). However, since a stem-basis related method requires circular crowns with a similar radius, such approach is more useful in homogeneous coniferous forest stands than in deciduous stands characterized by heterogeneous crown structures (Zirlewagen and von Wilpert, 2001). Third, the association between canopy architecture and the chemical composition of TF at small spatial scales has been reported for Norway spruce (Whelan *et al.*, 1998; Hug *et al.*, 2005) and black spruce (Carleton and Kavanagh, 1990), but not yet for deciduous species.

Systematic patterns of TF deposition can have important effects on spatially distributed processes in forest soils such as ion loading and water and solute transport. Furthermore, the spatial heterogeneity of TF fluxes within a forest stand is highly relevant for assessing sampling designs in TF studies and has importance for small-scale field experiments in biogeochemistry, like litterbag studies, soil columns, fertilizer, and tracer studies (Brodersen *et al.*, 2000). In a Douglas fir forest, spatial patterns of root water uptake were related to TF

patterns around trees, especially in dry months (Bouten *et al.*, 1992). However, spatial patterns of forest floor water content could not be related directly to TF water patterns, mainly as a result of drainage (Raaijmakers *et al.*, 2002). In a mature Norway spruce stand, the spatial heterogeneity of annual seepage water fluxes of SO_4^{2-} , Cl^- , and Mg^{2+} at 90 cm depth was largely explained by the heterogeneity of TF fluxes ($r^2 > 0.61$), while no such relationship was found for nitrogen (Manderscheid and Matzner, 1995). In the same Norway spruce stand, the SO_4^{2-} content of the forest floor reflected the gradients observed in TF, while no significant relations to stem distance were found for other investigated soil parameters and horizons (Seiler and Matzner, 1995).

In temperate hardwood forests, the spatial variability of TF deposition has mainly been quantified with the aim of deriving sample size requirements, while generally little attention is paid to spatio-temporal patterns of TF. In addition, reports on the variability of TF deposition throughout the year are scarce for deciduous forests. Kimmins (1973), Kostelnik *et al.* (1989), Puckett (1991), and Robson *et al.* (1994) measured the variability of TF concentration for only nine, six, five, and three rain events, respectively. The variability of TF deposition in a mixed hardwood forest has been quantified for six years, but during the growing season only (Houle *et al.*, 1999a). Since the small-scale spatial variability of TF may affect hydrological, biogeochemical, and ecological processes on the forest floor and beyond, more knowledge on the driving factors of the within-stand TF variability is needed. While some attempts have been made to relate TF chemistry to canopy structure in coniferous forests, little is known about the influence of deciduous canopies on the small-scale variability of TF. Therefore, the aims of this chapter were (i) to quantify the spatial heterogeneity of TF water amount and ion deposition to the forest soil under a beech (*Fagus sylvatica* L.) canopy, (ii) to examine the temporal stability of spatial TF input, and (iii) to relate the small-scale spatial variability of TF to easily measurable canopy characteristics.

6.3 Materials and methods

The study site is described in section 3.3.1.

6.3.1 Data collection

In this chapter, the same data were used as in Chapter 5 (see Fig. 5.1), but without considering stemflow deposition. Weekly collection of precipitation and throughfall water ($n = 12$) between 4 March 2003 to 4 March 2004, biweekly chemical analysis of the water samples,

and quality control are explained in section 5.3.1. Canopy cover fraction and plant area index were determined above the 12 throughfall collectors during foliated and defoliated conditions as described in section 4.3.1.2. To examine spatial patterns of throughfall deposition throughout time, the four phenological canopy phases distinguished in Chapter 5 (see section 5.3.2.2) were generally reduced to two periods: (i) the leafless season, and (ii) the leafed season (25 April until 18 November 2003), including leaf emergence, the fully leafed period, and leaf senescence.

6.3.2 Data analysis

Ion fluxes were calculated as described in section 5.3.2.1.

6.3.2.1 Spatial variability of throughfall

The areal coefficient of variation (CV, %) of each measured ion was calculated for the biweekly, semiannual (leafed and leafless season), and annual volume-weighted TF concentration, TF deposition, and net TF deposition. Net throughfall (NTF) was calculated as TF deposition minus wet deposition, which was assumed to be equal for all sampling points. The variation in spatial variability of ion deposition was studied in relation to variations in precipitation amount, ion deposition, and canopy phenology (Houle *et al.*, 1999a). Linear regression analysis was used to study the relationship between the CV of ion deposition on the one hand, and the amount of precipitation and ion deposition on the other hand. The CVs of TF water and ion depositions were compared between the leafed and the leafless season by the Wilcoxon rank sum test.

6.3.2.2 Temporal stability of spatial throughfall variability

Two techniques were applied to investigate the temporal stability of the spatial variability of TF ion depositions, in correspondence with the analysis of the amount of TF water (see section 4.3.2.2). First, non-parametric Spearman rank correlations were calculated between the TF during the leafless season and the TF during the leafed season or during the fully leafed period (excluding leaf emergence and senescence). Spearman correlations were also calculated between TF in all biweekly periods.

The second technique was the ‘time stability’ method (Vachaud *et al.*, 1985; Raat *et al.* 2002). For m periods and n locations, the method calculates the mean relative difference over time of the TF collected at location j ($\bar{\delta}_j$), as described in Eq. 4.2 to 4.4. The time stability of the

biweekly TF ion deposition ($n = 12$) was examined for the leafed season ($m = 13$), the leafless season ($m = 9$), and the annual study period ($m = 22$).

6.3.2.3 Relationship between throughfall and canopy structure

The relationship between the spatial variability of TF and canopy structure was studied by correlation analysis. Pearson correlation coefficients were calculated between canopy cover and plant area index (PAI) determined during the leafed and the leafless season on the one hand, and the TF water amount and ion depositions during the four phenological canopy phases, the semiannual seasons, and the annual study period on the other hand.

6.4 Results

6.4.1 Spatial variability of throughfall

The spatial variability of annual TF deposition, as expressed by the areal coefficient of variation (CV, Table 6.1), was highest for H^+ and NH_4^+ (~20%), intermediate for SO_4^{2-} , Mg^{2+} , K^+ , and Ca^{2+} (~15%), and lowest for NO_3^- , Na^+ and Cl^- (12-9%). The ratio of the maximum to minimum annual TF flux ranged from 2.0 (H^+) to 1.4 (Cl^-).

Table 6.1. Mean, standard deviation (SD), coefficient of variation (CV, %), minimum, maximum, and maximum/minimum ratio of annual throughfall water amount ($mm\ yr^{-1}$) and ion deposition ($mmol_e\ m^{-2}\ yr^{-1}$) for 12 throughfall collectors.

	Mean	SD	CV (%)	Minimum ^a	Maximum ^a	Max./min. ratio
Water	410.4	31.9	8	350.0 (6)	455.6 (9)	1.3
H^+	0.6	0.1	20	0.4 (6)	0.9 (11)	2.0
Na^+	77.3	7.3	9	64.8 (8)	88.6 (1)	1.4
K^+	49.6	6.9	14	38.8 (8)	64.4 (5)	1.7
Ca^{2+}	47.4	6.6	14	38.0 (8)	58.4 (5)	1.5
Mg^{2+}	25.7	3.7	15	20.5 (8)	31.8 (5)	1.5
NH_4^+	89.5	16.7	19	64.9 (8)	116.0 (5)	1.8
NO_3^-	38.8	4.5	12	32.2 (8)	47.6 (5)	1.5
SO_4^{2-}	105.0	16.5	16	78.2 (8)	129.2 (1)	1.7
Cl^-	100.4	10.6	11	84.3 (8)	114.1 (2)	1.4

^a Collector number (cf. Fig. 5.1) in brackets.

The variability of the biweekly TF deposition, as expressed by the median CV (Table 6.2), was highest for H^+ , K^+ , and NH_4^+ , and lowest for NO_3^- . The spatial variability of TF concentrations was higher than the spatial variability of TF depositions for all measured ions other than H^+ . Arranged according to deposition variability, the ion order in the leafed season (Table 6.2) was similar to the ion order at the annual level (Table 6.1). During the leafed

season, the variability in H^+ and NH_4^+ deposition was higher than the variability in TF water amount (CV = 18%), while during the leafless season all ion depositions were more variable than the TF amount (CV = 7%) (Table 6.2)

Table 6.2. Coefficient of variation (CV, %, $n = 12$) of throughfall water amount and volume weighted ion concentration (C), ion deposition (TF), and net ion deposition (NTF) during the biweekly sampling intervals (median CV value), the leafed season, and the leafless season.

Variable	Coefficient of variation (%) in sampling interval								
	Two weeks			Leafed season			Leafless season		
	C	TF	NTF	C	TF	NTF	C	TF	NTF
Water	-	15	32	-	18	24	-	7	47
H^+	31	36	7	13	28	1	21	21	10
Na^+	22	15	29	26	11	21	10	11	16
K^+	28	21	22	26	13	14	18	20	21
Ca^{2+}	27	16	24	29	14	19	16	16	22
Mg^{2+}	27	17	22	31	17	22	13	14	20
NH_4^+	31	20	41	37	23	40	15	17	24
NO_3^-	24	13	25	25	14	22	10	10	18
SO_4^{2-}	26	19	27	30	16	22	17	18	24
Cl^-	23	19	26	28	13	18	11	11	17

No significant ($p > 0.10$) relationship was found between precipitation amount and the variability of the biweekly ion depositions, as expressed by the CVs. For H^+ only, the logarithm of the CV of H^+ deposition in TF during the leafed season decreased significantly with increasing H^+ deposition ($r^2 = 0.43$, $p = 0.015$). The semi-annual variability of TF water amount, H^+ , NH_4^+ , Cl^- , NO_3^- , and Mg^{2+} deposition was greater in the leafed season than in the leafless season, while SO_4^{2-} , K^+ , and Ca^{2+} depositions were more variable during the leafless season (Table 6.2). However, the biweekly CVs of TF differed not significantly ($p > 0.10$) between the leafed and the leafless season, except for H^+ deposition ($p = 0.004$) and TF water amount ($p < 0.001$) (Fig. 6.1, $p = 0.09$ for K^+). An influence of leaf development stage on the spatial variability of ion fluxes was suggested by the high NO_3^- variability during the period of leaf emergence (CV = 66%, Fig. 6.1) and the increased TF variability of Mg^{2+} during leaf senescence (CV > 30%).

The spatial variability of net throughfall (NTF) deposition was greater than the variability of the TF deposition for all ions other than H^+ (Table 6.2). The median CV of biweekly NTF was highest for NH_4^+ (41%), lowest for H^+ , and ranged from 22 to 29% for the other ions. The ion order arranged to annual NTF variability was similar to the ion order arranged to TF variability, with the exception of NO_3^- , K^+ , and H^+ .

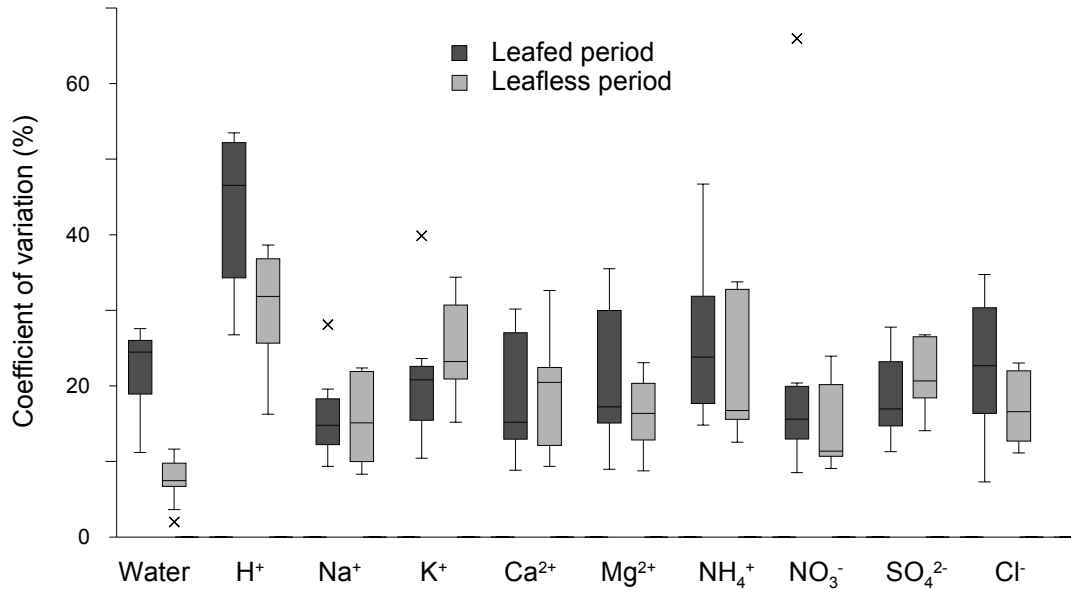


Fig. 6.1. Spatial coefficient of variation (%; $n = 12$) of biweekly throughfall water amount and ion deposition during the leafed season ($m = 13$ sampling periods) and the leafless season ($m = 9$). Boxplots indicate the minimum, lower quartile, median, upper quartile, and maximum values of the variation coefficient. Values outside the 1.5 interquartile ranges are indicated by x.

6.4.2 Time stability of spatial throughfall patterns

A significant relationship between the ranks of funnels in the leafed and the leafless season was found for the TF deposition of all measured ions ($r_s > 0.58$, $p < 0.05$, Table 6.3) except for NO_3^- and H^+ ($r_s < 0.45$, $p > 0.25$). The amount of TF water was negatively correlated between the two periods but not significantly ($r_s = -0.36$, $p = 0.25$, Table 6.3).

Table 6.3. Pearson correlation coefficients ($n = 12$) between throughfall water amount and ion deposition in the leafed season (values upper right) and in the leafless season (values lower left), and Spearman correlation coefficients ($n = 12$) between throughfall in the leafed and leafless season (bold values on the diagonal).

	Water	H^+	Na^+	K^+	Ca^{2+}	Mg^{2+}	NH_4^+	NO_3^-	SO_4^{2-}	Cl^-
Water	-0.36	0.92***	-0.53	-0.28	-0.54	-0.57	-0.63*	-0.26	-0.57	-0.52
H^+	0.07	0.45	-0.44	-0.26	-0.41	-0.44	-0.57	-0.21	-0.47	-0.38
Na^+	0.34	-0.37	0.58*	0.81**	0.88***	0.89***	0.96***	0.98***	0.98***	0.98***
K^+	0.48	-0.31	0.87***	0.69*	0.82**	0.87***	0.90***	0.84***	0.89***	0.88***
Ca^{2+}	0.21	-0.43	0.93***	0.88***	0.82**	0.98***	0.92***	0.91***	0.98***	0.91***
Mg^{2+}	0.29	-0.32	0.94***	0.86***	0.94***	0.86***	0.86***	0.90***	0.95***	0.96***
NH_4^+	0.41	-0.43	0.86***	0.89***	0.86***	0.93***	0.85**	0.87***	0.96***	0.92***
NO_3^-	0.41	-0.29	0.81**	0.92***	0.86***	0.88***	0.97***	0.38	0.93***	0.96***
SO_4^{2-}	0.31	-0.39	0.92***	0.88***	0.95***	0.98***	0.96***	0.97***	0.69**	0.96***
Cl^-	0.37	-0.28	0.92***	0.89***	0.87***	0.93***	0.92***	0.87***	0.94***	0.81***

Significance levels: * $p < 0.05$; ** $p < 0.01$; *** $p < 0.001$.

Spearman rank correlation coefficients between the TF water and ion fluxes in the leafless season and the fully leafed period (excluding leaf emergence and senescence) were generally similar to the correlations between the leafless and the leafed season. Spearman correlations increased for NO_3^- ($r_s = 0.54$, $p = 0.07$) and decreased for Na^+ ($r_s = 0.48$) and Cl^- ($r_s = 0.61$) by excluding leaf emergence and senescence.

The Spearman correlations for TF between all biweekly periods ($m = 22$) showed that the ranks of funnels for TF deposition of SO_4^{2-} , Mg^{2+} , and NH_4^+ were significantly positively ($p < 0.05$) correlated for 60, 55, and 45%, respectively, of the 231 pairs of biweekly periods. Significant positive correlations for TF water and the deposition of all other ions were found for only 22 to 36% of all pairs of biweekly periods. During the leafed season, the ranks of funnels for biweekly ion deposition were best correlated for TF water (73% of 78 pairs), SO_4^{2-} (65%), H^+ (60%), and Mg^{2+} (56%). During the leafless season, the biweekly fluxes were significantly positively correlated for more than half of the 36 pairs of biweekly periods, i.e. from 53% for Ca^{2+} to 89% for NH_4^+ and 94% for SO_4^{2-} , but only for 36% of the sampling pairs for the amount of TF water.

The error bars calculated by the ‘time stability method’ (Fig. 6.2) indicate the temporal spread around the average deviation for each sampling point in the two considered periods (Fig. 6.2a,b) and throughout the year (Fig. 6.2c). For example, sampling point 6 (cf. Fig. 5.1) received on average 35% less TF water than the plot average amount for the sampled biweekly periods in the leafed season (Fig. 6.2a), while sampling point 8 received on average 24% more TF water. The temporal stability of TF deposition patterns, e.g., of NO_3^- , was higher during the leafless season (Fig. 6.2b) than during the leafed season (Fig. 6.2a). The time stability method indicates that spatial TF patterns were consistent across the measured ions (cf. 6.4.3)

6.4.3 Relationship between throughfall chemistry and throughfall water amount

Annual volume-weighted (vw) mean TF concentrations were positively correlated with each other ($r > 0.89$, $p < 0.001$, $n = 12$) for all ions except for H^+ , and negatively ($r < -0.70$, $p < 0.05$) correlated with the amount of TF water. A highly significant negative relationship between vw ion concentrations and TF water amount was also found in the leafed season ($r < -0.89$, $p < 0.001$), but not in the leafless season ($p > 0.10$).

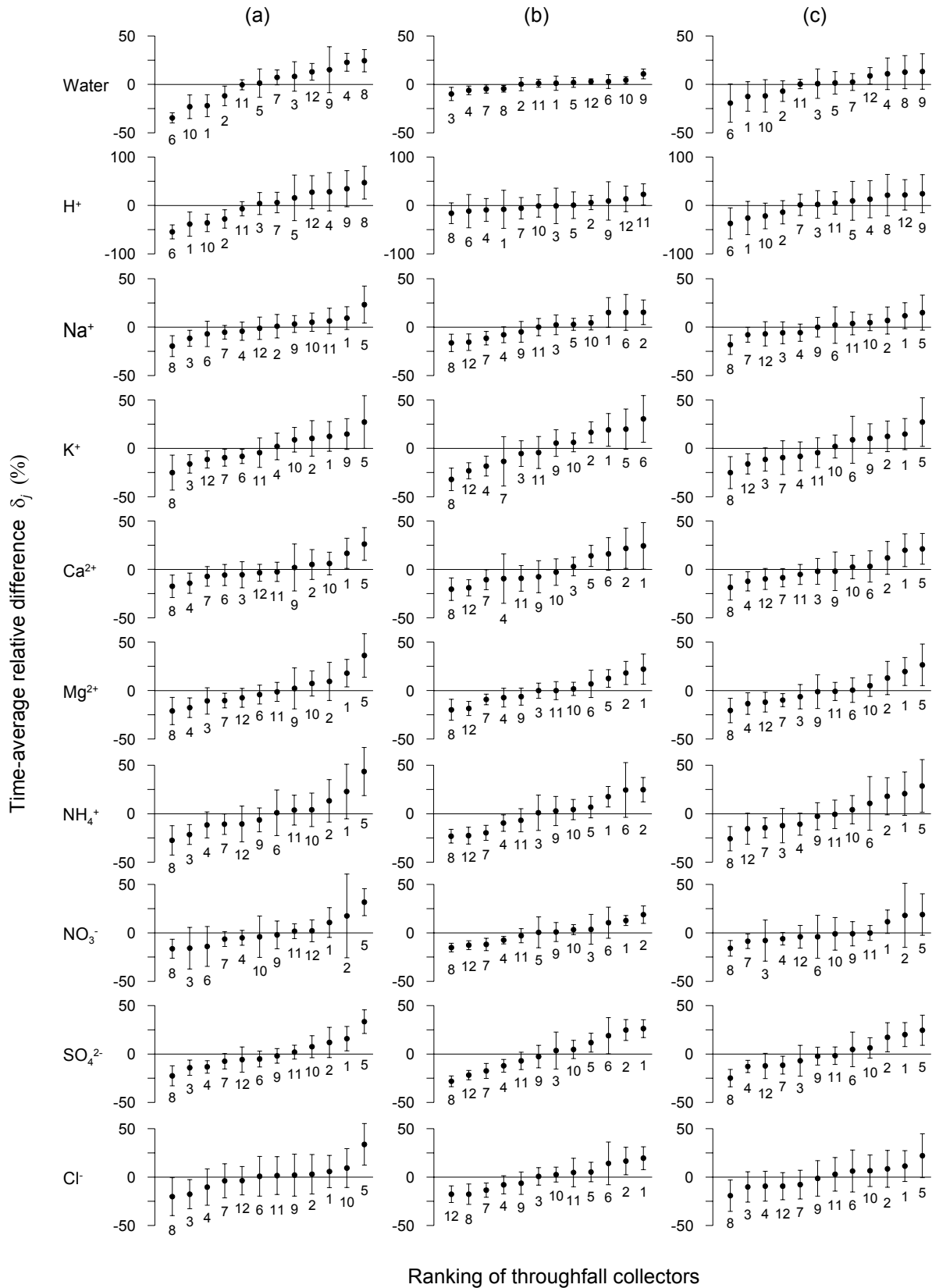


Fig. 6.2. Time stability plots for throughfall water amount and ion deposition. Time-average relative difference of throughfall in biweekly sampling intervals during (a) the leafed season ($m = 13$), (b) the leafless season ($m = 9$), and (c) the annual study period ($m = 22$). Error bars are plus and minus one standard deviation; numbers refer to throughfall collector number ($n = 12$) (cf. Fig. 5.1).

The throughfall fluxes of all ions other than H^+ were positively correlated ($r > 0.79$, $p < 0.01$) with each other during the annual period, the leafed season and the leafless season (Table 6.3). TF depositions, except for H^+ , were negatively related to the amount of TF water during the annual period and the leafed season, but not during the leafless season (Table 6.3). The inverse relationship between TF deposition and TF water amount was significant ($p < 0.05$) at the annual level for NH_4^+ , Cl^- , SO_4^{2-} , and Na^+ , and was suggested during the leafed season (Table 6.3) for all ions ($0.05 < p < 0.10$) other than K^+ and NO_3^- ($p > 0.37$). The TF flux of H^+ , in contrast to the other ions, was positively correlated with the amount of TF water at the annual level ($r = 0.68$, $p < 0.05$) and during the leafed season ($r = 0.92$, $p < 0.001$, Table 6.3), but not during the leafless season.

6.4.4 Relationship between throughfall and canopy structure

Canopy cover within a zenith angle of 5.7° above the 12 TF collectors ranged from 88 to 99% during the leafed season and from 44 to 69% during the leafless season. The corresponding plant area index (PAI) above the collectors ranged from 3.0 to 6.7 in the leafed season, with a plot-average of 4.5, and from 0.6 to 1.3 in the leafless season, with a plot-average of 0.9. The PAIs above the 12 sample locations were significantly correlated between the two periods ($r = 0.82$, $p = 0.001$).

Pearson correlation coefficients between TF and PAI during the leafed season (PAI_L) (Table 6.4) were slightly higher than correlations between TF and canopy cover (not shown), while TF was similarly related to PAI during the leafless season (PAI_{NL}) as to branch cover. TF was more closely correlated with the canopy structure determined using a zenith angle of 5.7° than using an angle of 1.9° or 3.8° (not shown). The value of the canopy extinction coefficient (k) used to derive PAI from canopy cover (Eq. 4.1) did not influence the calculated correlation coefficients. Correlations between PAI and the ratio of TF to wet-only deposition (Fig. 6.3) were exactly equal to correlations between PAI and TF (Table 6.4) and PAI and NTF.

The relationship between canopy structure and TF differed between the water amount and H^+ flux in TF on the one hand, and the TF flux of all other ions on the other hand. During the leafed season, the amount of TF water and H^+ in TF were negatively correlated with PAI in the leafed season (PAI_L), but more strongly correlated with PAI in the leafless season (PAI_{NL}) (Table 6.4). During the leafless season, TF water and H^+ deposition were not significantly related to canopy structure (Table 6.4).

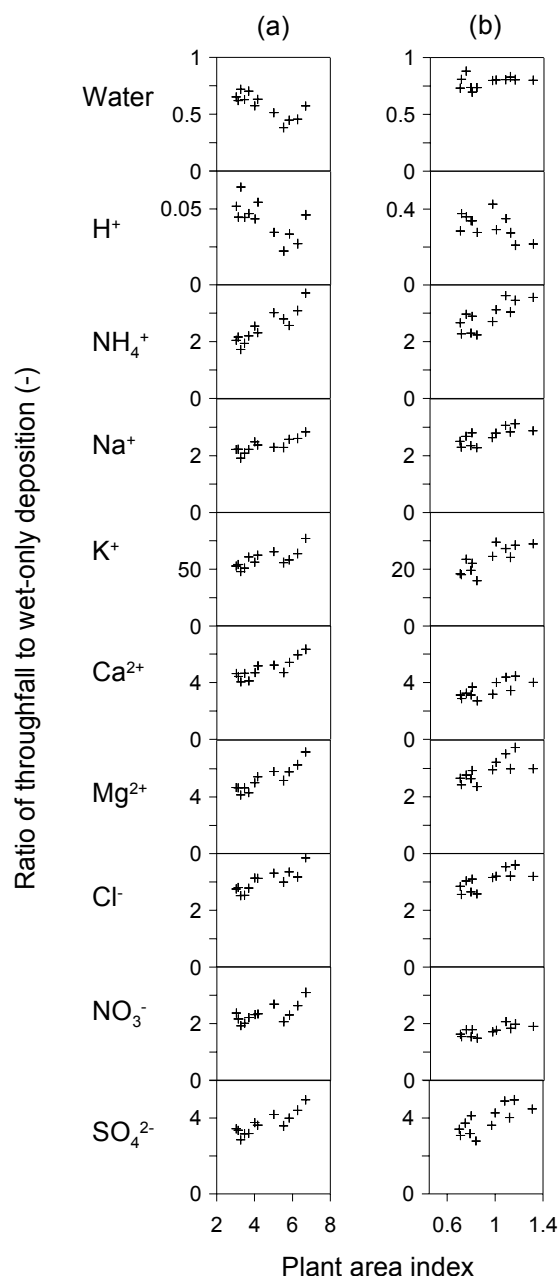


Fig. 6.3. Ratio of throughfall to wet-only (TF:WD) water amount and ion deposition in relationship to plant area index (PAI) in (a) the leafed season (TF:WD_L vs. PAI_L) and (b) the leafless season (TF:WD_{NL} vs. PAI_{NL}). Pearson correlation coefficients are given in Table 6.4.

In contrast to the TF water amount and H⁺ deposition, TF fluxes of all other ions were significantly positively correlated with canopy structure (Table 6.4). The ion fluxes, except for H⁺, were positively related to canopy cover and PAI_L during the leafed season ($r > 0.68$, $p < 0.05$) and to branch cover and PAI_{NL} during the leafless season ($r > 0.76$, $p < 0.01$) (Table 6.4). Like during the leafed season, annual TF water was more closely related to PAI_{NL} than to PAI_L, while the annual ion fluxes in TF were more closely related to PAI_L.

Table 6.4. Pearson correlation coefficients ($n = 12$) between semi-annual and annual throughfall (TF) water amount and ion deposition, and plant area index (PAI) in the leafed (L) and leafless (NL) season. PAI was derived from canopy cover in a zenith angle of 5.7° above TF collectors.

Variable	TF _L		TF _{NL}	TF _{year}	
	PAI _L	PAI _{NL}	PAI _{NL}	PAI _L	PAI _{NL}
Water	-0.76**	-0.89***	0.29	-0.63**	-0.92***
H ⁺	-0.65*	-0.92***	-0.47	-0.63**	-0.61*
Na ⁺	0.82**	0.58*	0.80**	0.88***	0.82**
K ⁺	0.75**	0.39	0.88***	0.85***	0.59*
Ca ²⁺	0.86***	0.58*	0.79**	0.90***	0.71**
Mg ²⁺	0.90***	0.63*	0.76**	0.90***	0.73**
NH ₄ ⁺	0.90***	0.72**	0.84***	0.92***	0.82**
NO ₃ ⁻	0.68*	0.35	0.79**	0.77**	0.51
SO ₄ ²⁻	0.87***	0.64*	0.82**	0.90***	0.79**
Cl ⁻	0.84***	0.59*	0.79**	0.88***	0.79**

Significance levels: * $p < 0.05$; ** $p < 0.01$; *** $p < 0.001$.

Lastly, the different canopy development phases during the leafed season were examined. The TF fluxes during the fully leafed period were generally more closely related to PAI_L than the TF fluxes during leaf emergence and leaf senescence (Fig. 6.4). There was no significant correlation with PAI_L for the TF deposition of K⁺ and NO₃⁻ during the short period of leaf emergence, and for the TF of Na⁺ and Cl⁻ during leaf senescence.

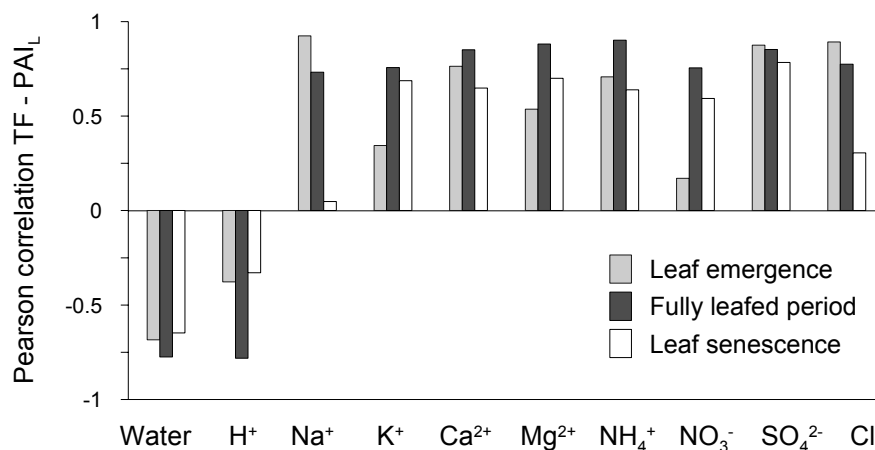


Fig. 6.4. Pearson correlation coefficients ($n = 12$) between plant area index in the leafed season (PAI_L) and throughfall (TF) water amount and ion deposition during each of three phenological canopy phases in the leafed season. PAI was derived from canopy cover in a zenith angle of 5.7° above TF collectors.

6.5 Discussion

6.5.1 Spatial variability and temporal stability of throughfall

The spatial heterogeneity of the annual and biweekly TF depositions under the studied beech tree was similar to the heterogeneity in a mixed oak-beech stand (Duijsings *et al.*, 1986), but relatively low compared with reported TF variability at the rain event scale (Kimmins, 1973; Kostelnik *et al.*, 1989; Puckett, 1991). Our results confirm that differences in TF concentration between collectors are generally greater than differences in TF volume (Kimmins, 1973; Kostelnik *et al.*, 1989; Lawrence and Fernandez, 1993; Houle *et al.*, 1999a). As a result, the variability in TF ion depositions was lower than in TF concentrations for all measured ions except H^+ (Table 6.2).

The observed ion ranking according to the heterogeneity of TF deposition generally corresponds to previous reports. H^+ and NH_4^+ were more spatially variable than other ions, while Na^+ and Cl^- were less variable (Houle *et al.*, 1999a; Duijsings *et al.*, 1986; Lin *et al.*, 1997). However, the spatial variation of K^+ deposition during the growing season was lower than observed under other mixed hardwood forests, which may be due to the fact that only one tree species was considered here and that all collectors were positioned under a closed canopy. The spatial variability of TF deposition has been reported to decline with increasing length of the sampling interval (Duijsings *et al.*, 1986; Lawrence and Fernandez, 1993; Houle *et al.*, 1999a), although Kimmins (1973) found that sampling at longer intervals did not reduce the variability of TF deposition of the studied ions (K^+ , Ca^{2+} , and Mg^{2+}). In the present study, little difference was observed between the variability of biweekly, semiannual, and annual TF deposition. While TF deposition represents the actual ion input to the forest floor, the variability of net throughfall ion input reflects the effects of dry deposition and canopy interactions on TF chemistry. The NTF variability was higher than the TF variability for all ions other than H^+ and K^+ (Table 6.2), indicating that in general the input by wet deposition partly masked the spatially heterogeneous ion enrichment in TF fluxes beneath the canopy. For K^+ , the variability of NTF and TF deposition was equal because of the very low precipitation input of K^+ relative to TF. For H^+ , in contrast, the spatial variation in NTF was low because the actual TF deposition of H^+ to the forest floor was much smaller than the H^+ input by wet deposition, indicating canopy retention of H^+ (Lovett *et al.*, 1996).

Few reports have been made of TF variability under defoliated conditions. We found no clear difference in the spatial variability of TF depositions between the leafed and the leafless season (Fig. 6.1), and TF fluxes were only significantly more variable in the leafed season for

TF water amount and H^+ deposition. This corresponds with the results of Duijsings *et al.* (1986) for a mixed oak-beech stand, while also Puckett (1991) found an unexpectedly high NTF variability for the single winter event measured.

The spatial distribution of TF water and chemistry can vary considerably between individual rain events (Kostelnik *et al.*, 1989; Puckett, 1991; Lin *et al.*, 1997) and between biweekly samplings (Houston *et al.*, 2002), although consistent storm-to-storm patterns have been observed under beech (Robson *et al.*, 1994), spruce (Whelan *et al.*, 1998), and Douglas fir (Raat *et al.*, 2002). However, temporal stability has mostly been assessed for few events and in a non-quantitative way. The temporal stability of spatial TF patterns in the present study depended on the ion and the period of the year considered. A systematic location effect on TF was found at the semiannual level, as TF deposition was significantly ($p < 0.05$) correlated between the leafed and leafless season for all measured ions other than NO_3^- and H^+ (Table 6.3) During the leafed season, the temporal stability of the TF water amount was greater than the temporal stability of TF ion fluxes, in agreement with results obtained for coniferous forests (Lawrence and Fernandez, 1993; Whelan *et al.*, 1998; Raat *et al.*, 2002). Nevertheless, spatial patterns of TF deposition demonstrated a relatively high temporal stability during the leafless season, particularly for NH_4^+ and SO_4^{2-} .

6.5.2 Spatial variability of throughfall in relationship to canopy structure

The observed spatial variability of TF under a deciduous beech tree was largely explained by a simple measure of canopy structure, i.e. the canopy cover or plant area index (PAI) above a sampling point. The TF deposition of all ions other than H^+ increased with increasing PAI, both during the leafed ($r^2 = 0.46-0.81$) and leafless season ($r^2 = 0.58- 0.77$) (Table 6.4). In contrast, the TF water amount and H^+ deposition during the growing season decreased with increasing PAI, and were better explained by the branch structure ($r^2 > 0.79$) than by leaves and branches together ($r^2 < 0.57$).

To our knowledge, relationships between canopy structure and TF chemistry within stands have only been reported for coniferous forests. In three black spruce stands, calculated canopy depth partly explained the growing season TF deposition of K^+ ($r^2 = 0.18-0.30$), and Ca^{2+} and Mg^{2+} ($r^2 = 0.30-0.55$) (Carleton and Kavanagh, 1990). In a spruce stand in which canopy cover ranged from 50 to 95%, bimonthly TF deposition of all major ions other than H^+ was linearly related to canopy cover ($r^2 = 0.32-0.54$), while exponential relationships better

described TF in a less homogeneous spruce stand where canopy cover ranged from 0 to 85% ($r^2 = 0.43-0.91$) (Hug *et al.*, 2005). In a spruce plantation, curvilinear relationships between canopy cover and TF deposition of different ions for six winter events were significant ($p < 0.05$) in 57% of the cases, with curve maxima occurring at canopy cover of 70 to 80% (Whelan *et al.*, 1998). At the stand level, annual NTF fluxes of major ions were significantly ($p < 0.01$) positively correlated with leaf area index (LAI) in 30 forests stands, while H^+ deposition was negatively correlated to LAI (Draaijers, 1993).

Similar spatial patterns were found for ions associated with dry deposition and canopy leaching, in agreement with previous studies (Robson *et al.*, 1994; Whelan *et al.*, 1998; Raat *et al.*, 2002) (Table 6.3, Fig. 6.2). Strong spatial correlations between TF depositions may be explained by the fact that the foliage density per area ground surface influences both foliar leaching and dry deposition. This was confirmed by the close relationships between local PAI and TF for ions mainly originating from dry deposition, like NH_4^+ , SO_4^{2-} , and Cl^- , and for ions that are partly leached from the canopy, like Ca^{2+} and Mg^{2+} (Table 6.4). The lower correlation between canopy measurements and the TF flux of K^+ and NO_3^- during the leafed season mainly resulted from a deviating spatial TF heterogeneity during leaf emergence (Fig. 6.4). TF deposition of H^+ was significantly negatively related to PAI, indicating the capacity of deciduous canopies to neutralize precipitation. As discussed in section 5.5.4, the lower acidity of throughfall water with increasing PAI may be due to H^+ uptake in plant tissue by cation exchange of K^+ , Ca^{2+} , Mg^{2+} (Lovett *et al.*, 1996), excretion of weak acids (Cronan and Reiners, 1983), uptake of HNO_3 (Stachurski and Zimka, 2002), and reduction of acidity by dry deposited atmospheric NH_3 (De Schrijver *et al.*, 2004) and Ca^{2+} compounds (Lee and Longhurst, 1992).

The relationship between TF and the canopy structure differed between TF chemistry and TF water amount (Table 6.4, Fig. 6.3). During the leafed season, the spatial heterogeneity of TF chemistry, except for H^+ , was more influenced by leaves than by branches, probably because of the higher collecting surface area and physiological activity of leaves than of branches. Nevertheless, during the leafless season, the spatial patterns of TF deposition of all ions other than H^+ were significantly related to the tree branch structure. Although the collecting surface of a forest during the dormant season is much smaller than during the growing season, atmospheric turbulence is high in open canopies due to the absence of leaves and the generally higher wind speeds in winter at the study site (see section 3.4.3), which enhances dry deposition onto branches in defoliated conditions (Beckett *et al.*, 2000; Freer-Smith *et al.*,

2004). Besides, seasonal differences in air concentrations of elements may be important, e.g., for Na^+ , Mg^{2+} , and Cl^- (see also section 5.5.2). In addition to wash-off of dry deposition, cation leaching from twigs and branches (Levia and Herwitz, 2002) may have contributed to the spatial heterogeneity of TF depositions observed during the dormant season, particularly for K^+ and to a lesser extent for Ca^{2+} (see section 5.5.3)

In contrast to TF chemistry, the spatial variability of the amount of TF water during the leafed season was more closely correlated with twig and branch cover (PAI_{NL}) than with foliated canopy cover (PAI_{L}) (Table 6.4). During the dormant season, however, the amount of TF water showed a low degree of spatial variability and could not be explained by the simple measure of branch structure used. These results, based on biweekly sampled TF during one year using 12 collectors, were also observed at the rain event level using 20 tipping bucket collectors over a two-year period (Chapter 4). A detailed discussion of these findings is given at the end of section 4.5.3.

6.6 Conclusions

The spatial variability of annual throughfall deposition under the studied beech tree was highest for H^+ and NH_4^+ , intermediate for SO_4^{2-} , Mg^{2+} , K^+ , and Ca^{2+} , and lowest for NO_3^- , Na^+ and Cl^- . While the spatial pattern of the amount of throughfall water was more consistent throughout the leafed season than the pattern of ion depositions in throughfall, the spatial variability of throughfall depositions demonstrated a relatively high temporal stability during the leafless season. Similar spatial patterns were found for ions associated with dry deposition and canopy leaching. The observed spatial heterogeneity of ion deposition was closely positively correlated with the local canopy cover or plant area index, not only during the leafed season but also in non-foliated conditions. Consequently, the biomass and distribution of both foliage and branches significantly influence the spatial pattern of throughfall deposition beneath the deciduous canopy studied. Besides the heterogeneous distribution of throughfall, stemflow fluxes in beech stands contribute substantially to the spatial variability of water and ion inputs to the forest floor (see Chapter 5, section 5.5.5). We conclude that calculations of percolation fluxes and element budgets in beech stands may be improved by considering the spatial heterogeneity of both throughfall and stemflow fluxes.

7 Quantifying atmospheric deposition onto a beech canopy using varying forms of the canopy budget method and an inferential technique

After: Staelens, J., De Schrijver, A., Neiryneck, J. and Verheyen, K. Quantifying atmospheric deposition onto a deciduous forest canopy using varying forms of the canopy budget method and an inferential technique. To be submitted to an international journal with peer review.

7.1 Abstract

The canopy budget model is a calculation scheme simulating the interaction of major ions within forest canopies based on throughfall and precipitation measurements. The method is often used to estimate dry deposition onto forest ecosystems, but varying forms have been reported. To examine the sensitivity of the estimated deposition fluxes to input data and model choices, variations on the canopy budget model were applied for two deciduous forest plots located in contrasting regions, i.e. a beech (*Fagus sylvatica* L.) plot in Belgium and a mixed sugar maple (*Acer saccharum* Marsh.) plot in Quebec. For both forest plots, a semi-annual time step in the model gave similar results as an annual time-step. Sodium was found to be more suitable as a tracer ion in the filtering approach than Cl^- or SO_4^{2-} . Using bulk instead of wet-only precipitation in the model may underestimate the acidifying deposition of nitrogen (N) and sulphur (S). Different canopy exchange equations had relatively little effect on the estimated NH_4^+ deposition at the beech plot but affected the estimated H^+ and NH_4^+ fluxes at the maple plot. Dry deposition of S and N onto the beech canopy was also calculated using measured air concentrations and deposition velocities from literature. This inferential technique resulted in a higher estimated N deposition than the canopy budget method when weak acid excretion was taken into account, but agreed well for S deposition.

7.2 Introduction

Air pollution and the associated high deposition levels of sulphur and nitrogen may have adverse effects on the structure and functioning of forest ecosystems (Aber *et al.*, 1998; Bouwman *et al.*, 2002). Therefore, quantifying atmospheric deposition is a key issue in large-scale forest monitoring programmes such as the Pan-European programme for intensive and continuous monitoring of forest ecosystems (de Vries *et al.*, 2003). Atmospheric deposition consists of wet, dry, and occult deposition. Wet deposition is defined as the process by which atmospheric compounds are attached to and dissolved in cloud and precipitation droplets and delivered to the earth's surface by rain, hail or snow (Krupa, 2002). Dry deposition is the direct deposition of particles and gases onto plant surfaces which is then washed off by precipitation (Lovett and Lindberg, 1984). Dry deposition onto forests is considerably higher than dry deposition in the open field due to canopy roughness, large foliage surface areas, and physical and physiological properties of tree leaves (Erisman and Draaijers, 2003). Occult deposition of nutrients occurs to receptor surfaces immersed in cloud or fog and can contribute significantly to forest ecosystems budgets at high-elevation sites (Oyarzún *et al.*, 2004), but is generally considered negligible for lowland forests (Vermeulen *et al.*, 1997).

Wet deposition is most accurately measured using wet-only precipitation collectors, but continuously open bulk collectors are often used in ecological studies (see section 2.2). Dry deposition can be measured directly using micrometeorological techniques or indirectly using surface wash techniques. Micrometeorological techniques such as the eddy correlation or the gradient method require large monitoring efforts and thus inferential models have been developed, which estimate pollutant-specific deposition velocities that are multiplied by measurements of near-surface air concentrations to estimate dry deposition (e.g., Hicks *et al.*, 1987, Zhang *et al.*, 2002). The most applied surface wash technique is the throughfall method, in which the amount and quality of water above and beneath a forest canopy is measured (Draaijers *et al.*, 1996; de Vries *et al.*, 2003). When throughfall measurements are used for quantifying atmospheric deposition to forests, a distinction has to be made between in-canopy sources and atmospheric sources of chemical compounds. The throughfall enrichment of a compound below the canopy provides an estimate of the dry and occult deposition onto the canopy only if all deposited material is washed off by rain and if canopy exchange is quantified. Canopy exchange processes comprise ion diffusion and/or exchange between the water layer covering plant tissue and the underlying apoplast, as well as stomatal uptake of gases (Draaijers *et al.*, 1997).

Separating internal and external ion sources in throughfall and stemflow has been an ongoing concern for several decades (White and Turner, 1970; Mayer and Ulrich, 1978; Lovett and Lindberg, 1984; Beier *et al.*, 1992; Draaijers and Erisman, 1995; Stachurski and Zimka, 2000). Two widely used methods are a multiple regression model developed by Lovett and Lindberg (1984) and extended by Lovett *et al.* (1996), and a canopy budget model proposed by Ulrich (1983) and extended by Bredemeier (1988), Van der Maas *et al.* (1991), and Draaijers and Erisman (1995). The regression model distinguishes net throughfall of individual rain events into dry deposition and canopy exchange based on the duration of the antecedent dry period and event precipitation amount (Lovett and Lindberg, 1984) and composition (Lovett *et al.*, 1996). The canopy budget model distinguishes between internal and external input sources to ecosystems using the so-called ‘filtering approach’ based on a tracer ion (Ulrich, 1983) and by estimating ion exchange processes occurring within the forest canopy (Draaijers and Erisman, 1995).

The canopy budget method has been used for a wide range of forest types and atmospheric pollution levels (Table 7.1), although several of its basic assumptions have not properly been evaluated for different environmental conditions (de Vries *et al.*, 2003). The method has been validated for a Douglas fir forest in an area with high nitrogen (N) and sulphur (S) deposition (Draaijers and Erisman, 1995), and except for oxidised N, deposition estimates were similar to estimates derived from micrometeorological measurements and inferential modelling. However, for 13 forest plots in Switzerland, the dry deposition of N and S derived from throughfall using the canopy budget method was significantly lower than results of an inferential method based on deposition velocities taken from literature (Thimonier *et al.*, 2005).

Since the publication of the canopy budget model by Draaijers and Erisman (1995), several variations have been reported. Applications differ in the type of precipitation input, tracer ion and time step used, and in the assumptions made about canopy exchange processes. Nevertheless, little is known about the impact of these model variations on the calculated dry and atmospheric deposition. Therefore, the aims of this chapter were (i) to give an overview of varying forms of the canopy budget method, (ii) to assess the effect of model variations on the estimated atmospheric deposition and canopy exchange for two contrasting case studies, i.e. deciduous forest canopies located in Western Europe and Canada, and (iii) to compare the dry deposition of nitrogen and sulphur calculated with a canopy budget method with results of an inferential method.

Table 7.1. Some reported applications of the canopy budget method: reference, country, forest type, model type, and precipitation deposition (PD) data used.

Reference	Country	Forest type / tree species ^a	Model ^b	PD ^c
<i>Filtering approach used for base cations, chloride, sulphate, and/or phosphate</i>				
Armbruster (2002) ^d	Europe	Coniferous (59), deciduous (12)	Na ⁺	BD
Asche (1988) ^e	Germany	Oak-hornbeam	Na ⁺	BD
Bélanger (2004)	U.S.A.	Deciduous (29)	Na ⁺	WD
Bouya <i>et al.</i> (1999)	Belgium	Norway spruce (2)	Cl ⁻	BD
Bredemeier (1988) ^e	Germany	Spruce (5), beech (3), oak-pine	Na ⁺	BD
Duchesne <i>et al.</i> (2001)	Canada	Mixed deciduous	Na ⁺	WD
Ignotavo and Dambrine (2000) ^e	France	Norway spruce (3)	Na ⁺ , SO ₄ ²⁻	BD
Houle <i>et al.</i> (1999b)	Canada	Mixed deciduous, coniferous	Na ⁺	WD
Langush <i>et al.</i> (2003) ^e	Europe	Coniferous (31), deciduous (6)	Na ⁺	BD
Lin <i>et al.</i> (2000, 2001)	Taiwan	Mixed subtropical rainforest	Na ⁺	BD
Oyarzún <i>et al.</i> (2004) ^e	Chile	Evergreen rainforest	Na ⁺	BD
Ukonmaanaho and Starr (2002) ^e	Finland	Boreal forest types (6)	SO ₄ ²⁻	BD
Ulrich (1983)	Germany	Norway spruce, beech	Na ⁺	BD
Van Ek and Draaijers (1994)	The Netherlands	Douglas fir, Scots pine, oak	Na ⁺	BD ^f
Yoshida and Ichikuni (1989)	Japan	Japanese oak, Japanese cedar	Al ³⁺	BD
<i>Filtering approach and canopy exchange between base cations and NH₄⁺ + H⁺</i>				
Balestrini and Tagliaferri (2001)	Italy	Norway spruce, silver fir	Na ⁺ + w.a.	BD
De Schrijver <i>et al.</i> (2004)	Belgium	Corsican pine, silver birch	Na ⁺	BD
de Vries <i>et al.</i> (1998)	Europe	(suggested modelling technique)	Na ⁺	BD
de Vries <i>et al.</i> (2003)	Europe	Coniferous and deciduous (255)	Na ⁺	BD
Devlaeminck <i>et al.</i> (2005)	Belgium	Beech (6)	Na ⁺	BD
Draaijers and Erisman (1995)	The Netherlands	Douglas fir	Na ⁺ + w.a.	BD
Draaijers <i>et al.</i> (1997)	The Netherlands	Douglas fir	Na ⁺ + w.a.	BD
Puxbaum and Gregori (1998)	Austria	Oak (6)	Na ⁺	BD
Schmitt <i>et al.</i> (2005)	Switzerland	Coniferous (4), deciduous (6)	Na ⁺ + w.a.	BD ^f
Thimonier <i>et al.</i> (2005)	Switzerland	Coniferous (6), deciduous (7)	Na ⁺ + w.a.	BD ^f
Van der Maas and Pape (1991)	The Netherlands	Douglas fir	Na ⁺ + w.a.	BD
Zeng <i>et al.</i> (2005)	China	Mixed subtropical forest	Na ⁺ + w.a.	BD

^a Number of forest plots given in brackets if different from one

^b Tracer ion used in the filtering approach; canopy uptake of NH₄⁺ and H⁺ calculated excluding or including canopy leaching of weak acids (+ w.a.)

^c BD: bulk precipitation deposition; WD: wet-only precipitation deposition

^d Filtering approach used for Mg²⁺ only

^e Filtering approach also used for H⁺, NH₄⁺, and/or NO₃⁻

^f Bulk precipitation deposition corrected for dry deposition onto collectors using correction factors taken from literature

7.3 Materials and methods

7.3.1 Study sites

To assess the impact of variations on the canopy budget method, data of two hardwood sites in different regions were used. First, the method was applied for a European beech (*Fagus sylvatica* L.) plot in Belgium. Throughfall was sampled from March 2003 to March 2004 with

12 collectors disposed in a 12 x 6 m plot under one dominant beech tree. Stemflow was sampled throughout the year, and was included for calculating net throughfall plus stemflow fluxes. More information on site description, data collection, and quality control is given in Chapter 5 (section 5.3). For this site, also an inferential technique was applied.

Second, the canopy budget method was tested for a mixed deciduous forest site located in the Lake Clair Watershed (46°57' N, 71°40' W, 270-390 m a.s.l.) in Quebec, Canada (Houle *et al.*, 1999b). The dominant species (82% of basal area) in the study plot is sugar maple (*Acer saccharum* Marsh.) with an admixture of American beech (*Fagus grandifolia* Ehrh.) and yellow birch (*Betula alleghaniensis* Britton). Leaf area index of the deciduous stand was 5.5 in 1991. Throughfall was sampled from June 1989 to December 1996 with 36 funnel collectors in a 40 x 90 m plot during the growing season (May to October) and 12 pails for snow collection during the dormant season (November to April). Major ions were analysed by ion chromatography (SO_4^{2-} , NO_3^- , Cl^-), colorimetry (NH_4^+), and flame emission spectrometry or inductively coupled plasma emission spectrometry (K^+ , Ca^{2+} , Mg^{2+} , and Na^+). The data used in this chapter are eight-year averages of wet-only precipitation and throughfall fluxes for the growing and dormant seasons (Table 2 in Houle *et al.* (1999b)). Stemflow was measured for four years during the growing season only, and its contribution to the forest floor input was estimated to be lower than 5% for all ions, except for K^+ (9%) (Houle *et al.*, 1999b). As no annual stemflow fluxes were available, only wet precipitation and throughfall fluxes were used. Further details on site description and data collection are given in Houle *et al.* (1999b). This study was chosen because it reports seasonal throughfall and wet-only deposition fluxes for all major ions. Other North American studies in deciduous hardwood forests were rejected because of lacking measurements in the dormant season or lacking wet-only precipitation or Na^+ fluxes. Houle *et al.* (1999b) used Na^+ as a tracer ion to determine the annual contribution of canopy leaching to the throughfall enrichment of K^+ , Ca^{2+} , and Mg^{2+} .

7.3.2 Canopy budget method

7.3.2.1 'Reference' canopy budget method

Dry deposition and canopy exchange were first estimated by the canopy budget model as described by de Vries *et al.* (2003). In this method, Na^+ is used as tracer ion for calculating the dry deposition of K^+ , Ca^{2+} , and Mg^{2+} . Dry deposition of reduced N is calculated by estimating canopy exchange processes without accounting for weak acid excretion by the canopy. All fluxes are expressed in $\text{mmol}_c \text{ m}^{-2} \text{ yr}^{-1}$ (= $\text{meq m}^{-2} \text{ yr}^{-1}$).

Ion deposition beneath a forest canopy by throughfall (TF) and stemflow (SF) results from total atmospheric deposition (TD) and canopy exchange (CE) (Lovett *et al.*, 1996):

$$TF + SF = TD + CE = WD + DD + CE \quad (7.1)$$

where WD is the wet deposition and DD is the dry deposition (plus occult deposition, if that is important in the system under study). The canopy exchange is positive when the canopy contributes ions (canopy leaching, CL) or negative when ions are absorbed by the canopy (canopy uptake, CU). The net throughfall and stemflow (NTF) flux is defined as:

$$NTF = TF + SF - WD = DD + CE \quad (7.2)$$

According to the canopy budget method, Na^+ is assumed to be inert with respect to the canopy, i.e. neither uptake nor leakage occurs ($CE = 0$). Dry deposition of base cations Ca^{2+} , Mg^{2+} , and K^+ is computed by the so-called ‘filtering approach’ (Ulrich, 1983) or Na^+ ratio method, assuming that the ratio between dry and wet deposition of Na^+ is similar for particles containing base cations:

$$DD_X = \frac{(TF + SF - WD)_{\text{Na}}}{WD_{\text{Na}}} \cdot WD_X \quad (7.3)$$

where X is Ca^{2+} , Mg^{2+} or K^+ . The NTF to WD ratio of Na^+ is called the dry deposition factor (DDF) of Na^+ . Canopy leaching of base cations is then determined by subtracting the calculated DD (Eq. 7.3) from the NTF deposition (Eq. 7.2). Canopy uptake of H^+ and NH_4^+ is assumed to equal the canopy leaching of base cations (BC) because of ion charge balance:

$$CU_{\text{NH}_4+\text{H}} = CL_{\text{BC}} \quad (7.4)$$

In allocating the uptake of H^+ and NH_4^+ , it is assumed that H^+ has per mol an exchange capacity six times larger than NH_4^+ ($xH = 6$), based on a laboratory experiment with Douglas fir branches (Van der Maas *et al.*, 1991):

$$CU_{\text{NH}_4} = \frac{(TF + SF)_{\text{NH}_4}}{(TF + SF)_{\text{NH}_4} + xH \cdot (TF + SF)_H} \cdot CL_{\text{BC}} \quad (7.5)$$

Knowing the canopy uptake of H^+ and NH_4^+ , the dry deposition flux of H^+ and NH_x (NH_3 and NH_4^+ aerosol) can be computed from Eq. 7.2. Nitrate, SO_4^{2-} , and Cl^- are assumed to flow passively through the canopy ($CE = 0$), so that the DD equals the NTF deposition.

7.3.2.2 Varying forms of the canopy budget method

Dry deposition and canopy exchange were also calculated using several reported variations on the canopy budget model. The impact of different assumptions on the calculated fluxes was assessed by comparing these results to those of the ‘reference version’ of de Vries *et al.* (2003) described above (7.3.2.1).

(1) Time step of the model. While the canopy budget model is generally calculated on an annual or seasonal basis, Duchesne *et al.* (2001) estimated DD at a 1-week time step, allowing to determine the temporal evolution of DD. We assessed the impact of different time steps by running the model on a biweekly, semiannual, and annual (reference version) basis.

(2) Precipitation data. Although wet-only precipitation measurements more accurately represent wet deposition fluxes (see Chapter 2), bulk deposition measurements are often used as precipitation input for the canopy budget method (Table 7.1). The model was run using wet-only (reference version) and bulk precipitation deposition data.

(3) Tracer ion. The vast majority of previous studies (Table 7.1) have used assumed sodium to be an inert tracer ion for calculating DD. Nevertheless, other ions such as chloride (Bouya *et al.*, 1999), aluminium (Yoshida and Ichikuni, 1989), and sulphate (Ignatova and Dambrine, 2000; Ukonmaanaho and Starr, 2002) have also been used. Since Al^{3+} was not measured in the case studies, the model was applied using Na^+ (reference version), Cl^- , and SO_4^{2-} as tracer ion in Eq. 7.3.

(4) Dry deposition factor (DDF) of Na^+ for all ions. The filtering approach used for estimating DD of K^+ , Ca^{2+} , and Mg^{2+} (Eq. 7.3) can be extended to other ions such as SO_4^{2-} (Bouya *et al.*, 1999), Cl^- (Draaijers and Erisman, 1995), and H^+ , NH_4^+ , and NO_3^- (Ulrich, 1983; Lin *et al.*, 2000; Langusch *et al.*, 2003). Following this approach, the DDF of Na^+ was used to estimate the (particulate) DD of all measured ions. The difference (if > 0) between the NTF and the (particulate) DD calculated in this way has been used to estimate the gaseous DD of HCl (Draaijers and Erisman, 1995), SO_2 (Langusch *et al.*, 2003), NO_x and NH_3 (Hug *et al.*, 2005).

(5) Weak acids (w.a.). Canopy uptake of H^+ and NH_4^+ due to canopy leaching of K^+ , Ca^{2+} , and Mg^{2+} can be corrected for the simultaneous canopy leaching of base cations and weak acids (CL_{wa}), which include bicarbonate and weak organic anions. Eq. 7.4 then becomes:

$$CU_{NH_4+H} = CL_{BC} - CL_{wa} \quad (7.6)$$

The CL_{wa} is calculated by subtracting TD from (TF+SF) of weak acids (Eq. 7.2). Therefore,

including leaching of weak acids requires an estimate of the generally unknown fluxes of weak acids in WD, DD, TF, and SF. The concentration of weak acids in WD, TF, and SF was estimated as the difference in concentration of the measured cations and strong acid anions (Chiwa *et al.*, 2004). Draaijers and Erisman (1995) assumed that DD_{wa} equalled WD_{wa} . To test the sensitivity of this assumption, DD_{wa} was also set equal to 0 (cf. Schaefer *et al.*, 1992).

(6) Leaching of Na^+ , Cl^- , and SO_4^{2-} . To our knowledge, reported applications of the canopy budget method all have assumed that TF and SF enrichment of Na^+ , Cl^- , and SO_4^{2-} were only due to wash-off of DD. However, the seasonal variation in TF chemistry beneath the studied beech canopy strongly suggested canopy leaching (CL) of these three ions during leaf emergence and/or leaf senescence (see 5.5.2 and 5.5.4). Therefore, CL of Na^+ during leaf emergence was estimated by calculating DD of Na^+ using the NTF:WD (DDF) of Na^+ during the fully leafed period (leafed season without leaf emergence and senescence). Likewise, CL of SO_4^{2-} during leaf senescence was estimated from its NTF:WD ratio during the rest of the year. Canopy leaching of Cl^- during leaf emergence and senescence was calculated using the $Na^+ : Cl^-$ ratio in the NTF deposition during the fully leafed period and leafless season. Then, canopy uptake of H^+ and NH_4^+ was computed as CL_{BC} (including CL_{Na}) minus CL of SO_4^{2-} and Cl^- (analogously to Eq. 7.6).

(7) NH_4^+ uptake. Different equations have been used for allocating the relative uptake of H^+ versus NH_4^+ . While Eq. 7.5 (Draaijers *et al.*, 1998; de Vries *et al.*, 2001, 2003) only takes TF (+SF) deposition into account, wet precipitation fluxes of H^+ of NH_4^+ have also been included (de Vries *et al.*, 1998; De Schrijver *et al.*, 2004; Devlaeminck *et al.*, 2005; all with $xH = 1$):

$$CU_{NH_4} = \frac{(WD + TF + SF)_{NH_4}}{(WD + TF + SF)_{NH_4} + xH \cdot (WD + TF + SF)_H} \cdot CL_{BC} \quad (7.7)$$

Furthermore, ratios of H^+ and NH_4^+ in TF (+SF) and WD have been used (Draaijers and Erisman, 1995; Zeng *et al.*, 2005):

$$CU_H = \frac{CL_{BC}}{1 + \frac{2}{xH \cdot \left[\frac{TF_H + SF_H}{TF_{NH_4} + SF_{NH_4}} + \frac{WD_H}{WD_{NH_4}} \right]}} \quad (7.8)$$

The method was tested using Eq. 7.5, 7.7, and 7.8, in which xH was set equal to 1, 6, and 10.

(8) NO_3^- uptake. When canopy exchange of NO_3^- is assumed to be zero, as in the reference version of the canopy budget method, DD of NO_3^- can be calculated directly. However, there

is much evidence of canopy uptake of oxidised N in experimental as well as field studies (Harrison *et al.*, 2000). Therefore, de Vries *et al.* (2001) suggested to calculate canopy uptake of NO_3^- based on TF fluxes of NH_4^+ and NO_3^- , using an efficiency factor of NH_4^+ vs. NO_3^- uptake ($x\text{NH}_4$) with a proposed value of six:

$$CU_{(\text{NO}_3^- + \text{NH}_4^+)} = \frac{x\text{NH}_4 \cdot (\text{TF} + \text{SF})_{\text{NH}_4} + (\text{TF} + \text{SF})_{\text{NO}_3^-}}{x\text{NH}_4 \cdot (\text{TF} + \text{SF})_{\text{NH}_4}} \cdot CU_{\text{NH}_4} \quad (7.9)$$

Nitrate uptake was calculated using Eq. 7.5 ($x\text{H} = 6$) and Eq. 7.9 with $x\text{NH}_4$ set equal to 1, 6, and 10. Note that the estimated NO_3^- uptake can also differ from zero when the dry deposition factor of Na^+ (DDF_{Na}) is used for all ions (approach 4). A weak point of calculating uptake of oxidised N with Eq. 7.9 is that the charge balance of the canopy is not maintained. When NO_3^- is taken up by the canopy, another anion should be released, or, more likely, a cation should be taken up. The study of Stachurski and Zimka (2002) indicates that H^+ retention in a beech canopy did not result from exchange with other cations, but was closely correlated with the retention of nitrate. Therefore, in approach 8, we also examined the effect of assuming that the calculated uptake of NO_3^- was accompanied by an equivalent uptake of H^+ . The leaching of base cations was then attributed entirely to the canopy uptake of NH_4^+ .

7.3.3 Inferential method

For the beech canopy, dry deposition of inorganic N and S was also calculated using an inferential method by multiplying measured air concentrations of NH_3 , NO_2 , and SO_2 with dry deposition velocities for deciduous forest canopies obtained from literature. Atmospheric concentration of NH_3 was measured at the study site during nine months in 2003 with passive samplers (see section 2.3.2). The NH_3 concentration for the other three months was derived from similar measurements at the Bourgoyen-Ossemeersen (15 km distance). As NO_2 and SO_2 were not measured at the study site, data measured by the Flemish Environment Agency were used (VMM, 2004). To obtain air concentrations representative for the beech site, measurements at rural and semi-urban sites in northern Belgium were used to calculate regional mean values. At each site, NO_2 and SO_2 concentrations were determined every 30 minutes by chemiluminescence and UV fluorescence, respectively (VMM, 2004).

Reported deposition velocities onto (deciduous) forests range from 0.8 to 2.2 cm s^{-1} for NH_3 , 0.1 to 0.3 cm s^{-1} for NO_2 , and 0.3 to 1.1 cm s^{-1} for SO_2 (e.g., Erisman, 1993; Hovmand and Kemp, 1996; Puxbaum and Gregory, 1998; Smith *et al.*, 2000; Kovács and Horváth, 2004;

Schmitt *et al.*, 2005). Dry deposition velocities depend on different rates of transport from the atmosphere to the canopy, represented by an aerodynamic, quasi-laminar boundary layer, and canopy resistance in the well known resistance analogy (Hicks *et al.*, 1987). As climate and air concentrations affect deposition rates (Andersen and Hovmand, 1999), we used mean values determined for the Netherlands, where atmospheric conditions are expected to be similar to those at the beech plot. The dry deposition rates used were 1.2, 0.2, and 1.0 cm s⁻¹ for NH₃, NO₂, and SO₂, respectively (Erisman, 1993).

Dry deposition of N compounds includes particulate NH₄⁺ and NO₃⁻, reduced N gas (NH₃), and many gaseous nitrogen oxides such as HNO₃, NO₂, NO, HNO₂, and peroxyacetyl nitrate (Lovett and Lindberg, 1993). However, the major load of dry deposition of gaseous N is due to NH₃, HNO₃, and NO₂ (Andersen and Hovmand, 1999). As no data on air concentrations of HNO₃ and particulate N were available for the beech site, dry deposition of these N forms was approximated from reported inferential modelling results. In the studies mentioned in Table 7.2, NH₃ contributed 74 to 86% of the dry deposition of NH_x, with an average of 79%. Dry deposition of particulate NH₄⁺ was therefore approximated as 21% of the NH_x deposition.

Table 7.2. Comparison of annual dry and wet nitrogen deposition (kg N ha⁻¹ yr⁻¹) at various sites. NH_x: sum of reduced nitrogen compounds; NO_y: sum of oxidised nitrogen compounds. Values between brackets are approximate; values in italic are estimated by a canopy budget method.

Deposition (kg N ha ⁻¹ yr ⁻¹)		The Netherlands ^a Douglas fir	Austria ^b Oak	Denmark ^c Spruce	Hungary ^d Spruce	Belgium ^e Pine	Belgium ^f Beech	Belgium ^g Beech
Dry								
Gaseous	NH ₃	17.9	4.1	10.0	5.6	18.5	16.5	-
	NO ₂	2.8 ^h	4.8 ^h	1.5	2.9	2.7	4.2	-
	HNO ₃	2.4 ⁱ	3.2	1.6	2.0	1.3		-
Particulate	NH ₄ ⁺	4.7	1.5	2.7	0.9	6.3	(4.4)	-
	NO ₃ ⁻	3.7	0.5	1.5	0.7	3.3		-
Total dry	NH _x	22.6	5.6	12.7	6.4	24.8	(20.9)	14.7
	NO _y	8.9	8.4	4.6	5.6	7.2	(10.5)	3.9
Wet	NH ₄ ⁺	11.3	4.7	4.8	4.3	8.5	4.7	4.7
	NO ₃ ⁻	5.2	2.5	4.3	3.1	4.0	2.5	2.5
Total	NH _x	33.9	10.3	17.5	10.7	33.3	(25.6)	19.4
	NO _y	14.1	10.9	8.9	8.8	11.1	(13.0)	6.4
	Inorg-N	48.0	21.2	26.4	19.4	44.5	(38.6)	25.8

^a Erisman *et al.* (1996); ^b Puxbaum and Gregori (1998); ^c Andersen and Hovmand (1999);

^d Horváth (2004); ^e Neiryneck *et al.* (2004, submitted); ^f Present study, inferential method;

^g Present study, canopy budget method (Table 7.4; approach 9).

^h Including NO; ⁱ including HNO₂.

The contribution of NO_2 , HNO_3 and NO_3^- aerosol to the deposition of oxidised N (NO_y) differed between sites, but dry deposition of NO_y was on average twice as high as the NO_2 deposition (Table 7.2). This generalisation was used to approximate dry deposition of NO_y at the beech plot. An analogous approach as for N was used to approximate dry deposition of particulate SO_4^{2-} . According to reported inferential model results (Table 7.3), dry deposition of SO_2 contributed on average 78% (70 to 89%) of the total dry deposition of S.

Table 7.3. Comparison of annual dry and wet sulphur deposition ($\text{kg S ha}^{-1} \text{ yr}^{-1}$) at various sites. Values between brackets are approximate; values in italic are estimated by a canopy budget method.

Deposition ($\text{kg S ha}^{-1} \text{ yr}^{-1}$)		The					
		Netherlands ^a Douglas fir	Austria ^b Oak	Hungary ^c Spruce	U.S.A. ^d Deciduous	Belgium ^e Beech	Belgium ^f Beech
Dry							
Gaseous	SO_2	14.2	11.6	19.4	6.9	9.2	-
Particulate	SO_4^{2-}	6.1	1.4	4.7	2.6	(2.6)	-
Total dry	S	20.3	13.0	24.1	9.5	(11.8)	13.6
Wet	SO_4^{2-}	-	6.1	8.9	6.1	4.4	4.4
Total	S	-	19.1	33.0	15.6	(16.2)	18.1

^a Wyers and Duyzer (1997); ^b Puxbaum and Gregori (1998); ^c Kovács and Horváth (2004); ^d Likens *et al.* (2002); ^e Present study, inferential method; ^f Present study, canopy budget method (Table 7.4; approach 9)

7.4 Results

7.4.1 Net throughfall (+ stemflow) deposition

Measured above-canopy and below-canopy ion fluxes differed strongly between the two forest plots (Fig. 7.1). The major cation in rainfall at the beech plot in Belgium was NH_4^+ , while H^+ was the dominant cation in wet precipitation at the maple plot in Quebec. Fluxes of ions originating from seasalt aerosols (Na^+ , Cl^- , Mg^{2+}) were much higher at the beech plot, which is located ca. 60 km from the North Sea, than at the maple plot. Throughfall ion fluxes beneath the deciduous beech canopy were significantly higher than the wet deposition throughout the year, except for H^+ (Fig. 7.1a) (see Chapter 5 for a more detailed discussion of the beech plot). Ion enrichment in throughfall (+ stemflow) compared to wet precipitation was much higher at the beech plot than at the maple plot. Nevertheless, the throughfall deposition beneath the maple canopy was significantly higher than the wet precipitation for Ca^{2+} , Mg^{2+} , K^+ , Na^+ , Cl^- , and SO_4^{2-} during the growing season, and for Ca^{2+} , Mg^{2+} , K^+ , Na^+ , and Cl^- during the dormant season (Houle *et al.*, 1999b) (Fig. 7.1b).

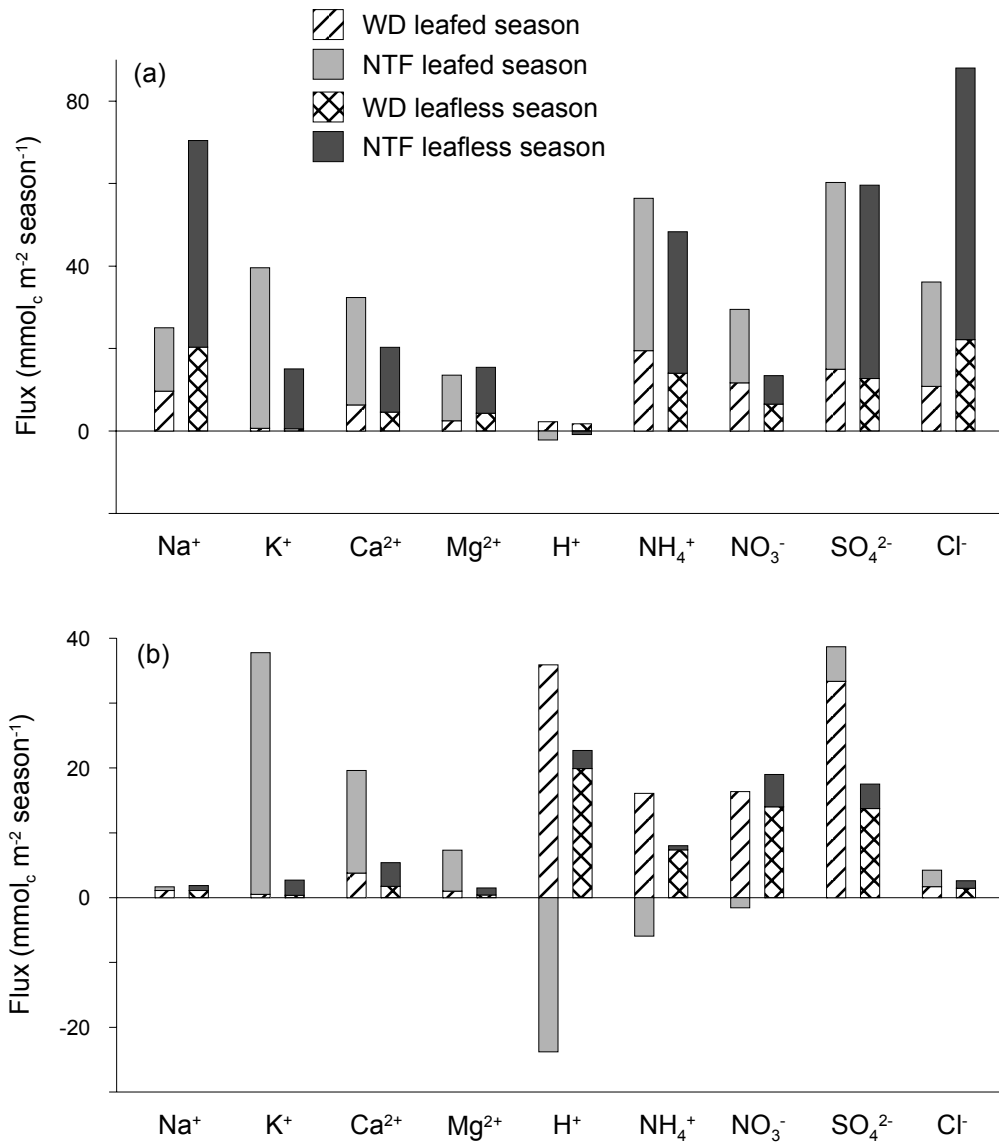


Fig. 7.1. Wet deposition and net throughfall (+ stemflow) deposition ($\text{mmol}_c \text{m}^{-2} \text{season}^{-1}$) of major ions during the leafed and leafless season for (a) a beech plot in Belgium (net throughfall + stemflow deposition), and (b) a mixed maple plot in Quebec (net throughfall deposition) (after Houle *et al.*, 1999b).

A significant net retention of NH_4^+ by the maple canopy was observed during the growing season (Houle *et al.*, 1999b) (Fig. 7.1b). Net retention of NO_3^- was observed during leaf senescence, but during the rest of the leafed season the possible NO_3^- uptake by the maple canopy was lower than its (unknown) dry deposition (Houle *et al.*, 1999b). During the leafed season, the input of free acidity (H^+) by rainfall was to a large extent retained by both canopies.

7.4.2 Canopy budget method

7.4.2.1 Beech plot

For the beech plot, the time step (method 1) used in the canopy budget model had more effect on the estimated H^+ deposition than on the estimated base cation deposition (Table 7.4). Dry deposition of base cations was up to 9% lower with a semiannual time step than with an annual time step, whilst DD was up to 30% higher with a biweekly time step. The calculated DD of H^+ was often slightly negative ($> -2.2 \text{ mmol}_e \text{ H m}^{-2} \text{ yr}^{-1}$), which is impossible. The use of bulk precipitation in stead of wet-only precipitation deposition (method 2) decreased the estimated DD of all ions other than K^+ and H^+ . Using bulk deposition increased the estimated total deposition (TD) of K^+ , Ca^{2+} and Mg^{2+} by 48, 19, and 2%, respectively, while TD of H^+ and NH_4^+ decreased with 9 and 5%, respectively. When Cl^- or SO_4^{2-} were used as a tracer ion (method 3), DD of base cations was 26 and 52% higher than with Na^+ as a tracer ion. The higher calculated DD of base cations in this approach resulted in lower canopy leaching of Ca^{2+} and Mg^{2+} and even canopy uptake of Na^+ . Consequently, canopy uptake and DD of H^+ and NH_4^+ were lower than with Na^+ as a tracer.

When Na^+ is used to estimate also the DD of NO_3^- , SO_4^{2-} , and Cl^- particles (method 4), the difference between NTF and estimated DD may be attributed to deposition of NO_y , SO_2 , and HCl (if the difference > 0) or to canopy exchange. The flux of NTF-DD was negative for NO_3^- , which may be due to canopy uptake of NO_y . Assuming that particles containing Cl^- and Na^+ have the same deposition velocity, a gaseous HCl deposition of $19 \text{ mmol}_e \text{ m}^{-2} \text{ yr}^{-1}$ was derived (Table 7.4). However, the estimated gaseous deposition of SO_2 ($32 \text{ mmol}_e \text{ m}^{-2} \text{ yr}^{-1}$) was 52% of the particulate SO_4^{2-} deposition, which appears not to be realistic according to micrometeorological studies (Table 7.3). When NTF-DD was attributed to canopy exchange in stead of gaseous deposition, the use of the Na^+ filtering approach for all major ions resulted in higher TD estimates than with the reference model for NO_3^- (35%) and H^+ (140%), but lower TD estimates for NH_4^+ , SO_4^{2-} and Cl^- (-15 to -40%). The low estimated DD of NH_4^+ and the high DD of H^+ in this approach resulted in a negligible estimate of NH_4^+ exchange within the beech canopy and a relatively high calculated H^+ uptake.

Correcting canopy exchange of base cations for weak acid excretion (method 5) decreased the canopy uptake of $NH_4^+ + H^+$ by approximately 50%, irrespective whether the DD of weak acids was assumed to be zero or equal to the WD of weak acids. Accounting for canopy leaching of Na^+ , Cl^- , and SO_4^{2-} (method 6) decreased the exchanged equivalent amount of $NH_4^+ + H^+$ charge by 20%.

Table 7.4. Wet deposition, estimated dry deposition and estimated canopy exchange ($\text{mmol}_c \text{ m}^{-2} \text{ yr}^{-1}$) for a beech plot in Belgium using varying forms of the canopy budget model. See text for details on the different model types used.

Type of precipitation data	Wet deposition ($\text{mmol}_c \text{ m}^{-2} \text{ yr}^{-1}$)					
	Na ⁺	K ⁺	Ca ²⁺	Mg ²⁺	H ⁺	Cl ⁻
WD Wet-only precipitation deposition	30	1.2	11	6.8	4.0	33
BD Bulk precipitation deposition	44	2.5	19	10.2	1.9	37
						28
						33
						36
						50
Form of canopy budget model	Dry deposition ($\text{mmol}_c \text{ m}^{-2} \text{ yr}^{-1}$)					
	Na ⁺	K ⁺	Ca ²⁺	Mg ²⁺	H ⁺	Cl ⁻
0 'Reference' (de Vries <i>et al.</i> , 2003)	65	2.5	24	15	1.3	143
1 Semi-annual time step	65	2.3	21	15	-0.3	148
Biweekly time step	65	2.8	31	15	-1.2	102
2 Bulk precipitation deposition	51	2.9	22	12	2.9	131
3 Cl ⁻ as tracer ion	83	3.2	30	19	-0.3	116
SO ₄ ²⁻ as tracer ion	100	3.8	36	23	-1.8	91
4 DDF _{Na} for all measured ions	65	2.5	24	15	8.8	73
5 Weak acids (w.a.), DD _{wa} = 0	65	2.5	24	15	-1.1	102
Weak acids (w.a.), DD _{wa} = WD _{wa}	65	2.5	24	15	-0.7	109
6 Leaching of Na ⁺ , Cl ⁻ , and SO ₄ ²⁻	61	2.3	22	14	0.7	134
7a NH ₄ ⁺ de Vries <i>et al.</i> (2003), xH = 1	65	2.5	24	15	-2.2	147
NH ₄ ⁺ de Vries <i>et al.</i> (2003), xH = 6	65	2.5	24	15	1.3	143
NH ₄ ⁺ de Vries <i>et al.</i> (2003), xH = 10	65	2.5	24	15	3.9	141
7b NH ₄ ⁺ de Vries <i>et al.</i> (1998), xH = 1	65	2.5	24	15	-0.3	145
NH ₄ ⁺ de Vries <i>et al.</i> (1998), xH = 6	65	2.5	24	15	10.8	134
NH ₄ ⁺ de Vries <i>et al.</i> (1998), xH = 10	65	2.5	24	15	17.5	127
7c NH ₄ ⁺ Draaijers and Erisman (1995), xH = 1	65	2.5	24	15	1.7	143
NH ₄ ⁺ Draaijers and Erisman (1995), xH = 6	65	2.5	24	15	18.4	126
NH ₄ ⁺ Draaijers and Erisman (1995), xH = 10	65	2.5	24	15	27.1	117
8 NO ₃ ⁻ de Vries <i>et al.</i> (2001), xNH ₄ = 1	65	2.5	24	15	26.5	147
NO ₃ ⁻ de Vries <i>et al.</i> (2001), xNH ₄ = 6	65	2.5	24	15	1.9	147
NO ₃ ⁻ de Vries <i>et al.</i> (2001), xNH ₄ = 10	65	2.5	24	15	0.0	147
9 Final estimate	61	2.1	19	13	0.2	105

^aThe positive difference between net throughfall and estimated dry particulate deposition may be attributed to gaseous dry deposition (HCl, SO₂).

Using different equations for calculating CE and varying the exchange efficiency factor (xH) (method 7) had only little effect on the estimated NH_4^+ deposition, but strongly influenced estimated H^+ loads. For example, according to the equation reported by Draaijers and Erisman (1995), the DD of H^+ increased twenty-fold when assuming similar ($xH = 1$) or much more efficient canopy uptake ($xH = 10$) of H^+ than of NH_4^+ , while the DD of NH_4^+ decreased only by 18%. Without accounting for weak acid or inorganic anion leaching, the calculated canopy uptake of NH_4^+ varied from 0.65 to 1.1 g N m⁻² yr⁻¹ (method 7a-c). Canopy uptake of NO_3^- calculated by Eq. 7.9 (method 8) was 7% of the estimated NH_4^+ uptake for $xNH_4 = 6$ and increased to 41% by assuming that the uptake rate of nitrate was equal to that of ammonium ($xNH_4 = 1$). Based on the results of Stachurski and Zimka (2002), NO_3^- was assumed to be taken up with H^+ as counter ion, and only NH_4^+ was considered to exchange with K^+ , Ca^{2+} , and Mg^{2+} . Using the NO_3^- uptake equation as suggested by de Vries *et al.* (2001), the canopy uptake and DD of H^+ and NH_4^+ in method 8 were the same as in the ‘reference’ (method 0).

Finally, the canopy budget method was applied at the beech site for four phenological canopy phases separately, using wet-only precipitation and Na^+ as tracer ion, and taking into account the estimated leaching of weak acids, Na^+ , Cl^- , and SO_4^{2-} to calculate the canopy uptake of NH_4^+ . As the estimated deposition of NH_4^+ at this plot was not sensitive to the value of the exchange efficiency xH , and as all values of xH in the range of 1 to 10 resulted in a negative DD of H^+ , only NH_4^+ was assumed to exchange with cations (K^+ , Ca^{2+} , and Mg^{2+}) that were not leached with anions (w.a., Cl^- , SO_4^{2-}). Following method 8, uptake of H^+ was calculated by allowing uptake of NO_y (xHN_4 set to 6). According to this modified seasonal canopy budget method (Table 7.4, method 9), DD contributed 58 to 76% of the annual total atmospheric deposition (TD) for the elements studied. There was little difference in the contribution of DD to the estimated TD between the leafed and leafless season (Fig. 7.2a). The relative importance of DD in the NTF flux was generally lower during the leafed season than during the leafless season because of ion leaching from the beech foliage, particularly for Ca^{2+} and Mg^{2+} . Annual canopy uptake of NH_x was computed at 0.48 g N m⁻² yr⁻¹, of which about half occurred during the leafed season.

7.4.2.2 Mixed maple plot

At the mixed maple plot (Houle *et al.*, 1999b), the use of an annual vs. semi-annual time step in the canopy budget model (method 1) had little impact on the estimated DD (< 10% difference), except for NH_4^+ (Table 7.5).

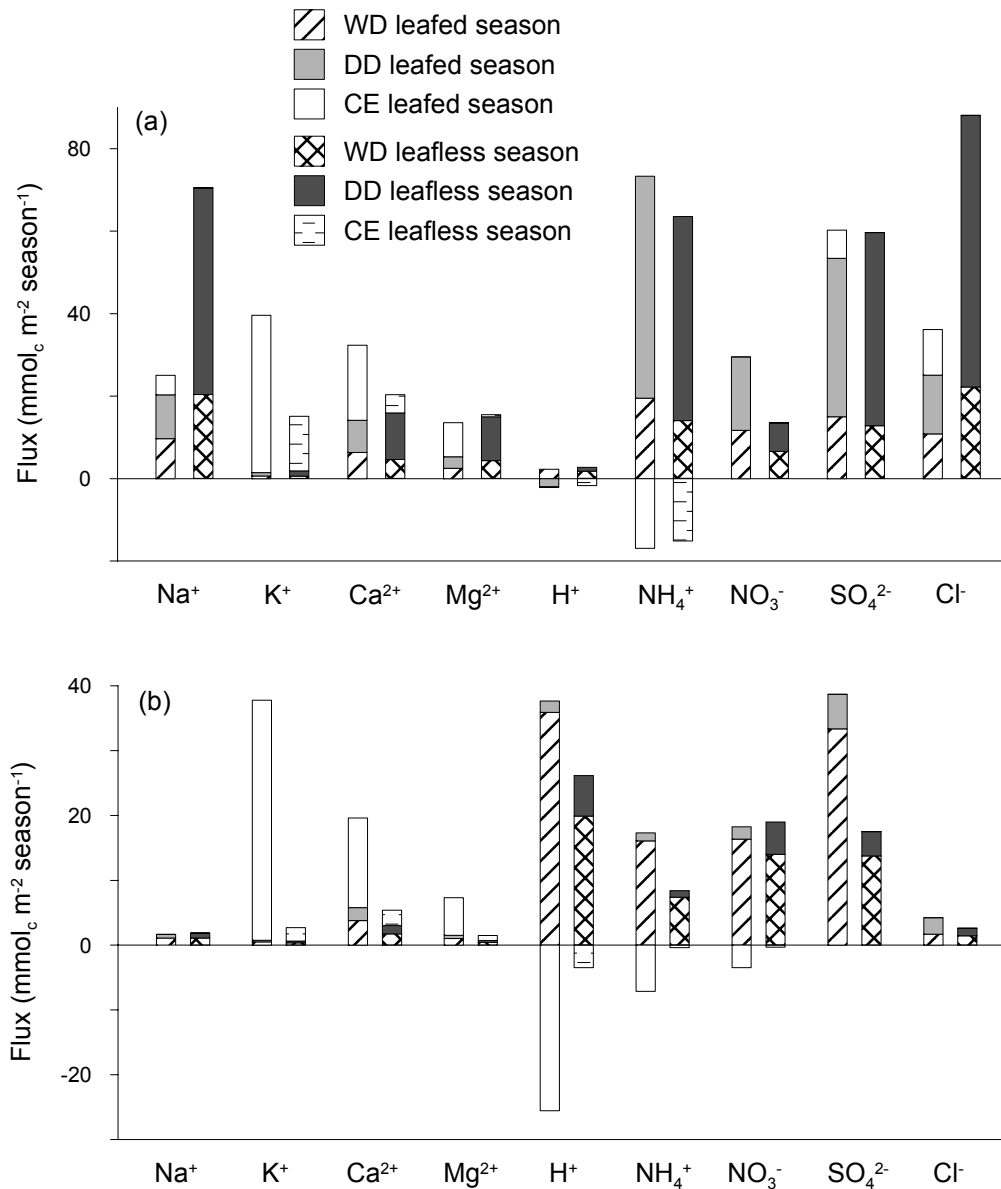


Fig. 7.2. Wet deposition, estimated dry deposition, and estimated canopy exchange ($\text{mmol}_c \text{m}^{-2} \text{season}^{-1}$) during the leafed and leafless season for (a) the beech plot in Belgium, and (b) the mixed maple plot in Quebec. The finally chosen canopy budget method (approach 9; Table 7.4 and Table 7.5) differed slightly between the two sites (see text).

For many tested forms of the canopy budget model, a small negative DD of NH_4^+ ($> -2.7 \text{ mmol}_c \text{m}^{-2} \text{yr}^{-1}$) was calculated for the maple canopy (Table 7.5), which is impossible. Using Cl^- as a tracer ion (method 3) almost doubled the estimated DD of base cations, while SO_4^{2-} as tracer resulted in 68% lower DD estimates than with Na^+ . When the dry deposition factor of Na^+ was used for all ions (method 4), a relatively high DD and canopy uptake of NO_3^- and SO_4^{2-} was calculated. For Cl^- only, a positive NTF-DD was found with method 4 that may be attributed to the DD of HCl gas.

Accounting for weak acid leaching (method 5) to calculate ion exchange within the canopy had a relatively large effect on the estimated DD of H^+ . When DD of weak acids was assumed to be zero or equal to the WD of weak acids, the DD of H^+ was 22% and 36% of the measured WD of H^+ , respectively. With respect to the three reported equations for allocating canopy uptake of H^+ and NH_4^+ (method 7), similar results were found for different equations, but the assumed exchange efficiency (xH) of H^+ vs. NH_4^+ affected the estimated canopy uptake and DD of these ions. When xH decreased from 6 to 1, the computed canopy uptake (no weak acid leaching assumed) increased five-fold for NH_4^+ and decreased by 30% for H^+ . When calculating canopy uptake of NO_3^- (method 8), it did not make sense to use the NO_3^- uptake to approximate H^+ uptake by the maple canopy, because this resulted in large negative DD values for H^+ (-10 to -20 $mmol_c m^{-2} yr^{-1}$).

Finally, the canopy budget method was applied semi-annually for the maple plot, using Na^+ as a tracer ion and accounting for weak acid leaching to calculate $H^+ + NH_4^+$ uptake (Table 7.5, method 9). A value of xH = 3 resulted in a computed uptake of NH_4^+ that corresponded well with the observed canopy retention of NH_4^+ during the growing season (-23.8 $mmol_c m^{-2}$) (Fig. 7.2b) and in positive DD estimates for both H^+ and NH_4^+ . The calculated canopy uptake of NO_3^- was in line with the observed NO_3^- retention by the maple canopy during the growing season (1.6 $mmol_c m^{-2}$) for a value of $xNH_4 = 3$. The DD of H^+ varied from 8 to 13 $mmol_c m^{-2} yr^{-1}$ by assuming that the DD of weak acids was 0 to 100% of the WD of weak acids.

7.4.3 Inferential method

The mean nine-monthly air concentration of NH_3 at the beech site was $4.6 \mu g N m^{-3}$. Based on the seasonal pattern at a neighbouring site, the average annual NH_3 concentration amounted to $4.4 \pm 0.1 \mu g N m^{-3}$ (mean \pm standard deviation, $n = 2$) (Fig. 7.3). The regional air concentration at rural and semi-urban sites during the study period was $8.8 \pm 2.1 \mu g NO_2-N m^{-3}$ ($n = 7$) and $3.0 \pm 0.9 \mu g SO_2-S m^{-3}$ ($n = 12$) (Fig. 7.3). The air concentrations were higher in the leafless season for NO_2 and SO_2 , in contrast to NH_3 (Table 7.6).

Table 7.6 compares the calculated dry deposition of N and S gases with the net throughfall (NTF) measurements and with the NTF corrected for ion exchange within the canopy using the final canopy budget method (approach 9). The annual deposition velocities of NH_3 and SO_2 were assumed to be similar in the leafed and leafless season to account for the low surface resistance of both gases in case of co-deposition onto wet surfaces ().

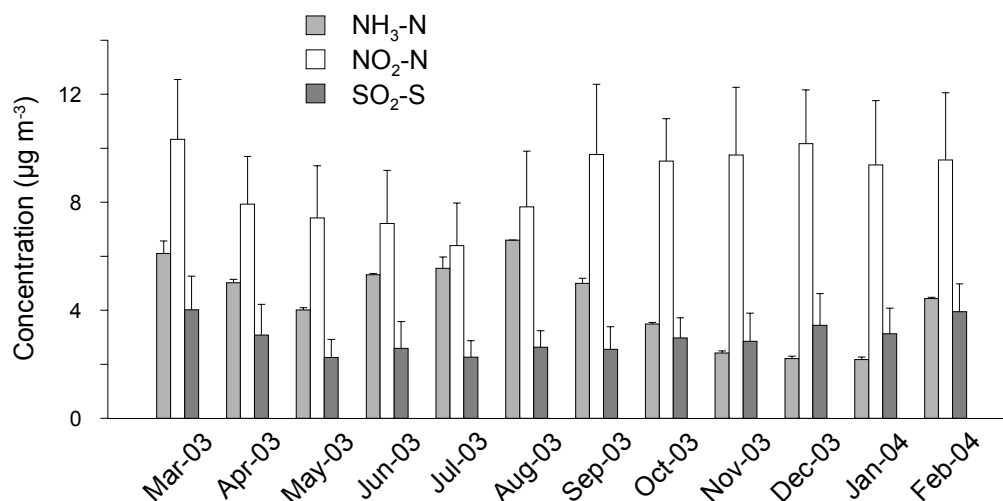


Fig. 7.3. Monthly air concentration of NH₃, NO₂, and SO₂ (µg N or S m⁻³) at the beech site. NH₃ was measured 4-weekly at the beech site from March to December 2003 using two samplers. NO₂ and SO₂ data are regional average concentrations at rural and semi-urban sites in northern Belgium (7 sites for NO₂, 12 for SO₂) measured every 30 min. The error bars indicate (spatial) standard deviations.

Since NO₂ deposition is closely related to stomatal opening (e.g., Gessler *et al.*, 2000), the deposition velocity of NO₂ was assumed to be equal to the value of Erisman (1993) in the leafed season (0.2 cm s⁻¹) and to 50% of this value in the leafless season. The particulate deposition of NH₄⁺ and SO₄²⁻ and the total NO_y deposition were derived from the calculated NH₃, SO₂, and NO₂ depositions based on reported inferential modelling results (Table 7.2 and Table 7.3).

Table 7.6. Dry deposition (DD) of nitrogen and sulphur compounds at the beech site during the leafed (L, 210 days) and leafless (NL, 154 days) season determined by inferential modelling and by the canopy budget method (semi-annual approach no. 1 and final approach no. 9; Table 7.4). The particulate DD in the inferential approach was approximated based on literature reports (see Table 7.2 and Table 7.3).

	NH ₃		NO ₂		SO ₂	
	L	NL	L	NL	L	NL
Air concentration (µg m ⁻³)	6.06	4.53	26.4	31.3	5.09	6.83
(µg N or S m ⁻³)	4.99	3.73	8.02	9.52	2.54	3.41
Deposition velocity (cm s ⁻¹)	1.2	1.2	0.2	0.1	1.0	1.0
Gaseous DD (g N or S m ⁻² period ⁻¹)	1.09	0.60	0.29	0.13	0.46	0.45
(mmol _c m ⁻² period ⁻¹)	78	43	21	9	29	28
Derived total DD (mmol _c m ⁻² period ⁻¹)	NH _x		NO _y		SO _x	
	L	NL	L	NL	L	NL
a. Inferential gas + particle DD	97	53	42	18	37	36
b. Net throughfall deposition	37	34	18	7	45	47
c. DD canopy budget method no. 1	97	51	18	7	45	47
d. DD canopy budget method no. 9	54	51	20	8	38	47

When the canopy budget method was applied semi-annually and leaching of K^+ , Ca^{2+} , and Mg^{2+} determined by the Na^+ filtering method was entirely attributed to uptake of $NH_4^+ + H^+$ (approach 1), the estimated DD of NH_x corresponded well to the results of the inferential technique (Table 7.6). The agreement for NH_x disappeared when other canopy processes (leaching of weak acids, SO_4^{2-} , and Cl^-) were taken into account (Table 7.6, approach 9). For NO_y , approach 9 allowed a small canopy uptake based on the estimated NH_x uptake, but the estimated DD of NO_y was still lower than the results of the inferential technique. For S, a better agreement was found between the different DD estimates (Table 7.6). The results of the inferential technique and final canopy budget method (approach 9) are also shown at the annual level (Table 7.2 and Table 7.3).

Using the mean NH_3 concentration measured at the beech plot during the leafed season ($5 \mu g N m^{-3}$) and the deposition velocity suggested by Erisman (1993) (Table 7.6), the difference between the calculated dry deposition of NH_3 and the NTF of NH_4^+ during the leafed season amounted to $41 mmol_e m^{-2}$ ($0.57 g N m^{-2}$). By adding an approximated dry deposition of NH_4^+ particles in the leafed season ($0.27 g N m^{-2}$), the estimated canopy uptake of NH_x during the growing season was $0.84 g N m^{-2}$.

7.5 Discussion

7.5.1 Time step, precipitation input, and tracer ion

The impact of varying forms of the canopy budget model on estimated dry deposition (DD) and total atmospheric deposition (TD) depended on the ion and forest plot considered. Applying the method at a semi-annual time step (method 1) hardly changed the calculated fluxes compared to an annual time step. For H^+ at the beech site and for NH_4^+ at the maple site, a shorter time step resulted in large proportional changes in dry deposition because of the small value of the calculated fluxes. For those two elements, negative dry deposition fluxes were often calculated, which is impossible (cf. infra). The impact of using bulk in stead of wet-only precipitation deposition on the estimated fluxes for a specific ion depends on the bulk:wet-only ratio and the throughfall enrichment of both the ion and tracer ion considered. Using bulk deposition results in lower calculated throughfall (+ stemflow) enrichment than using wet-only deposition, and thus in a lower sum of dry deposition and canopy leaching. Consequently, total deposition of neutralizing base cations onto the beech canopy was overestimated using bulk in stead of wet-only deposition, whilst total deposition of potentially acidifying NH_4^+ was underestimated. On the other hand, if throughfall deposition of NH_4^+ is

lower than in precipitation, bulk deposition overestimates canopy retention compared to wet-only deposition. For elements for which canopy exchange is assumed to be negligible, the precipitation type does not affect the determination of total atmospheric deposition.

The chosen tracer ion meaningfully affected estimated fluxes at both study sites. As discussed in Chapter 5, the assumption of negligible ion leaching from the beech canopy was more acceptable for Na^+ than for Cl^- . For the Canadian site, Houle *et al.* (1999b) concluded that Na^+ enrichment under the maple canopy was derived essentially from dry deposition, based on seasonal throughfall patterns of Na^+ , lacking correlation with dissolved organic carbon (approximated by colour measurements), and a lixivation experiment. For Cl^- , in contrast, a peak in net throughfall was observed during leaf senescence (Houle *et al.*, 1999b), suggesting Cl^- leaching from senescent maple leaves (cf. Neary and Gizyn, 1994). Furthermore, Cl^- is not useful as a tracer for dry deposition of particles containing base cations when significant deposition of gaseous HCl occurs. Likewise, SO_4^{2-} is less useful as a tracer for estimating particulate deposition because S is deposited both as particle (SO_4^{2-}) and as gas (SO_2) (cf. Table 7.3). In addition, the seasonal pattern of throughfall enrichment suggested some leaching of SO_4^{2-} from senescent beech leaves (see section 5.5.4). By comparing throughfall fluxes under artificial and real spruce trees, Ignatova and Dambrine (2000) also concluded that Na^+ was more suitable than SO_4^{2-} as a tracer ion for dry deposition. It should be noted that the assumption of negligible canopy exchange of Na^+ is most critical in regions with low Na^+ deposition rates, like at the maple site.

7.5.2 Canopy uptake of nitrogen and protons

The canopy budget method computes ion uptake within tree canopies by assuming that ion exchange in the interface water-plant surface is the main process governing uptake and release of the components considered. In its most simple form (method 0), excretion of salts or acids by vegetation is not accounted for (Van der Maas and Pape, 1991). Including leaching of weak acids with base cations (method 5) meaningfully decreased the estimated canopy uptake of H^+ and NH_4^+ . Furthermore, base cation leaching may also be accompanied by anions like Cl^- or SO_4^{2-} (see Chapter 5 for the beech canopy). Taking into account canopy leaching of organic and inorganic anions decreases the amount of base cations that is thought to exchange with H^+ and NH_4^+ , so that the computed canopy uptake of $\text{H}^+ + \text{NH}_4^+$ declines.

To determine weak acid (w.a.) leaching, an estimate of total w.a. deposition is required. The charge balance approach has generally been used to estimate weak acid fluxes in throughfall,

stemflow and precipitation, but the computed weak acid flux is sensitive to relatively small changes in water composition, in particular for rainfall. Draaijers (1993) reported that the canopy budget model yielded unrealistic results when used for the summer and winter period separately because of a negative charge balance in semi-annual bulk deposition. However, at the beech site slight negative charge balances in wet deposition were measured for only two of the 22 biweekly sampling intervals. The charge balance thus appears to be a reasonable approach for determining fluxes of weak acidity (Driscoll *et al.*, 1989; Chiwa *et al.*, 2004) given sufficiently long time steps and accurate chemical analyses. Estimating DD of w.a. introduces some uncertainty in the computed w.a. leaching. In the Integrated Forest Study, DD of weak ‘undissociated’ acidity was presumed to be negligible (Schaefer *et al.*, 1992), while Draaijers and Erisman (1995) estimated DD of w.a. to be equal to the WD of w.a. At the beech plot, we followed the latter approach because of the high throughfall enrichment of major ions. At sites with lower throughfall enrichment, such as the mixed maple plot, lower or negligible DD of weak acids (Schaefer *et al.*, 1992; de Vries *et al.*, 2001) is presumably more justified.

When weak acid leaching is included, the canopy budget model assumes that K^+ , Ca^{2+} and Mg^{2+} leaching from the canopy is due to H^+ and NH_4^+ uptake and weak acid excretion, and that all organic acids are leached in a neutral salt form. Previous research supports both cation exchange and the release of inorganic cations coupled with organic anions, but other canopy interactions may be involved too. A majority of experimental studies study has focused on canopy interactions of strongly acid precipitation ($pH < 4$) (Stachurski and Zimka, 2002). These results may not be representative for regions where N dominates acidifying deposition, which currently holds true for large parts of Europe (de Vries *et al.*, 2003) due to strongly declined S emission and deposition during the last decades (e.g., Hovmand and Kemp, 1996). Using artificial foliage and throughfall measurements, leaching of K^+ and Mg^{2+} from a beech canopy was found to result from ionic exchange of NH_4^+ for K^+ and Mg^{2+} (Stachurski and Zimka, 2002). However, H^+ retention in a beech canopy did not result from exchange with other cations, but was closely correlated with nitrate absorption, possibly due to HNO_3 uptake (Stachurski and Zimka, 2002). A positive relationship between canopy absorption of NH_4^+ and cation leaching has also been observed by Roelofs *et al.* (1985). H^+ retention in a Sitka spruce canopy sprayed with acid mist was partly related to increased TF fluxes of K^+ , Ca^{2+} , and Mg^{2+} , and partly attributed to weak organic acid leaching (Chiwa *et al.*, 2004) (cf. Cronan and Reiners, 1983; Schaefer *et al.*, 1992).

We tested different canopy exchange equations and efficiencies (xH) for computing the relative canopy uptake of H^+ vs. NH_4^+ . The chosen exchange equations had little effect on the estimated NH_4^+ uptake within the beech canopy due to the high NH_4^+ and low H^+ fluxes in throughfall and rainfall. For the maple plot, where H^+ fluxes were higher, computed uptake of H^+ and NH_4^+ was more sensitive to the value of the relative uptake efficiency (xH) than to the exact equation used. For both forest plots, the estimated dry deposition of H^+ or NH_4^+ in some cases was slightly negative for the ion with the smallest flux. To avoid this artefact, the value of the exchange efficiency can be modified (e.g., $xH \sim 3$ for the maple site). Alternatively, the contribution of H^+ and NH_4^+ to canopy uptake can be allocated without assuming an exchange equation. This approach only slightly affects estimated dry deposition when throughfall fluxes are much higher for NH_4^+ than for H^+ , as illustrated for the beech site.

Forest canopies can absorb and incorporate reduced as well as oxidised N compounds, but in field studies NH_4^+ is retained more preferentially than NO_3^- (Potter *et al.*, 1991; Lovett and Lindberg, 1993; Stachurski and Zimka, 2000, 2002). Experimental studies using ^{15}N labelled water solutions confirm the preferential uptake of NH_4^+ (Bowden *et al.*, 1989; Brumme *et al.*, 1992; Lumme, 1994; Boyce *et al.*, 1996), but the percentage of N retained by plants is usually lower than in field studies. This could be due to more efficient canopy uptake of dry than wet N deposition (Schaefer *et al.*, 1992; Boyce *et al.*, 1996; Horváth, 2004). In regions with elevated atmospheric N deposition, like at the beech site, possible canopy uptake of inorganic N is obscured by dry deposition (Lovett and Lindberg, 1993), resulting in a positive net throughfall flux of NH_4^+ and NO_3^- . As the assumption of negligible canopy exchange of NO_3^- is not valid (Draaijers and Erisman, 1995) we used the calculation procedure suggested by de Vries *et al.* (2001) and applied by Schmitt *et al.* (2005) and Thimonier *et al.* (2005). However, the calculated NO_3^- uptake entirely depends on the uncertain estimate of the NH_4^+ uptake and the unknown uptake efficiency of NO_3^- compared to NH_4^+ (xNH_4). In addition, the charge balance is not maintained, unless H^+ is considered to be taken up as a counter ion, as illustrated for the beech plot (approach 9).

Both gaseous (NH_3 , NO_2 , HNO_3) and dissolved (NH_4^+ , NO_3^-) nitrogen compounds can be taken up by tree leaves via stomatal uptake and cuticular absorption (Harrison *et al.*, 2000, Gessler *et al.*, 2002). In addition, N uptake by twigs and branches may be important (Boyce *et al.*, 1996; Macklon *et al.*, 1996; Wilson and Tiley, 1998). Nitrogen taken up by the canopy can be assimilated and used within trees (Rennenberg *et al.*, 1998), but inorganic nitrogen can also be retained by microbial action on canopy surfaces (Papen *et al.*, 2002) to be transformed

into organic N and partly released from the canopy in throughfall (Lovett and Lindberg, 1993; Ferm and Hultberg, 1999; Morris *et al.*, 2003). Epiphytic lichens on trunks and foliage have also been reported to remove inorganic N from water solutions (Houle *et al.*, 1999b), incorporating N in lichen biomass until litterfall (Morris *et al.*, 2003). Direct N uptake by forest canopies is not only important for quantifying total atmospheric deposition, e.g., to evaluate the exceedance of critical loads of acidification and eutrophication (Harrisson *et al.*, 2000). Retained and assimilated N may activate shoot-to-root transport of amino compounds and cytokinins (Gessler *et al.*, 1998; Collier *et al.*, 2003), thus reducing NH_4^+ and particularly NO_3^- uptake by roots (Pérez-Soba and van der Eerden, 1993; Gessler *et al.*, 1998, Rennenberg *et al.*, 1998). Canopy uptake has been reported to amount 1-12 kg N ha⁻¹ yr⁻¹ (e.g., Brumme *et al.*, 1992; Lovett and Lindberg, 1993). This is usually a small fraction of tree nutritional demand, except for forests at high elevation sites (Sievering *et al.*, 2000). However, canopy uptake values of 14-57 kg N ha⁻¹ yr⁻¹ were found by upscaling laboratory experiments to field conditions (Harrisson *et al.*, 2000).

7.5.3 Comparison with inferential method

For the beech site, dry deposition based on the inferential method was 16.5 and 4.2 kg N ha⁻¹ yr⁻¹ for NH_3 and NO_2 , respectively, compared to 14.5 and 3.5 kg N ha⁻¹ yr⁻¹ for reduced and oxidised N in the final canopy budget method (approach 9) (Table 7.2). Annual dry deposition of S was 11.8 kg S ha⁻¹ with the inferential technique and 13.6 kg S ha⁻¹ yr⁻¹ with the final canopy budget method (Table 7.3). Given the uncertainty in both approaches, these results correspond fairly well. However, the agreement between both methods for N decreased by accounting for the likely dry deposition of particulate N and HNO_3 . Dry deposition of reduced and oxidised N in the final canopy budget method was 6.2 and 6.6 kg N ha⁻¹ yr⁻¹ lower than approximated with the inferential method and literature data (Table 7.2). It should be noted that the dry deposition of NO_y estimated by the inferential method was higher than at other sites in the same region (Neiryneck *et al.*, 2004; Erisman *et al.*, 1996; Table 7.2), so that the actual difference for NO_y deposition between the canopy budget and inferential method may be smaller. The higher dry deposition of S during the leafless period according to the net throughfall measurements than by the inferential technique (Table 7.3) might partly be due to increased particulate SO_4^{2-} deposition in wintertime by enhanced atmospheric seasalt aerosols.

Our simple inferential approach estimated dry deposition by air concentrations that were not all measured at the study site and by deposition velocities taken from literature, and thus it is difficult to determine which of both methods is closest to the actual dry deposition value. Calculating the deposition flux as the product of a seasonal air concentration and deposition rate introduces considerable uncertainty in the estimate (Andersen and Hovmand, 1999). Nevertheless, correcting throughfall for ionic exchange within the canopy does not account for canopy uptake and assimilation of gases without the release of internally formed salts or acids (Puxbaum and Gregori, 1998), and consequently, the canopy budget method potentially underestimates canopy uptake and dry deposition of N. When the most certain compound in the inferential method (NH_3) was used to approximate the dry deposition of NH_x , the calculated canopy uptake of NH_x amounted to 8.4 kg N ha^{-1} during the leafed season (see section 7.4.3). Similar canopy uptake values were estimated by the canopy budget method when leaching of weak acids was not taken into account (Table 7.4; Table 7.6).

A Pan-European comparison of throughfall data corrected by the canopy budget method with inferential modelling in $150 \times 150 \text{ km}^2$ grid cells showed that the total acidifying deposition of S and N was usually overestimated by the canopy budget model, whereas the total eutrophying N deposition was underestimated, in particular at plots with high N loads. There was, however, a significant correlation between the SO_x and the NH_x deposition of the two methods (Van Leeuwen *et al.*, 2000). Similarly, for 13 Swiss forest plots, the two methods gave estimates of dry N and S deposition that correlated significantly with each other, but the inferential method yielded significantly higher estimates than the canopy budget method (Schmitt *et al.*, 2005; Thimonier *et al.*, 2005). For an oak forest, throughfall data of S and of reduced N corrected for canopy exchange were similar to inferential modelling results, while modelled dry deposition of oxidised N was $4 \text{ kg N ha}^{-1} \text{ yr}^{-1}$ higher than net throughfall (Puxbaum and Gregory, 1998). With respect to base cations, Draaijers *et al.* (1997) concluded that the dry deposition of Na^+ , Mg^{2+} , Ca^{2+} and K^+ can be estimated reasonably well using throughfall and precipitation measurements in association with the canopy budget model. A limiting condition for using the canopy budget method is that the studied forest stand should be free from insect plagues or diseases, since biotic stresses can enhance ion leaching from the canopy (Van Ek and Draaijers, 1994; Stadler *et al.*, 2001, 2005).

7.6 Conclusions

The canopy budget method is based on several presumptions, including the assumption that particles containing Mg^{2+} , Ca^{2+} and K^+ are deposited with equal efficiency onto the forest canopy as particles containing the tracer ion, and the assumed ion exchange processes within the canopy. The present research did not directly validate these presumptions, but tested varying forms of the canopy budget method for two contrasting forest sites to examine the sensitivity of estimated deposition fluxes to input data and model choices. Sodium appeared to be most appropriate tracer ion for estimating dry deposition and canopy interactions of other base cations, but the reliability of this filtering approach strongly depends on the actual atmospheric particle size distribution. For deciduous forest stands, the canopy budget method can easily be applied at the semi-annual level to increase insight in the seasonal pattern of the estimated fluxes. To compute the retention of NH_4^+ and H^+ within forest canopies, both ion exchange with K^+ , Ca^{2+} and Mg^{2+} as well as simultaneous cation and anion leaching should be taken into account from a physiological point of view. However, including weak acid leaching meaningfully decreased the computed canopy uptake of H^+ and NH_4^+ for both studied canopies. For the beech canopy, the calculated dry deposition of NH_x with the canopy budget method was similar to the N deposition estimated by an inferential technique when anion leaching from the canopy was neglected. As no detailed micrometeorological measurements were available for the studied forest plots, it is difficult to determine which method most closely approximates the actual atmospheric deposition. In future applications of the canopy budget method, varying forms could be tested to quantify the range of estimated dry deposition and canopy exchange for the forest stand under study. Additional research is required in order to improve our understanding of the processes involved in nitrogen retention within tree canopies under varying environmental conditions.

8 General discussion and conclusions

As the results of the present research have already been discussed extensively in the preceding chapters, the aim of this concluding section is to provide a more general discussion of the findings and implications of the study.

The amount of precipitation, throughfall, and stemflow water was continuously measured at high temporal resolution throughout two subsequent years. Chemical fluxes were determined for one year at a biweekly time interval. Hence, the effect of the forest canopy could be examined at the level of individual rain events for the water fluxes to the forest floor but not for the throughfall and stemflow chemistry. Continuous measurements over one or two years along a relatively dense grid allowed sound statements about the heterogeneity of the throughfall fluxes to the forest floor in space and time, during the growing as well as the dormant season. We found that the spatial and temporal variation in canopy cover significantly affected the water and ion fluxes beneath the beech tree studied. A clear effect of canopy structure on the spatial pattern of the amount of throughfall water was observed during the leafed season, but not during the leafless season. With respect to the ion fluxes, in contrast, the beech canopy significantly influenced the modification and spatial heterogeneity of throughfall ion composition during both the leafed and leafless season.

Accurate quantification of above-canopy precipitation is a prerequisite for assessing canopy effects on throughfall water amount and chemistry. With respect to the precipitation amount, quantifying occult precipitation by fog and clouds has been reported as a problem in studies on rainfall partitioning (e.g., Neal *et al.*, 1993). Despite negative interception values for a small fraction of rainfall events during the leafless season (Fig. 3.5), fog deposition could not be considered important at our lowland study site. To assess the measurement bias on rainfall chemistry by using continuously open funnel collectors, we compared two collector types. As expected, the commonly used bulk funnel collectors significantly overestimated the actual wet deposition of major ions due to dry deposited particles and gas onto the collectors (Table 2.2). The acidity of bulk precipitation was significantly lower than of wet-only precipitation. Therefore, wet-only samplers are preferred for determining wet deposition fluxes.

Like for precipitation samplers, dry deposition onto bulk throughfall collectors beneath the forest canopy cannot be ruled out. However, the inaccuracy introduced by using bulk instead of wet-only collectors for measuring throughfall deposition is expected to be much smaller than for measuring precipitation deposition because of two reasons. First, the concentration of gases and aerosols at throughfall collector height (1.5 m above the forest soil) is lower than above the canopy or in the open field due to effective filtering of particles and gases by the canopy (Lovett and Lindberg, 1992). In addition, lower wind speed at ground level does not favour dry deposition (Beckett *et al.*, 2000). At the study site, the annual ammonia deposition at 1.7 m height, as measured with passive sampling devices in 2000, was only 7% of the above-canopy deposition at 36 m height (De Schrijver *et al.*, 2001). Second, a certain amount of dry deposition will contribute less to throughfall than to precipitation deposition because of the ion enrichment of water passing through the forest canopy, except for H^+ . Unfortunately, few reports have been made of comparisons of wet-only and bulk throughfall below forest canopies. Bredemeier and Lindberg (1992) measured higher bulk than wet-only throughfall fluxes beneath a spruce canopy, but reported that their data set was too limited to set up final conclusions. Richter and Lindberg (1988) (see Table 2.1) only found significant differences between five-weekly bulk and event-based wet-only throughfall for H^+ and NO_3^- during the growing season. However, NO_3^- concentration was lower instead of higher in the bulk throughfall, indicating that the difference between collector types was not due to dry deposition but likely due to biochemical reactions in the bulk samplers during the extended sampling interval (Richter and Lindberg, 1988; Thimonier, 1998). We adopted a weekly sampling strategy with collecting bottles placed below ground level to minimize biochemical transformations. For logistic reasons, the chemical composition of throughfall was determined on biweekly pooled samples.

The present study is based on results obtained beneath the canopy of one dominant tree only. Nevertheless, the degree of spatial variability of throughfall water amounts was similar to studies in other deciduous stands (Table 4.1). The spatial variability in ion deposition was lower than in other deciduous stands, probably because the measurements occurred beneath the crown of a single tree rather than in a larger mixed species plot, and because the spatial variability was assessed for intervals of at least two weeks. The study design was chosen to minimize spatial variations in gross precipitation input, micrometeorological atmospheric conditions, and canopy composition. In mixed forest stands, both plant area index and compositional differences affect throughfall chemistry (Puckett, 1991; Hamburg and Lin,

1998). Canopy exchange strongly depends on tree species and ecological setting (Van Ek and Draaijers, 1994), while dry deposition onto tree crowns varies with micrometeorological conditions within a forest stand (Rustad *et al.*, 1994; Janson and Granat, 1999).

An important consequence of investigating one tree crown only is that no gaps between tree crowns are involved. Zirlewagen and von Wilpert (2001) demonstrated that spatial variability of throughfall at the scale of canopy gaps has control on water quantity and chemistry at the watershed scale. This means that the inferences at the smaller scale of our study should be considered within a broader context of heterogeneity in forest stands, including closed stand areas as well as treefall gaps and regeneration areas. More specifically, the linear relationship of canopy cover to throughfall water amount (negative relationship; Fig. 4.7) and throughfall ion fluxes (positive relationship; Fig. 6.3) observed in the present study cannot be simply generalized in case of more open forest stands. For example, in a very heterogeneous spruce stand where canopy cover ranged from 0 to 85%, an approximately linear decline of throughfall water amount with increasing canopy cover was only observed when canopy cover exceeded 60% (Hug *et al.*, 2005). Likewise, the increase of throughfall ion deposition with increasing canopy cover in the same stand was better described by an exponential function than a linear relationship. Furthermore, the impact of forest canopies on the water and ion fluxes beneath the canopy does not only depend on the biomass and distribution of the aboveground vegetation, but also on the composition and aerodynamic roughness of the canopy, as mentioned above. As dry deposition is influenced by wind speed and atmospheric turbulences (Erisman and Draaijers, 2003), tree height may interfere with the relation between canopy density and throughfall. To investigate the effect of the tree crown solely on throughfall patterns, the understory layer was removed in our research plot. Depending on its abundance and biomass, the understory layer may significantly affect water and nutrient cycling in forest stands. Canopy cover of shrubs and understory trees will have an additional effect on rainfall redistribution, although interception rates are expected to be low under closed forest canopies (Baldocchi and Vogel, 1996; Powell *et al.*, 2005).

For a given amount of rainfall, the presence of a leafed canopy significantly increased interception loss and decreased throughfall and stemflow amounts (Fig. 3.3). Although the partitioning of rainfall into throughfall, stemflow, and interception was significantly affected by event rainfall characteristics and meteorological conditions, foliation and event rainfall amount largely explained the observed water fluxes (Table 3.4). Consequently, the net precipitation to the forest floor depends on the temporal distribution of rainfall, as illustrated

by the different interception loss during the two growing seasons studied (Table 3.2). In view of expected climate change, there is currently much interest in understanding how ecosystems respond to changes in precipitation regimes, rising carbon dioxide and/or temperature (e.g., Schafer *et al.*, 2002; Weltzin *et al.*, 2003; Burkett *et al.*, 2005). As beech is known to be a drought sensitive tree species (Granier *et al.*, 2002; Lebourgeois *et al.*, 2005; Leuzinger *et al.*, 2005), particularly in its regeneration stage (Czajkowski *et al.*, 2005), it may suffer from climatic conditions prognosticated in West and Central Europe for the current century (Rennenberg *et al.*, 2004; Gessler *et al.*, 2004, but see Ammer *et al.*, 2005).

Time persistent spatial patterns of the amount of throughfall water were observed beneath the beech tree throughout the year, but particularly during the leafed season (Fig. 4.2). The spatial patterns of throughfall water amount were not significantly related between the leafed and the leafless season (Table 4.4), indicating a regulating effect of foliation on the spatial distribution of canopy drip to the forest floor. With increasing event rainfall amount, both the intercepted rainfall fraction (Fig. 3.5) and the spatial variability (Fig. 4.5) of throughfall water decreased. We found that a simple measure of canopy structure, like local canopy cover or derived plant area index, was closely related to the local amount of throughfall water during the growing season (Fig. 4.7, Fig. 4.8). Therefore, the throughfall water amount decreased with increasing amounts of leaves, twigs, and branches above a sampling point because of the enhanced interception and subsequent evaporation of rainfall water. An additional systematic influence of canopy architecture on throughfall inputs may result from lateral branch flow within the canopy. Besides a systematic component in the variability of throughfall, non-systematic throughfall variability occurs, which may be related to turbulence above the canopy, wind direction (Weihe, 1984), and wind speed (Fig. 4.9) (Hörmann *et al.*, 1996).

The amount of throughfall water during the dormant season showed a low degree of spatial variability (Fig. 4.3b) and could not be explained by the simple measure of branch structure used (Fig. 4.8). This may be related to the low interception loss (Fig. 3.5) and more frequent occurrence of dripping points in defoliated conditions. Stemflow generation by beech branches may contribute to the spatial heterogeneity of throughfall water, but the expected within-canopy variation in local stemflow generation apparently was too small and/or only weakly correlated to branch and twig cover to be detectable in the leafless season. However, also during the dormant season, the spatial pattern of throughfall water showed temporal stability (Fig. 4.6), which indicates that the branching structure influences throughfall water fluxes to the forest floor. The fact that the amount of throughfall water in defoliated

conditions did not decrease with increasing branch cover suggests that more detailed canopy structure measurements may be needed to describe rainfall redistribution and lateral within-canopy transport within leafless deciduous trees. A complete description of a canopy would require the specification of the position, size, and orientation of each element of surface in the canopy. Relevant branching properties may include branch diameter, length, and inclination angle (Levia and Herwitz, 2002), as well as intensity of ramification. Unfortunately, three-dimensional canopy characteristics above a specific point of the forest floor are not easily quantified neither synthesized into meaningful variables (Russel *et al.*, 1989; Frazer, 2005).

The spatial distribution of throughfall ion deposition in the leafless season was not correlated with the amount of throughfall water (Table 6.3). In contrast to the low influence of the leafless canopy on throughfall water fluxes, ion fluxes in throughfall and stemflow were significantly enriched during both the leafed and leafless season (Table 5.2, Fig. 5.2). This shows that defoliated deciduous canopies interact more actively with atmospheric deposition than is often thought. Furthermore, our results strongly suggest cation leaching from (the bark of) branches and twigs during the non-growing season (Table 5.3). Hence, the effect of foliation on the seasonal change in throughfall and stemflow chemistry was less pronounced than expected (Fig. 5.2). This finding was confirmed by the spatial variation of throughfall ion fluxes. For the major ions studied, similar spatial throughfall patterns were observed during the leafed and leafless season (Fig. 6.2). The spatial pattern of ion deposition beneath the beech crown was largely explained by the degree of leafed canopy cover in the growing season and by branch cover in the leafless season (Fig. 6.3). In addition, similar spatial patterns were observed for ions associated with dry deposition and canopy leaching (Table 6.3). Consequently, increasing amounts of leaves and/or woody components above a sampling point enhanced throughfall deposition throughout the year (Table 6.4) because both ion leaching and dry deposition increased with canopy density per ground surface area.

In forests, there are two major aboveground pathways that return nutrients to the forest floor: (i) throughfall and stemflow, and (ii) litterfall, i.e. shedding of organic material such as leaves and branches (Facelli, 1991; Staelens *et al.*, 2004). Depending on the nutrient and forest stand considered, one of both pathways can be the most important element source to the forest floor (Ukonmaanaho and Starr, 2002; Zimmermann *et al.*, 2002). However, from the viewpoint of the ecosystem, litterfall is a mostly internal cycling mechanism, while throughfall contains ions from internal and external sources. Even though litterfall may supply more material annually than throughfall, litterfall nutrients are only slowly released from organic matter,

while throughfall nutrients are nearly all dissolved and thus readily available for plant uptake (Parker, 1983; Gebauer *et al.*, 2000) or soil percolation (Quilchano *et al.*, 2002).

Systematic spatial throughfall patterns may have important implications for hydrological, biogeochemical, and ecological processes such as soil moisture, root growth, nitrification, soil solution chemistry, soil percolation, and trace gas fluxes (Bouten *et al.*, 1992; Manderscheid and Matzner, 1995; Schaap *et al.*, 1997; Beier, 1998; Bradford *et al.*, 2001; Raat *et al.*, 2002; Schume *et al.*, 2003). The temporal persistence of spatial throughfall patterns implies that forest floors may have consistently wetter and drier areas, although the spatial heterogeneity of forest floor water content also depends on differences in forest floor thickness and properties (Schume *et al.*, 2004), evaporation, root uptake, and drainage to the mineral soil (Schaap *et al.*, 1997; Raat *et al.*, 2002). For example, the spatial variance in net methane uptake in a temperate forest soil was partly explained by the variation in throughfall deposition and volume, which was attributed to spatial heterogeneity of the mixed deciduous canopy (Bradford *et al.*, 2001). Spatial throughfall patterns are reflected in patterns of water and ion percolation through the soil (Manderscheid and Matzner, 1995; Böttcher *et al.*, 1997; Beier, 1998). As a consequence of higher crown densities and higher fine root densities close to (coniferous) tree boles, lower throughfall amounts near the stem can lead to more strongly reduced percolation water fluxes below the rooting zone (Zirlewagen and von Wilpert, 2001). The impact of canopy cover on soil water contents will also depend on stand structure and composition, as tree species differ in rooting pattern (Rothe and Binkley, 2001) and corresponding spatio-temporal soil water depletion (Schume *et al.*, 2003, 2004).

In addition to the heterogeneous distribution of throughfall, large stemflow fluxes in beech stands contribute to the spatial variability of water and ion inputs to the forest floor. Significant effects of stemflow on hydrological budgets and soil processes close to tree boles have been reported, in particular for beech trees (Matschonat and Falkengren-Grerup, 2000; Chang and Matzner, 2000ab). However, stemflow infiltrates on a small area around tree trunks, while the spatial variability of TF water and ion deposition can affect ecological processes throughout a forest stand (Manderscheid and Matzner, 1995; Raat *et al.*, 2002). We conclude that calculations of percolation fluxes and element budgets in beech stands may be improved by considering the spatial heterogeneity of both throughfall (Beier, 1998) and stemflow fluxes (Chang and Matzner, 2000b), for example by distinguishing representative structural units within a forest stand (Zirlewagen and von Wilpert, 2001).

Furthermore, the spatial variation of throughfall fluxes within a forest stand is highly relevant for assessing sampling designs in throughfall studies, as discussed by other researchers (see references in Table 4.1). Our results confirmed that as the length of the sampling interval increased the spatial heterogeneity of throughfall water decreased while the temporal stability increased (Lawrence and Fernandez, 1993; Houle et al. 1999a). The down levelling effect of an increasing sampling interval on throughfall variability was less pronounced for the ion fluxes than for the water fluxes, but no results were available on the throughfall ion variability for individual rain events. The choice of the number of throughfall collectors that should be used in an experimental design depends on the temporal accuracy that is needed for the quantitative assessment of the process of interest (Thimonier, 1998). Finally, the influence of throughfall on forest floor water and chemistry implies that throughfall variability has importance for small-scale field experiments in biogeochemistry such as studies with litterbags, soil columns, tracers (Brodersen *et al.*, 2000), and trace gas fluxes (Bradford *et al.*, 2001).

We did not attempt to relate throughfall fluxes to a varying plant area index throughout the growing season (Holst *et al.*, 2004), but used the canopy measurements of August when plant area index was maximal (Mussche *et al.*, 2001). The impact of ignoring the seasonal evolution in canopy cover during the leafed season with respect to its relationship to throughfall is considered to be small because canopy cover changed more or less at the same time above all sampling locations. Regarding the water fluxes, there was even no clear difference in rainfall interception between events during the fully leafed period on the one hand and leaf unfolding or leaf senescence on the other hand. Only for events during the last week of leaf senescence, the interception of rainfall was relatively lower compared to the rest of the leafed season (Fig. 3.5), and this week was thus included in the leafless season to examine water fluxes (Chapters 3 and 4). In contrast, there was a clear effect of leaf emergence as well as leaf senescence on the chemistry of throughfall and stemflow (Fig. 5.2). During both canopy transition phases, increased throughfall enrichment compared to wet-only deposition was found for several ions (Fig. 5.3). Therefore, in addition to the leafless season, three phenological canopy phases were distinguished within the leafed season to study the spatio-temporal effect of the canopy on throughfall ion fluxes (Chapters 5 and 6).

Similar spatial patterns of throughfall deposition were found between ions originating mainly from dry deposition and mainly from canopy leaching (Table 6.3, Fig. 6.2), in agreement with previous research (Robson *et al.*, 1994; Whelan and Anderson, 1998; Raat *et al.*, 2002). This

spatial correlation highlights the problem of separating the contribution from external and internal ion sources to the enrichment of throughfall after canopy passage. Nevertheless, the measurement of throughfall ion fluxes for individual throughfall collectors allowed statistical analyses that are not possible when throughfall ion deposition is determined at the plot-average level only. For example, the difference of throughfall enrichment between the leafed and leafless seasons could statistically be tested by a related samples test (Table 5.2), which is more powerful than an unrelated samples test. The biweekly throughfall ion fluxes allowed to investigate relationships between ion pairs, which for example supported inferences on the leaching of weak acids (Fig. 5.5) and Cl⁻ (Fig. 5.7) from the canopy. The seasonal variation of throughfall and stemflow enrichment (Fig. 5.3) indicated that elements that are often thought to behave conservatively with respect to forest canopies may have been released from the beech canopy during leaf emergence and/or senescence, although the estimated contribution of canopy leaching was low compared to the annual dry deposition. More importantly, the relatively high throughfall enrichment ratios observed during the dormant season indicate that substantial amounts of gases and particles can be deposited onto a leafless deciduous canopy. The high dry deposition of nitrogen and sulphur estimated during the leafless season was most likely due to co-deposition of SO₂ and NH₃ (Derome *et al.*, 2004) and suggests that inferential deposition models have to take into account non-stomatal canopy uptake by wet surfaces (Wesely and Hicks, 2000).

Quantifying dry deposition onto forests goes along with some degree of uncertainty. Direct methods (eddy correlation and gradient techniques) to measure dry deposition are often not feasible because they require expensive instrumentation and a uniform, relatively large forest area (Horst and Weil, 1994; Wesely and Hicks, 2000). The generally small size of forest patches in the highly fragmented landscape in northern Belgium and other regions of Europe thus hampers the application of such direct micrometeorological methods. Inferential models are considered as the best practical way of quantifying seasonal and annual dry atmospheric deposition (Brook *et al.*, 1997; Zhang *et al.*, 2002), but a detailed parameterization of deposition velocities is needed to obtain reliable results (Andersen and Hovmand, 1999). Nevertheless, to estimate the spatial variation of atmospheric deposition within a forest stand in relation to the local canopy structure, the throughfall technique corrected for ion exchange within the canopy currently appears to be the only available method. Enhanced dry deposition of some atmospheric pollutants in forest edges has already been simulated using numerical models (De Jong and Klaassen, 1997; De Ridder *et al.*, 2004).

The present study has increased our understanding of the relationship between canopy structure and spatio-temporal patterns of water and ion fluxes beneath a broadleaf deciduous canopy, but several aspects deserve further research:

- The close relationship between canopy cover and throughfall water amount in the growing season suggests that a spatial interception model is feasible for hardwood stands. The central concept in dynamic interception models is the water storage capacity of the canopy (Rutter *et al.*, 1971; Whelan and Anderson, 1996). Such a spatially-explicit model should not only take spatial variations in water storage into account, but preferably also temporal variations due to canopy phenology (Link *et al.*, 2004). Furthermore, canopy storage is likely affected by rainfall intensity (Calder, 1996; Price and Carlyle-Moses, 2003) and wind speed (Hörmann *et al.*, 1996), although there is discussion on the physical interpretation of canopy storage values estimated by calibrating interception models (Vrugt *et al.*, 2003; Keim, 2004; Keim and Skaugset, 2004).
- Studies on throughfall and stemflow water in deciduous forests often focus on the growing season. More research is needed on the redistribution of precipitation water within leafless trees during the dormant season. This may include more advanced branch structure measurements than used in the present study and simulation of the lateral within-canopy transport (Xiao *et al.*, 2000a).
- Although ion leaching from forest canopies mainly originates from the foliage, woody components appear to contribute meaningfully to the release of some cations. Controlled experiments would be helpful to quantify ion leaching from leafless branches in relation to rainfall characteristics. Likewise, additional information is required on the retention of gaseous and dissolved nitrogen compounds by twigs and leaves, and on the processes involved in ion exchange within the canopy of different species in varying environmental conditions.
- The impact of heterogeneous throughfall fluxes on ecosystem processes has mainly been studied in coniferous stands. A systematic component of spatial throughfall patterns, as observed in the present study, is also expected beneath other deciduous forest canopies (e.g., Keim *et al.*, 2005). More research is needed to quantify the extent and ecological consequences of time persistent spatial throughfall patterns in broadleaved forests, e.g., with respect to soil moisture, microbiological processes, and soil percolation.

Summary

This study examined the amount and chemical composition of water reaching the forest floor, which is an important aspect of the hydrology and nutrient cycling in forest ecosystems. Throughfall is a major pathway of nutrients to the forest floor and is often used to quantify atmospheric deposition onto forest vegetation. Within coniferous forest stands, the spatial variation of throughfall has been found to affect a range of hydrological, biogeochemical, and ecological processes. Despite the general opinion that the canopy layer regulates water and ion fluxes in throughfall, few attempts have been made to relate fine-scale spatial throughfall variations to the canopy structure in a quantitative way, particularly in deciduous stands.

Therefore, the general objective of the study was to quantify and explain the spatio-temporal variation of water and ion fluxes to the forest floor beneath a deciduous canopy. The research focused on the canopy of one dominant beech (*Fagus sylvatica* L.) tree located in a temperate, mixed deciduous forest stand near Ghent (Belgium). The amounts as well as the chemical composition of precipitation, throughfall, and stemflow water were determined. The influence of canopy cover on the amount and composition of throughfall was analysed in time and in space. During the leafed season, increasing canopy cover decreased the water amount and increased ion deposition. During the leafless season, increasing branch cover increased ion deposition but did not significantly affect spatial variations in throughfall water fluxes.

First of all, the water and ion input by precipitation above the canopy layer was quantified as accurately as possible. At two sites located about 1 km from each other, precipitation water was measured by continuously open bulk collectors and by wet-only samplers that were open during rainfall only. The amount and chemistry of rainfall were almost identical at the two adjacent sites. However, the comparison of the two collector types showed that the often used bulk collectors significantly overestimated the actual wet deposition of all major ions, while the acidity of rainwater was underestimated. Consequently, wet-only precipitation data were used to determine the effect of the tree crown on the composition of throughfall water.

The research demonstrated that the temporal and spatial variation of the water amount beneath the beech canopy was significantly affected by foliation. At the level of individual rainfall events, the partitioning of rainfall water into throughfall, stemflow, and interception was

Summary

mainly determined by foliation and event rainfall amount, although other event characteristics such as rainfall intensity and wind speed also affected rainfall partitioning. For a given amount of rainfall, the presence of foliage significantly increased interception loss and decreased the amounts of throughfall and stemflow water. Likewise, foliation and event rainfall amount strongly affected the spatial variation of throughfall water amount, as the spatial heterogeneity declined in absence of leaves and for larger rain events. During the leafless season, the weak spatial pattern of throughfall water amount was not related to the photographically measured branch cover. However, canopy structure during the leafed season largely explained the spatial pattern of the water fluxes. The amount of throughfall water at the forest floor decreased with increasing cover of foliage and branches above a sampling point because of the enhanced interception and subsequent evaporation of rainfall water.

The modification of the composition of precipitation water after canopy passage was strongly influenced by canopy phenology and differed between the major ions studied. Throughout the year, the ion deposition beneath the canopy largely exceeded the above-canopy precipitation input for all ions other than H^+ . Although throughfall enrichment was generally higher during the leafed season, the presence of branches during the leafless season still markedly increased the ion fluxes to the forest floor compared to the wet-only precipitation. Dry deposition of gases and particles onto the canopy consequently was high during both the leafed and leafless season. According to a canopy budget method, dry deposition was estimated to contribute approximately two thirds of the total wet and dry atmospheric input to the forest. Ion leaching from the canopy was highest throughout the leafed season, and particularly during the periods of leaf emergence and senescence, but also woody components released cations. The results of varying forms of the canopy budget method were compared with an inferential technique. Despite uncertainties in estimating dry deposition, the results highlight the strong filtering capacity of forest canopies for atmospheric components of natural and anthropogenic origin.

In contrast to the amount of throughfall water, the spatial pattern of throughfall ion deposition was positively correlated with canopy cover during both the growing and the dormant season. Increasing amounts of leaves and/or branches and twigs above a sampling point resulted in higher throughfall deposition because of enhanced ion leaching from the beech canopy as well as dry deposition onto the canopy surfaces. Canopy cover as determined by skyward-looking photography is only a simple measure of canopy structure, particularly for broadleaved trees. Nevertheless, this canopy measure helped to explain the spatial patterns of throughfall water amount in the growing season and throughfall ion fluxes throughout the entire year.

Samenvatting

Deze studie onderzocht de hoeveelheid en de chemische samenstelling van de wateraanvoer naar de bosbodem, wat een essentieel onderdeel is van de hydrologie en nutriëntencyclus in bosccosystemen. Doorvalwater speelt een belangrijke rol bij de aanvoer van nutriënten naar de bosbodem en wordt vaak gebruikt om de totale atmosferische depositie op bosvegetatie te bepalen. Onderzoek in naaldbossen toont aan dat de kleinschalige ruimtelijke variatie van doorvalwater diverse hydrologische, biogeochemische en ecologische processen beïnvloedt. Ondanks de algemene overtuiging dat de kroonlaag van een bos een regulerend effect heeft op de water- en ionenfluxen in doorval, zijn er weinig pogingen gedaan om kleinschalige ruimtelijke variaties in doorval binnen een bosbestand op kwantitatieve wijze te relateren aan de kroonstructuur, in het bijzonder voor bladverliezende loofbestanden.

De algemene doelstelling van het onderzoek was daarom om de ruimtelijk en temporele variatie van de water- en ionenfluxen te kwantificeren en verklaren onder een bladverliezende kroonlaag. De studie richtte zich op een dominante beuk (*Fagus sylvatica* L.) gelegen in een gemengd loofbestand nabij Gent. Zowel de hoeveelheden als de chemische samenstelling van neerslag-, doorval- en stamafvloeiwaterv werden bepaald. De invloed van de kroon op het doorvalwater werd onderzocht in tijd en ruimte. Tijdens de bebladerde periode verminderde de waterhoeveelheid met toenemende kroonbedekking, terwijl de ionendepositie toenam. Tijdens de bladloze periode was een toenemende takbedekking gerelateerd aan toenemende ionendepositie maar niet aan ruimtelijke variaties in de hoeveelheid doorvalwater.

In eerste instantie werd de aanvoer van regenwater en ionen boven de kroonlaag zo accuraat mogelijk bepaald. Op twee locaties met tussenafstand van ongeveer 1 km werd het regenwater zowel gemeten met continu geopende bulk-collectoren als met wet-only toestellen die enkel open waren tijdens regenbuien. De hoeveelheid en de samenstelling van het regenwater was nagenoeg identiek op de twee nabijgelegen locaties. Uit de vergelijking van de twee types neerslagcollectoren bleek echter dat de algemeen gebruikte bulk-collectoren de ionenaanvoer via neerslag overschatten, terwijl de zuurtegraad van regenwater werd onderschat. Daarom werden de wet-only neerslagmetingen gebruikt om het effect van de kroonlaag op de samenstelling van doorvalwater te bepalen.

Het onderzoek toonde aan dat de temporele en ruimtelijke variatie van de waterhoeveelheid onder de kroonlaag significant werd beïnvloed door bebladering. Voor individuele regenbuien werd de opsplitsing van neerslagwater in doorval, stamafvloeï en interceptie vooral bepaald door bebladering en door de hoeveelheid regen van de bui, hoewel ook andere kenmerken van de buien de opsplitsing van neerslag beïnvloedden, zoals regenintensiteit en windsnelheid. De aanwezigheid van een bladerdek verhoogde de interceptie van neerslag en verlaagde de hoeveelheden van doorval- en stamafvloeïwater. Bebladering en buigrootte hadden ook een duidelijk effect op de ruimtelijke variatie van de hoeveelheid doorvalwater, aangezien de ruimtelijke heterogeniteit verminderde bij afwezigheid van bladeren en bij groter wordende regenbuien. Tijdens de bladloze periode stond het zwakke ruimtelijke patroon van de hoeveelheid doorval niet in verband met de takbedekking, die op fotografische wijze werd bepaald. Tijdens de bebladerde periode verklaarde de kroonstructuur echter grotendeels het ruimtelijke patroon van de waterfluxen. De aanvoer van doorvalwater naar de bosbodem verminderde met een toenemende blad- en takbedekking boven de meetpunten omwille van de grotere interceptie en daaropvolgende verdamping van regenwater.

De veranderende samenstelling van neerslagwater na contact met de kroonlaag werd duidelijk beïnvloed door de fenologie van de kroon en verschilde tussen de onderzochte ionen. Doorheen het volledige jaar was er voor alle ionen, behalve voor H^+ , een sterke aanrijking van de ionendepositie onder de kroonlaag in vergelijking met de regendepositie boven de kroonlaag. Hoewel de chemische aanrijking van doorvalwater over het algemeen hoger was tijdens de bebladerde periode, zorgden de takken en twijgen tijdens de bladloze periode ook voor een significante aanrijking van de ionenaanvoer naar de bosbodem. Er was bijgevolg een hoge droge depositie van gasvormige componenten en partikels op de kroonlaag, zowel tijdens de zomer- als winterperiode. Op basis van een kroonbudget-methode werd geschat dat de droge depositie ongeveer twee derden uitmaakte van de totale natte en droge atmosferische depositie op de kroonlaag. De afgifte van ionen door de kroonlaag was hoog gedurende de volledige bebladerde periode, en in het bijzonder bij het verschijnen van bladeren in de lente en in de periode voor de bladval in de herfst, maar ook de takken en twijgen gaven kationen af. De resultaten van diverse vormen van de kroonbudget-methode werden vergeleken met die van een inferentiële techniek. Ondanks de onzekerheden op de bepaalde droge depositie tonen de resultaten duidelijk aan dat de onderzochte kroonlaag een sterke filterwerking vertoont voor atmosferische componenten van natuurlijke en antropogene oorsprong.

In tegenstelling tot de waterhoeveelheden in doorval was het ruimtelijk patroon van de ionenfluxen onder de boomkruin positief gecorreleerd met de kroon- en takbedekking, zowel tijdens de bebladerde groeiperiode als tijdens de bladloze periode. Dit toonde opnieuw aan dat takken een belangrijke rol spelen bij de netto ionenaanvoer naar de bosbodem in afwezigheid van bladeren. Bij een toenemende hoeveelheid bladeren en/of houtachtige biomassa boven de meetpunten verhoogde de ionenaanvoer naar de bosbodem door de hogere ionenafgifte door de kroon en door de hogere droge depositie op de kroonelementen. De fotografisch bepaalde overscherming is slechts een eenvoudige kwantitatieve maat voor kroonstructuur, zeker bij loofbomen. Niettemin bleek deze kroonparameter in staat om ruimtelijke patronen te helpen verklaren van de hoeveelheid doorvalwater tijdens het groeiseizoen en van de ionenfluxen doorheen het volledige jaar.

References

- Aber, J., McDowell, W., Nadelhoffer, K., Magill, A., Berntson, G., Kamakea, M., McNulty, S., Currie, W., Rustad, L. and Fernandez, I. 1998. Nitrogen saturation in temperate forest ecosystems: hypotheses revisited. *BioScience* 48, 921-934.
- Aber, J.D., Nadelhoffer, K.J., Steudler, P. and Melillo, J.M. 1989. Nitrogen saturation in northern forest ecosystems. *BioScience* 39, 378-386.
- Aboal, J.R., Morales, D., Hernandez, M. and Jimenez, M.S. 1999. The measurement and modelling of the variation of stemflow in a laurel forest in Tenerife, Canary Islands. *Journal of Hydrology* 221, 161-175.
- Aikawa, M., Hiraki, T., Tamaki, M. and Shoga, M. 2003. Difference between filtering-type bulk and wet-only data sets based on site classification. *Atmospheric Environment* 37, 2597-2603.
- Akkoyunlu, B.O. and Tayanç, M. 2003. Analysis of wet and bulk deposition in four different regions of Istanbul, Turkey. *Atmospheric Environment* 37, 3571-3579.
- Allerup, P., Madsen, H. and Vejen, F. 1997. A comprehensive model for correcting point precipitation. *Nordic Hydrology* 28, 1-20.
- Ammer, V.C., Albrecht, L., Borchert, H., Brosinger, F., Dittmar, C., Elling, W., Ewald, J., Felbermeier, B., von Gilsa, H., Huss, J., Kenk, G., Kolling, C., Kohnle, U., Meyer, P., Mosandl, R., Moosmayer, H.U., Palmer, S., Reif, A., Rehfuess, K.E. and Stimm, B. 2005. Future suitability of beech (*Fagus sylvatica* L.) in Central Europe: critical remarks concerning a paper of Rennenberg *et al.* (2004). *Allgemeine Forst- und Jagdzeitung* 176, 60-67.
- Anonymous. 2000. Indicators for the sustainable management of French forests. A French document for implementing decisions taken by countries attending the ministerial conferences on the protection of European forests - 2000 edition. Ministry of Agriculture and Fisheries, Countryside and Forestry Department. Paris, France.
- Andersen, H.V. and Hovmand, M.F. 1999. Review of dry deposition measurements of ammonia and nitric acid to forest. *Forest Ecology and Management* 114, 5-18.
- Armbruster, M., MacDonald, J., Dise, N.B. and Matzner, E. 2002. Throughfall and output fluxes of Mg in European forest ecosystems: a regional assessment. *Forest Ecology and Management* 164, 137-147.
- Armbruster, M., Seeger, J. and Feger, K.H. 2004. Effects of changes in tree species composition on water flow dynamics - model applications and their limitations. *Plant and Soil* 264, 13-24.
- Arora, V. 2002. Modelling vegetation as a dynamic component in soil-vegetation-atmosphere transfer schemes and hydrological models. *Reviews of Geophysics* 40, Art. No. 1006.
- Asche, N. 1988. Deposition, Interception und Pflanzenauswaschung im Kronenraum eines Eichen/Hainbuchen-Bestandes. *Zeitschrift für Pflanzenernährung und Bodenkunde* 151, 103-107.
- Augusto, L., Ranger, J., Binkley, D. and Rothe, A. 2002. Impact of several common tree species of European temperate forests on soil fertility. *Annals of Forest Science* 59, 233-253.
- Aussenac, G. and Boulangeat, C. 1980. Interception des précipitations et évapotranspiration réelle dans des peuplements de feuillu (*Fagus sylvatica* L.) et de résineux (*Pseudotsuga meziessii* (Mirb) Franco). *Annales des Sciences forestières* 37, 91-107.
- Baldocchi, D.D. and Vogel, C.A. 1996. Energy and CO₂ flux densities above and below a temperate broadleaved forest and a boreal pine forest. *Tree Physiology* 16, 5-16.

References

- Balestrini, R. and Tagliaferri, A. 2001. Atmospheric deposition and canopy exchange processes in alpine forest ecosystems (northern Italy). *Atmospheric Environment* 35, 6421-6433.
- Becker, J.S., Bellis, D., Staton, I., McLeod, C.W. and Dombovari, J. 2000. Determination of trace elements including platinum in tree bark by ICP mass spectrometry. *Fresenius Journal of Analytical Chemistry* 368, 490-495.
- Beckett, K.P., Freer-Smith, P.H. and Taylor, G. 1998. Urban woodlands: their role in reducing the effects of particulate pollution. *Environmental Pollution* 99, 347-360.
- Beckett, K.P., Freer-Smith, P.H. and Taylor, G. 2000. Particulate pollution capture by urban trees: effect of species and windspeed. *Global Change Biology* 6, 995-1003.
- Beier, C. 1998. Water and element fluxes calculated in a sandy forest soil taking spatial variability into account. *Forest Ecology and Management* 101, 269-280.
- Beier, C., Gundersen, P. and Rasmussen, L. 1992. A new method for estimation of dry deposition of particles based on throughfall measurements in a forest edge. *Atmospheric Environment* 26A, 1553-1559.
- Beier, C., Hansen, K. and Gundersen, P. 1993. Spatial variability of throughfall fluxes in a spruce forest. *Environmental Pollution* 81, 257-267.
- Bélanger, N., Paré, D. and Courchesne, F. 2004. Regression equations for estimating throughfall nutrient fluxes using wet deposition data and their applicability for simulating the soil acid-base status using the dynamic forest soil-atmosphere model SAFE. *Ecological Modelling* 175, 151-167.
- Bellot, J. and Escarre, A. 1998. Stemflow and throughfall determination in a resprouted Mediterranean holm-oak forest. *Annals of Forest Science* 55, 847-865.
- Berger, T.W., Eager, C., Likens, G.E. and Stinger, G. 2001. Effects of calcium and aluminium chloride additions on foliar and throughfall chemistry in sugar maples. *Forest Ecology and Management* 149, 75-90.
- Binkley, D. and Högborg, P. 1997. Does atmospheric deposition of nitrogen threaten Swedish forests? *Forest Ecology and Management* 92, 119-152.
- Bolund, P. and Hunhammar, S. 1999. Ecosystem services in urban areas. *Ecological Economics* 29, 293-301.
- Böttcher, J., Lauer, S., Strebel, O. and Puhlman, M. 1997. Spatial variability of canopy throughfall and groundwater sulfate concentrations under a pine stand. *Journal of Environmental Quality* 26, 503-510.
- Bouten, W., Heimovaara, T.J. and Tiktak, A. 1992. Spatial patterns of throughfall and soil water dynamics in a Douglas fir stand. *Water Resources Research* 28, 3227-3233.
- Bouten, W., Schaap, M.G., Aerts, J. and Vermetten, A.W.M. 1996. Monitoring and modelling canopy water storage amounts in support of atmospheric deposition studies. *Journal of Hydrology* 181, 305-321.
- Bouwman, A.F., Van Vuuren, D.P., Derwent, R.G. and Posch, M. 2002. A global analysis of acidification and eutrophication of terrestrial ecosystems. *Water, Air, and Soil Pollution* 141, 349-382.
- Bouya, D., Myttenaere, C., Weissen, F. and Van Praag, H.J. 1999. Needle permeability of Norway spruce (*Picea abies* (L.) Karst.) as influenced by magnesium nutrition. *Belgian Journal of Botany* 132, 105-118.
- Bowden, R.D., Geballe, G.T. and Bowden, W.B. 1989. Foliar uptake of ¹⁵N from simulated cloud water by red spruce (*Picea rubens*) seedlings. *Canadian Journal of Forest Research* 19, 382-386.
- Boyce, R.L., Friedland, A.J., Chamberlain, C.P. and Poulson, S.R. 1996. Direct canopy nitrogen uptake from N-15-labeled wet deposition by mature red spruce. *Canadian Journal of Forest Research* 26, 1539-1547.

- Bradford, M.A., Wookey, P.A., Ineson, P. and Lappin-Scott, H.M. 2001. Controlling factors and effects of chronic nitrogen and sulphur deposition on methane oxidation in a temperate forest soil. *Soil Biology and Biochemistry* 33, 93-102.
- Bréda, N.J.J. 2003. Ground-based measurements of leaf area index: a review of methods, instruments and current controversies. *Journal of Experimental Botany* 392, 2403-2417.
- Bredemeier, M. 1988. Forest canopy transformation of atmospheric deposition. *Water, Air, and Soil Pollution* 40, 121-138.
- Bredemeier, M. and Lindberg, S.E. 1992. Element fluxes in precipitation samples - a comparison of bulk and event wet-only sampling in a spruce forest. *Staub Reinhaltung der Luft* 52, 67-72.
- Brodersen, C., Pohl, S., Lindenlaub, M., Leibundgut, C. and von Wilpert, K. 2000. Influence of vegetation structure on isotope content of throughfall and soil water. *Hydrological Processes* 14, 1439-1448.
- Brook, J.R., Di-Giovanni, F., Cakmak, S. and Meyers, T.P. 1997. Estimation of dry deposition velocity using inferential models and site-specific meteorology - uncertainty due to siting of meteorological towers. *Atmospheric Environment* 31, 3911-3919.
- Brumme, R., Leimcke, U. and Matzner, E. 1992. Interception and uptake of NH_4^+ and NO_3^- from wet deposition by aboveground parts of young beech (*Fagus sylvatica* L.) trees. *Plant and Soil* 142, 273-279.
- Burghouts, T.B.A., Van Straalen, N.M. and Bruijnzeel, L.A. 1998. Spatial heterogeneity of element and litter turnover in a Bornean rain forest. *Journal of Tropical Ecology* 114, 477-506.
- Burkett, V.R., Wilcox, D.A., Stottlemyer, R., Barrow, W., Fagre, D., Baron, J., Price, J., Nielsen, J.L., Allen, C.D., Peterson, D.L., Ruggerone, G. and Doyle, T. 2005. Nonlinear dynamics in ecosystem response to climatic change: case studies and policy implications. *Ecological Complexity* 2, 357-394.
- Butler, T.J. and Likens, G.E. 1995. A direct comparison of throughfall plus stemflow to estimates of dry and total deposition for sulfur and nitrogen. *Atmospheric Environment* 29, 1253-1265.
- Calder, I.R. 1996. Dependence of rainfall interception on drop size. I. Development of the two-layer stochastic model. *Journal of Hydrology* 185, 363-378.
- Cape, J.N. and Leith, I.D. 2002. The contribution of dry deposited ammonia and sulphur dioxide to the composition of precipitation from continuously open gauges. *Atmospheric Environment* 36, 5983-5992.
- Cape, J.N., Sheppard, L.J., Binnie, J. and Dickinson, A.L. 1998. Enhancement of the dry deposition of sulphur dioxide to a forest in the presence of ammonia. *Atmospheric Environment* 32, 519-524.
- Cappellato, R., Peters, N.E. and Meyers, T.P. 1998. Above-ground sulfur cycling in adjacent coniferous and deciduous forests and watershed sulfur retention in the Georgia Piedmont, U.S.A. *Water, Air, and Soil Pollution* 103, 151-171.
- Cappellato, R., Peters, N.E. and Ragsdale, H.L. 1993. Acidic atmospheric deposition and canopy interactions of adjacent deciduous and coniferous forests in the Georgia Piedmont. *Canadian Journal of Forest Research* 23, 1114-1125.
- Carleton, T.J. and Kavanagh, T. 1990. Influence of stand age and spatial location on throughfall chemistry beneath black spruce. *Canadian Journal of Forest Research* 20, 1917-1925.
- Carlyle-Moses, D.E., Fores Laureano, J.S. and Price, A. 2004. Throughfall and throughfall spatial variability in Madrean oak forest communities of northeastern Mexico. *Journal of Hydrology* 297, 124-135.
- Chamberlain, A.C. 1967. Interception and retention of radioactive aerosols by vegetation. *Atmospheric Environment* 4, 57-78.
- Chang, S.-C. and Matzner, E. 2000a. Soil nitrogen turnover in proximal and distal stem areas of European beech trees. *Plant and Soil* 218, 117-125.
- Chang, S.-C. and Matzner, E. 2000b. The effect of beech stemflow on spatial patterns of soil solution chemistry and seepage fluxes in a mixed beech/oak stand. *Hydrological Processes* 14, 135-144.

References

- Chiwa, M., Crossley, A., Sheppard, L.J., Sakugawa, H. and Cape, J.N. 2004. Throughfall chemistry and canopy interactions in a Sitka spruce plantation sprayed with six different simulated polluted mist treatments. *Environmental Pollution* 127, 57-64.
- Ciais, Ph., Reichstein, M., Viovy, N., Granier, A., Ogée, J., Allard, V., Aubinet, M., Buchmann, N., Bernhofer, Chr., Carrara, A., Chevallier, F., De Noblet, N., Friend, A.D., Friedlingstein, P., Grünwald, T., Heinesch, B., Keronen, P., Knohl, A., Krinner, G., Loustau, D., Manca, G., Matteucci, G., Miglietta, F., Ourcival, J.M., Papale, D., Pilegaard, K., Rambal, S., Seufert, G., Soussana, J.F., Sanz, M.J., Schulze, E.D., Vesala, T. and Valentini, R., 2005. Europe-wide reduction in primary productivity caused by the heat and drought in 2003. *Nature* 437, 529-534.
- Collier, M.D., Fotelli, M.N., Nahm, M., Kopriva, S.R.H., Hanke, D.E. and Gessler, A. 2003. Regulation of nitrogen uptake by *Fagus sylvatica* on a whole plant level - interactions between cytokinins and soluble N compounds. *Plant, Cell and Environment* 26, 1549-1560.
- Crockford, R.H. and Richardson, D.P. 2000. Partitioning of rainfall into throughfall, stemflow and interception: effect of forest type, ground cover and climate. *Hydrological Processes* 14, 2903-2920.
- Cronan, C.S. and Reiners, W.A. 1983. Canopy processing of acidic precipitation by coniferous and hardwood forests in New England. *Oecologia* 59, 216-223.
- Czajkowski, T., Kuhling, M. and Bolte, A. 2005. Impact of the 2003 summer drought on growth of beech sapling natural regeneration (*Fagus sylvatica* L.) in north-eastern Central Europe. *Allgemeine Forst- und Jagdzeitung* 176, 133-143.
- Davie, T.J.A. and Durocher, M.G. 1997. A model to consider the spatial variability of rainfall partitioning within a deciduous canopy: I. Model description. *Hydrological Processes* 11, 1509-1523.
- De Jong, J.J.M. and Klaassen, W. 1997. Simulated dry deposition of nitric acid near forest edges. *Atmospheric Environment* 22, 3681-3691.
- De Ridder, K., Neiryneck, K. and Mensink, C. 2004. Parameterising forest edge deposition using effective roughness length. *Agricultural and Forest Meteorology* 123, 1-11.
- Derome, J., Nieminen, T. and Saarsalmi, A. 2004. Sulphur dioxide adsorption in Scots pine canopies exposed to high ammonia emissions near a Cu-Ni smelter in SW Finland. *Environmental Pollution* 129, 79-88.
- De Schrijver, A., Nachtergale, L. and Lust, N. 2001. Deelaspecten van de intensieve monitoring van het boscysteem in het Vlaamse Gewest, meetjaar 2000. Eindverslag 2001. Contract no. IBW/1/2001. Ghent University, Laboratory of Forestry, Ghent, Belgium.
- De Schrijver, A., Nachtergale, L., Roskams, P., De Keersmaecker, L., Mussche, S. and Lust, N. 1998. Soil acidification along an ammonium deposition gradient in a Corsican pine stand in northern Belgium. *Environmental Pollution* 102 Suppl. 1, 427-431.
- De Schrijver, A., Nachtergale, L., Staelens, J., Luysaert, S. and De Keersmaecker, L. 2004. Comparison of throughfall and soil solution chemistry between a high-density Corsican pine stand and a naturally regenerated silver birch stand. *Environmental Pollution* 131, 93-105.
- de Vries, W., Reinds, G.J., Deelstra, H.D., Klap, J.M. and Vel, E.M. 1998. Intensive monitoring of forest ecosystems in Europe. Technical report 1998. EC-UN/ECE, Brussels, Geneva.
- de Vries, W., Reinds, G.J., van der Salm, C., Draaijers, G.P.J., Bleeker, A., Erisman, J.W., Auée, J., Gundersen, P., Kristensen, H.L., van Dobben, H., de Zwart, D., Derome, J., Voogd, J.C.H. and Vel, E.M. 2001. Intensive monitoring of forest ecosystems in Europe. Technical report 2001. EC-UN/ECE, Brussels, Geneva.
- de Vries, W., Reinds, G.J. and Vel, E. 2003. Intensive monitoring of forest ecosystems in Europe 2: Atmospheric deposition and its impact on soil solution chemistry. *Forest Ecology and Management* 174, 97-115.
- Deutsch, C.V. and Journel, A.G. 1998. *GSLIB - Geostatistical software library and user's guide*. Oxford University Press, New York.

- Devlaeminck, R., De Schrijver, A. and Hermy, M. 2005. Variation in throughfall deposition across a deciduous beech (*Fagus sylvatica* L.) forest edge in Flanders. *Science of the Total Environment* 337, 241-252.
- Dolman, A.J. 1986. Estimates of roughness length and zero plane displacement for a foliated and non-foliated oak canopy. *Agricultural and Forest Meteorology* 36, 241-248.
- Dolman, A.J. 1987. Summer and winter rainfall interception in an oak forest. Predictions with an analytical and a numerical simulation model. *Journal of Hydrology* 90, 1-9.
- Draaijers, G.P.J. 1993. The variability of atmospheric deposition to forests. Ph.D. thesis, University of Utrecht, the Netherlands.
- Draaijers, G.P.J. and Erisman, J.W. 1995. A canopy budget model to assess atmospheric deposition from throughfall measurements. *Water, Air, and Soil Pollution* 85, 2253-2258.
- Draaijers, G., Erisman, J., Lövblad, G., Spranger, T. and Vel, E. 1998. Quality and uncertainty aspects of forest deposition estimation using throughfall, stemflow and precipitation measurements. TNO-MEP-Report 98/003. TNO Institute of Environmental Sciences, Energy Research and Process Innovation, Apeldoorn, the Netherlands.
- Draaijers, G.P.J., Erisman, J.W., Spranger, T. and Wyers, G.P. 1996. The application of throughfall measurements for atmospheric deposition monitoring. *Atmospheric Environment* 30, 3349-3361.
- Draaijers, G.P.J., Erisman, J.W., Van Leeuwen, N.F.M., Romer, F.G., te Winkel, B.H., Veltkamp, A.C., Vermeulen, A.T. and Wyers, G.P. 1997. The impact of canopy exchange on differences observed between atmospheric deposition and throughfall fluxes. *Atmospheric Environment* 31, 387-397.
- Draaijers, G.P.J., Ivens, W.P.M.F. and Bleuten, W. 1988. Atmospheric deposition in forest edges measured by monitoring canopy throughfall. *Water, Air, and Soil Pollution* 42, 129-135.
- Draaijers, G.P.J., Van Ek, R. and Meijers, R. 1992. Research on the impact of forest stand structure on atmospheric deposition. *Environmental Pollution* 75, 243-249.
- Driscoll, C.T., Fuller, R.D. and Schecher, W.D. 1989. The role of organic acids in the acidification of surface waters in the eastern US. *Water, Air, and Soil Pollution* 43, 21-40.
- Duchesne, L., Ouimet, R., Camiré, C. and Houle, D. 2001. Seasonal nutrient transfers by foliar resorption, leaching, and litter fall in a northern hardwood forest at Lake Clair Watershed, Quebec, Canada. *Canadian Journal of Forest Research* 31, 333-344.
- Duijsings, J.J.H.M., Verstraten, J.M. and Bouten, W. 1986. Spatial variability in nutrient deposition under an oak/beech canopy. *Zeitschrift für Pflanzenernährung und Bodenkunde* 149, 718-727.
- Durocher, M.G. 1990. Monitoring spatial variability of forest interception. *Hydrological Processes* 4, 215-229.
- Duyzer, J. and Fowler, D. 1994. Modelling land atmosphere exchange of gaseous oxides of nitrogen in Europe. *Tellus* 46B, 353-372.
- Erisman, J.W. 1993. Acid deposition to nature areas in the Netherlands: Part I. Methods and results. *Water, Air, and Soil Pollution* 71, 51-80.
- Erisman, J.W. and Draaijers, G. 2003. Deposition to forests in Europe: most important factors influencing dry deposition and models used for generalisation. *Environmental Pollution* 124, 379-388.
- Erisman, J.W. and Wyers, G.P. 1993. Continuous measurements of surface exchange of SO₂ and NH₃: implications for their possible interaction in the deposition process. *Atmospheric Environment* 27A, 1937-1949.
- Erisman, J.W., Draaijers, G.P.J., Mennen, M.G., Hogenkamp, J.E.M., van Putten, E., Uiterwijk, W., Kemker, E., Wiese, H., Duyzer, J.H., Otjes, R. and Wyers, G.P. 1996. Towards development of a deposition monitoring network for air pollution in Europe: deposition monitoring over the Speulder forest. Report no. 722108041, RIVM, the Netherlands.

References

- Erisman, J.W., Möls, H., Fonteijn, P., Geusebroek, M., Draaijers, G., Bleeker, A. and van der Veen, D. 2003. Field intercomparison of precipitation measurements performed within the framework of the Pan European Intensive Monitoring Program of EU/ICP Forests. *Environmental Pollution* 125, 139-155.
- Facelli, J.M. 1991. Plant litter: its dynamics and effects on plant community structure. *The Botanical Review* 57, 1-32.
- Ferm, M. and Hultberg, H. 1999. Dry deposition and internal circulation of nitrogen, sulphur and base cations to a coniferous forest. *Atmospheric Environment* 33, 4421-4430.
- Forgeard, F., Gloaguen, J.C. and Touffet, J. 1980. Interception des précipitations et apport au sol d'éléments minéraux par les eaux de pluie et les pluviollessivats dans une hêtraie atlantique et dans quelques peuplements résineux en Bretagne. *Annales des Sciences forestières* 37, 53-71.
- Frazer, G.W., Wulder, M.A. and Niemann, K.O. 2005. Simulation and quantification of the fine-scale spatial pattern and heterogeneity of forest canopy structure: a lacunarity-based method designed for analysis of continuous canopy heights. *Forest Ecology and Management* 214, 65-90.
- Freer-Smith, P.H., El-Khatib, A.A. and Taylor, G. 2004. Capture of particulate pollution by trees: a comparison of species typical of semi-arid areas with European and North American species. *Water, Air, and Soil Pollution* 155, 173-187.
- Gash, J.H.C. 1979. An analytical model of rainfall interception by forest. *Quarterly Journal of the Royal Meteorological Society* 105, 43-55.
- Gebauer, G., Zeller, B., Schmidt, G., May, C., Buchmann, N., Colin-Belgrand, M., Dambrine, E., Martin, F., Schulze, E.-D. and Bottner, P. 2000. The fate of ¹⁵N-labelled nitrogen inputs to coniferous and broadleaf forests. In: Schulze, E.-D. (ed.). *Carbon and nitrogen cycling in European forest ecosystems*. Springer-Verlag, Berlin, pp. 144-170.
- Gessler, A., Keitel, C., Nahm, M. and Rennenberg, H. 2004. Water shortage affects the water and nitrogen balance in central European beech forests. *Plant Biology* 6, 289-298.
- Gessler, A., Rienks, M. and Rennenberg, H. 2000. NH₃ and NO₂ fluxes between beech trees and the atmosphere - correlation with climatic and physiological parameters. *New Phytologist* 147, 539-560.
- Gessler, A., Rienks, M. and Rennenberg, H. 2002. Stomatal uptake and cuticular adsorption contribute to dry deposition of NH₃ and NO₂ to needles of adult spruce (*Picea abies*) trees. *New Phytologist* 156, 179-194.
- Gessler, A., Schneider, S., von Sengbusch, D., Weber, P., Hanemann, H.C., Rothe, A., Kreutzer, K. and Rennenberg, H. 1998. Field and laboratory experiments on net uptake of nitrate and ammonium by the roots of spruce (*Picea abies*) and beech (*Fagus sylvatica*) trees. *New Phytologist* 138, 275-285.
- Giacomin, A. and Trucchi, P. 1992. Rainfall interception in a beech coppice (Acquerino, Italy). *Journal of Hydrology* 137, 141-147.
- Golden Software. 1999. Surfer 7 - a program for contouring and 3D surface mapping for scientists and engineers. Golden, Colorado, U.S.A.
- Gómez, J.A., Vanderlinden, K., Giráldez, J.V. and Fereres, E. 2002. Rainfall concentration under olive trees. *Agricultural Water Management* 55, 53-70.
- Granier, A., Biron, P. and Lemoine, D. 2000. Water balance, transpiration and canopy conductance in two beech stands. *Agricultural and Forest Meteorology* 100, 291-308.
- Granier, A., Pilegaard, K. and Jensen, N.O. 2002. Similar net ecosystem exchange of beech stands located in France and Denmark. *Agricultural and Forest Meteorology* 114, 75-82.
- Hahn, K. and Fanta, J (eds.). 2001. Contemporary beech forest management in Europe. NAT-MAN Working report 1. Available at <http://www.flec.kvl.dk/natman>.
- Hamburg, S.P. and Lin, T.C. 1998. Throughfall chemistry of an ecotonal forest on the edge of the Great Plains. *Canadian Journal of Forest Research* 28, 1456-1463.

- Hansen, K. 1996. In-canopy throughfall measurements of ion fluxes in Norway spruce. *Atmospheric Environment* 30, 4065-4076.
- Hansen, K., Draaijers, G.P., Ivens, W.P.M.F., Gundersen, P. and van Leeuwen, N.F.M. 1994. Concentration variations in rain and canopy throughfall collected sequentially during individual rain events. *Atmospheric Environment* 28, 3195-3205.
- Hanson, P.J. and Lindberg, S.E. 1991. Dry deposition of reactive nitrogen compounds: a review of leaf, canopy, and non-foliar measurements. *Atmospheric Environment* 25A, 1615-1634.
- Harrison, A.F., Schulze, E.-D., Gebauer, G. and Bruckner, G. 2000. Canopy uptake and utilization of atmospheric pollutant nitrogen. In: Schulze, E.-D. (ed.). *Carbon and nitrogen cycling in European forest ecosystems*. Springer-Verlag, Berlin, pp. 172-188.
- Herbst, M. and Hörmann, G. 1998. Predicting effects of temperature increases on the water balance of beech forest - an application of the 'KAUSHA' model. *Climatic Change* 40, 683-698.
- Herbst, M., Eschenbach, C. and Kappen, L. 1999. Water use in neighbouring stands of beech (*Fagus sylvatica* L.) and black alder (*Alnus glutinosa* (L.) Gaertn.). *Annals of Forest Science* 56, 107-120.
- Herwitz, S.R. 1985. Interception storage capacities of tropical rainforest canopy trees. *Journal of Hydrology* 77, 237-252.
- Herwitz, S.R. 1987. Raindrop impact and water flow on the vegetative surfaces of trees and the effects on stemflow and throughfall concentrations. *Earth Surface Processes and Landforms* 12, 425-432.
- Herwitz, S.R. and Levia, D.F. 1997. Mid-winter stemflow drainage from bigtooth aspen (*Populus grandidentata* Michx.) in central Massachusetts. *Hydrological Processes* 11, 169-175.
- Herwitz, S.R. and Slye, R.E. 1995. Three-dimensional modeling of canopy tree interception of wind-driven rainfall. *Journal of Hydrology* 168, 205-226.
- Hicks, B.B., Baldocchi, D.D., Meyers, T.P., Hosker, R.P.Jr. and Matt, D.R. 1987. A preliminary multiple resistance routine for deriving dry deposition velocities from measured quantities. *Water, Air, and Soil Pollution* 36, 311-330.
- Holst, T., Hauser, S., Kirchgassner, A., Matzarakis, A., Mayer, H. and Schindler, D. 2004. Measuring and modelling plant area index in beech stands. *International Journal of Biometeorology* 48, 192-201.
- Hörmann, G., Branding, A., Clemen, T., Herbst, M., Hinrichs, A. and Thamm, F. 1996. Calculation and simulation of wind controlled canopy interception of a beech forest in northern Germany. *Agricultural and Forest Meteorology* 79, 131-148.
- Horst, T.W. and Weil, J.C. 1994. How far is far enough - the fetch requirements for micrometeorological measurements of surface fluxes. *Journal of Atmospheric and Oceanic Technology* 11, 1018-1025.
- Horváth, L. 2004. Determination of the nitrogen compound balance between the atmosphere and a Norway spruce forest ecosystem. *Nutrient Cycling in Agroecosystems* 70, 143-146.
- Houle, D., Ouimet, R., Paquin, R. and Laflamme, J.-G. 1999a. Determination of sample size for estimating ion throughfall deposition under a mixed hardwood forest at the Lake Clair Watershed (Duchesnay, Quebec). *Canadian Journal of Forest Research* 29, 1935-1943.
- Houle, D., Ouimet, R., Paquin, R. and Laflamme, J.-G. 1999b. Interactions of atmospheric deposition with a mixed hardwood and coniferous forest canopy at the Lake Clair Watershed (Duchesnay, Quebec). *Canadian Journal of Forest Research* 29, 1944-1957.
- Houston, T.J., Durrant, D.W. and Benham, S.E. 2002. Sampling in a variable environment: selection of representative positions of throughfall collectors for volume and chemistry under three tree species in the UK. *Forest Ecology and Management* 158, 1-8.
- Hovmand, M.F. and Kemp, K. 1996. Downward trends of sulphur deposition to Danish spruce forest. *Atmospheric Environment* 30, 2989-2999.

References

- Huber, A. and Iroumé, A. 2001. Variability of annual rainfall partitioning for different sites and forest covers in Chile. *Journal of Hydrology* 248, 78-92.
- Hug, R., Hepp, R. and von Wilpert, K. 2005. 18 Jahre Depositionsmessnetz der forstlichen Versuchs- und Forschungsanstalt Baden-Württemberg. *Berichte Freiburger Forstliche Forschung*. Heft 59. Freiburg, Germany.
- Hutchings, N.J., Milne, R. and Crowther, J.M. 1988. Canopy storage capacity and its vertical distribution in a Sitka spruce canopy. *Journal of Hydrology* 104, 161-171.
- Ignatova, N. and Dambrine, E. 2000. Canopy uptake of N deposition in spruce (*Picea abies* L. Karst) stands. *Annals of Forest Science* 57, 113-120.
- Iroumé, A. and Huber, A. 2002. Comparison of interception losses in a broadleaved native forest and a *Pseudotsuga menziesii* (Douglas fir) plantation in the Andes mountains of southern Chile. *Hydrological Processes* 16, 2347-2361.
- ISS-ISRIC-FAO. 1998. World reference base for soil resources. *World Soil Resources Report* 84. FAO.
- Janson, R. and Granat, L. 1999. A foliar rinse study of the dry deposition of nitric acid to a coniferous forest. *Agricultural and Forest Meteorology* 98-99, 683-696.
- Johnson, D.W. and Lindberg, S.E. (eds). 1992. *Atmospheric deposition and forest nutrient cycling*. Ecological studies 91. Springer-Verlag, New York.
- Joslin, J.D., Wolfe, M.H. and Hanson, P.J. 2000. Effects of altered water regimes on forest root systems. *New Phytologist* 147, 117-129.
- Keim, R.F. 2004. Comment on "Measurement and modelling of growing-season canopy water fluxes in a mature mixed deciduous forest stand, southern Ontario, Canada". *Agricultural and Forest Meteorology* 124, 277-279.
- Keim, R.F. and Skaugset, A.E. 2004. A linear system model of dynamic throughfall rates beneath forest canopies. *Water Resources Research* 40, Art. WO5208. doi: 10.1029/2003WR002875.
- Keim, R.F. and Skaugset, A.E. 2003. Modelling effects of forest canopies on slope stability. *Hydrological Processes* 17, 1457-1467.
- Keim, R.F., Skaugset, A.E. and Weiler, M. 2005. Temporal persistence of spatial patterns in throughfall. *Journal of Hydrology* 314, 263-274.
- Kimmins, J.P. 1973. Some statistical aspects of sampling throughfall precipitation in nutrient cycling studies in British Columbian coastal forests. *Ecology* 54, 1008-1019.
- Klaassen, W. 2001. Evaporation from rain-wetted forest in relation to canopy wetness, canopy cover, and net radiation. *Water Resources Research* 37, 3227-3236.
- Klaassen, W., Lankreijer, H.J.M. and Veen, A.W.L. 1996. Rainfall interception near a forest edge. *Journal of Hydrology* 185, 349-361.
- Kostelnik, K.M., Lynch, J.A., Grimm, J.W. and Corbett, E.S. 1989. Sample size requirements for estimation of throughfall chemistry beneath a mixed hardwood forest. *Journal of Environmental Quality* 18, 274-280.
- Kovács, E.A. and Horváth, L. 2004. Determination of sulfur balance between the atmosphere and a Norway spruce forest ecosystem: comparison of gradient dry + wet and throughfall deposition measurements. *Journal of Atmospheric Chemistry* 48, 235-240.
- Krupa, S.V. 2002. Sampling and physico-chemical analysis of precipitation: a review. *Environmental Pollution* 120, 565-594.
- Kulshrestha, U.C., Sarkar, A., Srivastava, R.M. and Parashar, D.C. 1995. Wet-only and bulk deposition studies at New Delhi (India). *Water, Air, and Soil Pollution* 85, 2137-2142.
- Langusch, J.J., Borken, W., Armbuster, M., Dise, N.B. and Matzner, E. 2003. Canopy leaching of cations in Central European forest ecosystems - a regional assessment. *Journal of Plant Nutrition and Soil Science* 166, 168-174.
- Lawrence, G.B. and Fernandez, I.J. 1993. A reassessment of areal variability of throughfall deposition measurements. *Ecological Applications* 3, 473-480.

- Lebourgeois, F., Bréda, N., Ulrich, E. and Granier, A. 2005. Climate-tree-growth relationships of European beech (*Fagus sylvatica* L.) in the French permanent plot network (RENECOFOR). *Trees - Structure and Function* 19, 385-401.
- Lee, D.S. and Longhurst, A. 1992. A comparison between wet and bulk deposition at an urban site in the UK. *Water, Air, and Soil Pollution* 64, 635-648.
- Leuzinger, S., Zotz, G., Asshof, R. and Korner, C. 2005. Responses of deciduous forest trees to severe drought in Central Europe. *Tree Physiology* 25, 641-650.
- Levia, D.F. 2003. Winter stemflow nutrient inputs into a southern New England broadleaved deciduous forest. *Geografiska Annaler Series - Physical Geography* 85A, 13-23.
- Levia, D.F. and Frost, E.E. 2003. A review and evaluation of stemflow literature in the hydrologic and biogeochemical cycles of forested and agricultural ecosystems. *Journal of Hydrology* 274, 1-29.
- Levia, D.F. and Herwitz, S.R. 2000. Physical properties of water in relation to stemflow leachate dynamics: implications for nutrient cycling. *Canadian Journal of Forest Research* 30, 662-666.
- Levia, D.F. and Herwitz, S.R. 2002. Winter chemical leaching from deciduous tree branches as a function of branch inclination angle in central Massachusetts. *Hydrological Processes* 16, 2867-2879.
- Levia, D.F. and Underwood, S.J. 2004. Snowmelt induced stemflow in northern hardwood forests: a theoretical explanation on the causation of a neglected hydrological process. *Advances in Water Resources* 2, 121-128.
- Likens, G.E., Driscoll, C.T., Buso, C.T., Mitchell, M.J., Lovett, G.M., Bailey, S.W., Siccawa, T.G., Reiners, W.A. and Alewell, C. 2002. The biogeochemistry of sulfur at Hubbard Brook. *Biogeochemistry* 60, 235-316.
- Lin, T.-C., Hamburg, S., Hsia, Y.-J., King, H.-B., Wang, L.J. and Lin, K.C. 2001. Base cation leaching from the canopy of a subtropical rainforest in northeastern Taiwan. *Canadian Journal of Forest Research* 31, 1156-1163.
- Lin, T.-C., Hamburg, S.P. and King, H.-B. 2000. Throughfall patterns in a subtropical rain forest of northeastern Taiwan. *Journal of Environmental Quality* 29, 1186-1193.
- Lin, T.-C., Hamburg, S.P., King, H.-B. and Hsia, Y.-J. 1997. Spatial variability of throughfall in a subtropical rain forest in Taiwan. *Journal of Environmental Quality* 26, 172-180.
- Lindberg, S.E. and Garten, C.T. 1988. Sources of sulphur in forest canopy throughfall. *Nature* 336, 148-151.
- Link, T.E., Unsworth, M. and Marks, D. 2004. The dynamics of rainfall interception by a seasonal temperate rainforest. *Agricultural and Forest Meteorology* 124, 171-191.
- Liu, S. 1997. A new model for the prediction of rainfall interception in forest canopies. *Ecological Modelling* 99, 151-159.
- Llorens, P. and Gallart, F. 2000. A simplified method for forest water storage capacity measurement. *Journal of Hydrology* 240, 131-144.
- Llorens, P., Poch, R., Latron, J. and Gallart, F. 1997. Rainfall interception by a *Pinus sylvestris* forest patch overgrown in a Mediterranean mountainous abandoned area I. Monitoring design and results down to the event scale. *Journal of Hydrology* 199, 331-345.
- Lloyd, C.R. and Marques, F.A. de O. 1988. Spatial variability of throughfall and stemflow measurements in Amazonian rainforest. *Agricultural and Forest Meteorology* 42, 63-73.
- Lloyd, C.R., Gash, J.H.C. and Shuttleworth, W.J. 1988. The measurement and modelling of rainfall interception by Amazonian rain forest. *Agricultural and Forest Meteorology* 43, 277-294.
- Loescher, H.W., Powers, J.S. and Oberbauer, S.F. 2002. Spatial variation of throughfall volume in an old-growth tropical wet forest, Costa Rica. *Journal of Tropical Ecology* 18, 397-407.
- Loustau, D., Berbigier, P., Granier, A. and Moussa, F.E. 1992. Interception loss, throughfall and stemflow in a maritime pine stand. I. Variability of throughfall and stemflow beneath the pine canopy. *Journal of Hydrology* 138, 449-467.

References

- Lovett, G.M. and Lindberg, S.E. 1984. Dry deposition and canopy exchange in a mixed oak forest as determined by analysis of throughfall. *Journal of Applied Ecology* 21, 1013-1027.
- Lovett, G.M. and Lindberg, S.E. 1992. Concentration and deposition of particles and vapors in a vertical profile through a forest canopy. *Atmospheric Environment* 26A, 1469-1476.
- Lovett, G.M. and Lindberg, S.E. 1993. Atmospheric deposition and canopy interactions of nitrogen in forests. *Canadian Journal of Forest Research* 23, 1603-1616.
- Lovett, G.M., Nolan, S.S., Driscoll, C.T. and Fahey, T.J. 1996. Factors regulating throughfall flux in a New Hampshire forested landscape. *Canadian Journal of Forest Research* 26, 2134-2144.
- Lovett, G.M., Reiners, W.A. and Olson, R.K. 1982. Cloud droplet deposition in subalpine balsam fir forests: hydrological and chemical inputs. *Science* 218, 1303-1304.
- Lovett, G.M., Reiners, W.A. and Olson, R.K. 1989. Factors controlling throughfall chemistry in a balsam fir canopy - a modelling approach. *Biogeochemistry* 8, 239-264.
- Lumme, I. 1994. Nitrogen uptake of Norway spruce (*Picea abies* Karst.) seedlings from simulated wet deposition. *Forest Ecology and Management* 63, 87-96.
- Macklon, A.E.S., Sheppard, L.J., Sim, S. and Leith, I.D. 1996. Uptake of ammonium and nitrate ions from acid mist applied to Sitka spruce (*Picea sitchensis* (Bong.) Carr.) grafts over the course of one growing season. *Trees - Structure and Function* 10, 261-267.
- Manderscheid, B. and Matzner, E. 1995. Spatial and temporal variation of soil solution chemistry and ion fluxes through the soil in a mature Norway spruce (*Picea abies* (L.) Karst) stand. *Biogeochemistry* 30, 99-114.
- Marin, C.T., Bouten, W. and Sevink, J. 2000. Gross rainfall and its partitioning into throughfall, stemflow and evaporation of intercepted water in four forest ecosystems in western Amazonia. *Journal of Hydrology* 237, 40-57.
- Marschner, H. 1995. Mineral nutrition of higher plants. 2nd edition. Academic Press, San Diego.
- Matschonat, G. and Falkengren-Grerup, U. 2000. Recovery of soil pH, cation exchange capacity and the saturation of exchange sites from stemflow induced soil acidification in three Swedish beech (*Fagus sylvatica* L.) forests. *Scandinavian Journal of Forest Research* 15, 39-48.
- Mayer, R. and Ulrich, B. 1978. Input of atmospheric sulphur by dry and wet deposition to two central European forest ecosystems. *Atmospheric Environment* 12, 375-377.
- Meiwes, K.J. and Khanna, P.K. 1981. Distribution and cycling of sulphur in the vegetation of two forest ecosystems in an acid rain environment. *Plant and Soil* 60, 369-375.
- Michopoulos, P., Baloutsos, G., Nakos, G. and Economou, A. 2001. Effects of bulk precipitation pH and growth period on cation enrichment in precipitation beneath the canopy of a beech (*Fagus moesiaca*) forest stand. *Environmental Pollution* 281, 79-85.
- Monteith, J.L. 1965. Evaporation and environment. In: Fogg, G.F. (ed.). *The state and movement of water in living organisms*, 19th Symposium of the Society for Experimental Biology. Cambridge University Press, London, pp. 205-234.
- Morris, D.M., Gordon, A.G. and Gordon, A.M. 2003. Patterns of canopy interception and throughfall along a topographic sequence for black spruce dominated forest ecosystems in northwestern Ontario. *Canadian Journal of Forest Research* 33, 1046-1060.
- Mosello, R., Marchetto, A. and Tartari, G.A. 1988. Bulk and wet atmospheric deposition chemistry at Pallanza (N. Italy). *Water, Air, and Soil Pollution* 42, 137-151.
- Mussche, S., Samson, R., Nachtergale, L., De Schrijver, A., Lemeur, R. and Lust, N. 2001. A comparison of optical and direct methods for monitoring the seasonal dynamics of leaf area index in deciduous forests. *Silva Fennica* 35, 373-384.
- Nadkarni, N.M. and Sumera, M.M. 2004. Old-growth forest canopy structure and its relationship to throughfall interception. *Forest Science* 50, 290-298.
- Neal, C., Robson, A.J., Bhardwaj, C.L., Conway, T., Jeffery, H.A., Neal, M., Ryland, G.P., Smith, C.J. and Walls, J. 1993. Relationships between precipitation, stemflow and throughfall for a lowland

- beech plantation, Black Wood, Hampshire, southern England: findings on interception at a forest edge and the effects of storm damage. *Journal of Hydrology* 146, 221-233.
- Neary, A.J. and Gizyn, W.I. 1994. Throughfall and stemflow chemistry under deciduous and coniferous forest canopies in South-central Ontario. *Canadian Journal of Forest Research* 24, 1089-1100.
- Neiryneck, J., Genouw, G., Coenen, S. and Roskams, P. 2004. Depositie en luchtkwaliteit in Vlaamse bosgebieden [in Dutch with English summary]. Report IBW 2004-1. Institute for Forestry and Game Management, Geraardsbergen, Belgium.
- Neiryneck, J., Kowalski, A. S., Carrara, A., Berghmans, P., Genouw, G. and Ceulemans, R. Fluxes of oxidised and reduced nitrogen above a mixed coniferous forest exposed to various nitrogen emission sources. *Environmental Pollution*, submitted.
- Neter, J., Kutner, M.H., Nachtsheim, C.J. and Wasserman, W. 1996. *Applied linear statistical models*. WCB McGraw-Hill, Boston, Massachusetts.
- Oyarzun, C.E., Godoy, R., De Schrijver, A., Staelens, J. and Lust, N. 2004. Water chemistry and nutrient budgets in an undisturbed evergreen rainforest of southern Chile. *Biogeochemistry* 71, 107-123.
- Özyuvaci, N., Ozhan, S., Gokbulak, F., Serengil, Y. and Balci, A.N. 2004. Effect of selective cutting on streamflow in an oak-beech forest ecosystem. *Water Resources Management* 18, 249-262.
- Papen, H., Gessler, A., Zumbusch, E. and Rennenberg, H. 2002. Chemolithoautotrophic nitrifiers in the phyllosphere of a spruce ecosystem receiving high atmospheric nitrogen input. *Current Microbiology* 44, 56-60.
- Parker, G.G. 1983. Throughfall and stemflow in the forest nutrient cycle. *Advances in Ecological Research* 13, 57-133.
- Peck, A. and Mayer, H. 1996. Einfluss von Bestandesparametern auf die Verdunstung von Wäldern. *Forstwissenschaftliches Centralblatt* 115, 1-9.
- Pérez-Soba, M. and van der Eerden, L.J.M. 1993. Nitrogen uptake in needles of Scots pine (*Pinus sylvestris* L.) when exposed to gaseous ammonia and ammonium fertilizer in the soil. *Plant and Soil* 153, 231-242.
- Peterson, D.L. and Rolfe, G.L. 1979. Determining sample size in throughfall studies. *Forest Science* 25, 582-584.
- Potter, C.S., Ragsdale, H.L. and Swank, W.T. 1991. Atmospheric deposition and foliar leaching in a regenerating southern appalachian forest canopy. *Journal of Ecology* 79, 97-115.
- Powell, T.L., Starr, G., Clark, K.L., Martin, T.A. and Gholz, H.L. 2005. Ecosystem and understory water and energy exchange for a mature, naturally regenerated pine flatwoods forest in north Florida. *Canadian Journal of Forest Research* 35, 1568-1580.
- Price, A.G. and Carlyle-Moses, D.E. 2003. Measurement and modelling of growing-season canopy water fluxes in a mature mixed deciduous forest stand, northern Ontario, Canada. *Agricultural and Forest Meteorology* 119, 69-85.
- Pryor, S.C. and Barthelmie, R.J. 2005. Liquid and chemical fluxes in precipitation, throughfall and stemflow: observations from a deciduous forest and a red pine plantation in the midwestern U.S.A. *Water, Air, and Soil Pollution* 163, 203-227.
- Puckett, L.J. 1990. Estimates of ion sources in deciduous and coniferous throughfall. *Atmospheric Environment* 24A, 545-555.
- Puckett, L.J. 1991. Spatial variability and collector requirements for sampling throughfall volume and chemistry under a mixed-hardwood canopy. *Canadian Journal of Forest Research* 21, 1581-1588.
- Puxbaum, H. and Gregori, M. 1998. Seasonal and annual deposition rates of sulphur, nitrogen and chloride species to an oak forest in North-Eastern Austria (Wolkersdorf, 240 m asl). *Atmospheric Environment* 32, 3557-3568.

References

- Pypker, T.G., Bond, B.J., Link, T.E., Marks, D. and Unsworth, M.H. 2005. The importance of canopy structure in controlling the interception loss of rainfall: examples from a young and an old-growth Douglas-fir forest. *Agricultural and Forest Meteorology* 130, 113-129.
- Queveauviller, Ph., Van Renterghem, D., Griepink, B., Reijnders, H.F.R. and Van Der Jagt, H. The certification of the contents of ammonium, calcium, chloride, hydronium, magnesium, nitrate, potassium, sodium and sulphate in simulated rainwater. Low content (CRM 408), high content (CRM 409). Final Report EUR 15024 EN. Commission of the European Communities, Community Bureau of Reference, Luxembourg.
- Quilchano, C., Haneklaus, S., Gallardo, J.F., Schnug, E. and Moreno, G. 2002. Sulphur balance in a broadleaf, non-polluted forest ecosystem (central-western Spain). *Forest Ecology and Management* 161, 205-214.
- Raat, K.J., Draaijers, G.P.J., Schaap, M.G., Tietema, A. and Verstraten, J.M. 2002. Spatial variability of throughfall water and chemistry and forest floor water content in a Douglas fir forest stand. *Hydrology and Earth System Sciences* 6, 363-374.
- Rampazzo N. and Blum, W. 1992. Changes in chemistry and mineralogy of forest soils by acid rain. *Water, Air, and Soil Pollution* 61, 209-220.
- Ranalli, A.J., Turk, J.T. and Campbell, D.H. 1997. The use of bulk collectors in monitoring wet deposition at high-altitude sites in winter. *Water, Air, and Soil Pollution* 95, 237-255.
- Rao, P.S., Gavane, A.G., Ankam, S.S., Ansari, M.F., Pandit, V.I. and Nema, P. 2004. Performance evaluation of a green belt in a petroleum refinery: a case study. *Ecological Engineering* 23, 77-84.
- Reiners, W.A. and Olson, R.K. 1984. Effects of canopy components on throughfall chemistry: an experimental analysis. *Oecologia* 63, 320-330.
- Rennenberg, H., Seiler, W., Mayssek, R., Gessler, A. and Kreuzwieser, J. 2004. European beech (*Fagus sylvatica* L.) - a forest tree without future in the south of Central Europe? *Allgemeine Forst- Und Jagdzeitung* 175, 210-224.
- Rennenberg, H., Kreutzer, K., Papen, H. and Weber, P. 1998. Consequences of high loads of nitrogen for spruce (*Picea abies*) and beech (*Fagus sylvatica*) forests. *New Phytologist* 139, 71-86.
- Richter, D.D. and Lindberg, S.E. 1988. Wet deposition estimates from long-term bulk and event wet-only samples of incident precipitation and throughfall. *Journal of Environmental Quality* 17, 619-622.
- Robson, A.J., Neal, C., Ryland, G.P. and Harrow, M. 1994. Spatial variations in throughfall chemistry at the small plot scale. *Journal of Hydrology* 158, 107-122.
- Rodrigo, A. and Avila, A. 2001. Influence of sampling size in the estimation of mean throughfall in two Mediterranean holm oak. *Journal of Hydrology* 243, 216-227.
- Roelofs, J.G.M., Kempers, A.J., Houdijk, A.L.F.M. and Jansen, J. 1985. The effect of air-borne ammonium sulphate on *Pinus nigra* var. *maritima* in the Netherlands. *Plant and Soil* 84, 45-56.
- Rothe, A. and Binkley, D. 2001. Nutritional interactions in mixed species forests: a synthesis. *Canadian Journal of Forest Research* 31, 1855-1870.
- Ruijgrok, W., Tieben, H. and Eisinga, P. 1997. The dry deposition of particles to a forest canopy : a comparison of model and experimental results. *Atmospheric Environment* 31, 399-415.
- Russel, G., Marshall, G. and Jarvis, P.G. 1989. Plant canopies: their growth, form and function. Society for Experimental Biology, Seminar Series 31. Cambridge University Press, Cambridge.
- Rustad, L.E., Kahl, J.S., Norton, S.A. and Fernandez, I.J. 1994. Underestimation of dry deposition by throughfall in mixed northern hardwood forests. *Journal of Hydrology* 162, 319-336.
- Rutter, A.J., Kershaw, K.A., Robins, P.S. and Morton, A.J. 1971. A predictive model of rainfall interception in forests. I. Derivation of the model from observations in a plantation of Corsican pine. *Agricultural and Forest Meteorology* 9, 367-384.

- Rutter, A.J. and Morton, A.J. 1977. A predictive model of rainfall interception in forests. III. Sensitivity of the model to stand parameters and meteorological variables. *Journal of Applied Ecology* 14, 567-588.
- Rutter, A.J., Morton, A.J. and Robins, P.S. 1975. A predictive model of rainfall interception in forests. II. Generalization of the model and comparisons with observations in some coniferous and hardwood stands. *Journal of Applied Ecology* 12, 367-380.
- Sah, S.P. 1990. Vergleich des Stoffhaushaltes zweier Buchenwaldökosysteme auf Kalkgestein und auf Buntsandstein. *Berichte Forschung Waldökosysteme/Walsterben Universität Göttingen, Reihe A* 59, 1-140.
- Samson, R. and Lemeur, R. 2001. Energy balance storage terms and big-leaf evapotranspiration in a mixed deciduous forest. *Annals of Forest Science* 58, 529-541.
- Schaap, M.G., Bouten, W. and Verstraten, J.M. 1997. Forest floor water content dynamics in a Douglas fir stand. *Journal of Hydrology* 201, 367-383.
- Schaefer, D.A., Lindberg, S.E. and Lovett, G.M. 1992. Processing of acidic deposition: canopy interactions. In: Johnson, D.W. and Lindberg, S.E. (eds.). *Atmospheric deposition and forest nutrient cycling*. Ecological studies 91. Springer-Verlag, New York, pp. 444-449.
- Schaefer, D.A., Reiners, W.A. and Olson, R.K. 1988. Factors controlling the chemical alteration of throughfall in a subalpine balsam fir canopy. *Environmental and Experimental Botany* 28, 175-189.
- Schafer, K.V.R., Oren, R., Lai, C.T. and Katul, G.G. 2002. Hydrologic balance in an intact temperate forest ecosystem under ambient and elevated atmospheric CO₂ concentration. *Global Change Biology* 8, 895-911.
- Schmitt, M., Thöni, L., Waldner, P. and Thimonier, A. 2005. Total deposition of nitrogen on Swiss long-term forest ecosystem research (LWF) plots: comparison of the throughfall and the inferential method. *Atmospheric Environment* 39, 1079-1091.
- Schulze, E.-D. 1989. Air pollution and forest decline in spruce (*Picea abies*) forest. *Science* 244, 776-783.
- Schume, H., Jost, G. and Hager, H. 2004. Soil water depletion and recharge patterns in mixed and pure forest stands of European beech and Norway spruce. *Journal of Hydrology* 289, 258-274.
- Schume, H., Jost, G. and Katzensteiner, K. 2003. Spatio-temporal analysis of the soil water content in a mixed Norway spruce (*Picea abies* (L.) Karst.) - European beech (*Fagus sylvatica* L.) stand. *Geoderma* 112, 273-287.
- Seiler, J. and Matzner, E. 1995. Spatial variability of throughfall chemistry and selected soil properties as influenced by stem distance in a mature Norway spruce (*Picea abies* (L.) Karst.) stand. *Plant and Soil* 176, 139-147.
- Shuttleworth, W.J. 1989. Micrometeorology of temperate and tropical forest. *Philosophical Transactions of the Royal Society of London B* 324, 299-334.
- Sievering, H., Fernandez, I. and Lee, J. 2000. Forest canopy uptake of atmospheric nitrogen deposition at eastern US conifer sites: carbon storage implications? *Global Biogeochemical Cycles* 14, 1153-1159.
- Smith, W.H. 1981. *Air pollution and forests: interaction between air contaminants and forest ecosystems*. Springer-Verlag, New York.
- Smith, R.I., Fowler, D., Sutton, M.A., Flechard, C. and Coyle, M. 2000. Regional estimation of pollutant gas dry deposition in the UK: model description, sensitivity analysis and outputs. *Atmospheric Environment* 34, 3757-3777.
- SPSS Inc. 2003. *SPSS for Windows, Release 12.0.0*. Chicago, Illinois, U.S.A.
- Staaf, H. 1982. Plant nutrient changes in beech leaves during senescence as influenced by site characteristics. *Acta Oecologia* 3, 161-170.

References

- Stachurski, A. and Zimka, J.R. 2000. Atmospheric input of elements to forest ecosystems: a method of estimation using artificial foliage placed above rain collectors. *Environmental Pollution* 110, 345-356.
- Stachurski, A. and Zimka, J.R. 2002. Atmospheric deposition and ionic interactions within a beech canopy in the Karkonosze Mountains. *Environmental Pollution* 118, 75-87.
- Stadler, B., Müller, T., Orwig, D. and Cobb, R. 2005. Hemlock woolly adelgid in New England forests: canopy impacts transforming ecosystem processes and landscapes. *Ecosystems* 8, 233-247.
- Stadler, B., Sollinger, S. and Michalzik, B. 2001. Insect herbivores and the nutrient flow from the canopy to the soil in coniferous and deciduous forests. *Oecologia* 126, 104-113.
- Staelens, J., Nachtergale, L. and Luysaert, S. 2004. Predicting the spatial distribution of leaf litterfall in a mixed deciduous forest. *Forest Science* 50, 836-847.
- Stedman, J.R., Heyes, C.J. and Irwin, J.G. 1990. A comparison of bulk and wet-only precipitation collectors at rural sites in the United Kingdom. *Water, Air, and Soil Pollution* 52, 377-395.
- Swaans, W. and Aerts, W. 2004. Analyses van passieve samplers. Eindverslag. VITO report no. 2004/MIM/R/13. Flemish Institute for Technological Research, Mol, Belgium.
- Tanner, P.A. 1999. Analysis of Hong Kong daily bulk and wet deposition data from 1994 to 1995. *Atmospheric Environment* 33, 1757-1766.
- Teklehaimanot, Z. and Jarvis, P.G. 1991. Direct measurement of evaporation of intercepted water from forest canopies. *Journal of Applied Ecology* 28, 603-618.
- Thimonier, A. 1998. Measurement of atmospheric deposition under forest canopies: some recommendations for equipment and sampling design. *Environmental Monitoring and Assessment* 52, 353-387.
- Thimonier, A., Schmitt, M., Waldner, P. and Rihm, B. 2005. Atmospheric deposition on Swiss long-term forest ecosystem research (LWF) plots. *Environmental Monitoring and Assessment* 104, 81-188.
- Tukey, H.B. 1970. The leaching of substances from plants. *Annual Review of Plant Physiology* 21, 305-324.
- Ukonmaanaho, L. and Star, M. 2002. Major nutrients and acidity: budgets and trends at four remote boreal stands in Finland during the 1990s. *Science of the Total Environment* 297, 21-41.
- Ulrich, B. 1983. Interaction of forest canopies with atmospheric constituents: SO₂, alkali and earth alkali cations and chloride. In: Ulrich, B. and Pankrath, J. (eds.). *Effects of accumulation of air pollutants in forest ecosystems*. Reidel Publishing Company, Dordrecht, pp. 33-45.
- Ulrich, B. and Pankrath, J. (eds.). 1983. *Effects of accumulation of air pollutants in forest ecosystems*. Reidel Publishing Company, Dordrecht.
- UN/ECE. 2003. *The condition of forests in Europe. Executive report 2003*. United Nations Economic Commission for Europe, Geneva.
- UN/ECE. 2004. *Manual on methods and criteria for harmonised sampling, assessment, monitoring and analysis of the effects of air pollution on forests*. International Co-operative Programme on Assessment and Monitoring of Air Pollution Effects on Forests (ICP Forests). Federal Research Centre for Forestry and Forest Products (BFH), Hamburg, Germany. Available at <http://www.icp-forests.org>.
- Vachaud, G., Silans, A.P.D., Balabanis, P. and Vauclin, M. 1985. Temporal stability of spatially measured soil water probability density function. *Soil Science Society of America Journal* 49, 822-828.
- van Breemen, N., Burrough, P.A., Velthorst, E.J., van Dobben, H.F., de Wit, T., Ridder, T.B. and Reijnders, H.F.R. 1982. Soil acidification from atmospheric ammonium sulphate in forest canopy throughfall. *Nature* 299, 548-550.
- Van der Maas, M.P., van Breemen, N. and Van Langenvelde, I. 1991. Estimation of atmospheric deposition and canopy exchange in two Douglas forest stands in the Netherlands. Internal

- publication. Department of Soil Science and Geology, Agricultural University of Wageningen, the Netherlands,
- Vande Walle, I., Mussche, S., Schauvliege, M., Lemeur, R. and Lust, N. 1998. Inventaris proefbos Aelmoeseneie (Gontrode) 1997. Internal publication. Laboratory of Plant Ecology and Laboratory of Forestry, Ghent University, Belgium.
- Vande Walle, I., Van Camp, N., Perrin, D., Lemeur, R., Verheyen, K., Van Wesemael, B. and Laitat, E. 2005. Growing stock-based assessment of the carbon stock in the Belgian forest biomass. *Annals of Forest Science* 62, 853-864.
- Van Ek, R. and Draaijers, G.P.J. 1994. Estimates of atmospheric deposition and canopy exchange for three common tree species in the Netherlands. *Water, Air, and Soil Pollution* 73, 61-82.
- Van Leeuwen, E.P., Hendriks, K.C.M.A., Klap, J.M., de Vries, W., De Jong, E. and Erisman, J.W. 2000. Effects of environmental stress on forest crown condition in Europe. Part II: Estimation of stress induced by meteorology and air pollutants. *Water, Air, and Soil Pollution* 119, 335-362.
- Vermeulen, A.T., Wyers, G.P., Römer, F.G., Van Leeuwen, N.F.M., Draaijers, G.P.J. and Erisman, J.W. 1997. Fog deposition on a coniferous forest in the Netherlands. *Atmospheric Environment* 31, 375-386.
- VMM. 2002. 'Zure regen' in Vlaanderen. Depositie meetnet verzuring 2001. Flemish Environment Agency, Erembodegem, Belgium.
- VMM. 2004. Luchtkwaliteit in het Vlaamse Gewest. Jaarverslag immissiemeetnetten, kalenderjaar 2003 en meteorologisch jaar 2003-2004. Flemish Environment Agency, Erembodegem, Belgium.
- Vrugt, J.A., Dekker, S.C. and Bouten, W. 2003. Identification of rainfall interception model parameters from measurements of throughfall and forest canopy storage. *Water Resources Research* 39, Art. 9, 1251, doi: 10.1029/2003WR002013.
- Walker, J.T., Whittall, D.R., Robarge, W. and Paerl, H.W. 2004. Ambient ammonia and ammonium aerosol across a region of variable ammonia emission density. *Atmospheric Environment* 38, 1235-1246.
- Waterinckx, M. and Roelandt, B. 2001. De bosinventaris van het Vlaamse Gewest. Ministerie van de Vlaamse Gemeenschap, Afdeling Bos en Groen, Brussels, Belgium.
- Weihe, J. 1984. Benetzung und Interzeption von Buchen- und Fichtenbeständen. V. Die Verteilung des Regens unter Buchenkronen. *Allgemeine Forst- und Jagdzeitung* 156, 81-89.
- Weltzin, J.F., Loik, M.E., Schwinning, S., Williams, D.G., Fay, P.A., Haddad, B.M., Harte, J., Huxman, T.E., Knapp, A.K., Lin, G.H., Pockman, W.T., Shaw, M.R., Small, E.E., Smith, M.D., Smith, S.D., Tissue, D.T. and Zak, J.C. 2003. Assessing the response of terrestrial ecosystems to potential changes in precipitation. *BioScience* 53, 941-952.
- Wesely, M.L. 1989. Parameterization of surface resistances to gaseous dry deposition in regional-scale numerical models. *Atmospheric Environment* 23, 1293-1304.
- Wesely, M.L. and Hicks, B.B. 2000. A review of the current status of knowledge on dry deposition. *Atmospheric Environment* 34, 2261-2282.
- Whelan, M.J. and Anderson, J.M. 1996. Modelling spatial patterns of throughfall and interception loss in a Norway spruce (*Picea abies*) plantation at the plot scale. *Journal of Hydrology* 186, 335-354.
- Whelan, M.J., Sanger, L.J., Baker, M. and Anderson, J.M. 1998. Spatial patterns of throughfall and mineral ion deposition in a lowland Norway spruce (*Picea abies*) plantation at the plot scale. *Atmospheric Environment* 32, 3493-3501.
- White, E.J. and Turner, F. 1970. A method of estimating income of nutrients in a catch of airborne particles by a woodland canopy. *Journal of Applied Ecology* 4, 441-461.
- Wilson, E.J. and Tiley, C. 1998. Foliar uptake of wet-deposited nitrogen by Norway spruce: an experiment using ¹⁵N. *Atmospheric Environment* 32, 513-518.

References

- Wyers, G.P. and Duyzer, J.H. 1997. Micrometeorological measurement of the dry deposition flux of sulphate and nitrate aerosols to coniferous forest. *Atmospheric Environment* 31, 333-343.
- Xiao, Q., McPherson, E.G., Ustin, S.L. and Grismer, M.E. 2000a. A new approach to modeling tree rainfall interception. *Journal of Geophysical Research* 105, 173-187.
- Xiao, Q., McPherson, E.G., Ustin, S.L., Grismer, M.E. and Simpson, J.R. 2000b. Winter rainfall interception by two mature open-grown trees in Davis, California. *Hydrological Processes* 14, 763-784.
- Yang, J., McBride, J., Zhou, J. and Sun, Z. 2005. The urban forest in Beijing and its role in air pollution reduction. *Urban Forestry and Urban Greening* 3, 65-78.
- Yoshida, S. and Ichikuni, M. 1989. Role of forest canopies in the collection and neutralization of airborne acid substances. *Science of the Total Environment* 84, 35-43.
- Zeng, G.M., Zhang, G., Huang, G.H., Jiang, Y.M. and Liu, H.L. 2005. Exchange of Ca^{2+} , Mg^{2+} and K^+ and uptake of H^+ , NH_4^+ for the subtropical forest canopies influenced by acid rain in Shaoshan forest located in Central South China. *Plant Science* 168, 259-266.
- Zeng, N., Shuttleworth, J.W. and Gash, J.H.C. 2000. Influence of temporal variability of rainfall on interception loss. Part I. Point analysis. *Journal of Hydrology* 228, 228-241.
- Zhang, L., Moran, M.D., Makar, P.A., Brook, J.R. and Gong, S. 2002. Modelling gaseous dry deposition in AURAMS: a unified regional air-quality modelling system. *Atmospheric Environment* 36, 537-560.
- Zimmermann, L. and Zimmermann, F. 2002. Fog deposition to Norway spruce stands at high-elevation sites in the Eastern Erzgebirge (Germany). *Journal of Hydrology* 256, 166-175.
- Zimmermann, S., Braun, S., Conedera, M. and Blaser, P. 2002. Macronutrient inputs by litterfall as opposed to atmospheric deposition into two contrasting chestnut forest stands in southern Switzerland. *Forest Ecology and Management* 161, 289-302.
- Zirlewagen, D. and von Wilpert, K. 2001. Modeling water and ion fluxes in a highly structured, mixed-species stand. *Forest Ecology and Management* 143, 27-37.

Curriculum vitae

Personal data

Name Jeroen Staelens
Date of birth 11 February 1978
Place of birth Brugge
Nationality Belgian
Address Francisco Ferrerlaan 81, 9000 Gent, Belgium
Phone +32 474 75 87 05
E-mail jeroen_staelens@yahoo.com

Education

2001 - 2004 Ph.D. training in Applied Biological Sciences, Faculty of Bioscience Engineering, Ghent University
1996 - 2001 M.Sc. in Bioscience engineering, Faculty of Bioscience Engineering, Ghent University
1990 - 1996 Secondary school (Greek-Mathematics), Onze-Lieve-Vrouwecollege, Assebroek

Professional experience

August 2005 - present Scientific worker at the Research Institute for Nature and Forest (INBO), Geraardsbergen
2001 - 2005 Ph.D. research at the Department of Forest and Water Management, Faculty of Bioscience Engineering, Ghent University

Scientific publications

Publications in international journals with peer review cited in the Science Citation Index (IF: impact factor in 2004)

- Staelens, J., De Schrijver, A., Neiryneck, J. and Verheyen, K. Quantifying atmospheric deposition onto a deciduous forest canopy using varying forms of the canopy budget method and an inferential technique. *Water, Air, and Soil Pollution*, to be submitted. (IF: 1.058)
- De Schrijver, A., Geudens, G., Staelens, J., Mertens, J. and Verheyen, K. A meta-analysis of forest type effects on element deposition and leaching. *Ecosystems*, submitted. (IF: 3.283)

References

- Staelens, J., De Schrijver, A. and Verheyen, K. Seasonal variation in throughfall and stemflow chemistry beneath a beech (*Fagus sylvatica* L.) tree in relation to canopy phenology. Canadian Journal of Forest Research, submitted. (IF: 1.466)
- Van Camp, N., Biesemans, J., Staelens, J., Verdonck, F.A.M., Vande Walle, I. and Verheyen, K. Quantifying uncertainty and sample size dependency of forest inventory derived statistics by stochastic resampling. Canadian Journal of Forest Research, submitted. (IF: 1.466)
- Staelens, J., De Schrijver, A., Verheyen, K. and Verhoest, N.E.C. Spatial variability and temporal stability of throughfall water amount under a mature beech (*Fagus sylvatica* L.) tree in relationship to canopy structure. Journal of Hydrology, moderate revisions. (IF: 1.481)
- Staelens, J., De Schrijver, A., Verheyen, K. and Verhoest, N.E.C. Rainfall partitioning into throughfall, stemflow, and interception within a single beech (*Fagus sylvatica* L.) canopy: influence of foliation, rain event characteristics, and meteorology. Hydrological Processes, accepted with minor revisions. (IF: 1.457)
- De Schrijver, A., Mertens, J., Geudens, G., Staelens, J., Campforts E., Luysaert S., De Temmerman L., De Keersmaeker L., De Neve S. and Verheyen, K. Acidification of forested podzols in North Belgium during the period 1950-2000. Science of the Total Environment, in press. (IF: 1.952)
- Staelens, J., De Schrijver, Verheyen, K. and Verhoest, N.E.C. Spatial variability and temporal stability of throughfall deposition under beech (*Fagus sylvatica* L.) in relationship to canopy structure. Environmental Pollution, in press. (IF: 2.205)
- Luysaert, S., Staelens, J. and De Schrijver A. 2005. Does the commonly used estimator of nutrient resorption in tree foliage actually measure what it claims to? Oecologia 144, 177-186. (IF: 2.899)
- Staelens, J., De Schrijver, A., Van Avermaet, P., Genouw, G. and Verhoest, N. 2005. A comparison of bulk and wet-only deposition at two adjacent sites in Melle (Belgium). Atmospheric Environment 39, 7-15. (IF: 2.562)
- Tabari, M., Fayaz P., Espahbodi, K., Staelens, J., Nachtergale, L. 2005. Response of oriental beech (*Fagus orientalis* Lipski) seedlings to canopy gap size. Forestry 78, 443-450. (IF: 0.543)
- De Schrijver, A., Nachtergale, L., Staelens, J., Luysaert, S. and De Keersmaeker, L. 2004. Comparison of throughfall and soil solution chemistry between a high-density Corsican pine stand and a naturally regenerated silver birch stand. Environmental Pollution 131, 93-105. (IF: 2.205)
- Geudens, G., Staelens, J., Kint, V., Goris, R. and Lust, N. 2004. Allometric biomass equations for Scots pine (*Pinus sylvestris* L.) seedlings during the first years of establishment in dense natural regeneration. Annals of Forest Science 61, 653-659. (IF: 1.407)
- Oyarzún, C., Godoy, R., De Schrijver, A., Staelens, J. and Lust, N. 2004. Water chemistry and nutrient budgets in an undisturbed evergreen rainforest of southern Chile. Biogeochemistry 71, 107-123. (IF: 2.125)
- Staelens, J., Nachtergale, L. and Luysaert, S. 2004. Predicting the spatial distribution of leaf litterfall in a mixed deciduous forest. Forest Science 50, 836-847. (IF: 1.107)

Staelens, J., Nachtergale, L., Luyssaert S. and Lust, N. 2003. A model of wind-influenced leaf litterfall in a mixed hardwood forest. *Canadian Journal of Forest Research* 33, 201-209. (IF: 1.466)

Publications in international journals with peer review not cited in the Science Citation Index

Godoy, R., Haneke, J., Staelens, J., Oyarzún C., Paulino L. and Barrientos, M. Dry deposition of nitrogen to passive samplers in grassland and forest canopies in the central depression of southern Chile. *Gayana Botanica*, in press.

Oyarzún, C., Godoy, R., Staelens, J., Aracena, C. and Proschle, J.C. Nitrogen fluxes in a *Nothofagus obliqua* forest and a *Pinus radiata* plantation in the central depression of southern Chile. *Gayana Botanica*, in press.

Staelens, J., Godoy, R., Oyarzún, C., Thibo, K. and Verheyen, K. Nitrogen fluxes in throughfall and litterfall in two *Nothofagus* forests in southern Chile. *Gayana Botanica*, in press.

Staelens, J., De Schrijver, A., Oyarzún, C. and Lust, N. 2003. Comparison of dry deposition and canopy exchange of base cations in temperate hardwood forests in Flanders and Chile. *Gayana Botanica* 60, 9-16.

Publications in proceedings of scientific congresses

Nachtergale, L., Staelens, J. and Lust, N. 2002. Litterfall and litter decomposition in mixed species forests in Flanders. In: De Schrijver, A., Kint, V. and Lust, N. (eds.). Comparison of ecosystem functioning and biogeochemical cycles in temperate forests in southern Chile and Flanders. Proceedings of the workshop held at Ghent University, 17-19 September 2001. Academia press, Gent, pp. 107-117.

Staelens, J. and Nachtergale, L. 2001. Sampling strategies for leaf litterfall in a mixed *Betula pendula-Quercus robur-Quercus rubra* forest. In: Bréda, N. and Landman, G. Report on the ad hoc expert group meeting on litter fall assessment, 4-6 March 2001, Fontainebleau, France. Report from International co-operative program on assessment and monitoring of air pollution effects on forest (ICP Forests) and European scheme on the protection of forests against atmospheric deposition.

Abstracts of presentations at scientific congresses

Staelens, J., De Schrijver, A. and Van Avermaet, P. 2005. A comparison of bulk and wet-only deposition in Flanders (Belgium). Poster abstract in: Hůnová, I. (ed.). Conference abstracts of Acid Rain 2005, 7th International conference on acid deposition, 12-17 June 2005, Prague, Czech Republic, p. 130.

Staelens, J., Godoy, R. and Oyarzún, C. 2005. Aboveground nitrogen input by throughfall and litterfall in two *Nothofagus* forests in southern Chile. Abstract of oral presentation in: Risk assessment of agricultural intensification on N deposition on pristine forests and plantations in southern Chile, 2nd International workshop, Universidad Austral de Chile, 11 January 2005, Valdivia, Chile.

Staelens, J. and De Schrijver, A. 2004. Spatial variability of throughfall water under beech (*Fagus sylvatica* L.). Poster abstract in: Proceedings of the 10th PhD Symposium on Applied Biological Sciences. Communications in Agricultural and Applied Biological Sciences 69, 273-274.

References

- Staelens, J. and Geudens, G. 2004. Forest dynamics: fire disturbance and regeneration in forest ecosystems. Abstract of oral presentation in: Workshop of a bilateral scientific and technological cooperation between Chile and Flanders on history and ecology of fires in *Araucaria-Nothofagus* forest ecosystems in Chile, 18 April 2004, Valdivia, Chile.
- Staelens, J., De Schrijver, A., Oyarzún, C. and Lust, N. 2003. Atmospheric nitrogen input in temperate hardwood forests in Chile and Flanders. Abstract of oral presentation in: International workshop on risk assessment of agricultural intensification on N deposition on pristine forests and plantations in southern Chile, 22-26 April 2003, Ghent, Belgium.
- Staelens, J., De Schrijver, A., Oyarzún, C. and Lust, N. 2002. Comparison of dry deposition and canopy exchange of base cations in temperate hardwood forests in Flanders and Chile. Abstract of oral presentation in: International workshop on biogeochemical cycles in temperate forest ecosystems, 11-13 November 2002, Valdivia, Chile.

M.Sc. thesis

- Staelens J. 2001. Ruimtelijk expliciet modelleren van bladval in een gemengd loofbos. M.Sc. thesis, Ghent University, Belgium.

Scientific activities

Participation in congresses, symposia or workshops

Participation with oral presentation

- 23 March 2005. Ruimtelijke variabiliteit van doorvalwater onder beuk. 2^e Symposium Starters in het bosonderzoek, Brussels, Belgium.
- 11 January 2005. Aboveground nitrogen input by throughfall and litterfall in two *Nothofagus* forests in southern Chile. Risk assessment of agricultural intensification on N deposition on pristine forests and plantations in southern Chile, 2nd International workshop, Universidad Austral de Chile, Valdivia, Chile.
- 18 April 2004. Forest dynamics: fire disturbance and regeneration in forest ecosystems. Bilateral meeting Chile-Belgium on history and ecology of fires in *Araucaria-Nothofagus* forest ecosystems, Chile, Universidad Austral de Chile, Valdivia, Chile.
- 22-26 April 2004. Atmospheric nitrogen input in temperate hardwood forests in Flanders and Chile. International workshop of a bilateral scientific and technological co-operation between Flanders and Chile: Risk assessment of agricultural intensification on N deposition on pristine forests and plantations in southern Chile, Ghent University, Ghent, Belgium.
- 11-13 November 2002. Comparison of dry deposition and canopy exchange of base cations in temperate hardwood forests in Flanders and Chile. International workshop on Biogeochemical cycles in temperate forest ecosystems. Universidad Austral de Chile, Valdivia, Chile.
- 19-25 May 2002. Deposition of nitrogen onto forest ecosystems. Workshop of a bilateral scientific and technological co-operation between Flanders and Chile: Risk assessment of agricultural intensification on N deposition on pristine forests and plantations in southern Chile. Universidad Austral de Chile, Valdivia, Chile.

Participation with poster presentation

- 12-17 June 2005. A comparison of wet-only and bulk deposition in Flanders (Belgium). Acid Rain 2005, 7th International conference on acid deposition. Prague, Czech Republic.
- 29 September 2004. Spatial variability of throughfall water under beech (*Fagus sylvatica* L.). 10th PhD Symposium on Applied Biological Sciences. Ghent University, Ghent, Belgium.
- 25-27 June 2003. Spatial variability of throughfall water under beech. International symposium Forest ecosystem and landscape research: scientific challenges and opportunities. Tours, France.
- 15 February 2003. Spatial variability of throughfall water under beech. 1^o Symposium Starters in het bosonderzoek. Brussels, Belgium.

Participation without presentation

- 20 January 2003. Symposium on Environmental Statistics. Ghent University, Ghent, Belgium.
- 9 October 2002. 8th PhD Symposium on Applied Biological Sciences. Ghent University, Ghent, Belgium.
- 29 November 2001. Studiedag 'Bosomvorming, noodzaak en praktijk van een effectgerichte maatregel tegen verzuring en vermessing'. Ghent University, Ghent, Belgium.
- 17 November 2001. Symposium 'Bos, natuurlijk'. University of Leuven, Leuven, Belgium.

Supervision of M.Sc. thesis students

- 2003-2004 Karen Thibo. Belang van strooiselval en doorval in de nutriëntencyclus van *Nothofagus* bossen in Zuid-Chili. Promotors: Prof. dr. ir. N. Lust and Prof. dr. C. Oyarzún
- 2003-2004 Maarten Reynaert. Stamafvloei in *Nothofagus* bossen: hoeveelheid, samenstelling en invloedsfactoren. Promotors: Prof. dr. ir. N. Lust and Prof. dr. R. Godoy

Participation in scientific projects

Bilateral scientific and technological co-operation between Flanders (Ghent University, University of Leuven) and Chile (Universidad Austral de Chile), financed by the Ministry of the Flemish Community.

- 2004 - 2005 Effect of fire damage on regeneration and N loss from *Araucaria araucana* forests in southern Chile
- 2001 - 2004 Risk assessment of agricultural intensification on N deposition on pristine forests and plantations in southern Chile
- 1999 - 2002 Comparison of ecosystem functioning and biogeochemical cycles in temperate forests in southern Chile and Flanders

Review tasks for international journals

- 2005: Ecology (1), Forestry (1), Gayana Botanica (1)



ISBN 90-5989-104-X